From the Department of Internal Medicine III, Ludwig-Maximilians-University Munich
Faculty of Biology of the Ludwig-Maximilians-University Munich
GSF – Clinic Cooperative Group "Leukemia"

Identification and functional characterization of the human and murine *OSTL* gene, which encodes a RING-DRIL-RING domain protein possibly involved in B cell differentiation and leukemogenesis

Thesis for the attainment of the title Doctor in Biology from the Faculty of Biology of the
Ludwig-Maximilians-University Munich

By

Luciana M. Fontanari Krause

Santa Cruz das Palmeiras

Munich

2006

Identifizierung und funktionelle Charakterisierung des menschlichen und murinen *OSTL*-Gens, das für ein RING-DRIL-RING Domänen Protein kodiert und möglicherweise ein Rolle bei der B-Zell Differenzierung und der Leukämieentstehung spielt

Dissertation zur Erlangung des Doktorgrades an der Fakultät für Biologie der Ludwig-Maximilians-Universität München

Vorgelegt von

Luciana M. Fontanari Krause

Aus Santa Cruz das Palmeiras

München

2006

Betreuer: Prof. Dr. med. Stefan K. Bohlander

1. Gutachter: Prof. Dr. med. Thomas Cremer

2. Gutachter: Prof. Dr. Dirk Eick

3. Gutachterin: Prof. Dr. Elisabeth Weiss

4. Gutachter: Prof. Dr. Peter B. Becker

Tag der mündlichen Prüfung: 29.05.2006

1. Table of Contents

2. Abstract

The *OSTL* gene is localized at the band q23 in the chromosome 6. Its localization corresponds to a translocation breakpoint between chromosomes 6 and 12, the t(6;12)(q23;p13), that was characterized in our group in an acute lymphoblastic leukemia cell line. This translocation involves the *ETV6* (translocation ETs leukemia) gene localized in chromosome 12 with the *STL* (six twelve leukemia gene) gene localized in chromosome 6. The *STL* gene shares the first exon with a novel gene, that we named *OSTL* (opposite STL), but they are transcribed in opposite directions. Since the fusion gene *ETV6/STL* encodes only for a very small protein which lacks any known functional domain, we speculate that the main leukemogenic effect of this translocation is the deregulation of *OSTL*. *OSTL* has a RING-Finger motif that is highly conserved between species and has a significant homology with other genes in human as well as *C. elegans*, *D. melanogaster*, and *S. cerevisiae*. *OSTL* showed a very specific expression pattern during the mouse embryogenesis. The aim of this project was the functional characterization of *OSTL*, with special emphasis in normal hematopoiesis and leukemogenesis. Therefore we have sequenced the whole human and mouse *OSTL* cDNA by using *OSTL* cDNA clones from the RZPD ("Resource Zentrum Primäre Datenbank") in Berlin. These sequences encode for a 307 (mouse) and a 275 (human) amino acids length protein. The protein length differences between human and mouse are explained because of the existence of alternative spliced exons. The homology between human and mouse sequence is 99% at the protein level.

The expression of GFP-OSTL fusion protein in mouse fibroblast cell line enable us to observe the subcellular localization of OSTL protein. GFP-OSTL is localized mainly in the cytoplasm, showing small spots, probably in the mitochondrial region. In a mouse multiple tissue Northern blot, we could show that *OSTL* is expressed in testis, ovary and liver. In an human multiple tissue Northern, *OSTL* expression was observed in skeletal muscle, testis, ovary, heart, placenta, pancreas and prostate. Northern blotting with different human cell lines revealed expression of *OSTL* in three EBV (Epstein Barr Virus) transformed lymphoblastoid cell lines (LCL B, LCL D, and LCL R) and in one NHL (Non-Hodgkin Lymphoma) cell line (Karpas 422). In Reverse Transcriptase PCR experiments using B cell in different maturation stages, the expression of *OSTL* was observed in naive, memory B and plasma cells, and in leukemic patient samples, expression was observed in several AML and ALL cDNAs.

Whole mount *in situ* hybridization experiments were performed to investigate the temporo-spatial expression pattern of *OSTL* during mouse embryogenesis. There was distinct

expression of O*stl* in the somites (myotome), first and second branchial arches, optic and otic vesicles, in the hair follicles of the vibrissae, and limb buds in mouse embryos of embryonal days 9.5 to 14.5. This expression pattern suggests an important role for *Ostl* in the early development of these structures.

Aiming to find protein interaction partners of OSTL, we performed a Yeast Two Hybrid assay using a Hela cDNA library. Among others we found interaction of OSTL with the antiapoptotic protein, HAX-1 (HS1-associated protein X-1), that is involved in the regulation of B-cell signal transduction, and interaction with the pro-apoptotic protein, SIVA. SIVA was originally identified as an interaction partner of CD27 (TNFRSF7), a member of the TNF-receptor superfamily, which is expressed in B cells. These interactions were confirmed by *in vitro* (cotransformation in yeast, CoIP) and *in vivo* (colocalization of these proteins in mammalian cells and CoIP) assays.

Overexpression of *Ostl* in primary mouse hematopoietic cells followed by injection of the cells into lethally irradiated mice resulted in a T-Acute-Lymphoblastic-Leukemia (T-ALL) phenotype.

In summary, our experiments could demonstrate that *OSTL* is important in B cell development and signaling and deregulation of this gene can contribute to the development of hematologic malignancies.

3. Zusammenfassung

Das *OSTL*-Gen ist auf der Bande q23 von Chromosom 6 lokalisiert. Es liegt in unmittelbarer Nähe eines Translokationsbruchpunkts zwischen Chromosom 6 und Chromosom 12 (t(6;12)(q23;p13)), der in unserer Arbeitsgruppe in einer akuten lymphoblastischen Leukämie Zellinie kloniert wurde. Bei dieser Translokation kommt es zu einer Fusion des *ETV6*-Gens von Chromosom 12 mit dem *STL*-Gen auf Chromosom 6. Das erste Exon von *STL* wird jedoch in entgegengesetzter Richtung von einem zweiten Gen abgelesen, welches wir *OSTL* nannten (OSTL = Opposite STL). Es ist nicht klar, ob das ETV6-STL Fusionsprotein eine Rolle bei der Leukämieentstehung spielt, da es nur für ein sehr kleines Protein codiert, das keine bekannten funktionellen Domänen aufweist. Wir vermuten daher, dass die Regulation von *OSTL* durch die Translokation gestört wird und dass dies hauptsächlich zur Leukämieentstehung beiträgt. *OSTL* hat ein charakteristisches RING-Finger Motiv, das evolutionär hochkonserviert ist und signifikante Homologien zu anderen Genen des Menschen sowie von *C. elegans*, *D. melanogaster* und *S. cerevisiae* aufweist. *OSTL* hat ein zeitlich und räumlich sehr definiertes Expressionsmuster während der murinen Embryogenese. Es war das Ziel dieses Projektes, die Funktion von *OSTL* insbesondere im Hinblick auf die normale Hämatopoese und bei der Leukämieentstehung zu charakterisieren. An Hand von *OSTL* cDNA Klonen, die über das Ressourcen Zentrum Primäre Datenbank (RZPD) in Berlin bezogen wurden, konnten wir sowohl die Sequenz des menschlichen als auch des murinen *OSTL*-Gens ermittelt. Diese Sequenzen codieren ein 307 (Maus) bzw. 275 (Mensch) Aminosäuren langes Protein. Der Unterschied in der Proteinlänge zwischen Mensch und Maus ist durch die Zusammensetzung aus alternativ gespleißten Exonen bedingt. Das murine und das menschlichen OSTL Protein weisen eine erstaunlich hohe Homologie von 99% auf.

Durch Expression eines GFP-OSTL Fusionsproteins in Mausfibroblastenzellen konnten erste Hinweise auf die subzelluläre Verteilung des OSTL-Proteins gewonnen werden. Es zeigte sich eine deutliche Aussparung des Kerns und eine Lokalisation des GFP-OSTL Fusionsproteins in diskreten kleinen Flecken im Zytoplasma, wahrscheinlich in den Mitochondrien. Expressionsanalysen mit Hilfe von Multiple Tissue Northern Blots zeigten, dass die verwendete *OSTL*-Sonde Transkripte unterschiedlicher Größe detektiert, bei der Maus in Testis, Ovar und Leber und beim Menschen in Muskeln, Testis, Ovar, Herz, Plazenta, Pankreas, und Prostata. Die Untersuchung der Expression in humanen Zell-Linien zeigte, dass sich mit der *OSTL*-Sonde bei drei Epstein Barr Virus-transformierten

lymphoblastoiden Zellinien (LCL B, LCL D und LCL R) und bei einer NHL Zell Linie (Karpas 422) Transkripte nachweisen lassen. Mithilfe von *RT-PCR* konnte gezeit werden, dass *OSTL* während unterschiedlicher Entwicklungsstadien von B-Lymphozyten (naive, memory B, and plasma Zellen) und außerdem bei Leukämie-Patienten (AML und ALL) exprimiert wird.

Zur Analyse der räumlichen und zeitlichen Expression von *OSTL* während der Embryonalentwicklung der Maus wurden Embryonen der Entwicklungstage E9.5 bis 14.5 mittels Whole Mount *in situ* Hybridisierung untersucht. Es zeigte sich eine spezifische Expression von *OSTL* unter anderem in den Somiten (wahrscheinlich im Myotom), an der hinteren Öffnung des Neuralrohrs, in den Extremitätenknospen, in den Kieferbögen, in den Ohr- und Augenanlagen, in den Anlagen der Schnurrbarthaare und in den Extremitäten (Hand- und Fußwurzeln) in Mausembryonen der Stadien 9.5 bis 14.5. Diese vorläufigen Ergebnisse zeigen ein sehr spezifisches Expressionsmuster von *OSTL* in der Embryonalentwicklung der Maus, was eine Rolle dieses Gens bei der frühen Entwicklung und Differenzierung bestimmter Gewebe und Strukturen (z.B. der Muskeln) nahe legt.

Um Proteininteraktoren von OSTL zu identifizieren, wurde eine Hela cDNA Bank mittels *Yeast Two Hybrid Screen* durchsucht. Dabei fanden wir eine Interaktion von OSTL mit den Proteinen HAX1 (HS1-associated protein X-1), welches in der Signaltransduktion des B-Zellrezeptors eine Rolle spielt, und mit dem pro-apoptotischen Protein SIVA. SIVA wurde als Interaktionspartner von CD27 (TNFRSF7), einem Mitglied der TNF-Rezeptoren Superfamilie, der auf B-Zellen exprimiert wird. Diese Interaktionen wurden mit Hilfe von *in vitro* (Kotransformation in Hefe, CoIP nach) und *in vivo* (Kolokalization in Säugetierzellen, CoIP) Methoden bestätigt.

Durch Überexpression von *OSTL* in primären murinen Knochenmarkzellen, die in Mäuse transplantiert wurden, konnten wir eine T-ALL auslösen.

Zusammengefasst zeigen unsere Experimente, dass *OSTL* eine wichtige Rolle bei der B-Zellentwicklung spielt sowie dass eine deregulierte Expression von *OSTL* bösartige hämatologische Krankheiten verursachen kann.

4. Introduction

4.1. Hematopoiesis and hematopoietic stem cells

4.1.1. Yolk-sac hematopoiesis: the first blood cell of mouse and man

The yolk sac is the first site of blood-cell production during murine and human ontogeny. In the adult, hematopoiesis is in a steady state as all blood cells are synthesized from multipotent precursor cells produced by hematopoietic stem cells in the bone marrow. In the fetus, the liver serves as the principal hematopoietic organ. However, the early mammalian embryo requires red cells for growth and survival prior to the development of the liver. Large primitive red cells are produced in blood islands of the yolk sac after implantation of the embryo (Palis & Yoder, 2001). Figure 4.1 illustrates the development of yolk sac islands in the mouse embryo.
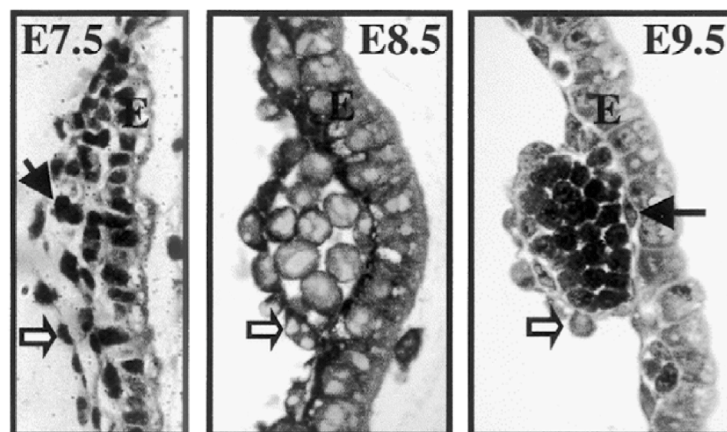
Figure 4.1: Development of yolk sac blood islands in the mouse embryo between E7.5 and E9.5. Yolk sac blood islands form between the single cell layer of endoderm cells (E) and mesothelial cells (open arrow). Blood islands develop from undifferentiated mesoderm cells (E7.5, closed arrow) that give rise to inner blood cells surrounded by an outer endothelial lining (E9.5, closed arrow) (figure from Palis, and Yoder, 2001).

4.1.2. Ontogenic emergence of the hematopoietic stem cell (HSC)

The developing tissues are supplied with oxygen and nutrients through the first hematopoietic cells that arise from extra-embryonic yolk sac, and circulate in the embryo. The primitive hematopoiesis, as the embryo develops is substituted by the definitive multilineage blood system. Pluripotent hematopoietic stem cells (HSC) sustained this definitive hematopoiesis and have the capacity of self-renewal, and are capable of long-term repopulation in

myeloablative recipients. The HSCs, in mouse embryos, appears beginning at mid-E10, in the yolk sac at E11, and at late-E11 in liver (Bonnet, 2003). In the zebrafish (Detrich, 1995) and frog (Turpen, 1997), both the ventral and dorsal mesoderm contribute to the initiation and perpetuation of hematopoiesis (Weissman, 2000). The human embryonic development significantly parallels mouse development, as shown schematically in figure 4.2 (Bonnet, 2003).
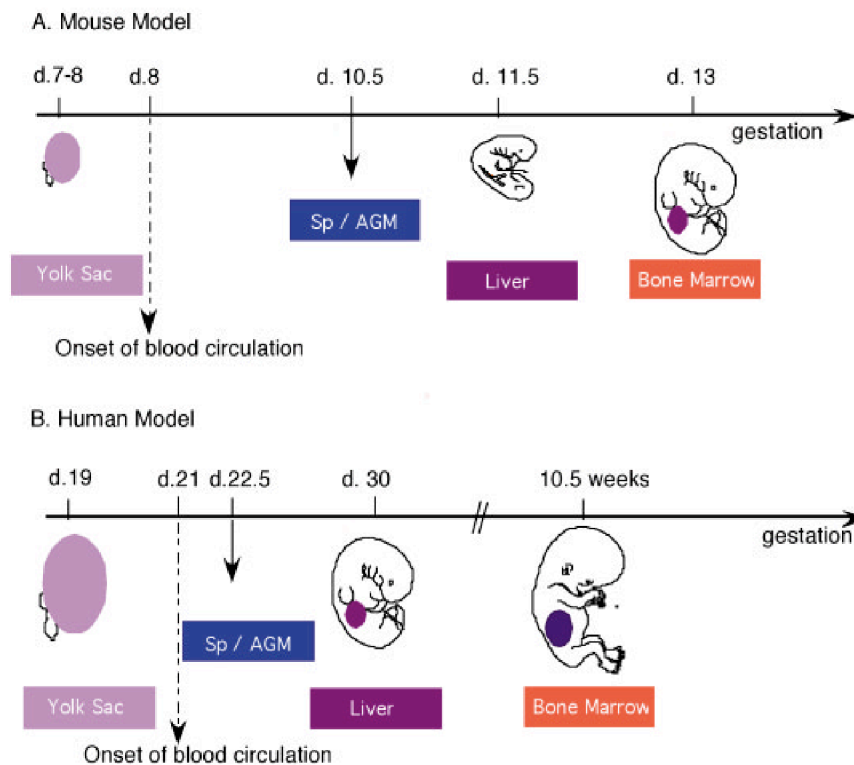
Figure 4.2: A and B Ontogenic emergence of the hematopoietic system in mouse and human.

4.1.3. Hematopoiesis

The human body produces, every day, billions of new white blood cells, red blood cells, and platelets to replace blood cells lost to normal cell turnover processes as well as to illness or trauma. A variety of homeostatic mechanisms allow blood cell production to respond quickly to stresses such as bleeding or infection and then return to normal levels when the stress is resolved. Hematopoiesis is the process of blood production and homeostasis. Alterations in the normal hematopoiesis can lead to several hematologic malignancies and other disorders such as leukemia, aplastic anemia, lymphoma, myelodysplasia, myeloproliferative disorders, and inborn errors of metabolism (Smith, 2003).

The complete number of mature blood cells in the body is derived from a relatively small number of hematopoietic stem cells and progenitors (Weissman, 2000; Lemischka, 2001). Murine models, particularly short- and long-term transplant studies, have provided a number of insights into the biology of HSCs and progenitors (Eaves, 1997; Jones, 1996). The results of these studies have demonstrated that HSCs are able to generate every lineage found in the hematopoietic system including red blood cells, platelets, and a variety of lymphoid and myeloid cells (Weissman, 2000; Lemischka, 2001; Eaves, 1997; Jones, 1996). Some of the most important lymphoid cells include natural killer (NK) cells, T cells, and B cells, while important myeloid cells include granulocytes, monocytes, macrophages, microglial cells, and dendritic cells (Akashi, 1999). Each of these cell types can be generated from a single HSC, and each HSC has an enormous capacity to generate large numbers of these cells over many years and perhaps even decades. In the mouse, a single HSC can reconstitute the entire hematopoietic system for the natural lifespan of the animal (Osawa, 1996). Murine HSCs are rare and are present at a frequency of 1/10.000 to 1/1.000.000 cells in the bone marrow depending on the species, age, and technical aspects of the model.

While HSCs are primarily found in the bone marrow, they are present in a variety of other tissues including peripheral blood and umbilical cord blood, and are found at low numbers in the liver, spleen, and perhaps many other organs (Holyoake, 1999).

These HSCs may have somewhat different properties, but they all have the ability to generate all the different blood lineages in large numbers for a prolonged period of time.

HSCs generate the multiple hematopoietic lineages through a successive series of intermediate progenitors. These include common lymphoid progenitors (CLPs), which can generate only B, T, and NK cells, and common myeloid progenitors (CMPs), which can generate only red cells, platelets, granulocytes, and monocytes (Akashi, 2000; Kondo, 1997). Downstream of the CLPs and CMPs are more mature progenitors that are further restricted in the number and type of lineages that they can generate (Akashi, 2000). Ultimately, terminally differentiated cells are produced that cannot divide and undergo apoptosis after a period of time ranging from hours (for neutrophils) to decades (for some lymphocytes). When a bone marrow or blood stem cell transplant is performed, it appears that progenitors contribute to engraftment for only a short period of time, while long-term blood production is derived primarily from HSCs (Jordan, 1990). Figure 4.3 (Smith, 2003) shows a summary of the blood development process.
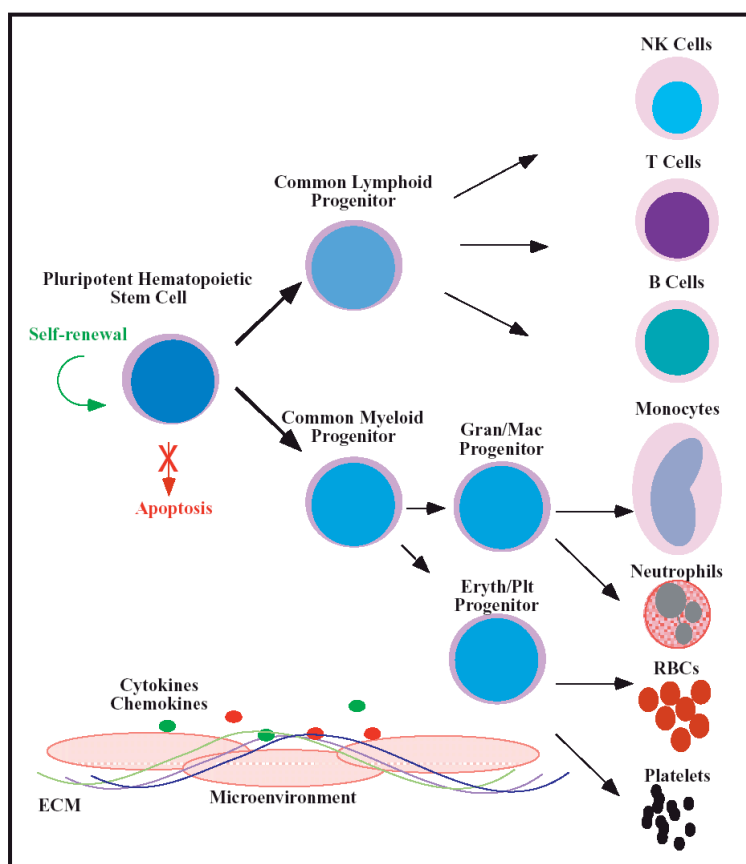
Figure 4.3: Process of blood development. ECM = extra-cellular matrix.

4.1.4. B cell development and signalling

The development of B lymphocytes from hematopoietic stem cells can be divided into distinct stages on the basis of the cytokine expression or loss of cell surface or intracellular proteins and of the rearrangement of the immunoglobulin (Ig) genes (Rolink, 1999; Hardy, 2000).

The loss of long-term self-renewal capacity by the HSCs is accompanied by expression of the tyrosine kinase receptor Flt3 (also known as Flk2) in multipotent progenitors (MPP) cells (Adolfsson, 2001; Christensen, 2001).

The Flt3$^+$ MPPs subsequently differentiate to the earliest lymphocyte progenitors (ELP), which initiate *RAG1* and *RAG2* expression and start to undergo D_H-J_H rearrangements at the immunoglobulin heavy-chain (*IgH*) locus (Igarashi, 2002; Jumaa, 2005) (Figure 4.4 A). The ELP cell is likely to give rise to the recently identified early T-lineage progenitor (ETP) in the thymus (Allman, 2003) and to the CLP in the bone marrow, which is able to develop into four distinct cell types: B, T, NK, and DC cells (Kondo, 1997; Traver, 2003) (Figure 4.4 A). Subsequent expression of the B cell marker B220 coincides with differentiation to CLP-2

cells (Gounari, 2002; Martin, 2003), constituting a subset fraction A cells (Li, 1996; Tudor, 2000) that enter the B cell pathway upon induction of CD19 expression and complete D_H-J_H rearrangements at the early pro-B cell stage (fraction B, figure 4.4 A) (Gounari, 2002; Hardy, 1991; Li, 1993). Productive V_H-DJ_H recombination in late pro-B cells (fraction C) results in cell surface expression of the Igμ proteins as part of the pre-B cell receptor (pre-BCR), which acts as a important checkpoint to control the transition from the pro-B to the pre-B cell stage. Signaling from the pre-BCR promotes allelic exclusion at the *IgH* locus, stimulates proliferative cell expansion, and induces differentiation to small pre-B cells, which start to recombine immunoglobulin light-chain genes (Meffre, 2000; Jumaa, 2005) (figure 4.4 B). Successful light-chain gene rearrangement leads to the emergence of immature IgM$^+$ B cells that emigrate from the bone marrow to peripheral lymphoid organs (Meffre, 2000**).**

Signaling via different transmembrane receptors is essential for guiding the differentiation of HSCs along the B cell pathway. Activation of the tyrosine kinase receptor c-Kit by its ligand SCF (stem cell factor) promotes the survival of long-term reconstituting HSCs *in vitro* (Adolfsson, 2001; Domen, 2000), although the absence of c-Kit does not affect the survival and engraftment of HSCs *in vivo* in a viable *c-kit$^{W/W}$* (Vickid) mouse strain (Waskow, 2002).

Similarly, signaling through the Flt3 receptor is required for efficient formation of the CLP and subsequent development of pro-B and pre-B cells, as these cell types are strongly reduced in the absence of the Flt3 ligand (FL) in the bone marrow of *FL$^{-/-}$* mouse (Mckenna, 2000; Sitnicka, 2002). In contrast, normal numbers of the CLP are generated in $\gamma_c^{-/-}$ mice lacking functional IL-7 receptor, which is composed of the IL-7Rα protein and the signalling γ_c chain (Miller, 2002). Consistent with this early developmental block, the lymphoid cytokine IL-7 not only signals pro-B cell survival, but also functions as a differentiation factor to induce B cell development of the CLP (Miller, 2002). Hence, the c-Kit, Flt3, and IL-7 signaling systems together account for the generation of all B-lymphocytes in the bone marrow of adult mice.

In addition to cytokine signaling, a multitude of lineage-restricted transcription factors control B cell development from the HSC to immunoglobulin-secreting plasma cells (Schebesta, 2002).

A

erythroid
myeloid
T cell
NK cell
DC
pre-BCR

CMP
ETP
CLP-2
early pro-B
late pro-B
pre-B
immature B cell

HSC → MPP → ELP → CLP → A1/2 → B → C → D → E

Lin-   Lin-   Lin-   Lin-   B220+   CD19+   BP1+   CD25+   IgM+

	HSC	MPP	ELP	CLP	A1/2	B	C	D	E
c-kit	high	high	high	low	low	low	low	-	-
Flt3	-	+	+	+	+	-	-	-	-
IL-7Ralpha	-	-	-	+	+	+	+	-	-
DH-JH	-	-	(+)	+	+	+	+	+	+
VH-DJH	-	-	-	-	-	(+)	+	+	+
VL-JL	-	-	-	-	-	-	-	+	+

B

pre-BCR   HC   SLC

MT
Ig-α, Ig-β
λ5, Vpre-B
Syk

Ig-α/Ig-β

SLP-65
Btk
PLC-γ2

BCR   HC   LC

Ig-α/Ig-β

pro-B cell (DJ GL) → pre-B cell (VDJ GL) → small pre-B cell (VDJ GL) → immature B cell (VDJ VJ)

Figure 4.4: A and B) A scheme of B cell development. A) The expression of signaling receptors, the rearrangement status of immunoglobulin genes and the initiation of expression of characteristic cell surface proteins are indicated for successive progenitor cell stages of mouse B-lymphopoiesis (adapted from Busslinger, 2004). **B)** Productive rearrangement of the heavy chain (HC) gene locus in pro-B cells results in pre-BCR expression on pre-B cells. Productive rearrangement of one of the LC gene loci in small pre-B cells leads to BCR expression on immature B cells. Inactivation of the indicated genes results in specific maturation arrests during B cell development. GL = germline configuration of the Ig genes (adapted from Jumaa, 2005).

4.1.5. Self-renewal of hematopoietic stem cells and leukemogenesis

In the hematopoietic system, stem cells are heterogeneous with respect to their ability to self-renew. Multipotent progenitors constitute 0.05% of mouse bone-marrow cells, and can be divided into three different populations: long-term self-renewing HSCs, short-term self-renewing HSCs, and multipotent progenitors without detectable self-renewal potential

(Morrison, 1994; Morrison, 1997). These populations form a lineage in which the long-term HSCs give rise to short-term HSCs, which in turn give rise to multipotent progenitors (Morrison, 1997). As HSCs mature from the long-term self-renewing pool to multipotent progenitors, they progressively lose their potential to self-renew but become mitotically active. Whereas long-term HSCs give rise to mature hematopoietic cells for the lifetime of the mouse, short-term HSCs and multipotent progenitors reconstitute lethally irradiated mice for less than eight weeks.

Because normal stem cells and cancer cells share the ability to self-renew, it seems reasonable to propose that newly arising cancer cells appropriate the machinery for self-renewing that is normally expressed in stem cells. Many pathways that are classically associated with cancer may also regulate normal stem cell development. For example the prevention of apoptosis by enforced expression of the oncogene *bcl-2* results in increased numbers of HSC *in vivo* suggesting that cell death has a role in regulating the homeostasis of HSCs (Domen, 1998; Domen, 2000).

Other signaling pathways associated with oncogenesis, such as the *Notch*, *Sonic hedgehog* (*Shh*) and *Wnt* signalling pathways, may also regulate stem cell self-renewal (Taipale, 2001) (Figure 4.5, adapted from Reya, 2001).

If the signaling pathways that normally regulate stem cell self-renewal lead to tumorigenesis when dysregulated then are stem cells themselves the target of transformation in certain types of cancer (Sell, 1994; Sawyers, 1991). There are two reasons to think that this hypothesize may be correct: first, because stem cells have the machinery for self-renewal already activated, maintaining this activation may be simpler than turning it on *de novo* in a more differentiated cell; that is, fewer mutations may be required to maintain self-renewal than to activate it ectopically. Second, by self-renewing, stem cells often persist for long periods of time, instead of dying after short periods of time like many mature cells in highly proliferative tissues. This means that there is a much greater opportunity for mutations to accumulate in individual stem cells than in most mature cell types. Though the molecular mechanisms of stem cell self-renewal are poorly understood, several genes and gene families have been implicated in the process including the *Hox* (Buske, 2002; Antonchuk, 2001) and *Wnt* gene families (Reya, 2003).
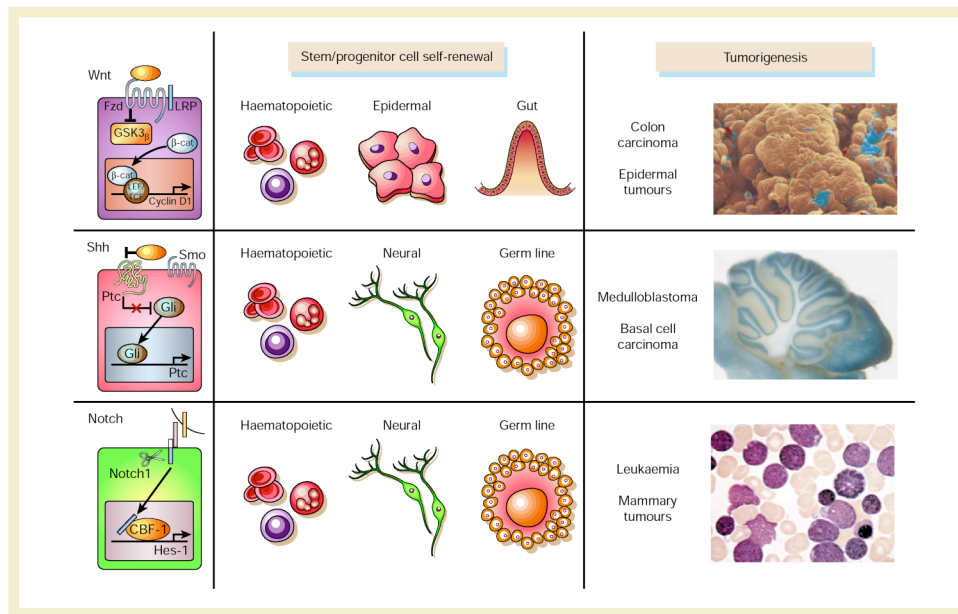
Figure 4.5: Signalling pathways that regulates self-renewal mechanisms during normal stem cell development and during transformation. *Wnt*, *Shh* and *Notch* pathways have been shown to contribute to the self-renewal of stem cells and/or progenitors in a variety of organs, including the hematopoietic and nervous systems. When dysregulated, these pathways can contribute to oncogenesis. Mutations of these pathways have been associated with a number of human tumors, including colon carcinoma and epidermal tumors (*Wnt*), medulloblastoma and basal cell carcinoma (*Shh*), and T-cell leukemias (*Notch*). Though the molecular mechanisms of stem cell self-renewal are poorly understood, several genes and gene families have been implicated in the process including the *Hox* and *Wnt* gene families (adapted from Reya, 2001).

4.2. Chromosomal translocations

Recurring chromosomal abnormalities have been identified in a variety of cancers, but are most frequently associated with leukemias, lymphomas and sarcomas (Rabbitts, 1994; Rowley, 1999). At present, more than 500 recurring cytogenetic abnormalities have been reported in hematological malignancies. Three main cytogenetic changes have been detected in hematological malignancies: deletions, inversions and translocations.

On the molecular level, there are two major mechanisms by which chromosomal translocations lead to malignant cell transformation: chromosomal breaks may occur within genes (usually within introns) and, if the reading frame is preserved, generate chimeric fusion genes with properties differing from those of the original ones or a chromosomal break may also occur near a cellular proto-oncogene that is then dysregulated in its pattern of expression (Rabbitts, 1994) (Figure 4.6 adapted from Burmeister, 2001).

a. Generation of novel fusion genes
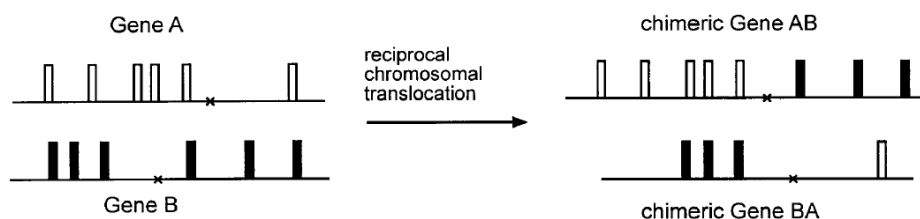
b. Activation of a cellular proto-oncogene
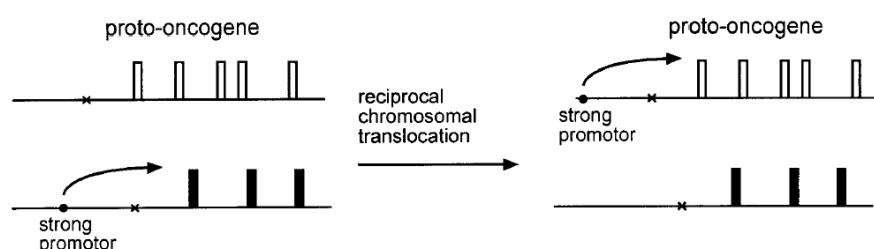
Figure 4.6: Two major mechanisms by which chromosomal translocations can lead to oncogenic transformation. a) If the chromosomal breaks occur within introns of two genes and if the reading frame is preserved, two new chimeric genes result from the translocation. One of them may act as an oncogene. **b)** If a strong promoter or enhancer element is translocated near a proto-oncogene, this may consecutively be activated.

4.2.1. Generation of fusion genes by chromosomal translocations

The first identified chromosomal translocation generating a fusion gene was the fusion of the *BCR* (22q11) and c-*ABL* genes (9q34) on the Philadelphia chromosome (Novell, 1960; Bartram, 1983; de Klein, 1986). This fusion creates a tumor-specific marker and the functional consequence of the BCR-ABL fusion is constitutively active tyrosine kinase activity of ABL. The studies of the BCR-ABL fusion have paved the way for many more descriptions of fusion proteins, often involving transcription factors.

There are at least seven different chromosomal translocations associated with myeloproliferative disease. These include the *BCR/ABL*, *ETV6/ABL*, *ETV6/PDGFRB*, *HIP1/PDGFRB*, *H4/PDGFRB*, *RAB5E/PDGFRB*, and *ETV6/JAK2* fusions (Table 4.1 adapted from Dash, 2001).

Table 4.1: Chromosomal translocations involving tyrosine kinases

Translocation	Genes	Major structures	Disease
t(9;22)(q34;q11)	*ABL1* *BCR*	TK GRB2/SOS binding	CML,ALL
t(8;13)(p11;q12)	*FGFR1* *ZNF198/FIM/RAMP*	TK Cysteine rich MYM	MPD
t(6;8)(q27;p11)	*FOP* *FGFR1*	Leucine rich TK	MPD
t(8;9)(p12;q33)	*FGFR1* *CEP110*	TK LZ	MPD
t(5;7)(q33;q11.2)	*PDGFRB* *HIP1*	TK Huntingtin interaction	CMML
t(5;14)(q33;q32)	*PDGFRB* *CEV14*	TK LZ	AML
t(5;10)(q33;q21)	*PDGFRB* *H4/D10S170*	TK LZ	MPD

MPD = myeloproliferative disease

Besides tyrosine kinases, transcription factors also play a crucial role in the development and maturation of blood cells. A coordinated action and timely expression of a whole set of transcription factors is necessary to insure the correct maturation of a progenitor cell into a fully functional cell of myeloid or lymphatic lineage. Inactivation of one transcription factor or alteration of its function or time-dependent expression pattern by a chromosomal break causing truncation and fusion with another gene may arrest the cell at a certain stage of differentiation. This immature differentiation-arrested cell may then undergo further genetic changes that ultimately result in malignant transformation and clonal outgrowth (Burmeister, 2001).

Approximately 20% of all cases of acute leukemia have chromosomal translocations involving the genes of the core-binding factor (CBF) family of transcription factor.

Two members of the family are involved in human leukemias, CBFα2 (also known as AML1) and CBFβ. AML1 is disrupted by the t(8;21)(q22;q22) in approximately 20% of AML-M2 cases, where its N-terminal part is fused to a gene known as ETO ("eight twenty-one"). In childhood but not adult ALL, the most frequent translocation (in some 20% of cases) is the cytogenetically invisible t(12;21)(p13;q22), leading to the fusion of the C-terminal part of AML1 with a protein called ETV6 (Ets variant translocation 6; previously called TEL = "translocation ETS leukemia"; ETS: a family of transcription factors) (Golub, 1995; Shurtleff, 1995).

Both translocations are associated with a remarkably favorable prognosis. Less frequently AML1 can also be found as a fusion partner with genes on 3q26 (EAP, MDS1, EVI1) in CML or myelodysplastic syndromes (Secker-Walker, 1995).

Approximately 5-10% of all clonal translocations found in acute leukemias involve the *MLL* gene on 11q23. MLL (for "mixed lineage leukemia") rearrangements have been indiscriminately found in myeloid, lymphatic, and biphenotypic leukemias, or as HTRX/HRX (due to its sequence homology to the *Drosophila thithorax* protein). There are more than 45 different partner genes leading to a wide variety of different fusion proteins that have been described in leukemias (Waring, 1997).

MLL rearrangements are particularly characteristic for infant ALL and therapy-related AML, where they can be found in 60-80% of cases (Hilden, 1997). The prognosis is usually poor in infants and therapy-related cases but has significantly improved in adults under intensified therapy regimens (Ludwig, 1998).

It is also known that most cases of AML-M3 are cytogenetically characterized by a balanced translocation, t(15;17)(q22-24;q12-21). This chromosomal translocation disrupts two genes, the gene coding for the retinoic acid receptor α subunit on chromosome 17 and the PML (for promyelocytic leukemia) on chromosome 15 (Borrow, 1990; de The, 1990; Lemons, 1990).

Two fusion genes result from the translocation, PML/RARα on chromosome 17 (expressed in nearly all cases) and RARα/PML on chromosome 15 (expressed in 80% of cases). PML/RARα is believed to mediate leukemogenesis, because it is not only expressed in nearly all cases but also retains the potentially important functional domains of both PML and RARα. The crucial event seems to be disruption of the RARα.

4.2.2. Dysregulation of a proto-oncogene due to a nearby chromosomal break

The term "proto-oncogene" refers to genes which play an important role in cell physiology, cell differentiation, regulation of cell growth, signaling cascades and others. If such a proto-oncogene is altered by genetic changes such as point mutations or deletions or becomes dysregulated in its expression, it can convert into a real "oncogene" (a gene that promotes malignant growth or transformation).

Many proto-oncogenes have first been detected in rapidly transforming animal retroviruses, where they were accidentally incorporated into the virus genome. The first example is ABL (from Adelson murine leukemia virus), second MYC (from avian myelocytomatosis), and third ERB (from murine erythroblastosis virus) (Burmeister, 2001).

The proto-oncogenes may be activated by a chromosomal break that relocates them near a strong enhancer element (Figure 4.6).

A very common mechanism of proto-oncogene activation in human leukemias is translocation of a proto-oncogene to gene loci of the immunoglobulin (Ig) or T-cell receptor (TCR) family (Burmeister, 2001). T-cell acute leukemias (T-ALL) have a number of different recurring translocations, most involve putative transcription factors that are involved in differentiation and are not normally expressed in T cells.

The *HOX11* gene, located on chromosome 10, band q24, which is activated by translocation t(10;14)(q24;q11) and t(7;10)(q35;q24) in T-ALL is an example (Dube, 1991; Hatano, 1991; Kennedy, 1991; Lu, 1991). This gene encodes a homeodomain protein that can bind DNA and transactivate transcription (Dear, 1993).

The *TAL1/SCL* gene, contains a b-HLH motif, is either involved in the t(1;14) or in up to 25% of childhood T-ALL cases (Baer, 1993). The chromosomal translocation probably causes ectopic TAL1 production, activating a specific set of target genes which are normally silent in T cells.

Other T-ALL-associated protein activated by chromosomal translocation is the RBTN/Ttg proteins (Sanchez-Garcia, 1993). These are produced after translocations t(11;14)(p13;q11) or t(11;14)(p15;q11) and encodes proteins with a LIM motif (Boehm, 1990).

The failure of certain fusion genes to induce leukemia on their own, in animal models, as well as the fact that more than 50% of acute myeloid leukemias do not have apparent cytogenetic abnormalities, point to the role of point mutations in or, alternatively, the aberrant expression of proto-oncogenes in the development of leukemia. These observations also suggest that the aberrant expression of proto-oncogenes might be more common than is generally believed.

The sheer number of *ETV6* fusions in AML allows for the study of a diverse group of leukemias in which more than one of the aforementioned mechanisms might be operating. The t(6;12) translocation is one of several that involve *ETV6*, in this case *ETV6* is fused to *STL* gene in a B-cell ALL cell line.

4.3. ETV6

ETV6 is a member of the *ets* (E-26 transforming specific) family of transcription factors. All *ets* family proteins share a highly conserved protein domain of about 88 amino acids in length the so-called *ets* domain. The *ets* domain is a sequence specific DNA binding domain but is also mediates protein-protein interaction (Figure 4.7, modified from Slupsky, 1998), it is

evolutionarily highly conserved and found in invertebrates such as *Drosophila* and *C. elegans* (Oikawa, 2003; Wasylyk, 1993).

The other evolutionarily conserved domain in the 652 amino acids of ETV6 is the N-terminally located *pointed* or sterile alpha motif (SAM) domain (Figure 4.7). This domain is also called HLH domain and is even more highly conserved in evolution and found in many *ets* family member. It is found in yeast proteins and has been shown to be involved in homo and heterodimerization in transcription factors and in signal transducing proteins (e.g. of the MAPK pathway) (Grimshaw, 2004). *ETV6* contains two alternative translational start codons (position 1 and position 43) leading to the expression of two isoforms of ETV6.
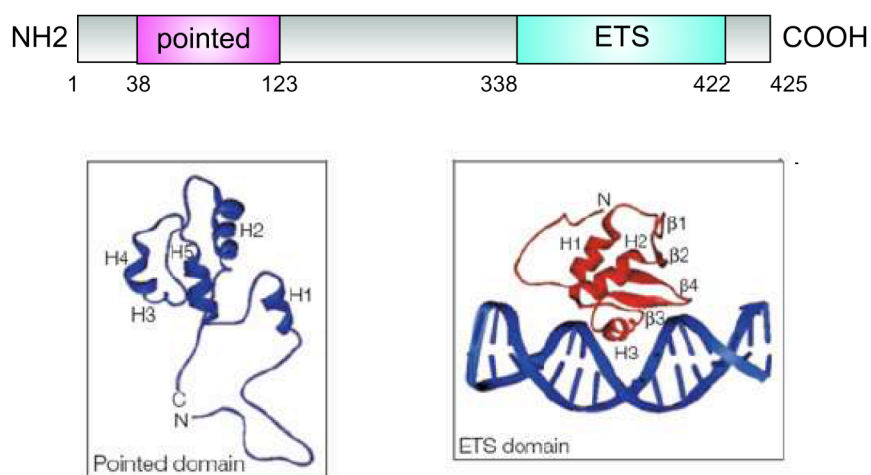
Figure 4.7: ETV6 protein structure. The pointed domain is represented between Nt 38 and Nt 123; ETS domain is between Nt 338 and Nt 422 (modified from Slupsky, 1998).

4.3.1. Role of ETV6 in hematopoiesis

ETV6 is widely expressed throughout embryonic development and in the adult. Embryos with a conventional knockout (KO) of the *Etv6* gene die by day 11 of embryonic development (E11) due to vascular abnormalities. Blood formation in the embryo is largely unperturbed (Wang, 1997). Yet, studies using chimeric mice from *Etv6*-deficient embryonic stem (ES) cells suggested a requirement of *Etv6* in bone marrow hematopoiesis. Inducible and lineage-specific gene disruption of *Etv6* in adult hematopoiesis in mice suggests that it plays two important roles in hematopoietic differentiation. First, *Etv6* controls the survival of HSCs so that its disruption indirectl*y* affects the majority of all hematopoietic cells which have limited clonal life spans and eventually will extinguish without constant regeneration from HSCs.

Secondly, *Etv6* is required late in the development of the megakaryocyte lineage, where it presumably acts in concert with transcriptional regulators previously implicated in megakaryopoiesis (Hock, 2004).

4.3.2. ETV6 fusion partners

Translocations involving the *ETV6* gene contribute to leukemogenesis through at least 3 different mechanisms. One mechanism is the activation of kinases. The second mechanism is the loss of function of critical transcription factors and/or the formation of aberrant transcription factors and the third mechanism is the induction of ectopic and aberrant expression of the proto-oncogene by the chromosomal translocation. Figure 4.8 shows the different breakpoints in the *ETV6* gene with regard to the different fusion partners.
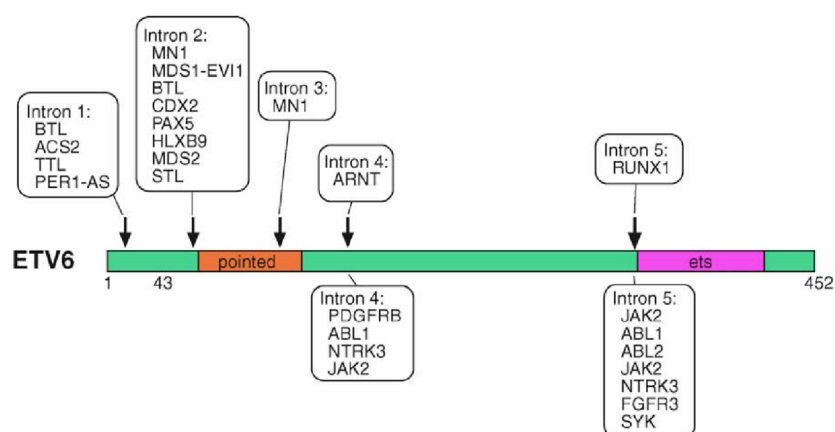
Figure 4.8: Diagram of ETV6 with protein domain and breakpoints (indicated by arrows) representing different partner genes of ETV6 (indicated in closed boxes) (adapted from Bohlander, 2005).

4.3.3. Protein tyrosine kinase fusion partners of ETV6

The first identified fusion partner of ETV6 was a protein tyrosine kinase (PTK), the platelet-derived growth factors receptor beta (*PDGFRB*) (Golub, 1994a). The fusion protein critical for the development of the chronic myelomonocytic leukemia is the ETV6/PDGFRB fusion, and not the reciprocal PDGFRB/ETV6 fusion. In the ETV6/PDGFRB fusion protein the N terminal portion of ETV6, which includes the *pointed* domain, is fused to the C-terminal two thirds of the PDGFRB protein, conserving the tyrosine kinase domain of PDGFRB. The fusion of the *pointed* domain of ETV6 in the N-terminal half with the tyrosine kinase domain in the C-terminal half of the fusion partner is characteristic of the class of *ETV6/PTK* fusions

and is found in the fusions of *ETV6* with *ABL1*, *ABL2*, *JAK2*, *NTRK3*, *FGFR3* and *SYK* (Table 4.2 adapted from Bohlander, 2005) (Papadopoulos, 1995; Cazzaniga, 1999; Kuno, 2001).

Table 4.2: Protein tyrosine kinase fusion partner of ETV6

Fusion partner	Translocation	Breakpoint in ETV6	Disease
PDGFRB	t(5;12)(q31;p13)	Intron 4	CMMoL
ABL1	t(9;12)(q34;p13)	Introns 4 and 5	AML, ALL
ABL2	t(1;12)(q25;p13)	Intron 5	AML-M3, -M4, T-ALL
JAK2	t(9;12)(p24;p13)	Intron 4 or 5	Pre-B cell ALL, T-ALL
NTRK3	t(12;15)(p13;q25)	Intron 4 or 5	Congenital fibrosarcoma, mesoblastic nephroma, Secretory breast carcinoma, AML
FGFR3	t(4;12)(p16;p13)	Intron 5	Peripheral T cell lymphoma
SYK	t(9;12)(q22;p12)	Intron 5	MDS

4.3.4. Transcription factors and other fusion partners of ETV6

The *ETV6/RUNX1* (*ETV6/AML1*) fusion is the most common fusion gene in childhood acute B cell lymphoblastic leukemia (Shurtleff, 1995). Reporter gene assays showed that the ETV6/RUNX1 fusion protein acts as a repressor by binding to the promoter and enhancer regions of RUNX1 target genes. This repression function is dependent on the *pointed* and on the central domain of ETV6, which are both part of the ETV6 portion of the ETV6/RUNX1 fusion protein (Fenrick, 1999). ETV6/ARNT and HLXB9/ETV6 chimeric proteins are other examples of this class of ETV6 fusions found in AML and the HLXB9/ETV6 hybrid is detected in up to 20% of pediatric cases with AML (Beverloo, 2001). A potential mechanism of transformation for these fusions is that the ETV6/ARNT and HLXB9/ETV6 proteins interact with the wild-type ETV6 through the *pointed* domain, thereby interfering with normal ETV6 function (Beverloo, 2001).

4.3.5. Ectopic and aberrant expression of a proto-oncogene gene

A number of *ETV6* translocations including the *ETV6-MDS1/EVI1* and the *ETV6-CDX2* fusion only contain the transcription/translation start of *ETV6* (Peeters, 1997; Chase, 1999). In these cases ectopic expression of the transcription factors *EVI1* and *CDX2* was detected in addition to the expression of the fusion gene.

The potential importance of the ectopic expression of a proto-oncogene in this class of *ETV6* fusions was further underlined by observations that the ectopic expression of the proto-oncogene also occurred when the fusion gene itself was not translated into a protein product: an example for this is the ectopic expression of the ParaHox gene GSH2 in patients with t(4;12) positive leukemia, even in cases, in which no protein expression of the CHIC2-ETV6 fusion generated by the chromosomal translocation, could be detected. Furthermore, expression of IL-3 was observed in a CML case with a t(5;12), lacking the *ETV6-ACS2* fusion protein. These results suggest that ectopic expression of *GSH2* and *IL-3* could be the key leukemogenic mechanism in these leukemias (Cools, 2002).
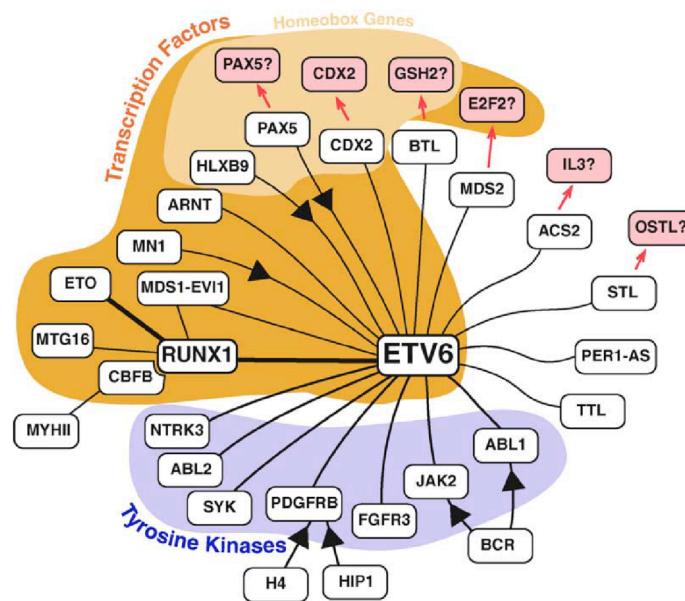
Figure 4.9: ETV6 fusion partner genes are represented in a network and sub-grouped in clusters with regard to their functional similarity. Transcription factors and the sub-class of homeobox genes, tyrosine kinases and others ETV6 fusion partners with unclear function (adapted from Bohlander, 2005).

There are some ETV6 fusion genes, such as *MDS2* and *STL* which are predicted to code for small proteins with no significant homology to any protein in the database. It is therefore very likely, in these cases, that upregulation of a neighboring gene (like *ID3*, *E2F2* or *RPL11* in the case of *MDS*2; and *OSTL* in the case of *STL* gene) is critical in these cases (Bohlander, 2005).

4.4. The translocation t(6;12)(q23;p13) in a B-cell ALL cell line

The translocation t(6;12)(q23;p13) was described by Zhang and coworkers in 1993 in the precursor B-cell ALL cell line SUB-B2 established from the leukemic cells from a 5-year-old boy with common ALL. The analysis of the balanced t(6;12)(q23;p13) led to the identification of *ETV6/STL* fusion gene (Suto, 1997). The *ETV6/STL* fusion gene codes for the first 54 amino acids of *ETV6* and an additional 14 amino acids from the Six Twelve Leukemia (*STL*) gene. However, the four codons from the *STL* gene do not belong to a reading frame starting with an ATG. The reciprocal *STL/ETV6* fusions are not in frame (Figure 4.10 adapted from Suto, 1997). The presumptive STL protein does not exhibit any homology to other proteins in the databases. Interestingly, the anti-sense strand of the first exon of *STL* is used to another gene which is transcribed in opposite direction. This gene was named *OSTL* (Opposite STL) by us. It codes for a 307 amino acid protein with two RING finger domains linked by an IBR (In Between RING fingers) or DRIL (Double RING fingers) motif. The OSTL protein is highly conserved (98% identity to its mouse and 86% to its *Fugu* homolog). OSTL interacts with several proteins involved in apoptotic signaling (Fontanari Krause, 2003). This makes it very likely that the overexpression of the RING finger *OSTL* gene is the main pathogenic mechanism in this translocation.

A.

ETV6/STL

```
        ETV6 187↓488 STL
CTGCCTGCGCACCTGCACCAAATTATGATTGTATGTCCCAGAAATTCACTTAGAAGCTAA
L   P   A   H   L   H   Q   I   M   I   V   C   P   R   N   S   L   R   S   ***
            54                                                  68
```

B.

STL/ETV6-L

```
              THE-1 INSERT                          ↓188 ETV6
TAGGCGGAAGGGATTTGCCTTGTCTCAGATGAGACTTTGGACTGTGGACTTTTGAGCTTGCAGCCAATT
***A   E   G   I   C   L   V   S   D   E   T   L   D   C   G   L   L   S   L   Q   P   I
                                                              56
```

STL/ETV6-M

```
                STL 487↓188 ETV6
TGAAAAGGATATGAGAAATCGGATTTTACGACATGCTTGCAGCCAATT
***K   G   Y   E   K   S   D   F   T   T   C   L   Q   P   I
                                          56
```

STL/ETV6-S

```
                  STL 333↓188 ETV6
TAGTCTATGACATGCATCATATGTGTGAGCAATCACAGAAGCTTGCAGCCAATT
***S   M   T   C   I   I   C   V   S   N   H   R   S   L   Q   P   I
                                              56
```

Figure 4.10: A) Nucleotide sequence and putative amino acid sequence (continuation of *ETV6* reading frame) of *ETV6/STL* fusion. **B)** Nucleotide sequence and putative amino acid sequence (5' continuation of *ETV*6 reading frame) of the three variant *STL/ETV6* fusions. Note that only *STL/ETV6* has an in frame start codon 5' of the *ETV6* reading frame (double-underlined). **C)** Diagram of ETV6, ETV6/STL, and STL/ETV6 proteins (Suto, 1997).

4.5. RING finger family of proteins

Freemont and coworkers in 1991 have first described a third class of zinc finger family in the *RING1* gene. The really interesting new gene (RING) is described as containing a cysteine-rich motif. The structure of this RING domain revealed that it did not assemble classical zinc fingers, but utilized its Cys/His residues to bind two zinc atoms in a unique cross-brace fashion, where the first and third pair of metal ligating residues binds the first zinc and the second and fourth pair binds the second zinc (Figure 4.11). The RING domain is thought to provide interfaces for protein interactions (Freemont, 1993; Schmeichel & Beckerle, 1994; Schwabe & Klug, 1994; Saurin, 1996; Dawid, 1998).

RING finger proteins may have either cytoplasmic or nuclear functions and are implicated in various processes such as cell lineage determination, oncogenesis, and embryogenesis (Freemont, 1993; Schwabe & Klug, 1994; Saurin, 1996; Dawid, 1998). The RING domain from KAP-1 is necessary for high-order oligomerization allowing KAP-1 to associate with the KRAB domain of KOX-1, thereby mediating transcriptional repression (Peng, 2000). The RING domains of PML and the viral protein Z directly bind eIF4E and alter its affinity for the 5' cap of mRNA. Thereby altering the mRNA transport and translational functions of eIF4E (Kentsis, 2001; Cohen, 2001). Finally, many RING domains function as E3 ubiquitin protein ligases in the ubiquitin conjugation pathway where they catalyze the transfer of an activated ubiquitin from an E2 ubiquitin conjugating enzyme to an intended substrate (Joazeiro, 2000; Fang, 2003).
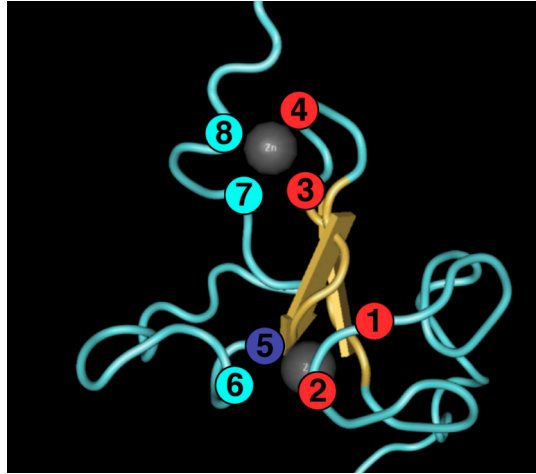
Figure 4.11: PHD (Plant Homeo Domain) finger of KAP-1, which has a similar structure as a RING finger. A three dimensional cross brace system, represented by seven cysteines and a histidine (#5), which are able to coordinate two zinc atoms (modified from Capili, 2001).

In 1999, Tyers and Willems after the biochemical characterization of the Skp1-Cdc53/CUL1-F-box (SCF) and anaphase promoting complex (APC) ubiquitination complex suggested that RING fingers play a central role in the combinatorial set of protein interactions that determine substrate specificity in the ubiquitin pathway. This pathway targets protein for degradation through the 26S proteasome (Hershko & Ciechanover, 1998; Weissman, 2001). Ubiquitination can quantitatively regulate substrates such as cyclins, transcription factors, hormone nuclear receptors, and oncoproteins. Four types of enzymes are known to mediate ubiquitination: an ubiquitin-activating enzyme (E1 or Uba), an ubiquitin-conjugating enzyme (E2 or Ubc), an ubiquitin ligase (E3 or Ubr) (Hershko & Ciechanover, 1998; Weissman, 2001), and a polyubiquitin ligase (E4) (Koegl, 1999). Ubiquitin conjugation occurs through the sequential action of these enzymes; first the E1 activates and forms a high-energy thioester bond with ubiquitin. Ubiquitin is then passed to the E2 by transthiolation and the E2, usually in cooperation with E3, transfers ubiquitin to a lysine side chain of the substrate. E3s specify the timing and substrate selection of ubiquitination reactions (Figure 4.12, adapted from Hicke & Dunn, 2003).
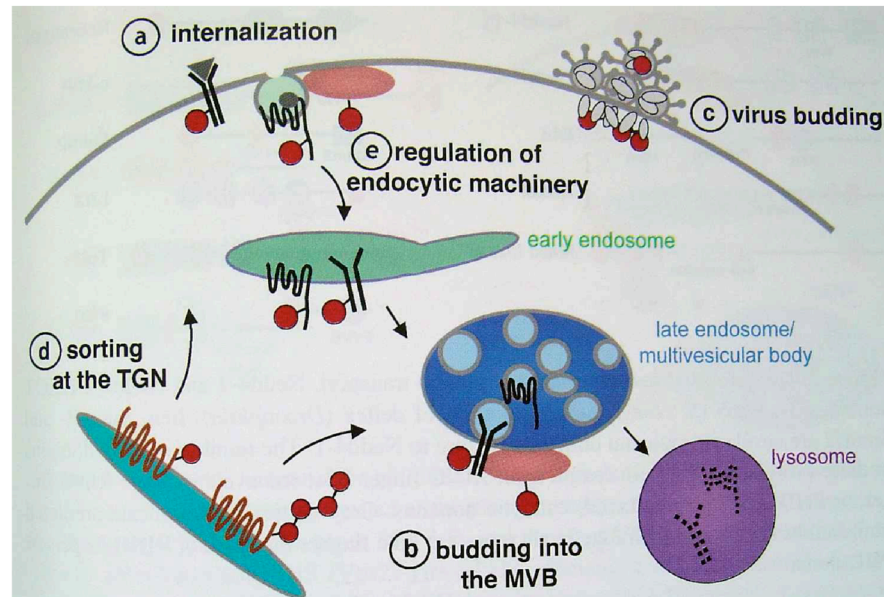
Figure 4.12: Regulation of protein transport by ubiquitin signals. a) Monoubiquitin and Lys63-linked di-ubiquitin chains serve as regulated internalization signals that can be appended to a plasma membrane protein to trigger entry into primary endocytic vesicles budding from the plasma membrane. **b)** Monoubiquitin serves as a signal for the entry of transmembrane proteins into MVB (multivesicular body) vesicles. **c)** Ubiquitin, ubiquitin-binding proteins, and ubiquitin ligases are important for the budding of envelop viruses. **d)** (Poly)ubiquitination regulates the sorting of proteins at the *trans*-Golgi network to the lysosome/vacuole. **e)** Ubiquitin modifies and regulates components of the endocytic machinery.

RING fingers are often found in conjunction with other cysteine-rich domains (Saurin, 1996). In the RING finger B-box coiled coil (RBCC) proteins, the RING fingers are linked to a specific cysteine-rich zinc-binding motif (B-Box) and a coiled coil domain (Reddy, 1992). Interstingly, the three RBCC proteins PML, TIF1, and Rfp were all identified as oncogenic products that are disrupted by chromosomal translocations (Saurin, 1996).

In 1999, van der Reijden and coworkes identified a novel conserved cysteine-rich motif called DRIL (for Double RING finger linked). Two RING fingers and DRIL (TRIAD) motifs defined the conserved tripartite motif.

The DRIL pattern differs from the consensus of the RING finger patterns with respect to the histidine location and the absence of length-variation in the C-terminal loop (Figure 4.13).

Recently, Capili and coworkers described in the human homologue of the *Drosophila Ariadne* (HHARI) protein a novel zinc-binding domain called RING2, which is related to the C-terminal RING of the protein family RING-IBR-RING (or TRIAD). Unlike classical RINGs, RING2 binds only a single zinc atom (Figure 4.14, adapted from Capili, 2004) and some conserved residues and metal binding ligands are charged.

C-x₂-   C-x₍₁₇₋₁₉₎-**H**-x₂-   C-x₂-   C-x₂-C-x₍₁₆₋₂₀₎-**H**-x₂-C   LIM pattern

C-x₂-   C-x₍₉₋₃₉₎- C-x₍₁₋₃₎-**H**-x₍₂₋₃₎-C-x₂-C-x₍₄₋₄₈₎- C-x₂-C   RING finger pattern

C-x₍₁₋₂₎-C-x₍₉₋₂₁₎- C-x₍₂₋₄₎-C-x₍₄₋₅₎-**H**-x₂-C-x₍₁₂₋₄₆₎- C-x₂-C   LAP/PHD pattern

C-x₄-   C-x₍₁₄₋₃₀₎-C-x₍₁₋₄₎-C-x₄-   C-x₂-C-x₄-   **H**-x₄-C   DRIL pattern

Figure 4.13: DRIL pattern consists of seven regularly spaced cysteine and one histidine residues and closely resembles the LAP/PHD (Leukemia-Associated Protein/Plant Homeo Domain), LIM (for the proteins in which it was first discovered: Lin11, Isl1, and Mec3), and RING finger patterns. C = cysteine, H = histidine (bold), x = any amino acid.

A)
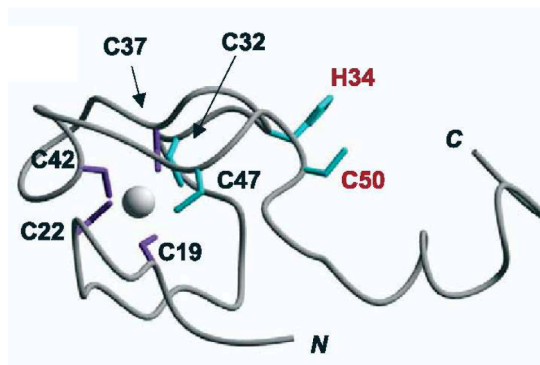
B)

Figure 4.14: A) RING2 structure. **B)** Sequence of HHARI RING2 showing the residues used to bind the zinc atom (Capili, 2005).

4.6. Aim of this work

Reciprocal translocations affecting band 12p13 are found as recurring chromosomal changes in myeloid and lymphoid malignancies. *ETV6* is involved in most of these balanced 12p13 translocations. The t(6;12)(q23;p13) translocation results in the fusion of *ETV6* with *STL* in a childhood B-cell ALL. Since the *ETV6/STL* fusion gene encodes only for a small protein, which lacks any know functional domain and has no homology to other proteins, we hypothesize that the main leukemogenic effect of this translocation is the deregulation of *OSTL*. The aim of this project was the characterization of the *OSTL* gene. For this we have sequenced the whole mouse and human cDNA and looked for the expression pattern of this gene in normal tissues, normal and malignant cell lines and patient samples. To be able to define the role of *OSTL* in the cells we searched and identified the protein-interaction partners of OSTL. Finally, to analyze the role of *Ostl* in leukemogenesis and assay whether ectopic expression of this gene can lead to the development of ALL leukemia, we established a mouse model where *Ostl* was overexpressed in bone marrow cells.

5. Materials and Methods

5.1. List of abbreviations and glossary

AA = aa	Amino acids
Ab	Antibody
AD	Activation Domain
AH 109	Yeast strain
APC	Allophycocyanin
Aqua bidest.	Water double deionized filtered trough Millipore filters
Aqua dest.	Water, deionized
BD	Binding Domain
BM	Bone Marrow
bp	Base pair(s)
BSA	Bovine Serum Albumin
C	Cysteine
°C	Degree Celsius
cDNA	Complementary DNA, synthetic DNA transcribed from a specific RNA through the action of the reverse transcriptase
cfu	Colony forming units
Cys = C	Cysteine
dCTP	Deoxycytosine triphosphate
DEPC	Diethyl pyrocarbonate
dGTP	Deoxyguanosine triphosphate
DMEM	Dulbecco's Modified Eagle Medium
DMF	Dimethylformamide
DMSO	Dimethylsulfoxide
DNA	Deoxyribonucleic acid
dNTP	Deoxynucleotide triphosphate
dTTP	Deoxythymidine triphosphate
DTT	Dithiothreitol
ECFP	Enhanced Cyan Fluorescent Protein

EDTA	Ethylenediaminetetraacetic acid
EGFP	Enhanced Green Fluorescent Protein
EtBr	Ethidium bromide
EtOH	Ethanol
EYFP	Enhanced yellow fluorescent protein
FBS	Fetal bovine serum
FCS	Fetal calf serum
G	Gram
G	Relative centrifugal acceleration
G	Glycine
Gal	Galactose
GAL1	Yeast promoter
Gal4	Yeast transcription factor
Glc	Glucose = dextrose
Gly = G	Glycine
GST	Glutathione S-transferase
H	Hour(s)
HEPES	N-(2-Hydroxythyl) piperazine-N'-2-ethan sulphuric acid
His = H	Histidine
HRP	Horse Radish Peroxidase
IBR	In Between RING fingers
Ile = I	Isoleucine
IPTG	Isopropyl-β-D-thio-galactopyranoside
KAc	Potassium acetate
kb	Kilobase(s)
KCl	Potassium chloride
kDa	Kilodalton
KH_2PO_4	Potassium dihydrogenphosphate
L	Liter
LB	Luria-Bertani bacterial medium
Leu = L	Leucine
LiAc	Lithium acetate

Lys = K	Lysine HCl
m	Meter
M	Molar
MCS	Multiple Cloning Site
MCSV	Murine Stem Cell Virus
Met = M	Methionine
μg	Microgram
$MgCl_2$	Magnesium chloride
$MgSO_4$	Magnesium sulfate
mIL-3	Mouse Interleukine-3
mIL-6	Mouse Interleukine-6
min	Minute(s)
mix	Mixture
ml	Milliliter
μl	Microliter
mM	Milimolar
μM	Micromolar
μm	Micrometer
MOPS	3-N-Morpholine-propanesulfonic acid
mRNA	Messenger RNA
M-SCF	Recombinant Murine Stem Cell Factor
msec	Mili seconds
MW	Molecular weight
NaAc	Sodium acetate
ng	Nanogram
NaH_2PO_4	Sodium dihydrogenphosphate
Na_2HPO_4	Disodium hydrogenphosphate
$(NH_4)_2SO_4$	Ammonium sulfate
nt	Nucleotide
N_2	Nitrogen
OD	Optical density
O/N	Overnight

ORF	Open reading frame
PAGE	Polyacrylamide gel electrophoresis
PBS	Phosphate buffered saline
PCR	Polymerase chain reaction
PE	Phycoerythrin
PEG	Polyethylene glycol
Pen/Strep	Penicillin/Streptomycin
pg	Picogram
Phe = F	Phenylalanine
PMSF	Phenylmethylsulfonyl fluoride
R	Adenine hemisulfate or Arginine HCl
rh	Recombinant human
RING1	Really Interesting Protein 1
RING2	Really Interesting Protein 2
rm	Recombinant mouse
RNase	Ribonuclease
RNA	Ribonucleic acid
RPMI	Roswell Park Memorial Institute culture medium
rRNA	Ribosomal RNA
RT	Room temperature
RT	Reverse transcription, or reverse transcriptase
RT-PCR	Method for amplifying cDNA from an RNA template
SD	Synthetic defined Dropout medium
SDS	Sodium dodecyl sulfate
sec	Second(s)
SSC	Saline-sodium citrate buffer
Taq	Thermus aquaticus (-Polymerase)
TBS	Tris-buffered saline
TE	Tris-EDTA buffer
TEMED	N,N,N',N'-Tetramethylethylendiamine
Thr = T	Threonine
Trp = W	Tryptophan

Tris	Trishydroxyaminomethan
tRNA	Transfer RNA
Tyr = Y	Tyrosine
u	Unit
U	Uracil
UV	Ultraviolet light
Val = V	Valine
Vector	Plasmid or phage chromosome used to carry cloned DNA segment
vol	Volume
v/v	Volume:volume ratio
WB	Western Blot
w/v	Weight:volume ratio
X-gal	5-bromo-4-chloro-3-indolyl-β-D-galactopyranoside
YPD	Yeast extract, peptone, dextrose

5.2. Materials

5.2.1. Chemicals, kits and materials

1-kb-DNA molecular weight marker	Life Technologies, Eggenstein, Germany
1.5 ml microcentrifuge tube	Eppendorf, Hamburg, Germany
15 ml polypropylene conical tubes	Becton Dickinson, Meylan, France
50 ml polypropylene conical tubes	Becton Dickinson, Meylan, France
Acetic acid	Merck, Darmstad, Germany
Acrylamide/Bis solution	Carl Roth, Karlsruhe, Germany
Agar	Carl Roth, Karlsruhe, Germany
Agarose	ICN Biomedicals Inc.
Amino acids (yeast two hybrid)	Sigma, Deisenhofen, Germany
Ammonium Chloride solution	CellSystems®, Vancouver, Canada
Ampicillin	Pan Biotech, Aidenbach, Germany
Amplify Fluorographic Reagent	Amersham, UK

Ampuwa® H_2O	Fresenius, Bad Homburg, Germany
Aprotinine	Sigma, Deisenhofen, Germany
Aqua bidest.	Millipore, Eschborn, Germany
BigDye™ terminator cycle sequencing v2.0	Applied Biosystems, Foster City, CA
Blocking reagent	Roche diagnostics – Boehringer, Germany
β-Mercaptoethanol	Sigma, Deisenhofen, Germany
Boehringer BM purple Ap substrate	Boehringer, Germany
Boric acid	Carl Roth, Karlsruhe, Germany
Bromophenol blue	Carl Roth, Karlsruhe, Germany
Bovine serum albumine	Life Technologies, Eggenstein, Germany
Cell culture medium DMEM	Pan Biotech, Aidenbach, Germany
Cell culture medium RPMI	Pan Biotech, Aidenbach, Germany
Chloroform	Sigma, Deisenhofen, Germany
Citric acid	Merck, Darmstadt, Germany
Coomassie® stain solution	BioRad, Hercules, CA
Cryotube™ vials	Nalge Nunc Internacional, Denmark
Deoxyribonuclease I, Amplification Grade	Life Technologies, Eggenstein, Germany
DEPC	Carl Roth, Karlsruhe, Germany
Dig antibody AP coupled	Boehringer, Germany
Dimethylsulfoxide (DMSF)	Carl Roth, Karlsruhe, Germany
DMF	Carl Roth, Karlsruhe, Germany
DMSO	Sigma, Deisenhofen, Germany
DNA Ligase buffer 10X	NewEngland Biolabs, Schwalbach, Germany
DNA polymerases (Taq, T4, Klenow)	MBI Fermentas, St. Leon-Rot, Germany
dNTP Set, PCR Grade	Life Technologies, Eggenstein, Germany
ECL™ Western Blot Detection reagents	Amersham, Braunschweig, Germany
EDTA	Carl Roth, Karlsruhe, Germany
Electroporation cuvettes	PeqLab, Erlangen, Germany
Eppendorf tubes	Eppendorf, Germany
Ethanol	Merck, Darmstadt, Germany
Ethidium bromide	Carl Roth, Karlsruhe, Germany
Falcon® 14 Polystrene round-bottom tube	Becton Dickinson, Meylan, France

Fetal Bovine Serum	Gibco, Life Technologies, Paisley, Scotland
Filter 0.22μm	Millipore, Belford, USA
Filterpaper (Gel-blotting-paper)	Schleicher & Schuell, Dassel, Germany
Fetal calf serum (FCS)	Life Technologies, Eggenstein, Germany
5-Fluorouracil	Medac
Formaldehyde 37%	Carl Roth, Karlsruhe, Germany
Formamide	Carl Roth, Karlsruhe, Germany
Genomed Plasmid Mega Kit	Genomed, St. Louis, USA
Giemsa, solution	Merck, Darmstadt, Germany
Glass beads (425-600 μ #G8772)	Sigma, Deisenhofen, Germany
Glutathione-Agarose (#G 4510)	Sigma, Deisenhofen, Germany
Gluthathione Sepharose™ 4B	Pharmacia Biotech, Freiburg, Germany
Glycerol	Carl Roth, Karlsruhe, Germany
Glycin	Merck, Darmstadt, Germany
Heparin	Sigma, Deisenhofen, Germany
HEPES	Sigma, Deisenhofen, Germany
Hybond™-P PVDF transfer membrane 0.45 μm	Amersham, Buckinghamshire, UK
Hydrochloridric acid 37%	Merck, Darmstadt, Germany
Hypercassete 18x24 cm	Amersham, Buckinghamshire, UK
Hyperfilm™ ECL chemiluminescence reagent	Amersham, Buckinghamshire, UK
Hyperfilm™ ECL high performance	Amersham, Buckinghamshire, UK
IPTG	Roche Molecular Biochemicals Mannheim
Isopropanol	Carl Roth, Karlsruhe, Germany
Kanamycin	Pan Biotech, Aidenbach, Germany
Klenow Fragment	MBI Fermentas, St. Leon-Rot, Germany
Lab-Tek II chambered coverglass w/cover	Nalge Nunc International, Naperville, USA
Leupeptine	Sigma, Deisenhofen, Germany
Levamisole	Sigma, Deisenhofen, Germany
Lithium acetate	Sigma, Deisenhofen, Germany
L-glutamine (cell culture)	Pan Biotech, Aidenbach, Germany
May-Grunwald's eosin-methylene blue solution	Merck, Darmstadt, Germany
Megaprime™ DNA labeling system	Pharmacia Biotech, Freiburg, Germany
Methanol	Merck, Darmstadt, Germany

Methocult™ GF M3434	CellSystems®, Vancouver, Canada
Methylene blue	Merck, Darmstadt, Germany
Microspin S-400 HR columns	Amersham, UK
mIL-3	Tebu-bio, USA
mIL-6	Tebu-bio, USA
Milk powder	Carl Roth, Karlsruhe, Germany
MOPS	Life Technologies, Eggenstein, Germany
M-SCF	Tebu-bio, USA
Nescofilm sealing film	Carl Roth, Karlsruhe, Germany
Nitrocellulose membrane (Hybond)	Amersham, UK
Oligo (dT)$_{12\text{-}18}$ Primer	Life Technologies, Eggenstein, Germany
Paraformaldehyde	Carl Roth, Karlsruhe, Germany
PBS	Pan Biotech, Aidenbach, Germany
Penicillin/Streptomycin	Pan Biotech, Aidenbach, Germany
Pepstatine	Sigma, Deisenhofen, Germany
Pepton, meat pancreatic digested	Merck, Darmstadt, Germany
Pipette tips	Carl Roth, Karlsruhe, Germany
Polyethylenglycol (PEG) 4000	Merck, Darmstadt, Germany
Phenol	Sigma, Deisenhofen, Germany
Phenol/Chloroform	Life Technologies, Eggenstein, Germany
Plastic cuvettes for OD	Carl Roth, Karlsruhe, Germany
Plastic material for cell culture	Greiner Labortechnik, Frickenhausen, Germany
"	Sarstedt, Nümbrecht, Germany
"	Corning, USA
Platinum® *Taq* DNA Polymerase	Life Technologies, Eggenstein, Germany
"	NewEngland Biolabs, Schwalbach, Germany
"	Pan Biotech, Aidenbach, Germany
PolyFect transfection reagent	Qiagen, Hilden, Germany
Propidium iodide	Calbiochem, San Diego, USA

Protamine sulfate	Sigma, Deisenhofen, Germany
Proteinase inhibitor cocktail	Sigma, Deisenhofen, Germany
Protein Agarose-G beads	Roche Molecular Biochemicals Mannheim
Proteinase K	Gibco, Life Technologies, Paisley, Scotland
Qiagen® Plasmid Midi Kit	Qiagen, Hilden, Germany
Qiagen® Plasmid Maxi Kit	Qiagen, Hilden, Germany
Qiagen® Plasmid MaxiEndofree Kit	Qiagen, Hilden, Germany
Qiagen RNEasy Mini Kit	Qiagen, Hilden, Germany
Qiashredder™ columns	Qiagen, Hilden, Germany
Restriction enzymes	MBI Fermentas, Germany
"	NewEngland Biolabs, Schwalbach, Germany
"	
Ribonuclease A	MBI Fermentas or Sigma, Germany
RNase Away	Carl Roth, Karlsruhe, Germany
Rneasy™ mini kit	Qiagen, Hilden, Germany
RothFect transfection reagent	Carl Roth, Karlsruhe, Germany
SDS	Carl Roth, Karlsruhe, Germany
SeeBlue® Plus2 pre-stained standard	Life Technologies, Eggenstein, Germany
Shrimp alkaline Phosphatase	MBI Fermentas, St. Leon-Rot, Germany
SOC medium	Sigma, Deisenhofen, Germany
Sodium acetate	Sigma, Deisenhofen, Germany
Sodium chloride	Merck, Darmstadt, Germany
Sodium citrate	Carl Roth, Karlsruhe-, Germany
Sodium hydroxide	Merck, Darmstadt, Germany
SuperScript™ II RNase H⁻ Reverse Transcriptase	Life Technologies, Eggenstein
Surgical blade	Feather Safety Razor Co. Med. Div., Japan
Syringe 10 ml	Braun, Melsungen, Germany
Syringe Driven Filter Unit Millex-GP 0.22 μm	Millipore, Carrigtwohill, Ireland
Syringe Driven Filter Unit Millex-HV 0.45 μm	Millipore, Carrigtwohill, Ireland
Syringe Driven Filter Unit Millex-LG 0.20 μm	Millipore, Japan

T4 DNA Ligase	NewEngland Biolabs, Schwalbach, Germany
T4 DNA Ligase	Life Technologies, Eggenstein, Germany
T4 DNA Ligase Buffer	NewEngland Biolabs, Schwalbach, Germany
"	Life Technologies, Eggenstein, Germany
T4 DNA Polymerase	NewEngland Biolabs, Schwalbach, Germany
TEMED	Carl Roth, Karlsruhe, Germany
Tris	Carl Roth, Karlsruhe, Germany
Triton X-100	Carl Roth, Karlsruhe, Germany
Trypan blue	Life Technologies, Eggenstein, Germany
Trypsin-EDTA solution	Biochrom AG, Berlin, Germany
Tween® 20	Carl Roth, Karlsruhe, Germany
Vektashield® mounting medium	Vector laboratories, Burlingame, CA
Yeast extract	Sigma, Deisenhofen, Germany
Yeast nitrogen base without aa	Difco, Detroit MI, USA
X - gal	Clontech, Heidelberg, Germany

5.2.2. Bacterial strains (*E. coli*)

BL21	Clontech, Heildelberg, Germany
XL1-Blue	Clontech, Heildelberg, Germany

5.2.3. Yeast strains (*S. cerevisiae*)

<u>CG 1945</u>:

MATa, ura3-52, his3-200, ade2-101, lys2-801, trp1-901, leu2-3, 112, gal4-542, gal80-538, cyh^{r}2, LYS2::GAL1$_{UAS}$-GAL1$_{TATA}$-HIS3, URA3::GAL4$_{17-mers(x3)}$-CYC1$_{TATA}$-lacZ (Clontech, Palo Alto, USA); Feilotter et al., 1994.

<u>AH 109</u>:

MATa, trp1-901, leu2-3, 112, ura3-52, his3-200, gal4Δ, gal80Δ, LYS2::GAL1$_{UAS}$-GAL1$_{TATA}$-HIS3, GAL2$_{UAS}$-GAL2$_{TATA}$-ADE2, URA3::MEL1$_{UAS}$-MEL1$_{TATA}$-lacZ (Clontech, Palo Alto, USA); James et al., 1996.

5.2.4. Murine cell lines

GP$^+$E86:

Mouse fibroblast cell line

NIH3T3:

Swiss mouse embryo fibroblast cell;

Aaronson et al., 1968; Jainchill et al., 1969; Copeland et al.,1979.

5.2.5. Human cell lines

DOHH2:

Mature EBV$^-$ B cell derived from follicular B-NHL

(provided by Dr. Martin Dreyling, GSF-CCG-Leukemia, Grosshadern, Munich);

Kluin-Nelemans et al., 1991.

Granta 519:

Mature EBV$^+$ B-cell line derived from B-NHL

(provided by Dr. Martin Dreyling, GSF-CCG-Leukemia, Grosshadern, Munich);

Rudolph et al., 2004; Jadayel et al.,1997.

HBL2:

Mature EBV$^-$ B cell line derived from B-NHL

(provided by Dr. Martin Dreyling, GSF-CCG-Leukemia, Grosshadern, Munich).

HBL4:

B-NHL EBV$^+$

(provided by Dr. Martin Dreyling, GSF-CCG-Leukemia, Grosshadern, Munich).

HEK293 T:

Human embryonal kidney cell line;

Graham et al., 1977.

Karpas 422:

Mature B cell line derived from B-NHL

(provided by Dr. Martin Dreyling, GSF-CCG-Leukemia, Grosshadern, Munich).

Dyer et al., 1990.

LCL B:

Lymphoblastoid transformed cell

(provided by Dr. Martin Schlee, GSF, Grosshadern, Munich).

LCL D:

Lymphoblastoid transformed cell

(provided by Dr. Martin Schlee, GSF, Grosshadern, Munich).

LCL R:

Lymphoblastoid transformed cell

(provided by Dr. Martin Schlee, GSF, Grosshadern, Munich).

Nalm 6:

Precursor B cell of type B-III;

Hurwitz et al., 1979.

NCEB-1:

Mature EBV$^+$ B cell derived from B-NHL

(provided by Dr. Martin Dreyling, GSF-CCG-Leukemia, Grosshadern, Munich);

Saltman et al., 1988.

SEM:

Precursor B cell of type B-I

(provided by Dr. Georg Bornkamm, GSF, Grosshadern, Munich)

Greil et al., 1994; Reichel et al., 1998.

Wsu-NHL:

Mature EBV⁻ B cell line derived from follicular B-NHL

(provided by Dr. Martin Dreyling, GSF-CCG-Leukemia, Grosshadern, Munich);

Mohamed et al., 1988.

5.2.6. Mice

Parental strain mice, for the bone marrow assays, and for the whole mount *in situ* hybridization assays (BALB/c mice) were bred and maintained at the GSF-Grosshadern, animal facility. Donors of primary BM cells were > 12-week-old (C57Bl/6Ly-Peb3b x C3H/HeJ) F1 (PebC3) mice and recipients were > 8 week old (C57Bl/6J x C3H/HeJ) F1 (B6C3) mice.

5.2.7. Antibodies

The following antibodies were used for Western blot analysis and for flow cytometry:

Anti-green fluorescent protein, rabbit IgG fraction (Molecular probes)

Anti-HAX1, clone 52, mouse IgG1 (Clontech)

Anti-SIVA, clone C-20, goat polyclonal IgG (Santa Cruz)

B220, clone RA3-6B2, APC labeled (BD Pharmingen)

CD4, clone GK1.5, PE labeled (BD Pharmingen)

CD8, clone 53-6.7, APC labeled (BD Pharmingen)

c-kit, clone 2B8, APC labeled (BD Pharmingen)

c-myc, mouse monoclonal IgG1 (Clontech)

Donkey anti-rabbit IgG-HRP (Santa Cruz)

Donkey anti-goat IgG-HRP (Santa Cruz)

Donkey anti-mouse IgG-HRP (Santa Cruz)

Gr-1, clone RB6-8C5, PE labeled (BD Pharmingen)

HA-tag, rabbit Ig polyclonal antibody (Clontech)

Mac-1 (CD11b), clone M1/70, APC labeled (BD Pharmingen)

Sca-1, clone D7, PE labeled (BD Pharmingen)

Ter119, PE labeled (BD Pharmingen)

5.2.8. Plasmids

The following mammalian expression plasmids pECFP/GFP/YFP, pcDNA6/V5-His A, and MCSV (MIG) were used for mouse cell transfections; the prokaryotic expression pGEX 4T-2 vector was used to produce GST-fusion proteins; the pGEMT-easy was used to subclone PCR product; and the yeast shuttle plasmids pGBT9, pGBKT7 and pGADT7 were used in the yeast two hybrid screen.

5.2.8.1. Mammalian expression plasmids

pECFP/pEGFP/pEYFP-C1:

pECFP/GFP/YFP vectors are used to generate fusion proteins for expression and localization studies. A gene of interest inserted into the MCS of these vectors will be expressed as a fusion to the C-terminus of the enhanced fluorescent protein (Cyane, Green or Yellow). The vectors carry a Kanamycin resistance gene for selection in bacteria (Clontech, Heidelberg).

pcDNA6/V5-His A:

The pcDNA6/V5-His A is used to express proteins with a V5 or HIS tag (Invitrogen).

MSCV (MIG):

For retroviral gene transfer into primary BM cells, the gene of interested was subcloned into the multiple cloning site of the modified murine stem cell virus (MSCV) 2.1 vector (Pineault et al., 2003) upstream of the internal ribosome entry site (IRES) and the enhanced GFP.

5.2.8.2. Prokaryotic expression plasmids

pGEX-4T2:

This vector was used for inducible, high-level intracellular expression of genes as fusion with Schistosoma japonicum glutathione S-transferase (GST) under the control of a *tac* promoter (inducible with IPTG 1-5mM). The vector includes an internal *lac* I^q gene for use in any *E.coli* host and a coding region for factor Xa protease recognition site for cleaving the protein of interest from the GST protein (Pharmacia Biotech).

5.2.8.3. T-vector

pGEM®-T easy:

The pGEM-T easy vector is used for the cloning of PCR products. It is provided ready for ligation with PCR products from the company. The vector contains T7 and SP6 RNA polymerase promoters flanking a multiple cloning region within the α-peptide coding region of the enzyme β-galactosidase (Promega, Madison, USA).

5.2.8.4. Yeast two hybrid expression plasmids

5.2.8.4.1. Bait-expression plasmids

pGBT9:

The vector pGBT9 is used for the expression of proteins of interest as fusions with the GAL4 DNA-BD. The vector has the TRP1 gene for selection for tryptophan autotrophy in yeast and a beta-lactamase gene for selection with Ampicillin in bacteria (Clontech, Palo Alto, USA).

PGBKT7:

The vector pGBKT7 is used for the expression of proteins of interest as fusions with the GAL4 DNA-BD. The vector has the TRP1 gene for selection for tryptophan autotrophy in yeast and a beta-lactamase gene for selection with kanamycin in bacteria.

It contains a c-Myc epitope that facilitates further in vitro assays, such as coimmunoprecipitation to confirm the interactions in yeast two hybrid system (Clontech, Palo Alto, USA).

5.2.8.4.2. Prey-expression plasmids

pGAD-GH:

The vector pGAD-GH is used for the expression of library (prey) proteins as fusion with the GAL4 DNA-AD. The vector has the LEU2 gene for selection for leucine autotrophy in yeast and a beta-lactamase gene for selection with Ampicillin in bacteria (Clontech, Palo Alto, USA).

PGADT7:

The vector pGADT7 is used for the expression of library (prey) proteins as fusion with the GAL4 DNA-AD. The vector has the LEU2 gene for selection for leucine autothrophy in yeast and a beta-lactamase gene for selection with Ampicillin in bacteria. It contains a HA epitope

that facilitates further in vitro assays, such as coimmunoprecipitation to confirm the interactions in yeast two hybrid system (Clontech, Palo Alto, USA).

5.2.8.5. Packaging plasmid

Ecopac:

The Ecopac is a packaging vector coding for the gag, pol, and env viral proteins. In this work it was used for transfection of HEK293T cells.

5.2.9. Primers

Oligonucleotides used for DNA amplification and sequence analysis (Table 2.1) were designed using the software program MacVector ™ 7.0 and were purchased from Metabion GmbH (Martinsried, München).

Table 5.1: Oligonucleotides used in the project

Oligoname	Sequence	Nucleotide position in cDNA sequence•	Ann °C
OSTLEx1dATGXhoI	5'-CTACCTCGAGAGATGAAGGTACAACTTGGCC-3'	(235-246) Exon 1d	55
OSTL58TxhoI	5'-CTACCTCGAGATATGCCCAGCCTGTTGGGAGC-3'	(58-77) Exon 1d	55
OSTLE06205T	5'-GAGTGCCTCAAAGTCTACCTG-3'	(205-225) Exon 1	55
OSTL983BpstI	5'-CATACTGCAGTGTTACCAGTGCATACCTGTCCG-3'	(983-961) Exon 6	55
hGAPDHT	5'-GCACCACCAACTGCTTAGCACC-3'	(530-551) Exon 7	56
hGAPDHB	5'-GTCTGAGTGTGGCAGGGACTC-3'	(1166-1146) Exon 9	56
mGAPDHT	5'-CATCACCATCTTCCAGGAGC-3'	(271-291)	60
mGAPDHB	5'-ATGACGTTGCCCACAGCCTT-3'	(714-695)	60
pEGFP-C11240	5'-AAAGACCCCAACGAGAAGC-3'	(1240-1258)	55
pGEX5'	5'-GGGCTGGCAAGCCACGTTTGGTG-3'	Seq primer	55
Seqf464OSTL	5'-CAAAATCCAGTGCCCTACC-3'	(464-482) Exon 3	55
M13/pUCRevSeqP	5'-AGCGGATAACAATTTCACACAGG-3'	Seq primer	55
J16-183T	5'-CTGCTCCGTGTACTGCGTGG-3'	(78-97) Exon 1d	55
J16-251T	5'-AGTCCCCACCTCAAGCAC-3'	(146-163) Exon 1d	55
G01-M13-295F	5'-AGTCTAAAAGGGAGTGGGC-3'	(295-568) Exon 2	55
OSTL1431B	5'-CTCTTATCTTCTGAAAAGTGGC-3'	(1431-1410) Exon 6	55
G01-295-468	5'-CAATCCAAGAAGGAGAAG-3'	(295-4680 Exon 2	55
OSTL281B	5'-AAAACACTCTGTGATGGGG-3'	(282-264) Exon 2	55
J16c-979T	5'-GACCACACATCAAACCTCAG-3'	(979-998) Exon 4	55
J16T7-256T	5'-TCCTTACATAGACGGACCAG-3'	(256-275) Exon 1d	55
J16-(390-414)	5'-CCATGAGGACTCTATCAAGTATAAG-3'	(557-582) Exon 2	55
Y2H1	5'-TCATCGGAAGAGAGTAG-3'	(1155-1171)	55
T7	5'-GTAATACGACTCACTATAGGGC-3'	Seq primer	55
T3	5'-AATTAACCCTCACTAAAGGG-3'	Seq primer	55

Oligoname	Sequence	Nucleotide position in cDNA sequence*	Ann °C
SP6	5'-AGGTGACACTATAGAATAC-3'	Seq primer	55
J16-836TEcoRI	5'-CATAGAATTCGGCAGAGAAATGCCCAGAAG-3'	(836-855) Exon 3	55
J16-1218BXhoI	5'CAGCTCGAGTTACCAGTGCATACCTGT-3'-	(1218-1197) Exon 6	55
J16-982TEcoRI	5'-CATCGAATTCACACATCAAACCTCAGTAT-3'	(983-1001) Exon 4	55
OSTLj16T302XhoI	5'-CAGCTCGAGGCCTATTAGGGGCTCCACCC-3'	(302-321) Exon 1d	55
OSTLj16B1272XhoI	5'-CAGCTCGAGATCCTGCATGGCTCCTCCCG-3'	(1272-1253) Exon 6	55
OSTLJ16B1217XhoI	5'-CAGCTCGAGCCAGTGCATACCTGTCCG-3'	(1217-1198) Exon 6	55
mOSTLJ16364NcoI	5'-CAGCCATGGTGCTGATGTGCCGGGTG-3'	(364-384) Exon 1d	55
Y2H3'AD	5'-AGATGGTGCACGATGCACAG-3'	(2078-2046)	55
Y2H2-729-751	5'-CGTTTGGAATCACTACAGGGATG-3'	(729-751)	55
J16-838TNcoI	5'-CATACCATGGGCAGAGAAATGCCCAGAAG-3'	(838-855) Exon 3	55
J16-996BPstI	5'-CATACTGCAGGAGGTTTGATGTGTGGTC-3'	(996-978) Exon 4	55
J16-949TNcoI	5'-CATACCATGGATGTGGAGAGAGATACCGC-3'	(942-960) Exon 4	55
J16-295TNcoI	5'-CTATCCATGGCGTGCCTGGCCTATTAGGG-3'	(294-312) Exon 1d	55
J16ATG1dNcoI	5'-CTACCATGGTCAGGTACAACTTGGC-3'	(468-483) Exon 2	55
J16-605BpstI	5'-CATACTGCAGTGGCTTGGTGCTGGAGTC-3'	(624-607) Exon 2	55
J16-855BPstI	5'-CATCCTGCAGCTTCTGGGCATTTCTCTG-3'	(855-838) Exon 3	55
HAX162TEcoRI	5'-CAGGAATTCATGAGCCTCTTTGATCTCTT-3'	(162-181)	55
HAX976BEcoRI	5'-CAGGAATTCGGGACCGGAACCAACGTCCCA-3'	(996-976)	55
SIVA33TEcoRI	5'-CAGGAATTCGCGGCCATGCCCAAGCGGAG-3'	(32-51) Exon 1	55
SIVA562BXhoI	5'-CAGCTCGAGGGTCTCGAACATGGCACA-3'	(562-545) Exon 4	55
OSTLJ16T358EcoRI	5'-GACGAATTCCCCTCATGGTGCTGATG-3'	(359-375) Exon 1d	55
OSTLJ16T358BamHI	5'-GACGGATCCCCTCATGGTGCTGATG-3'	(359-375) Exon 1d	55
E06OSTL601T	5'-AGAGGAATGCCCAGAAGTGTCC-3'	(602-623) Exon 3	57
E06OSTL761B	5'-ACTGAGGTTTGATGTGTGGTCTCC-3'	(762-739) Exon 4	57
E06OSTL196T	5'-TGTGCGAGGAGTGCCTCAAAG-3'	(197-217) Exon 1d	57
E06OSTL381B	5'-TGGTGCTGGAATCAATACGGC-3'	(382-364) Exon 2	57
E06OSTL374T	5'-CAGCACCAAGCCATGTCCTC-3'	(375-394) Exon 2	57
E06OSTL501B	5'-AACACCAGACGAATTGGCAGG-3'	(502-482) Exon 3	57
E06OSTL734B	5'-AAATCGGAGCTGGCGGTATC-3'	(735-761) Exon 4	57
pMSCV-F	5'-CCCTTGAACCTCCTCGTTCGACC-3'	(1333-1355)	60
A-pMSCV-F	5'-CAGCCCTCACTCCTTCTCTA-3'	(1378-1397)	58
pMSCV-R	5'-CCTAGCAATGCTCGTCAAG-3'	(1498-1479)	58
hTBP-F	5'-GCACAGGAGCCAAGAGTGAA-3'	(653-672)Exons 5 and 6	57
hTBP-R	5'-TCACAGCTCCCCACCATGTT-3'	(779-760) Exon 6	57

* GenBank acc. Nr.: BF165105 (mouse OSTL J16), AA992964 (human OSTL E06), NM_006118.2 (HAX1), NM_006427 (SIVA 1), NM_021709 (SIVA 2); NM_001001303 (mouse GAPDH); NM_007583.11 (human TBP).

5.2.10. Buffers and solutions

All the solutions used for cell culture, bacterial and yeast work were sterilized (autoclaved or filtered with 0.22μm or 0.45 μm filters).

Ammonium Chloride Solution

    0.8% NH_4Cl in sterile water

    0.1 mM EDTA

Ampicillin stock

    100 mg/ml Ampicillin

    Aqua bidest.

    Sterilized by filtration. Aliquots 1 ml; stored -20°C

Blotto A for Western Blot

    1 x TBS

    5% milk powder

    0.05% Tween 20

Buffer E1 resuspension buffer

    50 mM Tris/HCl pH 8.0

    10 mM EDTA

    100 μg/ml RNAse A

Buffer E2 lysis buffer

    200 mM NaOH

    1%SDS

Buffer E3 neutralization buffer

    3 M Potassium acetate pH 5.5

Buffer QBT equilibration buffer (Qiagen)

    750 mM NaCl

    50 mM MOPS

    15% EtOH

    0.15% Triton X-100

Buffer QC wash buffer (Qiagen)

    50mM MOPS pH 7.0

    15% EtOH

Buffer QF elution buffer (Qiagen)

    1.25M NaCl

    50mM Tris/HCl pH 8.5

    15% EtOH

Denhardt's solution 50X

1% BSA (fraction V)

1% Ficoll (type 400) Polyvinylpyrrolidone

1% Aqua bidest.

Sterilized by filtration (0.45μm). Stored -20°C

DEPC water

0.1% diethylpyrocarbonate in bi-distilled water

shacked vigorously and autoclaved

Dithiothreitol (DTT) solution

1M DTT

0.01M Sodium acetate pH 5.2

Sterilized by filtration (0.22μm). Aliquots 1mL; stored -20°C

DNA loading buffer

0.25% Bromophenol blue

0.25% Xylencyanol FF

15% Ficoll in Aqua bidest.

Electrophoresis running buffer

250 mM Tris HCl, pH 8,5

2 M glycin

1% SDS

Electrophoresis sample (or loading) buffer

125 mM Tris

4% SDS

20% glycerol

10%β-Mercaptoethanol

0.01% bromophenol blue

FACS Buffer

PBS

2% FCS

1 mg/l propidium iodide

Frozen Storage Buffer (FSB 1) for chemically competent cells

Reagent	Amount per liter	Final concentration
1 M potassium acetate (pH 7.5)	10 ml	10 mM
$MnCl_2 \cdot 4\,H_2O$	8.91 g	45 mM
$CaCl_2 \cdot 2H_2O$	1.47 g	10 mM
KCl	7.46 g	10 mM
Glycerol	100 ml	10% (v/v)
Bidest. H_2O	to 1 l	

Sterilized by filtration (0.45 μm). Aliquots 40 ml; stored -20°C

Frozen Storage Buffer (FSB 2) for chemically competent cells

Reagent	Amount per liter	Final concentration
Na-MOPS	2.3 g	10 mM
$CaCl_2 \cdot 2H_2O$	11 g	75 mM
KCl	0.75 g	10 mM
Glycerol	150 g	15% (v/v)
Bidest. H_2O	to 1 l	

Sterilized by filtration (0.45 μm). Aliquots 24 ml; stored -20°C

Formaldehyde 3.7%

3.7% Formaldehyde (stock 37%)

in PBS

Gel fixation solution

20% methanol (v/v)

10% acetic acid (v/v)

IPTG

0.2% w/v Isopropyl-β-D-thio-galactopyranoside

Aqua bidest.

Sterilized by filtration (0.2μm). Aliquots 1ml; stored at -20°C

Kanamycin stock

50mg/ml Kanamycin Aqua bidest.

Sterilized by filtration. Aliquots 1 ml; stored at -20°C

Lithium acetate stock solution 10X pH 7.5

1M Lithium acetate

pH 7.5 with diluted acetic acid

autoclaved

Methocult™ GF M3434

　　1% Methylcellulose in Iscove's MDM

　　15% Fetal Bovine Serum

　　1% Bovine Serum Albumine

　　10 μg/ml rh Insulin

　　200 μg/ml Human Transferrin (iron-saturated)

　　0.1 mM 2-Mercaptoethanol

　　2 mM L-glutamine

　　50 ng/ml rm SCF

　　10 ng/ml rm IL-3

　　10 ng/ml rh IL-6

　　3 units/ml rh Erythropoietin

10x MOPS electrophoresis buffer for Northern blot

　　0.2 M MOPS pH 7.0

　　20 mM sodium acetate

　　10 mM EDTA pH 8.0

　　Add water to 1l

　　pH 7.0 with 2 N NaOH

Na_2HPO_4 1M pH 7.2

　　1M Na_2HPO_4

　　Aqua bidest.

　　Autoclaved

Neutralization solution for Southern Blot

　　1 M Tris HCl pH 7.4

　　1.5 M NaCl

50% PEG 4000 solution

　　50% w/v PEG 4000

　　Aqua bidest.

Phosphate buffer saline (PBS) pH 7.4

　　140 mM NaCl

　　5.4 mM KCl

　　9.7 mM Na_2HPO_4 x $2H_2O$

　　2 mM KH_2PO_4

RIPA buffer (lysis buffer for Western blot)

50 mM HEPES pH 7.5 (1 M stock)

150 mM NaCl (5 M stock)

1 mM EGTA (200 mM stock)

10% Glycerol (50% stock)

1% Triton X 100

100 mM NaF

10 mM $Na_4P_2O_7$ x 10 H_2O

Protease inhibitors (freshly added):

PMSF (stock 10 mg/ml diluted in isopropanol) 10 µl per 1 ml RIPA

1:100 protease inhibitor cocktail stock (Sigma) in lysis buffer:

104 mM AEBSF

0.08 mM Aprotinin

2 mM Leupeptin

4 mM Bestatin

1.5 mM Pepstatin A

1.4 mM E-64

Saline sodium citrate buffer (20xSSC)

3 M NaCl

0.3 M Sodium citrate pH 7.0

DEPC-treated Aqua bidest. (for RNA experiments)

Autoclaved

Sample Buffer (for *in vivo* CoIP)

150 mM Tris-HCl pH 8.0

50 mM NaCl

0.5% Triton X100

SDS-electrophoresis running buffer 10x pH 8.3

250 mM Tris Base

1.92 M Glycin

1% (w/v) SDS

Aqua bidest.

SDS-protein running gel	**10% (10 ml)**	**12% (10 ml)**
Tris/HCl (stock 1.5M pH 8.8)	2.5 ml	2.5 ml
Acrylamide + Bisacrylamide (stock 30%)	3.3 ml	4.0 ml
SDS (stock 10%)	0.1 ml	0.1 ml
Aqua bidest	4.0 ml	3.3 ml
TEMED	0.004 ml	0.004 ml
APS (stock 10%)	0.1 ml	0.1 ml

SDS-protein stacking gel	**4.4% (8 ml)**
Tris/HCl (stock 1.5M pH 8.8)	1.0 ml
Acrylamide + Bisacrylamide (stock 30%)	1.3 ml
SDS (stock 10%)	0.08 ml
Aqua bidest	5.5 ml
TEMED	0.008 ml
APS (stock 10%)	0.08 ml

Separating electrophoresis gel buffer

1.5 M Tris-HCl pH 8.8

2% SDS

Sodium dodecylsulfate (SDS) 10%

10% (w/v) Sodium dodecyl sulfate

Aqua bidest.

Autoclaved

Stacking Gel buffer

1.5 M Tris-HCl pH 6.8

2% SDS

Stripping buffer for WB

62.5mM Tris/HCl (stock 1M pH 6.7)

2%SDS

β-Mercaptoethanol 100mM

Aqua bidest.

Stripping buffer for Northern Blot

0.1x SSC

2% SDS

TBS-T wash buffer 5X pH 7.5

    250 mM Tris Base

    750 mM NaCl

    0.1% Tween 20 (1X)

    Aqua bidest.

TE buffer

    10 mM Tris/HCl (stock 1M pH 8.0)

    1 mM EDTA

    Aqua bidest.

Transfer buffer for Western Blot pH 8.8

    25 mM Tris Base

    20% Methanol

    1.44% (w/v) Glycin

    Aqua bidest.

Triton X-100 cell lysis buffer

    0.5% Triton X-100

    in 1X PBS

Trypan blue solution

    0.9% NaCl

    0.5% Trypan blue dyestuff

    Aqua bidest.

X-gal

    2% 5-Bromo-4-chloro-3-indolyl-β-D-galactopyranoside

    in 100% N,N-dimethylformamide

    Stored in dark glass at -20°C

5.2.11. Media

5.2.11.1. Bacterial media

E.coli bacteria were grown in Luria Bertani (LB) medium. Transfected bacteria containing the ampicillin resistance gene cells were grown in LB containing ampicillin (Amp) at the concentration of 100 μg/ml or transfected bacteria containing the kanamycin resistance gene cells were grown in LB containing kanamycin (Kan) at the concentration of 50 μg/ml.

LB medium pH 7.5

    1% w/vol Bacto-trypton

    0.5% w/vol Bacto-yeast extract

    0.5% w/vol NaCl

    Aqua bidest.

    Autoclaved

LB agar plates

    LB medium 100 ml

    Bacto-agar 15 g

    Autoclaved

    Ampicillin 100 μg/ml or Kanamycin 50 μg/ml

SOC medium

    Complete *E.coli* medium without selection (Sigma)

    950 ml dH_2O

    20 g Tryptone

    5 g Yeast extract

    0.5 g NaCl

    250 mM KCl (10 ml to 1 liter)

    autoclaved and cooled to 60°C to add 20 mM glucose (1 M stock solution)

Glycerol freezing solution

    1/3 Glycerol

    2/3 LB medium

5.2.11.2. Yeast media

Ingredients for liquid or solid media were dissolved in aqua bidest., mixed until completely dissolved and autoclaved in bottles (250-500-1000 ml). Amino acids (dropout solution) were prepared in water as 10X stock solution, autoclaved and added (50 ml/l) to medium without amino acids as required to obtain the desired SD medium. The dropout stock solution was prepared lacking the amino acids adenine, histidine, leucine, and tryptophan.

Dropout solution

Amount in dropout powder	10x concentration (mg/ml)
L-adenine hemisulfate salt[*]	200
L-arginine HCl	200
L-histidine HCl monohydrate[*]	200
L-isoleucine	300
L-leucine[*]	1000
L-lysine HCl	300
L-methionine	200
L-phenylalanine	500
L-threonine	2000
L-tryptophan[*]	200
L-tyrosine	300
L-uracil	200
L-valine	1500

[*]These amino acids were added separately for each selective Dropout medium

(SD medium)

YPD medium liquid

1% w/v Yeast extract

Peptone 2%

Dextrose 2%

For YPD plates 2% agar and 0.01% NaOH were added

SD -T, -L plates

6.7 g Yeast nitrogen base without aa

20 g Agar

850 ml Bidest. water

100 ml sterile 10X –T, -L, -H, -A Dropout solution

200 mg Adenine

200 mg Histidine

Autoclaved. Medium was allowed to cool to ~ 55°C before adding 2% glucose

SD -T, -L, -H plates

6.7 g Yeast nitrogen base without aa

20 g Agar

850 ml Bidest. water

100 ml sterile 10X –T, -L, -H, -A Dropout solution

200 mg Adenine

Autoclaved. Medium was allowed to cool to ~ 55°C before adding 2% glucose

SD -T, -L, -H, -A plates

6.7 g Yeast nitrogen base without aa

20 g Agar

850 ml Bidest. water

100 ml sterile 10X –T, -L, -H, -A Dropout solution

Autoclaved. Medium was allowed to cool to ~ 55°C before adding 2% glucose

SD -T, -L, -H, -A X-gal plates

6.7 g Yeast nitrogen base without aa

20 g Agar

850 ml Bidest. water

100 ml sterile 10X –T, -L, -H, -A Dropout solution

Autoclaved. Medium was allowed to cool to ~ 55°C before adding 2% glucose and 20 mg/ml X-α-gal solution in 1 ml DMF

PEG/LiAc solution

40% PEG 4000

1X TE buffer

1X LiAc

Stock solutions (see 2.2.9)

5.2.11.3. Cell culture media

Complete RPMI or DMEM medium

10% Fetal calf serum (heat-inactivated)

1% penicillin/streptomycin solution (10.000 U/ml Penicillin, 10 mg/ml Streptomycin)

RPMI1640 or DMEM to 500 ml volume

DMSO freezing medium

10% DMSO sterile-filtered

in filter sterilized and heat-inactivated FCS

Roswell Park Memorial Institute culture medium (RPMI 1640)

0.02 g/l L-Glutamine

2.0 g/l $NaHCO_3$

Sterile filtered

Dulbecco´s Modified Eagle medium (DMEM)

4.5 g/l glucose

0.5 g/l L-Glutamine

0.1 g/l Sodium Pyruvate

3.7 g $NaHCO_3$

Sterile filtered

Penicillin/Streptomycin solution

10,000 U/ml penicillin

10 mg/ml streptomycin

Trypsin/EDTA Solution

0.05% Trypsin

0.02% EDTA

in PBS without Ca^{2+}, Mg^{2+}

5.2.12. Equipment

Cytospin (Cytospin 2 Shandon)

DNA Cross linker (GS Gene linker Bio-Rad)

Flow Cytometry (BD FACS Calibur System)

Fluorescence Activated cell sorting (BD FACSVantage SE System)

Microscope (Zeiss Axiovert 200 M, Zeiss Axiovert 135)

Sorvall RC SB Plus and RC-5 centrifuge (Kendro Laboratory Products)

Microcentrifuge 5417 C (Eppendorf))

Spectrophotometer (Bio-Rad)

5.3. Molecular biology methods

Many of the molecular biology procedures were performed as described (Sambrook and Russel, 2001).

5.3.1. Plasmid DNA isolation from *E. coli*

5.3.1.1. DNA Mini preparation

This procedure, which rapidly isolates plasmid DNA from bacteria using the alkaline lysis method followed by Isopropanol precipitation, was used during the cloning process to isolate small amount of DNA from a large number of clones.

Briefly, each single colony was inoculated into 3 ml of LB medium (plus 100 μg/ml Amp or 50 μg/ml Kana) in plastic culture tubes and grown O/N at 37°C with vigorous shaking (260 rpm). The next day 1.5 ml of the culture was transferred in Eppendorf tubes and bacterial cells were harvested by centrifugation at 14000 rpm for 2 min.

The pellet was resuspended in 250 μl of cold Buffer E1 containing RNase (0.1 mg/ml) and 250 μl of Buffer E2 were added, mixed gently, and the mixture was incubated at RT for 5 min. 250 μl of Buffer E3 were added and mixed gently. The mixture was centrifuged at 14000 rpm 15 min. The supernatant (~ 800 μl) was transferred to a new Eppendorf tube and 0.7 vol of isopropanol was added. The suspension was vortexed and incubated at -20°C for 10-20 min and then recentrifuged at 14000 rpm for 20 min. The pellet was washed with 500 μl of 70% ethanol, vortexed, and centrifuged 10 min at 14000 rpm, dried for 10-20 min and redissolved in 20 μl of sterile bidest. water. The DNA was stored at -20°C.

5.3.1.2. DNA Maxi or MaxiEndofree preparation

The plasmids used in the transfection experiments were prepared with the Qiagen maxi endofree kit, according to the manufacturer's instructions. Qiagen plasmid purification protocols are based on a modified alkaline lysis procedure, followed by binding of plasmid DNA to Qiagen anion-exchange resin under appropriate salt and pH conditions. RNA, proteins, dyes, and low molecular weight impurities are removed by a medium salt wash.

Plasmid DNA was eluted in a high salt buffer concentrated and desalted by isopropanol precipitation. Briefly, plasmids were prepared from *E.coli* XL-1 bacterial cultures grown in the presence of a selective antibiotic.

A single colony (or 50 μl of a glycerol stock) was inoculated into 5 ml of standard LB medium in the presence of ampicillin (50 μg/ml) or kanamycin (25 μg/ml), and grown for 6 h at 37°C with vigorous shaking (260 rpm). The preculture was diluted 1:100 into a larger volume of selective medium and grown to saturation (O/N) at 37°C with gently shaking (190 rpm).

The bacterial cells were harvested and centrifuged at 4000 rpm for 20 min at 4°C in Sorvall RC-5 with GS-3 rotor. The pellet was resuspended in 10 ml of Buffer P1 containing Rnase (0.1 mg/1ml) and transferred to non-glass tubes for the SS3H rotor. 10 ml of Buffer P2 was added, mixed by inversion, and the mixture was incubated at RT for 5 min. 10 ml of ice-cold Buffer P3 were added, mixed gently and the mixture incubated on ice for 20 min. The suspension was centrifuged at 16000 rpm 30 min at 4°C and the supernatant was transferred into new tube and recentrifuged at 16000 rpm for 15 min at 4°C.

Qiagen column was equilibrated with 10 ml Buffer QBT. Subsequently, the supernatant from the cell lysate was applied to the column. Plasmid DNA bound to Qiagen anion-exchange resin was washed twice with 30 ml Buffer QC and eluted with 15 ml Buffer QF, collecting it in a 50 ml Falcon tube. The DNA was precipitated with 0.7 vol of isopropanol, incubated 10-20 min at -20°C and centrifuged 5000 rpm for 30 min. The DNA pellet was washed with 15 ml of 70% ethanol, vortexed, centrifuged 20 min at 5000 rpm, dried for 10-20 min and redissolved in 500 μl of sterile bidest. water. The DNA was stored at -20°C.

5.3.2. Qualitative and quantitative DNA analysis

To determine the quality and yield, the DNA was measured in an UV spectrophotometer (Pharmacia Biotech) at 260 and 280 nm, normally diluting 2 μl in 198 μl of sterile bidest. water. The DNA concentration was calculated by the spectrophotometric conversion $1A_{260}$ unit of double-stranded DNA = 50 μg/ml (Sambrook, 1989). In addition, the ratio A_{260}/A_{280} was measured. Preparations with a DNA concentration of less than 0.2 μg/ml and a ratio below 1.5 were discarded.

To ensure the correct preparation of the DNA plasmids, the DNAs were analyzed by one or more restriction enzyme digestions. 0.5 μg-1μg DNA (from maxiprep) or 1 μl DNA (from 20 μl miniprep) were digested in 1.5 ml Eppendorf tubes in 20 μl of total volume containing:

1 µl of enzyme (10 U)

2 µl of buffer (10X)

x µl of sterile bidest. water up to 20 µl

The mixture was spun down and incubates at 37°C (or recommended temperature) for 2-3 h. A 0.5-1.5% agarose gel in TBE 1X buffer with Ethidium bromide (final concentration 0.2 µg/ml) was prepared. 1-2 µl of DNA loading buffer (10X) was added and mixed to each DNA sample and the complete content was loaded on the gel and run for 1 h at 60-100 V. An appropriate molecular weight marker (e.g. 1 kb DNA ladder from Life technologies) was used.

5.3.3. DNA transformation into bacteria

Two different protocols were used for bacterial transformation. The electroporation procedure was performed to transform electrocompetent *Epicurian coli* XL1-blue supercompetent cells (see 5.3.3.1) and the heat shock protocol was performed to transform chemically competent cells such as BL21 cells (see 5.3.3.3).

5.3.3.1. Preparation of XL1 Blue electrocompetent cells

A 40 µl aliquot of the frozen bacterial stock was inoculated in 5 ml of LB medium in a 50 ml Falcon tube and incubate O/N at 37°C with constant shaking (100 rpm). The next morning the O/N culture (5ml) was inoculated in 500 ml of LB medium in a 1 l Erlenmeyer glass flask and cells were grown for 2-3 h to reach $OD_{600} \sim 0.5\text{-}0.6$. Subsequently, the cells were transferred into Beckman centrifuge-tubes on ice and centrifuged 15 min at 4000 g in a precooled GS-3 rotor at 4°C. Each cell pellet was washed twice in 100% vol with cold and sterile bidest. water, then in bidest. water 10% sterile glycerol. Cells were re-centrifuged 10 min at 4000 g, resuspended in 500 µl of cold bidest. water 10% glycerol, transferred to sterile Eppendorf tubes in 40 µl aliquots, shock frozen in liquid N_2 and stored in -80°C freezer.

5.3.3.2. Plasmid DNA transformation with electroporation

For electroporation, XL1-Blue electrocompetent bacteria cells were thawed on ice. 1 µl of plasmid DNA (50-100 ng) or 5-10 µl of ligation reaction (from a 20 µl total ligation) were added to 40 µl thawed electrocompetent cells and mixed by pipetting. The cells were

incubated on ice 1-2 min and then added to ice-cold electroporation cuvettes for bacteria. The cells were shocked by 1 pulse of 2.5 kV in 3-4 msec. immediately after each pulse, 1 ml of RT SOC medium was added and the suspension was transferred back to the original microtube, then incubated for 1 h at 37°C with shaking. After 15 sec of high speed centrifugation, 800-900 μl of medium was removed, the rest was resuspended and 100-200 μl of the suspension was plated on prewarmed LB/Amp or LB/Kana plates and incubated at 37°C O/N.

5.3.3.3. Preparation of BL21 chemically competent cells

An aliquot of 100 μl from the frozen bacterial stock was inoculated in 20 ml LB medium in a 100 ml Erlenmeyer glass flask and incubate O/N at 37°C shaking. The next morning the O/N culture (20 ml) was inoculated in 600 ml of LB medium in a 1 l Erlenmeyer glass flask and cells were grown for 2-3 h to reach $OD_{600} \sim 0.5$-0.7. Subsequently, the cells were transferred into Beckman centrifuge-tubes on ice and centrifuged for 10 min at 4000 rpm in a precooled GS-3 rotor at 4°C. Each cell pellet was resuspended in 240 ml sterile and cold FSB 1 (see 5.2.9), then the suspension was incubated on ice 15 min. Cells were re-centrifuged for 10 min at 4000 rpm, resuspended in 24 ml of sterile and cold FSB 2 (see 5.2.9) solution, aliquoted in sterile Eppendorf tubes in 100 μl aliquots, shock frozen in liquid N_2 and stored in -80°C freezer.

5.3.3.4. Plasmid DNA transformation with chemically BL 21 competent cells

For chemically transformation of XL1-Blue competent bacteria cells, 1 μl of plasmid DNA (50-100 ng) or 20 μl of ligation reaction (from a 20 μl total ligation) was added to 100 μl thawed competent cells and mixed by pipetting. The cells were incubated on ice 50 min. The cells were then incubated 90 sec at 42°C. After 15 sec of high speed centrifugation, 800-900 μl of medium was removed, the rest was resuspended and 100-200 μl of the suspension was plated on prewarmed LB/Amp or LB/Kana plates and incubated at 37°C O/N.

5.3.4. Cloning of PCR products

The plasmids generated in this work were prepared by amplifying the desired DNA inserts by PCR with primers containing appropriate restriction sites at their 5' termini. Then the PCR products were digested with the appropriate restriction enzymes and cloned into the recipient vector.

The strategy followed was:

1) Design and synthesize 5' and 3'-end PCR primers with the desired restriction sites;

2) Perform the PCR with the appropriate primers and DNA template;

3) Prepare the vector and insert for cloning (preparative gel/DNA purification or DNA ethanol precipitation);

4) Ligate vector and insert DNAs;

5) Transform the ligation products into *E.coli* electrocompetent cells or chemically competent cells;

6) Plate on appropriate selection plates;

7) Pick colonies and perform plasmid DNA minipreps;

8) Restriction analysis to identify the clones containing the correct DNA insert;

9) Sequence the insert or at least the cloning junction;

10) Store the correct plasmid as DNA and bacteria glycerol stock at -20°C.

5.3.4.1. Amplification of DNA by the polymerase chain reaction (PCR)

To amplify DNA, the Platinum *Taq* DNA Polymerase (NewEngland Biolabs or Invitrogen) was used. The system is composed of the thermostable Taq DNA enzyme and the appropriate 10X Taq DNA buffer, the NEB Taq DNA buffer already contains magnesium, the Invitrogen PCR kit provide the magnesium 50 mM to be added to the PCR mixture. The DNA amplification was performed according to the manufacturer's instructions and some adjustments depending on the template and primer pairs. First, one master mix was prepared using sterile tubes, pipettes, and pipette tips (sterilized in the UV Stratalinker) with all reagents on ice as follows:

PCR mix:

10X PCR buffer	2.5 μl
MnCl$_2$ 50 mM	0.6 μl
dNTPs 2 mM	2.5 μl
5' Primer (10 μM)	0.5 μl
3' Primer (10 μM)	0.5 μl
Bidest. water	up to 19 μl

The reagent mix was pipetted into thin wall PCR tubes (0.2 ml), 1 μl of template (~ 100 ng) was added and the sample was placed immediately in the thermocycler and the PCR performed.

Second, the cycle conditions in the Thermocycler (Perkin Elmer PCR System 2400 or PE Applied GenAmp PCR System 9700) were adjusted.

Generally the PCR reaction used for PCR fragment with length up to 1.0 kb were performed with the following conditions:

1.	95°C 2 min	denaturation of template
2.	94°C 30 sec	denaturation
3.	55-60°C (primer dependent) 30 sec-1 min	Annealing
4.	72°C 1 min (template dependent)	elongation
5.	72°C 5 min	finish elongation
6.	4°C ∞	reaction end

(steps 2–4: 20 cycles)

At the end of the PCR, 5 μl for each sample was analyzed on a 0.5-1% agarose gel.

5.3.4.2. Vector and insert preparation

In this work DNA was purified from agarose gels using the Qiagen gel purification kit, the procedure was performed according to the manufacturer's instructions.

Both vector (1-5 μg) and insert (1-5 μg) were digested with the compatible restriction enzymes in 20-50 μl reaction for 3 h to O/N:

1-5 μg of DNA

10-50 U of appropriate enzyme

5-10 μl of enzyme buffer 5X

x μl of sterile water up to 20 or 50 μl

The cleavage reaction was pipetted in a 1.5 ml Eppendorf tube and incubated in a thermoblock at the optimal temperature as recommended for each enzyme.

If the ends of the prepared vector were identical (e.g., following a single digestion), the vector DNA was treated for 30 min at RT with 1-2 μl of calf intestinal alkaline phosphatase (CAIP)

64

(Invitrogen) to remove the phosphate groups from the 5' ends to prevent self-ligation of the vector. After 30 min incubation CAIP was inactivated for 15 min at 60°C. After digestion reaction the DNAs were precipitated for the ligation.

DNA precipitation procedure:

Add the following reagents to a 1.5 ml Eppendorf tube:

1) 20 µl of digestion reaction

2) 10% v/v 3 M NaAc

3) 2.5 vol 100% ethanol

4) mixed by vortexing

5) incubated at -20°C for 10 min

6) centrifuged 13000 rpm at 4°C for 20 min

7) pellet was washed in 72 µl 70% ethanol

8) centrifuged 13000 rpm at 4°C for 10 min

9) the fluid was removed and the pellet dried at RT for 10-20 min

10) DNA pellet was resuspended in 20 µl sterile water

11) DNA was stored at -20°C

5.3.4.3. Ligation of plasmid vector and insert DNAs

After the vector and insert DNAs have been purified, the concentration of DNA was estimated by agarose gel electrophoresis in comparison to a molecular weight standard. The ligation was performed using T4 DNA Ligase (New England Biolabs) according to the manufacturer's instructions.

The typical ligation reaction was performed at RT for 2 h or at 16°C O/N, with 50-200 ng of vector and 50 to 200 ng of insert DNA (molar ratio of vector to insert 1:3) in 20 µl of final volume:

1-2 µl of vector (50 to 200 ng)

3-6 µl of insert (1:1 to 1:3 molar ratio of vector to insert)

2 µl of DNA Ligase buffer (5X)

1 µl T4 DNA Ligase

x µl of water up to 20 µl

To monitor the efficiency of ligation between vector and insert, the linear vector was transformed in the absence of the DNA insert.

At the end of the reaction, the samples were placed on ice and 5-10 μl was transformed into electro-competent or chemically competent cells (*E.coli* XL1-blue competent cells).

5.3.5. Analysis of RNA by Northern hybridization

To analyze the size and the expression of the OSTL RNA, Northern analysis was performed. Total RNA was isolated from cells in cell culture or from mouse tissues, run on an agarose gel, transferred to nylon membranes and detected by hybridization with a radiolabeled DNA-probe. To successfully isolate and analyze intact RNA some important precautions were used: effective disruption of cells, denaturation of nucleoprotein complexes, inactivation of endogenous ribonuclease (RNase) activity and purification of RNA away from contaminating DNA and protein (Sambrook, 1989). All disposable plastic ware were sterile. Many solutions as well as nondisposable plastic ware were pretreated with diethyl pyrocarbonate (DEPC) 0.05% O/N before sterilization.

5.3.5.1. Qiagen isolation of total RNA

The isolation and purification of RNA from tissue culture cells or mouse tissues was performed using the Qiagen RNEasy mini kit according to the manufacturer's instructions.

Briefly, cells were washed with sterile PBS, trypsinized (adherent cells), diluted in the complete medium, counted and centrifuged at 1000 rpm for 5 min. 10 μl of β-mercaptoethanol were added per 1 ml of RLT lysis buffer.

Cell pellets or tissue pellets were resuspended in RLT buffer (350 μl for up to $5x10^6$ cells or 600 μl for up to $1x10^7$ cells or 350 μl for up to 20 mg of tissues or 600 μl for up to 30 mg of tissues) and frozen at -80°C. Frozen lysates were thawed at 37°C for 10 min, transferred directly into QIAshreder columns sitting in 2 ml collection tubes and centrifuged at maximum speed for 2 min. Samples were collected into new tubes and 1 vol of 70% ethanol was added, creating conditions which promote selective binding of RNA to the RNEasy membrane. 700 μl of sample were applied to RNEasy mini spin column sitting in 2 ml collection tubes and centrifuged at 13000 rpm for 15 sec to allow absorption of RNA to the membrane. If the volume of lysate cells exceeded 700 μl, the rest of the suspension was applied to the same RNEasy spin column, using the same collection tube but discarding the flow-through each time.

The columns were washed with 700 μl of RW buffer and centrifuged at 13000 rpm for 15 sec. After having transferred the RNEasy spin columns into new collection tubes, 500 μl of RPE buffer (containing ethanol) were added and centrifuged at 13000 rpm for 15 sec. reusing the collection tubes and discarding the flow-through, the columns were centrifuged at maximum speed to dry the membrane. The RNEasy spin columns were then transferred into 1.5 ml collection tubes and the RNA was eluted with two centrifugation steps at 13000 rpm for 1 min with 30 μl of DEPC-treated water and stored at -80°C. After this step all procedures were performed keeping RNA samples on ice.

Yield and quality of the RNA were analyzed by UV spectrophotometer. The concentration of RNA was determined by the spectrophotometric conversion $1A_{260}$ unit of single-stranded RNA = 40 μg/ml. The absorbance ratio A_{260}/A_{280} was determined and good RNA preparations were considered exhibiting a ratio A_{260}/A_{280} grater than 1.8 (Sambrook, 1989). RNA (1.0 μl) was also analyzed by agarose gel electrophoresis and the 28S and 18S ribosomal bands were observed.

5.3.5.2. Agarose gel electrophoresis (formaldehyde-agarose gel)

To perform Northern analysis, a formaldehyde-agarose gel (Sambrook and Russel, 2001) was used.

Two hours before starting, the electrophoresis chamber, combs and tray were washed with DEPC-treated Millipore water.

To prepare 100 ml of a 1% agarose gel containing 2.2 M formaldehyde:

1) 1 g of agarose was added to 74 ml DEPC-treated Millipore water;
2) the agarose was dissolved by boiling in a microwave oven,
3) the solution was cooled to 55°C;
4) 10 ml of 10X MOPS electrophoresis buffer was added;
5) 16 ml of deionized formaldehyde was added

In a chemical fume hood, the agarose gel was poured using a 3-mm comb with at least four more wells than the number of RNA samples to be tested. These extra lanes were used for RNA size markers and running dyes. The gel was allowed to set for at least 1 hour at RT then wrapped with Saran Wrap until the samples were ready to be loaded.

20 μg of total RNA were dried in a speed vac and resuspended in 18 μl of formaldehyde-mixture, mixed well by pipetting and incubated for 1 h in a water bath at 50°C.

Formaldehyde mixture for RNA samples:

2 µl of RNA (up to 20 µg)

2 µl of 10X MOPS electrophoresis buffer (2.2.9)

4 µl of formaldehyde

10 µl of formamide

1 µl of Ethidium bromide (200 µg/ml)

_____

18 µl

After 10 min incubation on ice, the samples were centrifuged for 5 sec to deposit all of the fluid in the bottom of the centrifuge tubes.

2 µl of 10x formaldehyde gel-loading buffer were added to each sample and load them into the previously prepared 1% agarose gel. The electrophoresis was performed for 4-5 h at 80 V (in a 15 cm electrophoresis chamber) until the bromophenol blue had migrated 2/3 of the gel.

10x formaldehyde gel-loading buffer:

50% glycerol (diluted in DEPC-treated Millipore water)

10 mM EDTA pH 8.0

0.25% (w/v) bromophenol blue

0.25% /(w/v) xylene cyanol FF

5.3.5.3. Transfer of RNA to membrane

At the end of the electrophoresis, the gel was rinsed in sterile DEPC-treated Millipore water to remove the formaldehyde. In the meanwhile twenty-eight pieces of Whatman 3MM paper and one piece of nylon membrane (Zeta-Probe® GT blotting membrane, BioRad) were cut to the exact size of the gel, soaked first in sterile DEPC-treated Millipore water and then in 20xSSC (prepared with DEPC-treated Millipore water and autoclaved). The transfer of the RNA to membrane was performed by capillary blotting O/N at RT (Sambrook, 1989). After the blotting, the RNA was fixed to the membrane using a UV-crosslinker (Bio-Rad) with the auto cross linker program. The membrane was marked under the UV-light with a special pen and stored in a plastic bag at 4°C until the hybridization.

5.3.5.4. Probe hybridization

Before the hybridization step, the membrane was washed in 2xSSC at RT for 20-30 min, changing several times the buffer.

The membrane was then placed in a glass tube and pre-hybridized for 3 h with rotation at 65°C in 20 ml hybridization solution with 150 µl (10-15 µg) of denatured Lacks DNA (to block unspecific ligations of the probe). The DNA probe was prepared (2.3.5.5.1), denatured at 100°C for 5 min, quick chilled on ice and added in 20 ml of fresh prepared and prewarmed hybridization solution at the final concentration of 10^6 cpm/ml. The membrane was hybridized with the radioactive probe with continuous rotation O/N at 65°C.

After hybridization, the membrane was washed twice with 50 ml of wash buffer I at RT for 10-20 min and twice with 50 ml of wash buffer II at 65°C for 10-20 min, and once with wash buffer III at 65°C for 5-10 min. The radioactive membrane was wrapped in plastic and autoradiography was performed.

To reprobe the membrane, it was washed in a large volume of stripping buffer at 65°C for 2 h. As a positive control for RNA levels, the filter was re-hybridized with a GAPDH [α^{32}P]-probe, using a PCR amplified GAPDH fragment (5' primer: mGAPDHF and 3' primer: mGADHR).

Hybridization solution
25% 20xSSC (see 2.2.10)
10% 50xDenhardt's solution (see 2.2.10)
10% dextransulfat
0.5% SDS
Millipore water was added to final volume
10% SDS
10% w/v SDS powder in 1% DEPC-treated water
Wash buffer I
2xSSC
Wash buffer II
2xSSC
0.1% w/v SDS
Wash buffer III
0.2xSSC
0.1% w/v SDS

Stripping wash buffer

1 M Tris HCl pH 8.0

0.5 M EDTA pH8.0

0.1xDenhardt's solution

For the human multiple tissue northern blot (hMTN blot), a commercial MTN blot (Clontech) was used. The hybridization was performed with the ExpressHyb™ hybridization solution at 68°C. For the human B cells Northern, the same protocol as above was used.

5.3.5.5. Radioactive labeling of DNA

5.3.5.5.1. Megaprime DNA labeling system

The Megaprime™ kit (Pharmacia), which uses random hexanucleotides to prime DNA synthesis on denatured template DNA, was used to label DNA. The Klenow fragment of DNA polymerase I is used in this kit. According to the manufacturer's instructions, 25 ng of DNA was diluted in TE buffer pH 8.0 to a final volume of 34 μl in a 1.5 ml sterile centrifuge tube, heat denatured at 95°C for 5 min and snap cooled on ice for 5 min. After a brief spin down, the denatured DNA was added to the Megaprime™ tube reaction. 5 μl of α[^{32}P] dCTP were added, mixed by pipetting up and down about 12 times, and the reaction mixture was incubated at 37°C for 1 h. Then the DNA was denatured by heating to 95°C for 5 min and snap cooled on ice for 5 min. After a brief spin down, the radiolabeled DNA was purified using Bio-Spin Chromatography columns (BioRad) according to the manufacturer's instructions.

5.3.6. Analyzing OSTL expression by Reverse Transcriptase PCR (RT-PCR)

5.3.6.1. RNA extraction from culture cells or frozen cells and from mouse tissues

The RNA extraction was performed using a denaturing guanidine isothiocyanate-containing buffer for cell lysis and a silica-gel-based membrane for RNA isolation. The reagents and the protocol from the RNeasy® Minikit (Qiagen) were used as described in 5.3.5.1.

5.3.6.2. cDNA synthesis (Reverse Transcriptase Reaction)

The reagents and protocols used for cDNA synthesis were from Invitrogen. To avoid DNA contamination, the RNA was treated with Deoxyribonuclease I before the cDNA synthesis.

For DNase I treatment, 1 μg RNA was mixed with 1 μl 10x DNase I reaction buffer (supplied in the kit), 1 μl DNase I (1 U/μl) in a total volume of 10 μl. The tube was incubated at RT for 40 min and DNase I was inactivated by adding 1 μl of 25 mM EDTA to the reaction tube. After DNase treatment, a RNA aliquot was loaded on an agarose gel for quality control and to estimate the RNA concentration.

For the Reverse Transcriptase reaction, 2 to 4 μl of RNA (approximately 2 μg) were pipetted into an 1.5 ml RNase-free Eppendorf tube together with 1 μl of Oligo (dT)$_{12-18}$, 1 μl of 10 mM dNTP mix (containing 10 mM each dATP, dTTP, dCTP, dGTP at neutral pH) and sterile water to a total volume of 12 μl. The mixture was heated to 65°C for 5 min and quickly chilled on ice. To the tube contents, 4 μl of 5X First-Strand buffer, 2 μl of 0.1 M DTT, and 1 μl of RNaseOUT™ were added. The tube contents was mixed and incubated at 42°C for 2 min. Afterwards, 1 μl of Superscript™ II Reverse Transcriptase was added, and the reaction was incubated at 42°C for 50 min. The reverse transcriptase was then heat-inactivated at 70°C for 15 min.

5.4. Identification of Protein-Protein Interactions with the Yeast Two Hybrid System

5.4.1. Background

To identify OSTL-interacting proteins the yeast two-hybrid system has been used (Fields and Song, 1989; Chien et al., 1991). This method is a useful sensitive approach to detect protein-protein interactions that uses yeast as a test vehicle and transcriptional activation of a reporter system. The two-hybrid approach takes advantage of the modular domain structure of eukaryotic transcription factors. This modular structure consists at least of two distinct functional domains, one that directs binding to specific DNA sequences (BD) and one that activates transcription (AD). The DNA binding and activation domains need not be covalently attached to each other for activation; and they can be exchanged between transcriptional factors and retain their function. In this work the GAL 4 based two-hybrid system 3 (Clontech) was used (Fig 5.1). To analyze the interaction of two different proteins X and Y, two constructs with encode separate fusion of protein X with GAL4 DBD and of Y with GAL4 AD domains are used. Our bait protein, OSTL, was cloned into the pGBKT7 vector (see 5.2.8.4.1), which then expressed a GAL4-DBD-OSTL fusion. A commercially available

Hela-cDNA-Library cloned into the pGAD-GH vector was used for screening (the "prey" proteins are expressed as GAL4-AD fusions). Interaction between bait and a prey plasmid in a single yeast clone can be scored by assaying the activation of reporter genes.

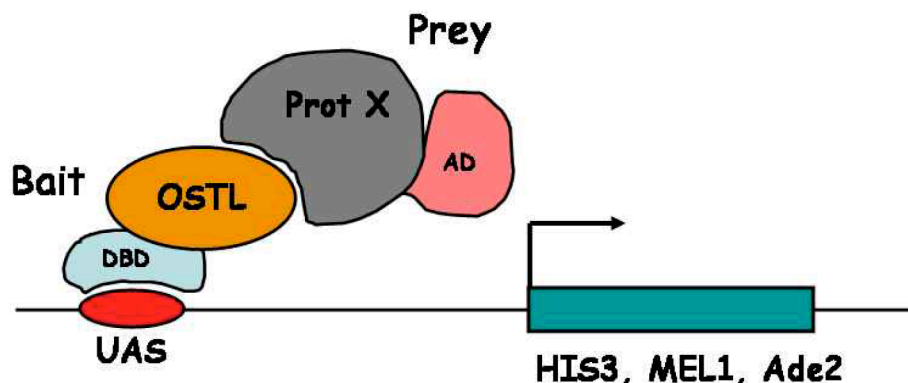The following reporter genes are present in the yeast strain AH109: His1, Mel1, Ade2.

Figure 5.1: Scheme of the yeast two hybrid system

Briefly, the main steps of the yeast two hybrid screen to identify OSTL-interacting proteins were:

1) Construction of bait protein plasmids pGBT9-E06 (Ampicillin resistance) (used for expression and activity tests) and pGBKT7-E06 (used for the large transformation, because of the advantage in the selection (Kanamycin resistance);

2) Transformation of yeast CG1945 cells with pGBT9;

3) Characterization of bait protein expression and activity (spurious activation of reporters);

4) Two Large scale transformation of yeast AH109 cells (AH109 cells have His1, Ade2, and Mel1 as reporter genes) with pGBKT7-E06 and with Hela S3-cDNA library plasmid (pGAD-GH);

5) Collection of primary transformants in medium stringency (SD-T,L,H) plates (100 cm) for the first transformation and in high stringency (SD-T,L,H,A) plates (100 cm) for the second one;

6) X-α-Gal test (Mel1 reporter gene activity):
   Plate colonies from medium and high stringency transformants onto SD-T,L,H,A + X-α-Gal plates. The blue clones (Mel1 reporter active) were selected;

7) Isolation of plasmid-DNA from yeast clones and transformation in XL1-blue-bacteria;

8) Selection of colonies containing the prey plasmid by growth on Ampicillin plates;

9) Isolation of plasmid-DNA by miniprep, restriction analysis;

10) Sequence analysis of positive clones and DNA maxiprep of the relevant positive clones.

5.4.2. Determination of yeast cell density

The density of cells in culture was determined spectrophotometrically by measuring its optical density (OD) at 600 nm. For reliable measurements, cultures were diluted such that the OD_{600} was < 1. In this range, each 0.1 OD_{600} unit correspond to $\sim 3 \times 10^6$ cells/ml.

5.4.3. DNA transformation into yeast cells using the lithium acetate procedure

The lithium acetate method is based on the fact that alkali cations make yeast competent to take up DNA providing high transformation efficiency of 10^4 to 10^6 transformants/µg.

One day before the experiment one or more AH 109 colonies (≤ 4 weeks old) were inoculated in 1 ml YPD medium with 2% of glucose and grown O/N to saturation at 30°C with vigorous shaking.

On the next day the O/N culture was inoculated into 50 ml YPD with 2% glucose in a 500 ml flask and incubated until it reached an OD_{600} of 0.2-0.3 ($\sim 3 \times 10^6$ cells/ml). At this point, the cells were grown for another 1 to 2 generations (2 to 5 h) at 30°C.

After that procedure, the yeast cells were harvested by centrifuging 10 min at 4000 rpm at RT in a Rotanata 46 R (Hettinge) centrifuge, resuspended in 25 ml of sterile water and recentrifuged 10 min at 4000 rpm at RT. Pelleted cells were resuspended in 1.5 ml buffered lithium acetate solution, freshly prepared as follows:

1 vol 10x TE buffer, pH 7.5
1 vol 10x lithium acetate stock solution
8 vol sterile water

For each transformation reaction, 0.1 mg freshly denatured high-molecular-weight carrier DNA with 0.1 to 1.0 µg plasmid DNA were mixed in a sterile 1.5 ml microcentrifuge tube. Immediately, 100 µl of competent yeast cells and 600 µl of PEG/LiAc solution were added.

PEG/LiAc solution:

1 vol 10x TE buffer, pH 7.5

1 vol 10x lithium acetate stock solution

8 vol 50% PEG 4000

Cells were incubated for 30 min at 30°C; 70 μl of DMSO was added to each tube and gently mixed by inversion; the cells were then heat shocked 15 min at 42°C, chilled on ice and centrifuged for 5 sec at top speed in a microcentrifuge. Finally, the pellet was resuspended in 1 ml of 1x TE buffer. 100-200 μl of the yeast suspension were plated on appropriate SD plates, and incubated at 30°C until colonies appeared (normally 2-7 days).

5.4.4. Preparation and test of the bait protein

Firstly, the pGBT9 bait plasmid expressing human OSTL (E06 clone) was constructed (for details see 6.6.1). In a second step, using the lithium acetate transformation protocol, pGBT9-E06 and the empty pGBT9 as a control were transformed separately into yeast strain CG 1945. The cells were plated on SD –W plates. Then the transformed yeast cells were replated on SD –W, -H. Growth on SD –W, -H plates would indicate activation of the HIS3 reporter gene through the bait protein alone. If this had been the case, the bait protein would have to be modified to remove any protein domains that happen to function as activation domains in this setting.

To determine the degree of growth on –H plates, serial dilution plating was performed. This was done by dissolving a yeast colony in 500 μl sterile water. 100 μl of the suspension were diluted into 1 ml sterile water and a series of 1/20 dilutions were prepared to cover a 1000-fold concentration range. 100 μl from each dilution (undiluted, 1/10, 1/100, 1/1000) were spread on 100 mm SD-T and SD-TRP, HIS dropout plates and then incubated at 30°C. The growth of the cells was monitored for several days.

For the further yeast screens we have cloned E06 DNA into pGBKT7 vector, which has different selections in yeast and bacteria (see 5.2.8.4.1) and facilitates the selection for positive interactors and confirmation of these interactions.

5.4.5. Large scale cDNA library transformation

In order to obtain a high number of transformants expressing an individual library plasmid, a large scale transformation protocol was used.

The DNA transformation into yeast cells AH109 was prepared in the same way as by 5.4.3. Selected transformed colonies (AH109-pGBKT7/OSTL) from SD –TRP yeast selection medium were prepared (see 5.4.3) in 2 ml of total volume and completely used for the transformation with the cDNA-Library.

55 μg of plasmid DNA was used to obtain a maximal amount of transformation efficiency (this detail was checked before with series of pilot experiments to obtain the maximum number of colonies), that is this case was 4×10^4 transformants/μg DNA.

After transformation the cells were incubated 1 h at 30°C with 22.5 ml of YPD yeast medium. The pellet was washed with 1X TE buffer and resuspended in 22.5 ml of the same buffer. 250 μl of the transformed yeast cells was divided into 50 SD –TRP, LEU, HIS yeast selection plates and incubated at 30°C for 3 to 7 days (until the colonies appear). As a control, 2 μl of the transformation mixture was plated into SD –LEU and SD –TRP, LEU yeast selection plates and incubated in the same conditions.

5.4.5.1. Selection of clones containing interacting prey proteins

Through the selection, only the transformants that contain the DNA-BD/OSTL-fusion-protein interacting with an AD-fusion-protein must be examined. The yeast strain AH109 has three reporter genes (*HIS3, ADE2, MEL1/lacZ*) under control of the GAL4 DNA binding sites. This is a great advantage, because it reduces the number of false positives, if only those clones are analyzed that show activation of all three reporter genes. The colonies expressing HIS3, ADE2 have been selected through grown into SD –TRP, LEU, HIS, ADE yeast selection plates. These colonies were tested by expression of the MEL1-gene or through the activity of the α-Galactosidase. The primary transformants from 50 SD –TRP, LEU, HIS yeast selection plates were replated into ADE plates and finally into x-α-Gal plates. The selected colonies from the second screen (using high selective plates) were replated into x-α-Gal plates. After 4 to 7 days incubation at 30°C, the positive colonies wee selected through it blue color.

5.4.6. Rapid isolation of plasmid-DNA from yeast

Plasmid DNA is released from yeast transformants together with chromosomal DNA in a rapid protocol by vortexing cells with glass beads in the presence of detergents, phenol, chloroform, and isoamyl alcohol.

A single yeast colony was inoculated into 2 ml of medium in a sterile 14 ml falcon tube. The yeast cells were grown O/N at 30°C at 200 rpm. 1.5 ml of the O/N cultures was transferred into a microcentrifuge tube and spun 5 sec at high speed. The supernatant was removed and

the pellet was briefly vortexed. Cells were resuspended in 200 μl of breaking buffer (5.2.9). 0.3 g of glass beads (0.45-0.52 mm acid-washed, ~ 200 μl) and 200 μl of phenol/chloroform/isoamyl (25:24:1) were added and vortexed for 2 min at high speed. The suspension was centrifuged 5 min at high speed at RT, and 50 μl of the aqueous layer was transferred in a new microcentrifuge tube and stored at -20°C.

5.4.7. Transformation of plasmid DNA in E. coli

Firstly *E.coli* XL1-blue were made electrocompetent and aliquoted at –80°C (5.3.3.1). To perform the electroporation with plasmid DNA isolated from the yeast clones, XL1-blue bacteria cells and DNA were thawed on ice.

2 μl (1-2 μg) of plasmid DNA was added to the thawed bacteria, mixed, and the solution was transferred to ice-cold electroporation cuvettes (2 mm Equibio). After 1-2 min incubation, the cells were electroporated with a 2.5 mV in 3-4 msec pulse (Easyject-Equibio, 2500 V or 1800 V, 6.125 kV/cm maximum field strength). Immediately after the pulse, 1 ml of SOC medium were added and the suspension was transferred back to the original microtube, then incubated 1 hour at 37°C shaking. After 5 sec of centrifugation at high speed, 800 μl of medium was removed, the rest was resuspended and 100 μl of the suspension was spread on LB/Amp plates and incubated at 37°C O/N.

5.4.8. Confirmation assays for specific interacting proteins

5.4.8.1 Confirming potential interactions by co-transformation of bait and prey plasmid

The specific interaction between two fusion proteins was first proved through cotransformation assay in yeast cells. The above candidates (pGAD-GH/cDNA-clone) were cotransformed with the DNA-BD-plasmid pGBKT7/OSTL into AH109 competent yeast cells (5.4.3).

5.4.8.2. Transient cotransfection of mouse fibroblast cells (NIH3T3)

Detailed procedure in section 5.5.1.1.

5.4.8.3. *In-vitro*-expression and radioactive label of the interacting proteins for coimmunoprecipitation assay

Radioactively labeled (35S-methionine incorporation) proteins were produced using an *in vitro* expression system: the TNT®-reticulocyte-lysate system (Promega). The proteins to be

expressed were cloned into the vectors pGBKT7 or pGADT7 (see 5.2.7.4). These vectors contain a T7 promoter sequence 5' of the multiple cloning site. Using T7-RNA-polymerase, cDNAs in these vectors can be transcribed at high copy numbers in the above mentioned reticulocyte lysate and the resulting RNA is translated into the appropriate proteins. Proteins translated from the pGBKT7 vector will have a Myc epitope tag at their N-termini, and proteins translated from the pGADT7 vector will have an HA epitope tag at their N-termini. The procedure was performed as follows:

25 μl of TNT Rabbit Reticulocyte Lysate

2 μl of Reaction buffer

1 μl of T7 RNA Polymerase

1 μl of amino acid, without Methionin (1mM)

2 μl of [^{35}S] Methionin (>1.000Ci/mmol at 10mCi/ml, Amersham)

1 μl of RNasin Ribonuclease Inhibitor (40u/μl)

2 μl of DNA Template(s) (0.5 μg/μl)

Nuclease-Free Water up to 50 μl

The reaction was incubated at 30°C for 90 min.

In vitro co-immunoprecipitation assay

The above amino acid methionine radioactive lysates (see 5.4.9.2) expressed *in vitro* were used for the CoiP assay.

The procedure was performed as follows:

10 μl of *in vitro* translated (^{35}S-methionine-labeled) Myc-tagged bait protein

10 μl of *in vitro* translated (^{35}S-methionine-labeled) HA-tagged prey protein

were mixed in an Eppendorf tube (the CoiP reaction).

The reaction was incubated 1 h at RT on a rotating platform. Then 10 μl of a c-myc monoclonal antibody or a HA polyclonal antibody was added to the reaction and the incubation was continued for one more hour at RT.

Meanwhile, protein A beads were prepared as follows:

The beads were mixed by inverting the tube several times. A sufficient volume (~ 10 μl) of beads were placed into a 1.5 ml microcentrifuge tube and washed twice with 200 μl of PBS.

The bead / PBS suspension was centrifuged at 7000 rpm for 30 sec and the supernatant was removed. Finally, the beads were resuspended in the original volume (~ 10 µl) with PBS.

3 µl of washed protein A beads were added the CoIP reaction and incubated for 1 h at RT, rotating. Then the reaction tube was centrifuged at 7000 rpm for 10 sec, the supernatant was discarded and the beads were washed five times with wash buffer 1 (supplied in the kit (Clontech). After each wash, the beads were centrifuged at 7000 rpm for 10 sec. Finally, the beads were washed twice with wash buffer 2 (supplied in the kit) (Clontech) and after centrifugation the beads were resuspended in 20 µl of SDS-PAGE loading buffer (see 5.2.9 The sample was heated at 80°C for 5 min for denaturation, and 10 µl of the sample was loaded on a gradient 8-12% minigel (BioRad) following standard procedures.

After electrophoresis, the gel was fixed with a gel fixation solution (see 5.2.10) at RT for 10min, the fixation solution was changed once and the gel was incubated for 30 min at RT. After rinsing the gel with H_2O, fluorographic amplification reagent (Amersham, CAT #NAMP100) was added according to manufacturer's instructions, and incubated on a rotary shaker for 20 min at RT. The gel was placed onto pre-wetted 3 MM Whatman paper, covered with Saran wrap and dried at 80°C under constant vacuum.

After the gel was dry, the Saran wrap was removed and the gel was exposed to an X-ray film (Kodak) O/N at RT. The film was developed using standard techniques.

5.4.8.4. *In-vivo*-expression of the interacting proteins for coimmunoprecipitation assay

The pECFP plasmid expressing OSTL (see 6.3) protein was cotransfected with pEYFP-HAX1 or pEYFP-SIVA (see 6.6.5 – figure 6.32) to HEK293T cells by the lipofectamin method (see 5.5.1). Cells were lysate 24 h post-transfection in a lyses buffer (see 5.2.10). Lysates from 4.10^6 or 6.10^6 cells were precleared with protein G-Agarose beads (Roche). Total cell lysate ($\cong$ 800 µg or 1400 µg) were divided and incubated with mouse anti-HAX1 clone 52 (Clontech) or with polyclonal goat anti-Siva antibody clone C-20 (Santa Cruz) (reaction B) or control polyclonal mouse or goat IgG antibody (Santa Cruz) (reaction A) and protein G-Agarose beads for 1:30 h. Then supernatant from reaction A was mixed with beads in reaction B and incubated for 5 h. The beads were washed twice with sample buffer (see 5.2.10). The immunoprecipitated proteins were analyzed by 10% SDS-PAGE (see 5.2.10), blotted, and probed with a rabbit anti-GFP antibody (Molecular Probes). Horseradish peroxidase-coupled rabbit anti-mouse IgG (Santa Cruz) was used with ECL detection system (Amersham Biosciences).

5.5. Cell Culture

The cell culture procedures were carried out in a vertical laminar flow hood (BDK Luft- und Reinraumtechnick GmbH) to ensure sterile conditions required for mammalian cell culture. The cells were grown in commercially available cell culture flasks or dishes (5.2.1) and incubated at 37°C in a humid atmosphere containing 5% CO_2. The cell culture medium used for adherent and suspension cells was commercial-available DMEM and RPMI, respectively, supplemented with 10% FCS and antibiotics (100 U penicillin and 100 ng streptomycin/ml medium). E 86 and bone marrow (BM) cells were grown with the described DMEM complete medium, supplemented with 15% FCS and 1.6 mg/ml cyprobay. The complete medium for BM cells grown was also supplemented with an growth factor cocktail, depending on the culture condition: for myeloid condition 6 ng/ml IL-3, 10 ng/ml IL-6, 10 ng/ml SCF, and for lymphoid condition 10 ng/ml IL-7, 10 ng/ml SCF, and 6 ng/ml Flt3 ligand. The cells were split according to the cell growth rate and density.

In order preserve a the cell lines, $\sim 6x10^6$-$1x10^7$ healthy cells in the logarithmic growth phase were suspended in 1.5 ml of FCS with 10% DMSO in 1.8 ml cryotubes, the tubes were transferred to an -80°C freezer for 24 h and then stored permanently in liquid nitrogen.

5.5.1. Transfection of adherent cells

For co-localization and protein expression, mouse (NIH3T3) or human (HEK293 T) cell lines were transiently transected using cationic polymers from two commercial suppliers (RothFect® transfection kit, Carl Roth or PolyFect® transfection kit, Qiagen).

The day before transfection, 35 mm 6 well culture dishes were seeded with 1-$4x10^5$ cells/well in 3 ml complete DMEM growth medium and grew O/N (12-18 h). For the transfection, 1.5 μg of DNA was diluted in DMEM without serum and antibiotics to a final volume of 100 μl. 10 μl of transfection reagent (PolyFect® or RothFect®) were added to the DNA sample and mixed by pipetting up and down for 5 times.

The mixture was incubated at RT for 10 min to allow complex formation. While the complex formation took place, the DMEM medium was removed from the cells and the cells were washed once with 3 ml of PBS. 1.5 ml of fresh complete DMEM was added to the cells. 600 μl of complete DMEM was added to the transfection complexes and mixed by pipetting. The transfection complexes were gently transferred to the 35 mm dishes and evenly distributed by gently swirling the dishes. Cells were grown O/N (12-24 h); after O/N incubation, cells were analyzed in a fluorescence microscope and prepared by fixation.

5.5.2. Fixation of cells

Cells grown on cover slips were fixed in 3% formaldehyde solution in PBS as described by Dernburg and Sedat, 1998. Briefly, the cell culture medium was removed, the cells were washed twice with cold 1X PBS solution at RT for 3 min. 3% formaldehyde in PBS was added to the cells and they were incubated for 10 min at RT in the dark. The cells were washed twice with cold 1X PBS, then the coverslips were covered with Vektashield reagent, inverted, put on microscope slides and sealed with nail-varnish.

5.5.3. Fluorescence microscopy

After fixation, the cells were analyzed using an inverted fluorescence microscope (Zeiss Axiovert 200 M). Phase contrast (bright field) and fluorescent images of the cells were taken with 100X objectives with a greyscale CCD camera and appropriate filter settings (488 nm for GFP, 433-453 nm for pECFP and DAPI, 513 nm for YFP). The image data were directly transferred to a Macintosh computer (G4) running the Openlab 3.0 image acquisition program.

5.6. Western Blot

To analyze protein expression, SDS polyacrylamide gel electrophoresis (SDS-PAGE) followed by immunoblotting was performed.

5.6.1. Sample preparation

First, cellular protein extracts were prepared. Cell cultures were washed with cold sterile PBS, trypsinized, diluted in PBS, centrifuged at 1000 rpm for 5 min, rewashed in PBS, counted, centrifuged and resuspended in cellular lysis buffer (RIPA buffer – see 5.2.9) 150 μl / $5x10^7$ cells. The cells were incubated for 30 min at 4°C and mixed by inversion (Labinco machine). The sample was centrifuged at 14000 rpm for 30 min and the supernatant was transferred to a new Eppendorf tube, the protein concentration was determined by the Bradford method (5.5.6) and stored at -80°C.

5.6.2. Total protein determination (Bradford-Bio-Rad)

Protein concentrations were determined with the Bradford method. The assay is based on the observation that the absorbance maximum for an acidic solution of Coomassie Brilliant Blue

G-250 shifts from 465 nm to 595 nm when binding to protein occurs. Both hydrophobic and ionic interactions stabilize the anionic form of the dye, causing a visible color change. The extinction of a dye-albumin complex solution is proportional to the protein concentration over a 10-fold range (5-25 µg/ml). The protein concentration of the sample was determined by comparing the extinction of the sample to values obtained from a range of protein standards. The protein standard used was Bovine Serum Albumine (BSA). Six different amounts of albumine (2.5 µg, 5µg, 10 µg, 15 µg, 20 µg, and 25 µg) were diluted in distilled water to a final volume of 800 µl. 1 µl of cell lysate was diluted in distilled water for the measurement. 200 µl of protein assay solution was added to the tubes. The tubes were incubated at RT for 15 min. For the measurements, polystyrol spectrophotometer cuvettes (10x4x45 mm Sarstedt) were used.

5.6.3. SDS polyacrylamide-gel electrophoresis (SDS-PAGE)

Total cell extract (TCE) protein was separated on SDS-PAGE gels (see 5.2.10); some gels were purchased ready to use (BioRad). A 10-12% separation gel (tris-glycine buffer) and a 5% stacking gel were used.

5.6.4. Immunoblotting

Proteins separated on SDS-PAGE were transferred to nitrocellulose membranes (BioRad) using a semi-dry-electroblotter (BioRad). Six pieces of Whatman 3MM paper and one piece of nitrocellulose membrane were cutted to the exact size of the gel, soaked first in water and afterwards in transfer buffer. The transfer occurred over 1-2 h at 150 mA (mA = cm^2 membrane x 0.8). Membranes were blocked in the presence of blotto A (5.2.9) at 4°C O/N. Membranes were then incubated with the respective antibodies diluted in blotto A (1:100-1:3000) at RT for 1 h in continuous rotation, washed with TBS-T wash buffer once for 15 min and twice for 5 min in continuous rotation. Membranes were stained with the secondary anti-mouse or anti-rabbit antibodies horseradish Peroxidase-conjugate (1:1000-1:6000) and finally proteins were detected using the enhanced chemiluminescence (ECL) assay (Amersham).

5.7. Preparation and purification of GST fusion proteins

The coding region of proteins to be expressed as GST fusion protein was cloned into the pGEX-4T2 vector (5.2.7.2). BL21 E. coli cells were transformed with the pGEX constructs. Transformant cells were selected in LB/Amp plate and individual colonies were picked and diluted into 10 ml of LB/Amp medium and incubated O/N at 37°C.

The next day 10 ml of the culture were diluted 1:10 in 100 ml of LB/Amp medium and incubated at 37°C for 1-3 h (OD_{600} ~ 0.8). The expression of the fusion protein was induced by addition of IPTG (1 mM) for other 3-4 h. After induction, cells were centrifuged at 4000 rpm and 4°C for 15 min. Cells were then resuspended in a freshly prepared lysis buffer, vortexed, and lysed by mild sonication.

Lysis Buffer:

1x PBS

20% glycerol

1% Triton 100

1 mM DTT

1 mM EDTA

1 mM PMSF (diluted in isopropanol)

10 μg Leupeptin (diluted in H_2O)

10 μg Pepstatin (diluted in DMSO)

10 μg Aprotinin (diluted in H_2O)

After the sonication, the lysate was transferred to 1.5 ml microcentrifuge tubes and centrifuged at 14000 rpm for 5 min. The purification of the GST fusion protein was performed with glutathione Sepharose 4B (Pharmacia) according to the manufacturer's instructions. Bacterial lysates was incubated with glutathione Sepharose 4B (500 μl / 50 ml lysate) and the GST fusion protein was eluted using a 15 mM glutathione solution in PBS. The purified proteins were examined on 12% SDS PAGE and Coomassie blue staining.

5.8. *Whole mount in situ hybridization*

To analyze the expression pattern of *OSTL* during the mouse embryonic development, a whole mount *in situ* hybridization analysis using digoxigenin-labeled RNA *OSTL* probe was performed as described (Kispert et al., 1996; Lescher et al., 1998).

An antisense-RNA-probe and as control a sense-RNA-probe were hybridized to mouse embryos of different developmental stages (9.5 until 14.5 mouse embryo days).

This part of the work was performed in the Prof. Hrabé de Angelis laboratory at the GSF, Neuherberg, in collaboration with Dr. Gerhard Pzemeck.

5.8.1. Preparation of RNA probe

The DNA template used as probe was a PCR product from murine OSTL, which had been PCR amplified and subcloned into pGEMT-easy vector (see 5.2.7.3). Briefly, the steps of the procedure were as follows:

1) 10 μg of DNA template was linearized with the restriction enzymes: *NcoI* for the sense-probe, and *SalI* for the antisense-probe;

2) The reactions were incubated at 37°C for 2 h;

3) The enzymes were inactivated by heating at 65°C for 15 min;

4) Template DNAs were purified using a QIAquick spin column following the manufacturer's instructions (Qiagen);

5) The single-stranded RNA probes were synthesized using purified RNA polymerases (T7 for the antisense-probe, and SP6 for the sense-probe) to transcribe sequences downstream of the appropriate polymerase promoter site. This reaction was performed in a sterile microcentrifuge tubes on ice as follows:

   10 μl linearized DNA (10 μg)

   3 μl Ampuwa water

   2 μl TS-buffer

   2 μl rNTPs DigMix

   1 μl Rnase inhibitor

   2 μl RNA-polymerase (depends on DNA-template: T7 for antisense-probe) and sp6 for sense-probe

   The reaction was incubated at 37°C for 2 h;

2 µl of DNase was added and the mixture incubated at 37°C for 15 min;

6) The RNAs were precipitated with 400 µl of 100% EtOH, 1µl of tRNA (as a carrier), and 33 µl of 7.5 M NH$_4$Ac, the reagents were gently mixed and incubated at -80°C for 1 h;

7) The RNA was pelleted at 4°C and 15000 rpm for 15 min;

8) The RNA-pellets were resuspended in 100 µl of Ampuwa water, 1 µl of Rnase-inhibitor was added and the pellets were stored at -20°C;

9) The RNA synthesis quality was assayed by running 2 µl of RNA on a 1% agarose gel

5.8.2. Preparation of mouse embryos

Pregnant Balb-c female mice were obtained from the animal facilities GSF-Grosshadern. The mouse embryos from different development stages (9.5 until14.5 days) were collected using standard procedure (Kaufman, 2001). The embryos were prepared in PBS in DEPC-treated water (see 5.2.9). The embryos were fixed in a 4% paraformaldehyd solution diluted in PBS O/N at 4°C, rotating. After fixation the embryos were dehydrated (on ice) through 25%, 50%, and 75% MetOH diluted in PBS with DEPC-treated water for 10 min at each MetOH dilution. Afterwards the embryos were bleached with MetOH/H$_2$O$_2$ (6:1 v/v) for 1 h on ice.

Finally, the embryos were dehydrated twice (on ice) with a large amount of 100% MetOH for 5-10 min each time. They were stored in 100% MetOH at -20°C.

5.8.3. Hybridization of probe to mouse embryos

The embryos were rehydrated (on ice) through 75%, 50%, and 25% MetOH diluted in PBS (DEPC-treated water) for 10 min at each MetOH dilution with shaking. They were washed twice with PBT for 10 min on ice, and once for 5 min with shaking. For mouse embryos from 10.5 until 14.5 days, a proteinase K treatment was performed. 10 µg/ml proteinase K was added and the embryos were incubated (10.5 days: 3 min, 11.5 days: 4 min, 12.5 days: 5 min, 13.5 days: 6 min, and 14.5 days: 7 min) in proteinase K buffer at 37°C with shaking. Then washed twice with freshly prepared PBT/glycin for 5 min on ice, and twice with PBT on ice for 5 min with shaking. They were incubated in RIPA buffer on ice for 10 min, without shaking. Then, washed twice with PBT for 5 min on ice and fixed with freshly prepared 4% paraformaldehyd /0.2% glutaraldehyd in PBT for 20 min at RT, without shaking.

After washing twice in PBT buffer for 5 min at RT, the embryos were incubated in hybridiyation buffer/PBT (1:1 mixture) for 10 min at RT, then washed with hybridization buffer for 10 min at RT.

Prehybridization was performed as follows: hybridization buffer with 100 μg/ml tRNA at 68°C for 3 h. The probes were denatured at 90°C for 3 min and hybridization was performed as follows: 1:100 diluted DIG labeled probe (0.25 μg/ml) with 100 μg/ml tRNA in hybridization buffer at 68°C O/N.

The next day, the hybridization buffer with the probe was removed and the embryos were washed twice with heated hybridization buffer at 65°C for 30 min, then they were cooled to RT and washed once with hybridization buffer/RNAse solution (1:1 mixture). After wash once with RNAse solution for 5 min at RT, they were incubated with RNAse solution containing 100 μg/ml RNase A for 60 min at 37°C. Then a wash with RNase solution/SSC/FA/Tween 20 mixture for 5 min at RT was performed. Embryos were heated in SSC/FA/Tween 20 from RT to 65°C and washed twice with SSC/FA/Tween 20 for 5 min at 65°C, then washed three times with SSC/FA/Tween solution for 10 min at 65°C and five times with SSC/FA/Tween solution for 30 min at the same temperature. Embryos were cooled down to RT and washed once with SSC/FA/Tween 20/1X TBST (1:1 mixture) for 5 min at RT, twice with 1X TBST for 10 min at RT and, finally, twice with MABT for 10 min at RT.

Incubation with 10% blocking solution in MABT for 1 h at RT was performed. Meanwhile, DIG antibody was pre-adsorbed in 1% blocking solution/MABT (1:5000 dilution) for 1 h at 4°C. Embryos were incubated in this antibody solution O/N at 4°C with shaking. To remove unbounded antibody, the embryos were washed three times with TBST for 5 min at RT, and about eight times with TBST for 1 h at RT. They were incubated in TBST for 72 hours at 4°C with shaking.

5.8.4. Staining of probe and visualization

The TBST solution was changed and the embryos were incubated with fresh TBST solution for 4 h at RT. Afterwards, washed twice with fresh made alkaline phosphatase buffer for 5 min at RT, then stained in staining solution (solution was changed before it turned from yellow to pink) O/N at 4°C.

Embryos were fixed in 4% paraformaldehyd in 1x PBS for 1 h at RT and photographed in 30% sucrose in 1x PBS or in 0.8% agarose in PBS with a digital camera (JVC Ky-F70) on a Leica MZ APO microscope and images processed in Corel Photopaint and Adobe Photoshop.

5.8.5. Dissections of stained mouse embryos

Stained whole embryo was incubated in 7.5% gelatine/30% sucrose in 1x PBS solution for 2 h at 42°C in a water bath. The gelatin solution with the embryos was poured in a 10 cm dish and kept at 4°C O/N. On a microscope the gelatin was cut in blocks of around 1 cm^2 and frozen on dry ice. The blocks were incubated at -80°C at least O/N and then cut into 35 μm thick slice in a Cryotom (Kryostat Leica CM 1850). The Cryotom cuts were spread on glass slides with glycerin/gelatin and dried at RT. The glass slides were photographed with a digital camera (JVC Ky-F70) on a Zeiss Axiocan HRC microscope and images processed in Corel Photopaint and Adobe Photoshop.

Solutions:

All solutions used before and for *in situ* hybridization had to be absolutely Rnase-free. DEPC-treated water was used for preparation of Rnase-free solutions and they were autoclaved. For Tris-buffer, DEPC-treated water is not sufficient; the solution was autoclaved twice.

4% Paraformaldehyd/PBS

4 g paraformaldehyd were added to 100 ml of 1x PBS

Few drops of 10 N NaOH were added and the solution was heated to 55°C, until the paraformaldehyd was completely dissolved;

Solution was cooled on ice and pH was adjusted to 7.0 with HCl (pH indicator paper was used).

PBT

PBS with 0.1% (v/v) of Tween 20

tRNA

10 μg/μl tRNA in DEPC-treated water

stored in aliquots at -20°C

Proteinase K buffer

2% Tris-HCl (pH 7.0)

0.2% 0.5 M EDTA

water was added to complete 500 ml

PBT/glycine

2 mg/ml glycine in PBT

Solution made fresh just before use

RIPA

0.1% SDS

150 mM NaCl

1% NP40

0.5% Sodium deoxycholate

5 mM EDTA

50 mM Tris-HCl ph 8.0

DEPC water was added to 500 ml

Hybridization buffer

5 ml of deionized formamide

2.5 ml of 20x SSC

5 μl of heparin solution

0.1% of Tween 20

DEPC-treated water was added to 10 ml

pH was adjusted to 6.0 with 1 M citric acid (4.5% 1 M citric acid was added)

SSC/FA/Tween 20

10 ml of 20X SSC

25 ml of formamide

0.5% Tween 20

Water was added to 50 ml

RNase solution

500 mM NaCl

10 mM Tris-HCl (pH 7.5)

0.01% Tween 20

Water was added to 10 ml

RNase A

10 μg/μl RNase A in 0.01 M NaAc (Sigma) (pH 5.2)

The solution was heated to 100°C for 15 min, and slowly cooled to RT;

The pH was adjusted by adding 0.1 vol of 1 M Tris-HCl pH 7.4;

Aliquots were stored at -20°C

MAB

0.1 M maleic acid

0.15 M NaCl

pH was adjusted to 7.5 with solid NaOH;

Water was added to 1 l

For MABT buffer:

0.1% Tween 20 was added/l

Blocking stock solution

Blocking reagent (Roche) was dissolved in MAB buffer to 10% (w/v);

Solution was mixed with shaking and heating in a microwave oven;

Stock solution was autoclaved, then 0.1% Tween 20 was added to the solution;

Aliquots were stored at -20°C

Alkaline phosphate buffer

The solution was freshly made just before use:

500 mM NaCl

50 mM MgCl$_2$

0.01% vol of Tween 20

100 mM Tris-HCl (pH 9.5)

2 mM Levamisol (diluted in TBST solution)

Water was added to 50 ml final volume

Staining solution

Boehringer BM purple Ap substrate (Boehringer)

2 mM of Levamisole

0.1% vol of Tween 20

Solution was centrifuged and only the supernatant was used

5.9. *Test for ubiquitination of a putative substrate protein*

The principle of this assay is based on a His-tagged version of ubiquitin, which is co-expressed with the putative ubiquitin substrate. His-ubiquitin conjugates are recovered by precipitation on Ni-NTA beads and analyzed by Western blotting with antibodies directed against the putative substrate protein (modified from Treier et al., 1994).

The procedure performed to test for ubiquitination of a putative substrate protein is as follows:

1) One day before the transfection, 1.3 x 10^6 HEK293T cells were plated on 60 mm culture dish with 3 ml of complete DMEM culture medium;

2) At noon, the cells were co-transfected with the putative ubiquitin ligase (OSTL) as well as with the putative substrate proteins (HAX1 or SIVA) together with either the His-Ubiquitin or the HA-Ubiquitin expression vector (HA-Ubiquitin was used as negative control). 1 μg of DNA for each vector (His-Ubi and HA-Ubi) and 3 μg DNA for OSTL, HAX1 and/or SIVA (mOSTL in GFP and HAX1 and SIVA in YFP) in 1 ml of Calcium-phosphate was used. 0.5 ml of the mixture has been added to the cells and they were incubated for 48 h;

3) Four hours before the cells were lysed, 20 μM (final concentration) of the proteasome inhibitor MG132 in 1.5 ml DMEM was added to the cells;

4) The cells were washed once with PBS and lysed in 0.8 ml of lysis buffer, the extracts were transferred to FACS-tubes;

5) The cells were briefly sonicated (twice for 15 sec at low power to shear the DNA. After sonication the cells were transferred to 1.5 ml microcentrifuge tubes and centrifuged at 13000 rpm for 1 min at RT;

6) 600 μl of supernatant was transferred to a new microcentrifuge tube (50 μl of the lysate was kept for TCA-precipitation (see below);

7) The 550 μl remaining lysate was incubated with 15 μl of magnetic Ni-Agarose beads (Qiagen), vortexed and incubated O/N at RT, rotating;

8) The tubes with the lysate were placed in a magnetic stand and the supernatants were removed with a 26G needle;

9) 750 μl of wash buffer A was added to the beads, they were vortexed and rotated for 5 min at RT;

10) Steps 8 and 9 were repeated twice;

11) The beads were washed three times with wash buffer B, and a final wash was performed with PBS;

12) PBS has been removed and 60 μl of 1 x SDS-PAGE sample buffer was added, the beads were boiled for 10 min;

13) 15 μl of the Ni-precipitate together with 15 μl of TCA precipitated extract (see below) were loaded on a 10% SDS-PAGE gel and analyzed by immunoblotting with anti HAX1 N17 antibody (sc-16636, Santa Cruz) diluted 1:1000 or anti SIVA antibody (sc-7250, Santa Cruz) diluted 1:1000.

TCA precipitation:

50 μl of 10% TCA was added to the extract (approximately 5 μg), the tubes were placed on ice and vortexed until a precipitate appeared (~ 2 min) and then incubated on ice for 15 min. The supernatant was removed after high speed centrifugation for 15 min. The pellets were washed with 200 μl ice-cold ethanol by vortexing until they dissolved (~ 2 min) and high speed centrifugation was performed for 15 min. The pellets were dried in the speed vac for 10 min and resuspended in 50 μl sample buffer and boiled for 5 min.

Lysis buffer

6 M guanidine-HCl

0.1 M NaH_2PO_4

0.01 M Tris (pH 8.0 adjusted with NaOH)

Wash buffer A

8 M urea

0.1 M NaH_2PO_4

0.01 M Tris (pH 8.0)

Wash buffer B

8 M urea

0.1 M NaH_2PO_4

0.01 M Tris (pH 6.4)

5.10. Overexpression of OSTL in primary hematopoietic cells

5.10.1. cDNA constructs and retroviral vectors

For retroviral gene transfer into primary bone marrow (BM) cells, the murine *OSTL* (clone J16) was subcloned into the multiple cloning site of the modified MSCV 2.1 vector (Pineault et al., 2003) upstream of the internal ribosomal entry site (IRES) and the enhanced green fluorescent protein (GFP) gene (2.2.7.1). As a control, the empty MSCV vector carrying was used.

5.10.2. Retrovirus Production

Retrovirus was produced with the constructs mentioned above by co-transfecting 30 μg of the construct plasmid DNA with equal amounts of Ecopac DNA into 293T cells using the

calcium phosphate precipitation method (Pineault et al., 2003). Virus conditioned medium (VCM) was collected 48h after transfection at time intervals of eight hours for forty-eight hours. Production of high-titer helper-free retrovirus was achieved by transducing the ecotropic packaging cell line GP⁺E86 (Pineault et al., 2003) with virus conditioned medium (VCM) from 293T transfected cells. Successfully transduced GP⁺E86 cells were sorted out by FACS using GFP as a marker 4 days after transduction using standard procedures (Pineault et al., 2003).

5.10.3. Retroviral infection of primary BM cells

Primary mouse bone marrow (BM) cells were transduced as previously described (Pineault et al., 2003). Briefly, BM cells were obtained by flushing both femurs and tibias of donor mice treated 4 days previously with 150 mg/kg 5-fluorouracil (myeloid condition) injected into the tail vein. Mice without 5-fluorouracil treatment (for lymphoid condition) were also used in this work. 5-flourouracil eliminates cycling cells hematopoietic cells from the animal, thus enriching the bone marrow for primitive hematopoietic progenitors, which are non-cycling or quiescent in nature (Reya, 2001). Cells were stimulated for 48 hrs in DMEM supplemented with 15% FBS, 10 ng/ml IL6, 6 ng/ml IL3 and 10 ng/ml mSCF.

For lymphoid condition assays, cells were stimulated for 24 h in DMEM supplemented with 15% FBS, 10 ng/ml IL7, 6 ng/ml mutant FLT3 and 10 ng/ml mSCF.

For transduction, cells were co-cultured for 48h with irradiated (40 Gy) GP⁺E86 virus producing cells in the same medium with the addition of 5 µg/ml protamine sulfate. Protamine sulfate prevents aggregation of viral particles, thus increasing efficiency of transduction. Loosely adherent and non-adherent BM cells were harvested from the co-culture 48h post transduction, BM cells were furtherer cultured in fresh medium with cytokine cocktail for 48 h or 24 h (myeloid or lymphoid condition) to allow expression of EGFP. Transduced BM cells were sorted by fluorescence activated cell sorting (FACS) using EGFP as a marker.

5.10.4. *In Vitro* Assays

5.10.4.1. Proliferation Assay

To study the proliferative potential *in vitro* of BM cells transduced with *OSTL* expressing retroviruses, a proliferation assay was performed by plating successfully transduced bone marrow cells directly after sorting in DMEM supplemented with 15% FBS, 10 ng/ml mIL-

6, 6 ng/ml mIL-3 and 100 ng/ml murine stem cell factor (SCF) (standard medium) (Tebu-bio GmbH, Offenbach, Germany) at 37°C in a humidified 5% CO_2 incubator. The cells were subjected to half-media change every 7 days and their proliferation assessed on the day of media change by counting viable cells after trypan exclusion. To generate IL-3 dependent cell lines, successfully transduced bone marrow cells were cultured directly after sorting in DMEM, 15% FBS with IL-3 alone (6 ng/ml). A half-media change was done every 7 days.

5.10.4.2. Colony Forming Cells Assay (CFC-assay)

To analyze the differentiation and clonogenic potential of the transduced BM cells, we performed CFC assays by testing colony formation in methylcellulose. The CFC–assay was done by culture highly purified transduced cells (500/dish) in 35mm-diameter Petri dishes directly after sorting in 1ml methylcellulose supplemented with cytokines (Methocult M3434).

Colonies were counted microscopically on 7 to 9 days after plating according to standard criteria (Schwaller, 1998). Re-plating capacity of clonogenic progenitors was assayed by re-plating the primary colonies (500 cells/dish) on secondary methylcellulose dishes. Again colonies were counted at 7 to 9 days after the secondary re-plating.

5.10.5. Cyto-Morphology

Cyto-morphological analysis of bone marrow cells was done by transferring 5×10^4 to 1×10^5 bone marrow cells on glass slide by centrifugation at 500 rpm for 10 minute using a Shandon Cytospin2 centrifuge. Slides were stained with May-Grunwald's eosine-methylene blue and Giemsa solution using the standard protocol supplied by Merck.

5.10.6. Immunophenotyping

Cell differentiation was determined and lineage distribution was analyzed by immunophenotyping. 5×10^4 to 1×10^4 cells were rinsed with PBS and stained for 30 minutes on ice with an appropriate concentration of phycoerythrin (PE) conjugated antibody to Gr-1, Sca-1, Ter-119, CD4, and allophycocyanin-conjugated antibody for lineage markers Mac-1, cKit, B220 or CD8 (all Pharmingen Heidelberg, Germany). The cells were then

washed with PBS and stained with propidium iodide, and viable cells were analyzed with the FACS Calibur system.

5.10.7. BM transplantation and assessment of mice

For the bone marrow transplantation procedures, 8–10 week old recipient F1 (B6C3) mice were irradiated with 850 cGy from a ^{137}Cs γ-radiation source. FACS purified transduced BM cells or defined ratios of transduced and unpurified and untransduced cells were injected into the tail vein of irradiated recipient mice.

PB or BM cell progeny of transduced cells were tracked using GFP fluorescence (Feuring Buske, 2002). Lineage distribution was determined by flow cytometric analysis as previously described (Pineault et al., 2003).

For histological analyses, sections of selected organs were prepared and H&E stained at the Academic Pathology Laboratory, GSF, Munich, using standard protocols. The mice were under observation for early signs of leukemia. Aspiration of the blood and bone marrow was performed at 8 weeks and subsequently at four week intervals and assessed for engraftment of the mice with transduced cells and progression of disease. The early signs of disease (leukemia) development were paleness of the feet, limited mobility or lethargy, shortness of breaths or ruffled body hair. Moribund mice were sacrificed and analyzed as described.

5.10.8. Analysis of sacrificed/dead experimental mice

The PB, spleen and BM of sacrificed mice were analyzed carefully. PB was aspirated from heart with 1 ml insulin syringes; Heparin was used for anticoagulation. PB was used for blood smears on glass slides and RBC count. WBC count and immunophenotyping was performed after lysing the RBC with ammonium chloride. The spleen size was measured in diseased mice, and then homogenized for single cell suspension in DMEM medium, for further analysis by FACS, cytospin or *ex vivo* assays. BM cells were obtained by flushing both femurs and tibias and subjected to WBC count, cytospin and immunophenotyping.

5.10.9. Preparation for histopathology

The four limbs, tail and head of mice were pinned to a cork plate with needles after sacrificing the animals for histological analyses. Then the skin from the chin to the anus and also the abdominal muscles were opened in the median and also pinned down (Fig.2.3). The mice were then bled by cut one of the renal arteries, and the blood was sucked out with a tissue paper. Then the diaphragm was carefully cut away to allow the fixing liquid to penetrate into the thorax. After this the whole mouse was placed into formalin (37%) over night, packed and sent to the department of pathology (PD. Dr. Leticia Quintanilla-Fend), where the organs were cut and stained for analyses.

Fig 5.3: Schematic representation of an OSTL diseased mouse before fixation for the histopathologic analysis.

5.11. Statistical analysis

Data were evaluated using the t-test for dependent or independent samples (Microsoft Excel). Differences with p-values < 0.05 were considered statistically significant.

5.12. Computer programs

Program	Origin	Application
Adobe PhotoShop® (Mac)	Adobe Systems, USA	Conversion of scanned files
Macromedia Freehand 10.0 (Mac)	Freehand Systems, USA	Graphics
Mac Vector^{TM} 7.0	Oxford Molecular Group	Sequence analysis, primer design
Microsoft Word 98 (Mac)	Microsoft Corporation, USA	Text processing
Microsoft Excel 98 (Mac)	Microsoft Corporation, USA	Table calculations, diagrams
Microsoft Internet Explorer 5.2 (Mac)	Microsoft Corporation, USA	Internet search
Microsoft Power Point 98 (Mac)	Microsoft Corporation, USA	Graphics
OpenLab 3.1 (Mac)	OpenLab Systems, USA	Microscopy pictures

Analysis via the Internet	www Address	Application
BLAST search (Basic Local Alignment Search Tool)	http://www.ncbi.nlm.nih.gov/BLAST/	DNA or protein sequence homology search
PROSITE pattern search	http://www2.ebi.ac.uk/ppsearch/	Protein motifs search
PubMed	http://www.ncbi.nlm.nih.gov/entrez/query.fcgi?db=PubMed	Scientific Literature

6. Results

6.1. Identification of OSTL gene by sequencing

The Opposite Six Twelve Leukemia gene (*OSTL*) was identified as overlapping with the Six Twelve Leukemia gene (*STL*), which was identified as a fusion partner of *ETV6* in the SUP B2-ALL cell line (see 4.4). The *ETV6-STL* fusion gene encodes a very small protein, which lacks any known functional domains (Suto et al., 1997). Therefore we hypothesized that the main leukemogenic effect of this translocation might be the deregulation of the *OSTL* gene. *OSTL* is localized in the long arm of chromosome 6 band q23 (Figure 6.1) and shares the first exon with *STL*, but is transcribed in the opposite direction. To characterize this novel gene we completely sequenced the human and mouse *OSTL* cDNA. The *OSTL* gene used in all experiments was cloned from the human clone IMAGp998**E06**4109Q2 (reference AA992964) and from the mouse clone IMAGp998**J16**9272Q2 (reference BF165105). We have named the human *OSTL* as E06 and the mouse *Ostl* as J16. The human sequence (E06) has three alternative exons (1b, 1c, and 1d) instead of exon 1, exons 2 to exon 5, and a splice variant of exon 5 (5b), and the complete exon 6 (Figure 6.2 and tables 6.1, 6.3 and 6.4). The mouse sequence (J16) revealed the complete cDNA of *Ostl* (from exons 1 to 6) as observed in the figure 6.3, tables 6.2, 6.3, and 6.4.

In the human *OSTL* cDNA sequence the second start codon (ATG, underlined) probably represents the true translational start site, because it contains a better Kozak sequence and it is homologous to the ATG in the mouse *Ostl*. The start (ATG) and stop (TAA) codons are in bold and underlined in both human and mouse *OSTL* cDNA sequences (Figures 6.2 and 6.3).
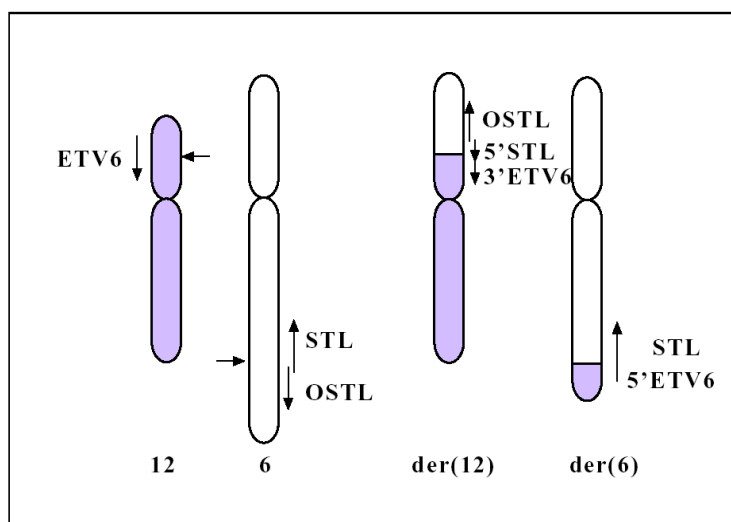
Figure 6.1: Diagram of the chromosomal localization of *OSTL*. *OSTL* and *STL* localize to the long arm of chromosome 6. They share the first exon, but are transcribed in opposite directions. *ETV6* is located in the short arm of chromosome 12. In the chromosomes on the right side the *ETV6-STL* fusion is shown.

```
1        GGCACGAGCGGCAGCATCGAGCTGGAGTTCTACCTGGCGCCCGAGCCGTTCTCCATGCCC      60
                                                                    M  P
61       AGCCTGTTGGGAGCTCCACCCTACTCTGGCCTGGGCGGTGTAGGGGATCCCTATGTGCCC      121
         S  L  L  G  A  P  P  Y  S  G  L  G  G  V  G  D  P  Y  V  P
122      CTCATGGTGCTGATGTGCCGGGTGTGCCTGGAAGACAAGCCCATCAAGCCCCTGCCTTGC      182
         L  M  V  L  M  C  R  V  C  L  E  D  K  P  I  K  P  L  P  C
183      TGCAAGAAGGCCGTGTGCGAGGAGTGCCTCAAAGTCTACCTGAGCGCCCAGGTACAACTT      243
         C  K  K  A  V  C  E  E  C  L  K  V  Y  L  S  A  Q  V  Q  L
244      GGCCAAGTAGAAATCAAATGCCCCATCACAGAGTGTTTTGAATTCTTGGAAGAAACAACT      304
         G  Q  V  E  I  K  C  P  I  T  E  C  F  E  F  L  E  E  T  T
305      GTTGTCTATAACTTAACGCATGAAGACTCCATCAAGTATAAGTACTTCTTGGAACTTGGC      365
         V  V  Y  N  L  T  H  E  D  S  I  K  Y  K  Y  F  L  E  L  G
366      CGTATTGATTCCAGCACCAAGCCATGTCCTCAGTGCAAGCACTTTACAACCTTCAAGAAA      426
         R  I  D  S  S  T  K  P  C  P  Q  C  K  H  F  T  T  F  K  K
427      AAAGGACATATTCCCACCCCTTCCAGATCAGAAAGCAAATACAAAATCCAGTGCCCTACC      487
         K  G  H  I  P  T  P  S  R  S  E  S  K  Y  K  I  Q  C  P  T
488      TGCCAATTCGTCTGGTGTTTTAAGTGCCACTCTCCTTGGCATGAAGGTGTTAACTGCAAG      548
         C  Q  F  V  W  C  F  K  C  H  S  P  W  H  E  G  V  N  C  K
549      GAGTACAAAAAAGGAGACAAAATTGTTGCGTCACTGGGCCAGCGAAATTGAGCATGGGCAG      609
         E  Y  K  K  G  D  K  L  L  R  H  W  A  S  E  I  E  H  G  Q
610      AGGAATGCCCAGAAGTGTCCAAAGTGCAAGATCCACATCCAGCGAACTGAAGGATGTGAC      670
         R  N  A  Q  K  C  P  K  C  K  I  H  I  Q  R  T  E  G  C  D
671      CATATGACCTGCTCACAATGTAACACTAATTTTTGTTACCGATGTGGTGAGAGATACCGC      731
         H  M  T  C  S  Q  C  N  T  N  F  C  Y  R  C  G  E  R  Y  R
732      CAGCTCCGATTTTTTGGAGACCACACATCAAACCTCAGTATATTTGGATGCAAATATCGC      792
         Q  L  R  F  F  G  D  H  T  S  N  L  S  I  F  G  C  K  Y  R
793      TACCTCCCAGAGAGACCTCATTTAAGGAGATTAGTGCGAGGGTCAGTCTGTGCTGGAAAA      853
         Y  L  P  E  R  P  H  L  R  R  L  V  R  G  S  V  C  A  G  K
854      TTATTCATTGCACCTCTAATTATGGTTTTGGGATTGGCACTAGGGGCCATAGCGGTTGTA      914
         L  F  I  A  P  L  I  M  V  L  G  L  A  L  G  A  I  A  V  V
915      ATCGGTTTATTTGTATTTCCTATCTATTGCCTTTGTAAAAAACAGAGAAAACGATCACGG      975
         I  G  L  F  V  F  P  I  Y  C  L  C  K  K  Q  R  K  R  S  R
976      ACAGGTATGCACTGGTAACATGCAGATGATTTCATCCAGCTAAGCTGGTTGGAGTAGGAG      1036
         T  G  M  H  W  *
1037     CGATACCAAAGGGTACACCCATCTGTGAGTCACATCTTGAAAAACACTGAGAGGAACCTT      1097
1098     CTACCATCTCATCTCCCAGTGATTCTCCGTGGGCCACAATGCCTCTAGCTATGGTGCACT      1158
1159     CCCAACATGGTATCCTGTCCTTTCCCTAAACAAATTGCTGCTGCTTTTAAAAAATGGTCA      1219
1220     CTTTCATAAACTATAAACATCTATATCATAACTCTGACCTTTGTGGTTCTTGGAAGAAGA      1280
1281     TATTTTAAGAACCAGTTATCCTAAGAATTCTGAGCACGCCTCTTCTGAGAATTGCTTGGA      1341
1342     CTGTCTTTGAACTCTGCACCTCCTCCAGGCCATCTTGTGAGACTTGGTGTTAATAGCTGA      1402
1403     AGTCCTATCTGTACCAACAAGCAAGGCCACTTTTCAGAAGATAAGAGTTCACTGAATGCA      1463
1464     CCTATTATAATCTGTGGCCCCAGCAGTATAATTCTTTTATCTTTCAAATGTTATAATTGC      1524
```

97

```
1525    AAAAAATCTCAATGTCCAAAAGGGAATGAGTGAAACTAAATTAATGAGAAGAATATTAAG    1585
1586    TTACTGAAGTGTATATGCGTAGGGGCGTGAATGTGTGTGTATATAAATATGTATTAAAAC    1640
1641    TAGGCCCAGTAACCTTGTACTTACCCAGTTCCATGCCGCTACACTATTTTTCCACATTTT    1701
1702    CATAGACCTATTGAAAGATGATGGCTCCTTTGTGGACATAATTTAGCAATGTATTAAATT    1762
1763    AAAGTCAATGTAGACAACAGGCCATTTCGATACTGAACTTTTCTATTTCTTGCTCTTTCT    1823
1824    TTTTGTCACACAAACACAGAAATTTGTGCAACGTCACCCCAAGGAGTATTAAGCTTTGTA    1884
1885    AACTGACAAACTGGCTGCTTTTAGGAAATTCTCAAGACACAAATATTCAGTCTTTTTAA    1945
1946    AATTCTTACATTTTGGAAAACATGCTTCACTCTATAGATAGATCCTTCACATTGGGATTA    2006
2007    TTTAATCCCAAAAACAAGTTTGCTGTAGACAACTGCTTAAGCCTTTAAAAAATTCCTATT    2067
2068    CTGCTAATTTTTTAACCAACTTGTAATTATAGATAATTCTGCTTTAGGTCAAGGTCTTAC    2128
2129    ATCATTTAATATCCTAACCTTGTTATCTCTTGCCTCCTCCTC                      2170
```

Figure 6.2: cDNA sequence of human *OSTL* (E06) from exon 1b to exon 6. The start and stop codons are shown in bold and underlined.

```
1      GGCCAGCAGCCCCCCGACGGTCTGCTCCTGGACGTGCTGGCCCAGCGACACCCGCCCCCC    60
61     GCCAAGCCGCAAGTCCTCTGCTCCGTGTACTGCGTGGAGAGCGACTTGCCCGAGGCCCCC    121
122    TCCGCCGAGTCCCCGTCGCCGTCGGAGTCCCCACCTCAAGCACCGCTGGGGCCGATTCCC    182
183    GCCAGCCCGCCGCCCTCCTTCCCCAGCTCCCCGCTGTCGCTCCCGGCTGACCCCCTTTCC    243
244    CCCGACGGCGGCAGCATCGAGCTGGAGTTCTACCTGGCTCCGGAGCCCTTCTCCGTGCCT    304
305    GGCCTATTAGGGGCTCCACCCTACTCTGGCCTGGGGGGAGTAGGGGACCCCTATGCGCCC    365
366    CTCATGGTGCTGATGTGCCGGGTGTGCCTGGAAGACAAACCCATCAAGCCCCTGCCCTGC    426
           M   V   L   M   C   R   V   C   L   E   D   K   P   I   K   P   L   P   C
427    TGCAAGAAGGCGGTGTGCGAGGAGTGCCTCAAAATCTACCTGAGCTCTCAGGTACAACTT    487
           C   K   K   A   V   C   E   E   C   L   K   I   Y   L   S   S   Q   V   Q   L
488    GGCCAAGTAGAAATCAAATGCCCAGTCACAGAGTGTTTCGAATTCCTGGAGGAAACAACT    548
           G   Q   V   E   I   K   C   P   V   T   E   C   F   E   F   L   E   E   T   T
549    GTTGTCTACAATTTAACCCATGAGGACTCTATCAAGTATAAGTACTTCTTGGAACTTGGC    609
           V   V   Y   N   L   T   H   E   D   S   I   K   Y   K   Y   F   L   E   L   G
610    CGAATTGACTCCAGCACCAAGCCATGTCCTCAATGCAAACACTTCACAACCTTTAAGAAA    670
           R   I   D   S   S   T   K   P   C   P   Q   C   K   H   F   T   T   F   K   K
671    AAAGGACATATCCCCACTCCTTCCAGATCAGAAAGCAGATACAAAATCCAGTGTCCCACT    731
           K   G   H   I   P   T   P   S   R   S   E   S   R   Y   K   I   Q   C   P   T
732    TGCCAATTGATCTGGTGTTTTAAGTGCCACTCTCCTTGGCATGAAGGTGTTAACTGCAAG    792
           C   Q   L   I   W   C   F   Q   C   H   S   P   W   H   E   G   V   N   C   K
793    GAGTACAAAAAGGAGACAAGTTACTGCGTCACTGGGCCAGTGAGATTGAGCACGGGCAG    853
           E   Y   K   K   G   D   K   L   L   R   H   W   A   S   E   I   E   H   G   Q
854    AGAAATGCCCAGAAGTGTCCAAAGTGCAAGATCCATATCCAGAGAACAGAAGGGTGTGAC    914
           R   N   A   Q   K   C   P   K   C   K   I   H   I   Q   R   T   E   G   C   D
915    CATATGACTTGTTCACAGTGTAACACTAATTTTTGCTATCGATGTGGAGAGAGATACCGC    975
           H   M   T   C   S   Q   C   N   T   N   F   C   Y   R   C   G   E   R   Y   R
976    CAGCTCCGATTTTTCGGAGACCACACATCAAACCTCAGTATATTTGGATGCAAATATCGC    1036
           Q   L   R   F   F   G   D   H   T   S   N   L   S   I   F   G   C   K   Y   R
1037   TACCTCCCAGAGAGACCTCATTTAAGAAGATTAGTTCGAGGGTCAGTCTGTGCTGGAAAG    1097
           Y   L   P   E   R   P   H   L   R   R   L   V   R   G   S   V   C   A   G   K
1098   CTCTTCATTGCGCCTCTCATCCTGGTTTTGGGATTGGCACTAGGGGCCATAGCAGTTGTA    1158
           L   F   I   A   P   L   I   L   V   L   G   L   A   L   G   A   I   A   V   V
1159   ATCGGTTTATTTGTATTTCCTATATATTGCCTTTGTAAAAAACAGAGAAAGCGATCACGG    1219
           I   G   L   F   V   F   P   I   Y   C   L   C   K   K   Q   R   K   R   S   R
1220   ACAGGTATGCACTGGTAATCCACAGAGGATTTCACATGATGTCAGCCGGTACCGGGAGGA    1280
           T   G   M   H   W   *
1281   GCCATGCAGGATGGTGCACTTGTCTGTGAGTTGGATCCTTAAAACTACCTAGAGGAACTT    1341
1342   CTGCCATCTTGTCTCCTGTGGTTCTCTGCAGACCACAGTGCCTCTAGCTACGGTGCACTC    1402
1403   TCAACATGGCATCCTGTCCTTTCCTTAAGCAGATTCGTGCTTTTTAAAAAAATGGTCACT    1463
1464   TTCGTTAACTATATACATTTATATAGTAACTCTCACCTTTGTGGTTCTTGGAAGAAAATA    1524
1525   TTTTGAGAACAGGATATCCTCAGATGTCTTTTGAGGATACCTCACCTGGAGTGTTATTTG    1585
1586   GATTGTCTGAACCTTGTGCTTCCCCCGGGCTGTCTCTGAGACATGGTATGCATAGCTGAA    1640
1641   TCCGGCCTGTCTCAACAAACAAGGCCACTTTTCAGAAGATAAATCAAGTTCACCAAATGT    1701
1702   ACCTAATTGTCCTCTGTAACCCAAATGGTATCATCGTTTTGTTTTTTGGATACTGTAATT    1762
1763   GCTTTAAAAAAAAAGTGTCAGCACCCAGAGGGAATTAATGAAACTAAATTAATGAAAGA    1823
1824   ACCATGAGTTACTGGTCCGTCTATGTAAGGATGTGAATGTGTGTATATAAACACGTATTA    1884
1885   AACCAGGCTCCATAACCATGTGCTTGCCTATTTCCATGTCTATTTTCATAGAACCTTTCA    1945
1946   GGCCTTGATGGTTATTTTTGTGGGCCTAACTTGGTAATGTACTGAATTAAAGCCAATGTC    2006
2007   AACAACAAAAAAAAAA                                                2022
```

Figure 6.3: cDNA sequence of mouse *Ostl* (J16). The whole mouse *Ostl* sequence from exon 1 to exon 6. The start and stop codons are shown in bold and underlined.

6.1.1. Characterization of the OSTL protein

We searched the protein databases for homologous protein sequences using the OSTL protein. After sequence analysis and comparison with known proteins in the database, we were able to identify the OSTL protein domains.

As represented in figure 6.4, we could identify three domains, one at the N terminal region from aa 5 until aa 51 (46 aa), representing a variant RING finger domain, a second domain, from aa 88 until aa 138 (50 aa) representing an in-between-RING finger domain (IBR) also known as double RING finger linked motif (DRIL) and a consensus RING finger was found in the C terminal region from aa 165 until aa 194 (29 aa).

In the variant N terminal RING finger of OSTL, there is a lysine (K) instead of an histidine (H) in the 4th position.

We searched the *Fugu rubripes* database for homologous sequences using segments of the human and mouse OSTL protein. *Fugu* genome is the smallest vertebrate genome and has proved to be a valuable reference genome for identifying genes.

There are two possible start codons in the human *OSTL* as commented in 6.1. In our studies, we used the second ATG (Figure 6.2 and 6.3), which was homology in the human and mouse *OSTL* sequence and is embedded in a better Kozak sequence. The ORFs (open reading frames) obtained encoded a 275 aa protein for human OSTL and a 307 aa protein for mouse Ostl as shown in table 6.1.

Human and mouse protein show 98% identity over their amino acid sequence, there are only 8 aa that are not identical (underlined in figure 6.5). The homology between human OSTL and *Fugu* Ostl is 86%, indicating that *OSTL* is highly conserved between species. The three domains of OSTL are 100% conserved in *Fugu*, human and mouse. The domains of OSTL are color-coded in figures 6.4 and 6.5.

IBR (in Between RING fingers) or DRIL (Double RING finger Linked) Domain (C6HC) aa 88-138

```
Consensus:     C-x4-C-x(14-30)-C-x(1-4)-C-x4-C-x2-C-x4-H-x4-C
In OSTL:       C-x2-C-x24      -C-x2    -C-x4-C-x2-C-x4-H-x4-C
```

Variant RING-finger 1 (C8) and canonical RING-finger 2 motif (C3HC4) aa 5-51 and aa 165-194

```
Consensus:   C-x2-C-x(9-39)-C-x(1-3)-H-x(2-3)-C-x2-C-x(4-48)-C-x2-C
Variant 1:   C-x2-C-x10     -C       -K-x2     -C-x2-C-x17     -C-x4-C
In OSTL (2): C-x2-C-x9      -C-x      -H-x2     -C-x2-C-x4      -C-x2-C
```

Figure 6.4: OSTL protein domains and comparison with consensus motifs. The three domains are schematically represented in color (pink: variant RING 1; blue: IBR; yellow: RING 2), the amino acids correspond to the human OSTL protein.

```
Fugu OSTL     1 AVRGCRVCLEGKSIAPLPCCRKAVCNECLGLYVSSQVRLAKSHINCPIYE  50
human OSTL    1 MVLMCRVCLEDKPIKPLPCCKKAVCEECLKVYLSAQVQLGQVEIKCPITE  50
mouse OSTL    1 MVLMCRVCLEDKPIKPLPCCKKAVCEECLKIYLSSQVQLGQVEIKCPVTE  50
                *  ****** * * ***** **** ***  .* .*.**.* .   * **. *

Fugu OSTL    51 CRGYLEEGVVISNLSKEDAEKYHYFLELSQLDSSTKPCPQCSQFTTLR--  98
human OSTL   51 CPEFLEETTVVYNLTHEDSIKYKYFLELGRIDSSTKPCPQCKHFTTFKKK 100
mouse OSTL   51 CFEFLEETTVVYNLTHEDSIKYKYFLELGRIDSSTKPCPQCKHFTTFKKK 100
                *  .***  *. **..**. **.***** ..********** .*** .

Fugu OSTL    99 EHNSN--RSEHKYKIQCSNCQFLWCFKCHAPWHNGLKCRQYRKGDKLLRT 146
human OSTL  101 GHIPTPSRSESKYKIQCPTCQFVWCFKCHSPWHEGVNCKEYKKGDKLLRH 150
mouse OSTL  101 GHIPTPSRSESRYKIQCPTCQLIWCFKCHSPWHEGVNCKEYKKGDKLLRH 150
                *   .   *** .***** .** .****.*** *. *...*.*******

Fugu OSTL   147 WASVIEHGQRNAQKCPQCKIHIQRTEGCDHMTCTQCSTNFCYRCGERYRH 196
human OSTL  151 WASEIEHGQRNAQKCPKCKIHIQRTEGCDHMTCSQCNTNFCYRCGERYRQ 200
mouse OSTL  151 WASEIEHGQRNAQKCPKCKIHIQRTEGCDHMTCSQCNTNFCYRCGERYRQ 200
                *** ************* .***************.** *********** .

Fugu OSTL   197 LRFFGDHTSNLSVFGCKYRYLPDKPHLRRFIRGSVCATKLLIAPVVLLLV 246
human OSTL  201 LRFFGDHTSNLSIFGCKYRYLPERPHLRRLVRGSVCAGKLFIAPLIMVLG 250
mouse OSTL  201 LRFFGDHTSNLSIFGCKYRYLPERPHLRRLVRGSVCAGKLFIAPLILVLG 250
                ************.********** .***** .****** ** ***...*

Fugu OSTL   247 VVVGALALVI                       256
human OSTL  251 LALGAIAVIGLFVFPIYCLCKKQRKRSRTGMHW 283
mouse OSTL  251 LALGAIAVVIGLFVFPIYCLCKKQRKRSRTGMHW 283
                . .**.*.*******************
```

Figure 6.5: Domains of OSTL protein and comparison between *Fugu*, human and mouse sequences. The differences between human and mouse aa sequences are underlined. The color bars represent the three protein domains of OSTL (pink: variant RING finger 1; blue: IBR or DRIL; yellow: RING finger 2). The aa without grey background are different between human, mouse, and fugu OSTL protein.

6.1.2. Genomic map of the *STL/OSTL* loci

The *STL* and *OSTL* genes share the first exon (as represented in figures 6.1 and 6.6), but they are transcribed in the opposite directions (striped bar in figure 6.6). Comparison of genomic and cDNA sequences suggested that the cDNA fragment of human clone AA992964 (E06) comprises exons 1b (nt 138710 to 138810 from EST AL355296), 1c (nt 140938 to 141125 from EST AL355296), 1d (nt 141657 to 141765 from AL355296), 2 (nt 18684 to 18917 from AL136128), 3 (nt 31415 to 31579 from AL136128), 4 (nt 50130 to 50331 from AL136128), 5 (nt 54909 to 54980 from AL136128), 5b (nt 55922 to 56036 from AL136128), and 6 (nt 56337 to 57575 from AL136128), and the cDNA sequence of mouse clone BF165105 (J16) corresponds to human exons 1 (nt95694 to 95912 from AL355296), 2, 3, 4, 5, and 6 as observed in figure 6.6, and tables 6.1, 6.2 and 6.4.

OSTL is composed for six exons, with a total cDNA length of 2125 bp and several splice variants (see 6.1.3). The exon-intron boundaries of human and mouse *OSTL* are listed in tables 6.1 and 6.2.

There are only two nucleotides in the splice donors not identical in both sequences (human and mouse *OSTL*), shown in the table 6.2 (in bold), in the intron 1 (were a guanine and a cystosine in the human sequence are replaced by thymidines in the mouse sequence).
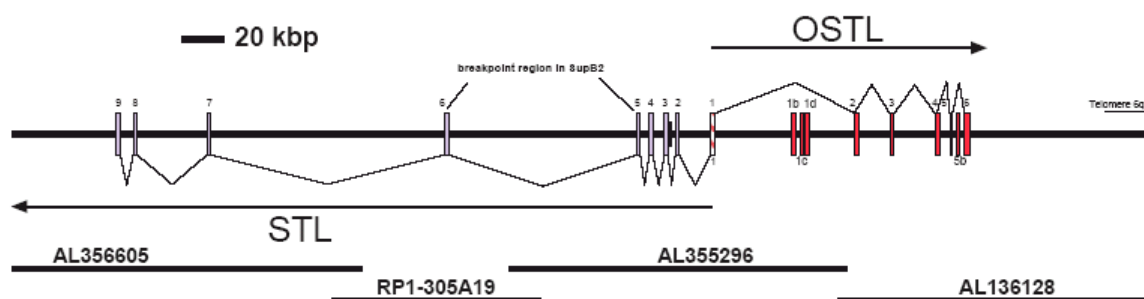
Figure 6.6: Map of *STL/OSTL* loci and position in the genomic sequence. The 6 *STL* exons are shown in pink bars, the exons and splice variants of *OSTL* from exon 1 (1b, 1c, and 1d) and from exon 5 (5b) are represented with red bars. The genomic sequences AL355296 and AL136128 and respective position in the map are represented in the lower black bars.

Table 6.1: Exon-intron boundaries of h*OSTL*

Intron	Splice acceptor	Exon	Splice donor
		Exon 1 (218 bp)	AGCGCCCAGgtaacttcac
Intron 1 (77kbp)	ccatcatgcagGTACAACTT	Exon 2 (233 bp)	AAATACAAAgtaagcattt
Intron 2 (12kbp)	ttcttacacagATCCAGTGC	Exon 3 (164 bp)	AAGTGCAAGgtgagataac
Intron 3 (18kbp)	tgctgatacagATCCACATC	Exon 4 (201 bp)	CAGTCTGTGgtgagtgtct
Intron 4 (4 kbp)	ttgttttccagCTGGAAAAT	Exon 5 (71 bp)	TTGTAATCGgtaagaaacac
Intron 5 (1 kbp)	cttatccctagGTTTATTTG	Exon 6 (1238 bp)	

Table 6.2: Exon-intron boundaries of m*Ostl*

Intron	Splice acceptor	Exon	Splice donor
		Exon 1 (218 bp)	AGC**TCT**CAGgtaacttcac
Intron 1 (77kbp)	ccatcatgcagGTACAACTT	Exon 2 (233 bp)	AAATACAAAgtaagcattt
Intron 2 (12kbp)	ttcttacacagATCCAGTGC	Exon 3 (164 bp)	AAGTGCAAGgtgagataac
Intron 3 (18kbp)	tgctgatacagATCCACATC	Exon 4 (201 bp)	CAGTCTGTGgtgagtgtct
Intron 4 (4 kbp)	ttgttttccagCTGGAAAGC	Exon 5 (71 bp)	TTGTAATCGgtaagaaacac
Intron 5 (1 kbp)	cttatccctagGTTTATTTG	Exon 6 (1238 bp)	

6.1.3. Identification of splice variants of the *OSTL* gene

In order to characterize and identify other possible splice variant of *OSTL,* we analyzed the EST clones AW859482, AA776581, AA373303. The exons contained in these EST clones and the proteins encoded by each clone are shown in the table 6.3, together with mouse (J16) and human (E06) *OSTL* clones. For a complete overview of the *OSTL* splice variant forms we included in our analysis the data obtained from the RT-PCR experiments of *OSTL* during B cell development (Figure 6.12). The RT-PCRs were performed in Markus Müschen's Laboratory (Düsseldorf). The sequence analysis observed for each expression bands (fragments of 848, 778, and 543 bp) of *OSTL* in the RT-PCR are represented in the table 6.3. There are seven splice variant forms of *OSTL* that transcribe significant OSTL protein as observed in table 6.4. The complete map of *OSTL* with the seven splice variant forms is demonstrated in figure 6.7.

Table 6.3: Characterization of *OSTL* splice variants and the corresponding proteins

OSTL no.	Clone/sequence reference	Exons	Transcribed Protein
1	Mouse BF165105	1, 2, 3, 4, 5, and 6	Ostl no.1 307 aa
2	Human AA992964	1b, 1c, 1d, 2, 3, 4, 5, 5b, and 6	OSTL no.2 275 aa
3	AW859482 and AA776581	2, 2a, 2b, and 3	OSTL no.3 ~ 91 aa
4	AA373303	1, and p1a (partial 1a)	OSTL no. 4 ~ 99 aa
5	Fragment from naïve B cells of 848 bp	2, 3, 4, 4b, 5, and 6	OSTL no. 5 ~ 256 aa
6	Fragment from naïve, memory and plasma B cell of 778 bp	2, 3, 4, 5, and 6	OSTL no. 6 ~ 248 aa
7	Fragement from memory B cell of 543 bp	3, 4, 5, and 6	OSTL no. 7 ~ 205 aa

Table 6.4: *OSTL* exon names, nucleotide positions in the genomic sequence and splice variants

Exon no.	Nt from to (access no.)	Splice 1	Splice 2	Splice 3	Splice 4	Splice 5	Splice 6	Splice 7
1	95694-95912 AL355296	X			X			
p1a	103960-104081 AL355296				X			
1b	138710-138810 AL355296		X					
1c	140938-141125 AL355296		X					
1d	141657-141765 AL355296		X					
2	18684-18917 AL136128	X	X	X		X	X	
2a	20080-20134 AL136128			X				
2b	21625-21732 AL136128			X				
3	31415-31579 AL136128	X	X	X		X	X	X
4	50130-50331 AL136128	X	X			X	X	X
4b	54568-54637 AL136128					X		
5	54909-54980 AL136128	X	X			X	X	X
5b	55922-56036 AL136128		X			X		
6	56337-57575 AL136128	X	X			X	X	X
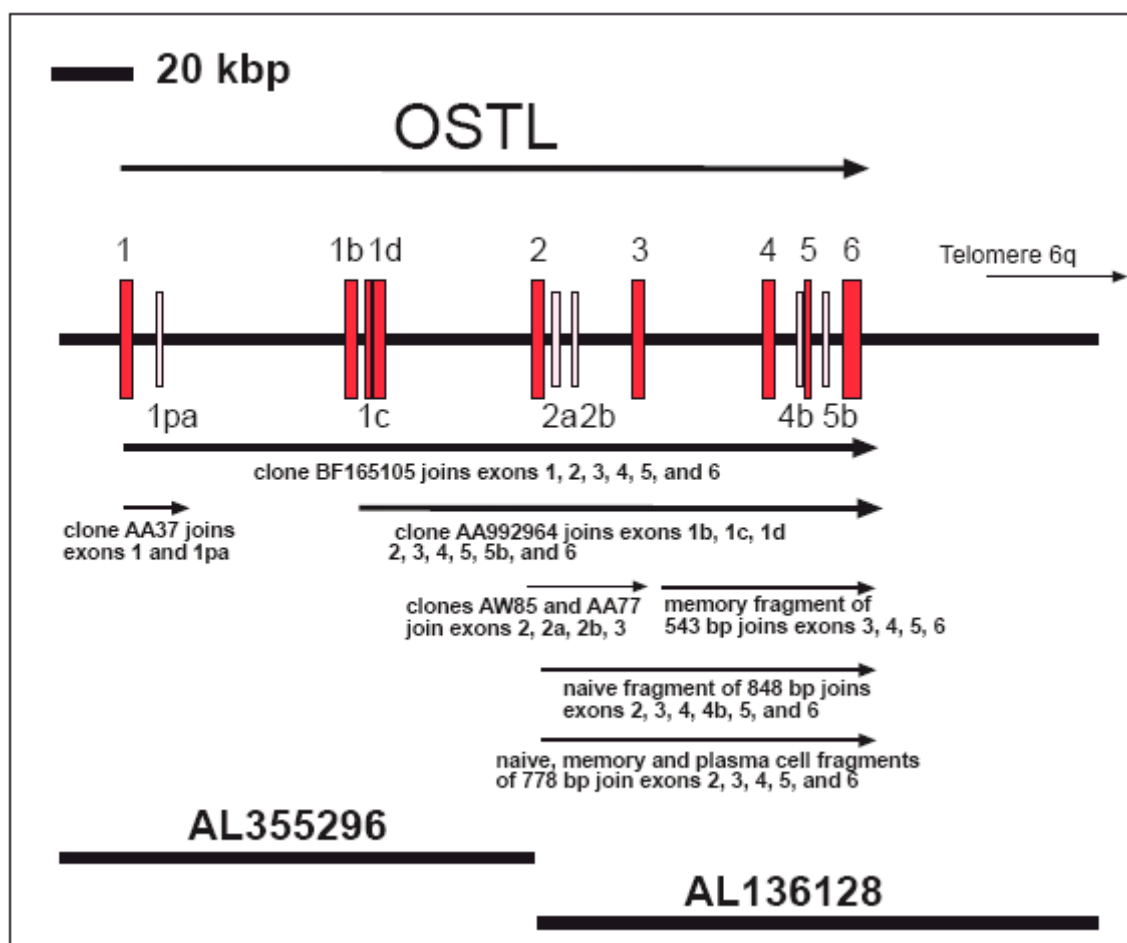
Figure 6.7: Map of *OSTL* locus showing seven splice variants and their position in the genomic sequence. The 6 *OSTL* exons are represented with pink bars, the splice variants from exon 1 (1pa, 1b, 1c, and 1d), exon 2 (2a, and 2b), exon 4 (4b), and exon 5 (5b) are represented with red bars. The arrows correspond to the seven splice variants of *OSTL*. The genomic sequences AL355296 and AL136128 are indicated with the lower black bars.

6.2. Expression of OSTL at RNA level

6.2.1. Mouse multiple tissue Northern Blot

To analyze the expression of *Ostl* in different mouse tissues, RNA was extracted from heart, liver, ovary, spleen, testis, kidney, thymus, bone marrow, and brain (see 5.3.5) from a normal 4 weeks old BALB/c mouse. A Northern blot with these mouse tissues was hybridized with a 748 bp *OSTL* cDNA probe (see 5.3.5), PCR amplified from mouse testis with primers OSTLEx1dATGXhoI and OSTL983BPstI (see table 5.1). An *Ostl* tanscript of 3.5 kbp could be clearly detected in liver, ovary and testis RNAs (Figure 6.8). A GAPDH probe was used as control for RNA quality (see 5.3.5.4).
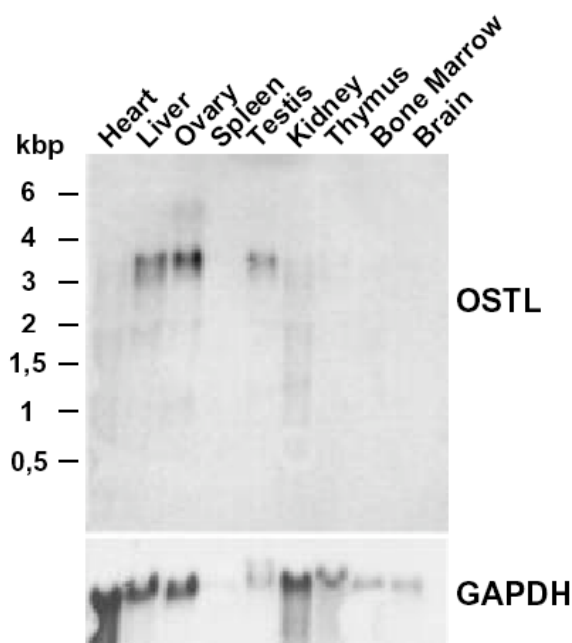
Figure 6.8: Mouse multiple tissue Northern Blot. *mOstl* is expressed in liver, ovary and testis.

6.2.2. Human multiple tissue Northern blot

To analyze the expression of *OSTL* in different human tissues, a commercial human multiple tissues Northern (Clontech) was hybridized with the same *OSTL* probe as for the mouse Northern (see 6.2.1). *OSTL* transcripts of 9.5, 4.4, and 1.35 kbp were detected in testis and *OSTL* transcripts of 9.5, 4.4, and 2.4 kbp were detected in skeletal muscle (Fig. 6.9). Weak *OSTL* transcripts could be observed in prostate, ovary, heart, placenta, liver, and pancreas. An actin was used as control for RNA quality.
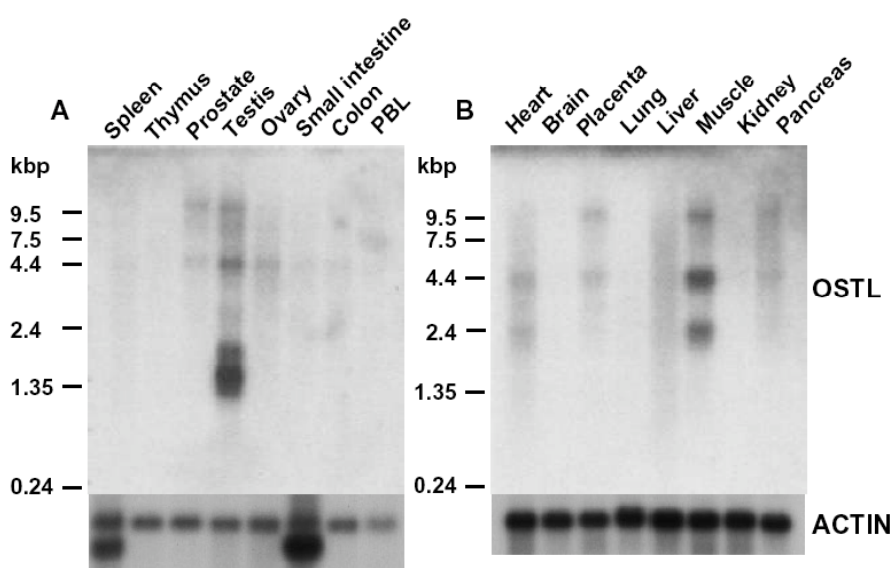
Figure 6.9 A and B: Human multiple tissue Northern blot. h*OSTL* is highly expressed in testis, and skeletal muscle; weak expression is observed in prostate, ovary, small intestine, heart, placenta, liver, and pancreas.

6.2.3. Human cells Northern Blot

To analyze the expression of *OSTL* in different human cell lines, RNA was extracted from BL2, BL41, BL70, DOHH2, Granta 519, Karpas 422, NCEB-1, three transformed lymphoblastoid cells from different patients (LCL B, LCL D, and LCL R), and Wsu-NHL cells (see 5.2.5 and 5.3.5). The Northern blot from human cell lines was hybridized with the same *OSTL* probe as described before (6.2.1). An *OSTL* transcript of 5.0 kbp was be detected in Karpas and in the three LCL samples (Figure 6.10). An actin probe was used as control for RNA quality.
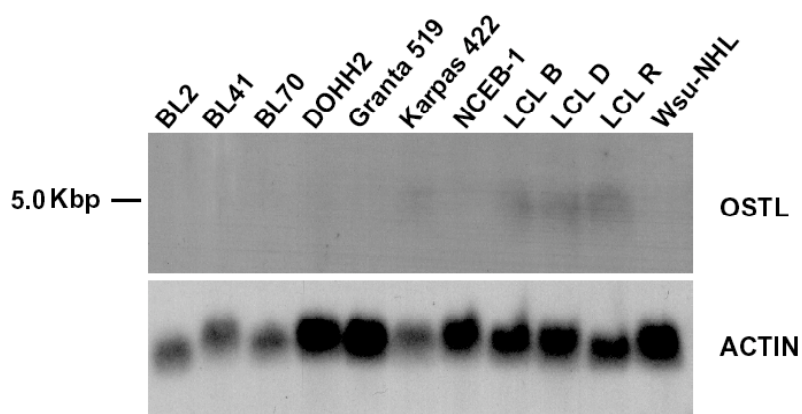
Figure 6.10: Human cell line Northern blot. h*OSTL* is expressed in Karpas 422, and LCLs cells (B, D, and R).

6.2.4. RT-PCR with Human cells

In order to confirm the expression of *OSTL* observed by the Northern blot in the different human cell lines (figure 6.10) we performed RT-PCR on RNA from the above cell lines and from two additional lines: SEM and Nalm6 (see 5.2.5). cDNA was synthesized from each cell line (see 5.3.6) after treatment of the RNA samples with *DNaseI*. *OSTL* primer pairs 5': E06OSTL601T and 3': E06OSTL761B (see table 5.1) were used for amplification. PCR reaction was performed as described in the section 5.3.4.1, using 35 cycles.

Amplification of a 1.16 kbp fragment was observed in Granta 519, two transformed lymphoblastoid patient cells (LCL B, and LCL D) and by SEM cell line. TATA binding protein (TBP) primers (see table 5.1) were used as controls for cDNAs quality (figure 6.11). Interestingly, the expression pattern observed in the Northern cell lines was not the same as the one obtained in the RT-PCR which could be due to the presence of alternatively spliced transcripts in the cell lines which can not be amplified with the primers used.
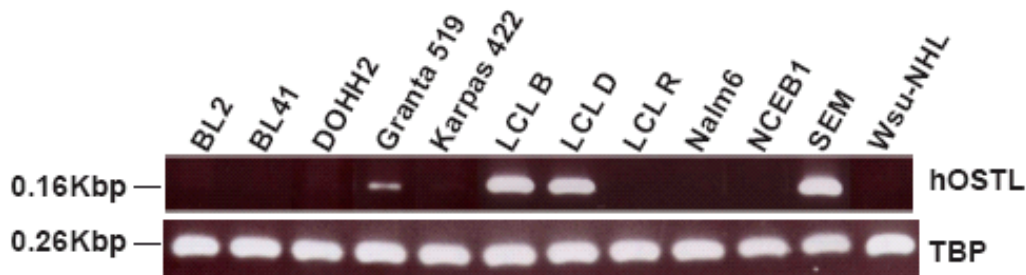
Figure 6.11: Human cells RT-PCR. h*OSTL* is expressed in Granta 519, LCL B and LCL D cells.

6.2.5. RT-PCR with B cells of different developmental stages

In order to analyze the *OSTL* expression during B cell development, RT-PCR was performed in Markus Müschen's laboratory using B cells from the early developmental stages Pre-B, and B1, Naïve, and from B cells from the later stages, plasma B cell and memory B cells. The SEM cell line was used as positive control for *OSTL* expression. GAPDH was used as control for cDNAs quality. *OSTL* primer pairs 5': OSTLE06205T and 3': OSTL983BPstI (see table 5.1) were used for amplification (figure 6.12).

The PCR reaction was performed as described in section 5.3.4.1, using 30 cycles. As observed in the figure 6.12, a 1.1 kbp *OSTL* fragment could be detected in Pre-B cells; three fragments of 1.2, 1.0, and 0.76 kbp were detected in B1; four fragments of 1.3, 0.91, 0.85, and 0.78 kbp were observed by naïve; four fragments of 0.95, 0.86, 0.78, and 0.54 kbp were detected by memory B cell and finally two *OSTL* fragments of 0.93, and 0.78 kbp were observed in plasma B cell. All the fragments were purified from the gel and sequenced. Naïve, memory, and plasma B cells fragments (see table 6.3) can encode bigger OSTL proteins.
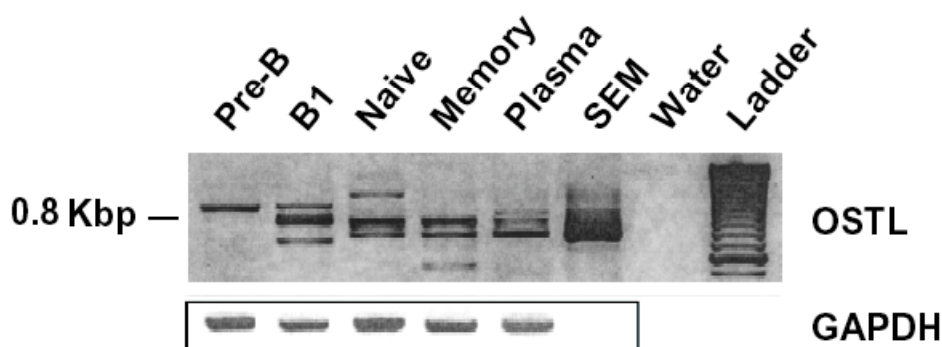
Figure 6.12: RT-PCR with B cells in different developmental stages. *OSTL* is expressed is all B cell stages. SEM cell line was used as positive control for *OSTL* expression.

6.2.6. RT-PCR with leukemic and normal patient bone marrow samples

In order to analyze the expression of *OSTL* in different leukemia patient samples, RT-PCRs were performed. For *OSTL* expression the same primer pairs and PCR program as for the human cell lines RT-PCR (see 6.2.4) were used.

For the first RT-PCR (Figure 6.13), three AML samples (AML M1, AML M4, and an AML with a *CALM-AF10* translocation), and two ALLs (ALL with *CALM-AF10* translocation and T-ALL with *CALM-AF10* translocation) were used.

A 0.16 kbp fragment was amplified in all leukemia patient cDNAs, as shown in figure 6.13. RT-PCR was also performed with normal human bone marrow sample, three pro-B-ALL patient samples, one pre-T-ALL, and two pro-T-ALLs as shown in figure 6.14. *OSTL* expression was observed in all the patient cDNAs (human normal BM, pro-B-ALL, pre-T-ALL, and pro-T-ALL), with a very weak expression in the pro-T-ALL 25 samples (Figure 6.14).
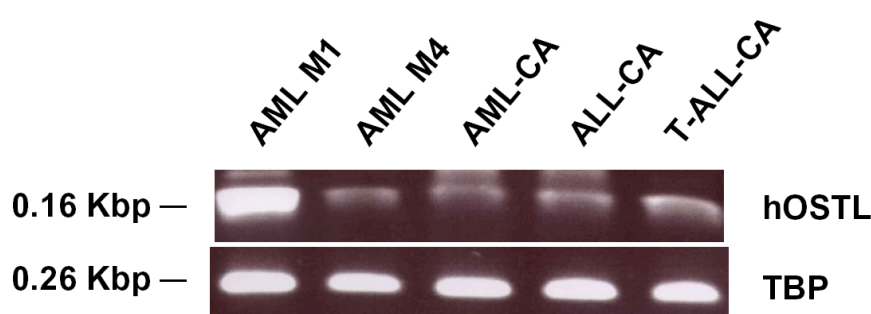
Figure 6.13: RT-PCR with leukemia patient cDNAs.
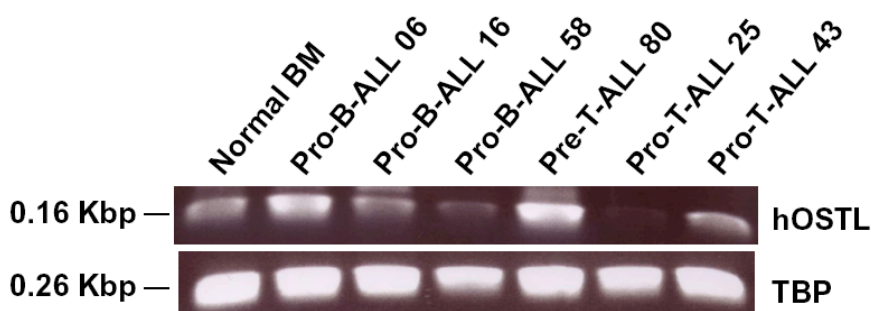
Figure 6.14: RT-PCR with normal bone marrow, B-ALL and T-ALL leukemia patient cDNAs.

6.3. Sub-cellular localization of OSTL

Cloning

In order to analyse the sub-cellular localization of *OSTL*, the *OSTL* encoding cDNA was cloned into pEGFP (Clontech) for the OSTL protein to be expressed as a fusion with the enhanced green fluorescent protein.

The *OSTL* insert was PCR amplified from the human clone E06, using the primers 5': OSTLEx1dATGXhoI and 3': OSTL983BPstI (table 5.1).

The recombinant plasmid was sequenced across the 5' cloning site with the primer pEGFP-C11240 (table 5.1) to confirm that the insert was in frame with the GFP open reading frame. The pEGFP-C1-*OSTL* (E06) construct is schematically shown in the figure 6.15.

Figure 6.15: Schematic representation of the protein encoded by the pEGFP-*OSTL* construct. The human *OSTL* insert (E06) is shown in blue (Nt 233 – Nt 983). The open reading frame (ATG) and stop codon (TAA) of *OSTL* insert are underlined. The restriction enzymes used to clone *OSTL* into pEGPF vector are shown in red (*XhoI* and *PstI*).

Transfection and sub-cellular localization experiments

We analysed the sub-cellular localization of fluorescent protein tagged OSTL protein by transiently expressing these proteins in the mouse fibroblast cell line NIH3T3 (see 5.5.1). Cells were observed 24 hours after transfection with an inverted epi-fluorescence microscope (Zeiss Axiovert 200 M) (see 5.5.3). After formaldehyde fixation, the transfected cells were photographed (see 5.5.2 and 5.5.3). OSTL localizes to the cytoplasm of the cells (figure 6.16 A). The transfected cells were counterstained with DAPI (figure 6.16 B). A merged image the GFP and DAPI channel is shown in figure 6.16 C. Figure 6.16 D shows a phase contrast picure of the same cell.
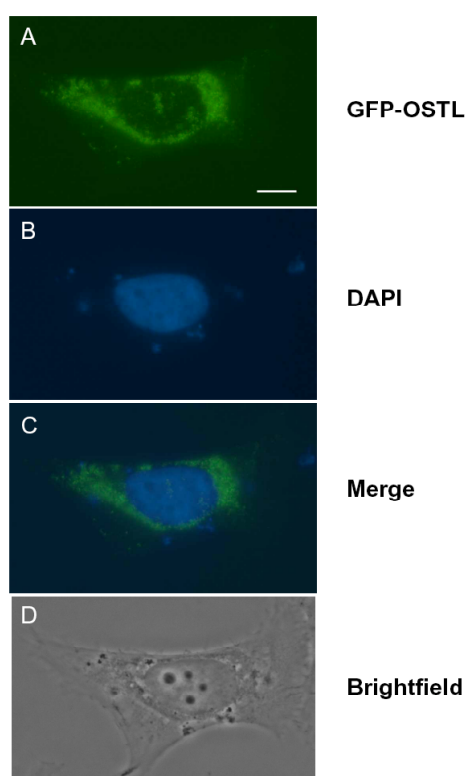
Figure 6.16: Sub-cellular localization of OSTL. A NIH3T3 cell transiently transfected with pEGFP-*OSTL* was visualized with a GFP filter, a DAPI filter and in phase contrast. Scale bar = 10 μm.

Protein expression

In order to confirm the expression of the OSTL protein from our fluorescent construct, we over-expressed the protein in the embryonal kidney cell line HEK293T and performed Western analysis (see 5.6.). The GFP-OSTL protein was detected with a commercial anti-GFP antibody (figure 6.17).
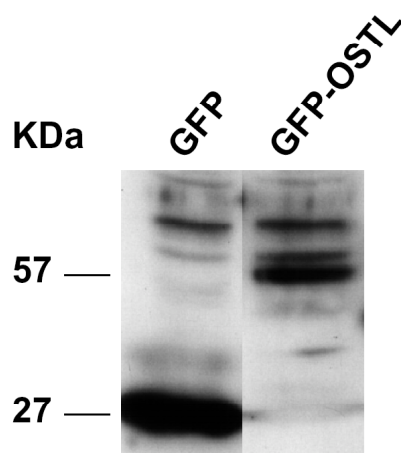
Figure 6.17: 10% SDS PAGE gel. Western blot of protein extract (10 μg/lane) from HEK 293T cells transiently-transfected with pEGFP empty (GFP lane) or pEGFP-OSTL (GFP-OSTL lane). Protein extracts were incubated with a rabbit anti-GFP antibody (1:3000) for 1 hour at RT and secondary antibody, donkey anti-rabbit HRP-conjugated. Detection was performed using ECL chemiluminescence kit, with exposure-time of 3 sec. Bands of 27 and 57 kDa molecular weight, correspond to the GFP and to the GFP-OSTL proteins.

6.4. Whole mount in situ hybridization

In order to analyze the expression pattern of *Ostl* during mouse embryonic development, we performed whole mount *in situ* hybridization experiments. *OSTL* RNA samples were prepared to hybridize BALB/c mouse embryos from 9.5 days post coitum (d.p.c.) on until 14.5 d.p.c. An *OSTL* insert of 748 bp was PCR amplified (see 5.3.4.1) from mouse testis with primers, 5': OSTLEx1dATGXhoI and 3': OSTL983BPstI (see table 5.1). The insert was gel purified and subcloned into pGEMT-easy vector (see 5.2.8.3).

Ostl showed a distinct expression pattern during mouse embryonal development. Figure 6.18 shows the expression of *Ostl* in mouse embryos of 9.5 (A1-4), 10.5 (B1-5), 11.5 (C1-4), and 12.5 (D1-4) d.p.c. The expression is observed in otic vesicle, optic vesicle, nostrils, prominent in somites, first and second limb buds, branchial arches, and closed posterior neuropore.

Ostl is strongly expressed in limb development (Figure 6.19).

In the earlier stages, expression is more prominent in the anterior region of the limb buds (Figures 6.19 A and B -limb buds of 11.5 d.p.c. embryo). At 12.5 d.p.c. expression divides into a proximal domain in the region of the prospective handplate and a distal domain including the mesodermal ridge (Figures 6.19 C and D).

Horizontal, transverse, and sagital sections of whole-mounts stained from 9.5 on until 13.5 d.p.c. embryos, showed expression of *Ostl* mainly in the somites and limb buds (figure 6.20).
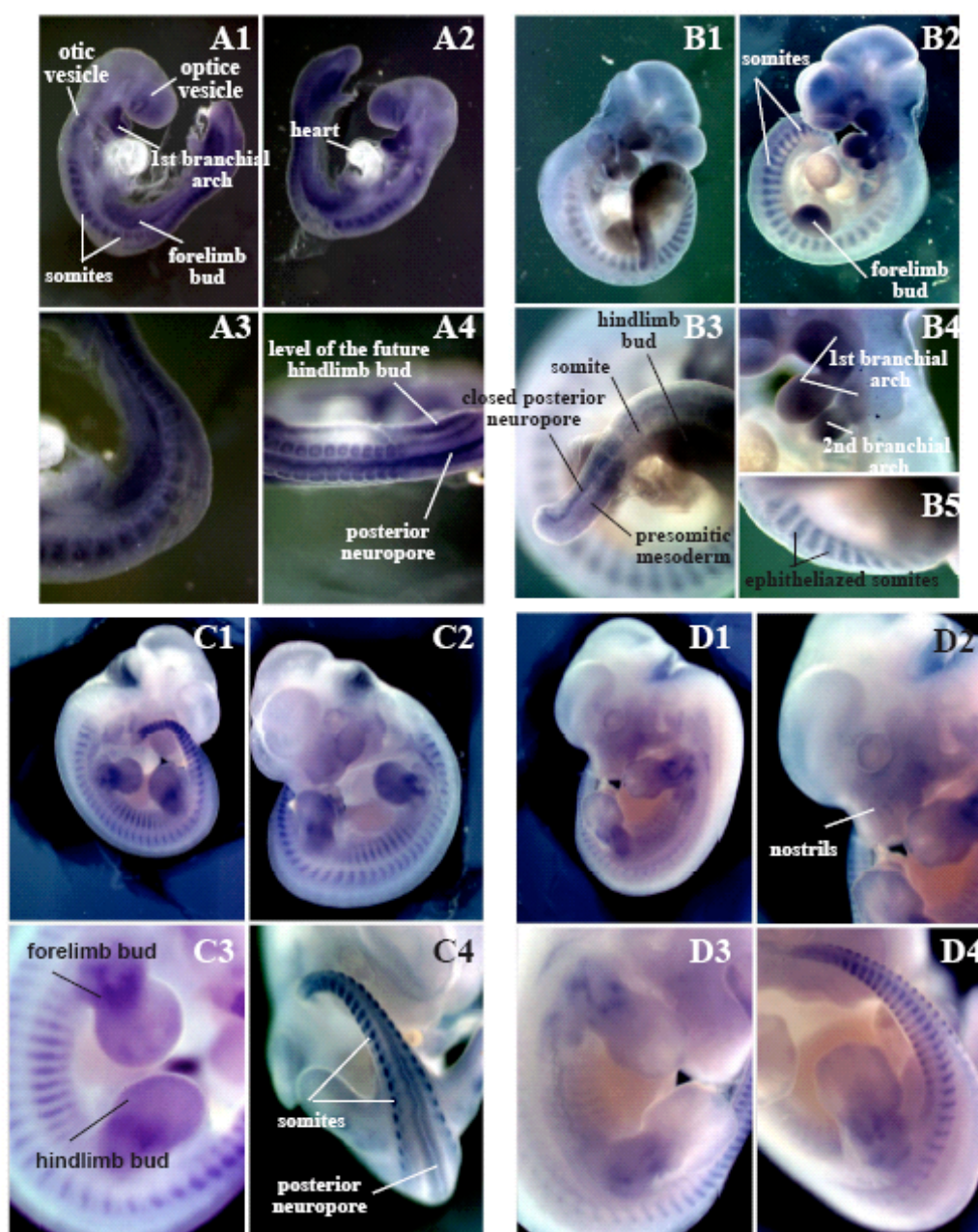
Figure 6.18: (A-D) Whole mount *in situ* hybridization of *Ostl* in mouse embryos. (A1) right lateral, **(A2)** left lateral, **(A3)** caudal lateral, **(A4)** caudal view of a 9.5 d.p.c. mouse embryo; **(B1)** right lateral, **(B2)** left lateral, **(B3)** caudal, **(B4)** branchial arches, **(B5)** caudal view of a 10.5 d.p.c. embryo; **(C1)** right lateral, **(C2)** left lateral, **(C3)** limb buds, **(C4)** frontal caudal view of a 11.5 d.p.c. mouse embryo; **(D1)** left lateral, **(D2)** nostrils, **(D3)** limb buds, **(D4)** hind limb bud and caudal view of a 12.5 d.p.c. embryo.
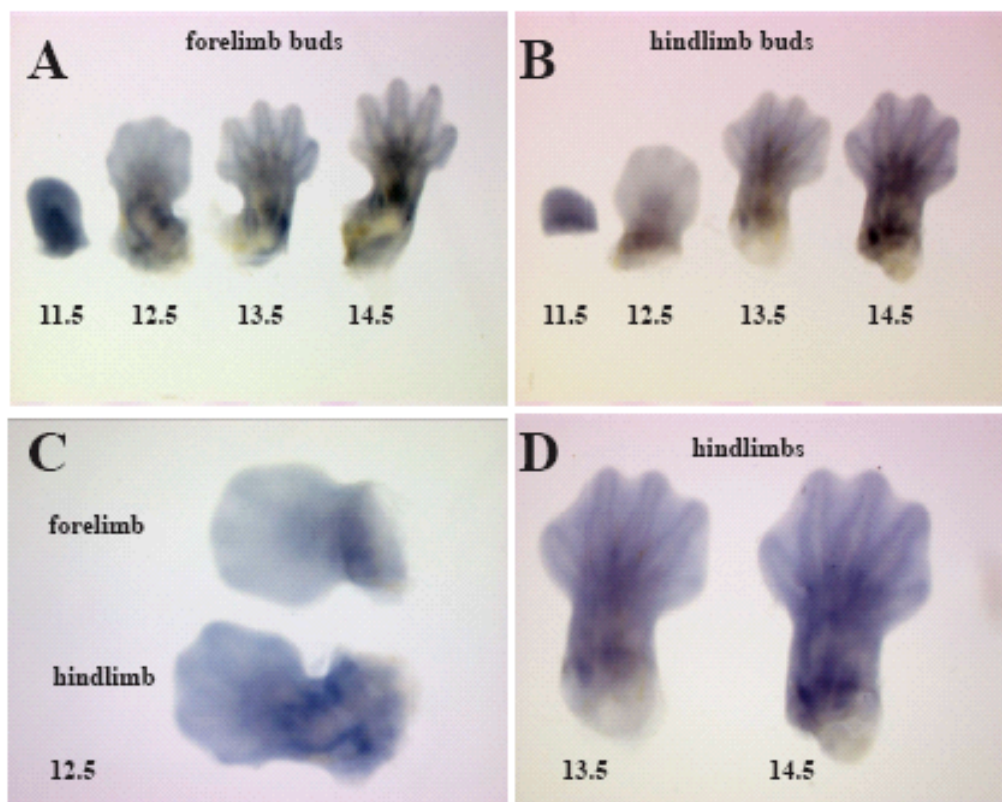
Figure 6.19: **(A-D)** *Ostl* **expression during limb development. (A)** forelimb buds from 11.5 until 14.5 d.p.c. embryos; **(B)** hindlimb buds from 11.5 until 14.5 d.p.c. embryos ; **(C)** limb buds of 12.5 d.p.c. embryos, and **(D)** hindlimb buds of 13.5 and 14.5 d.p.c. embryos.

113
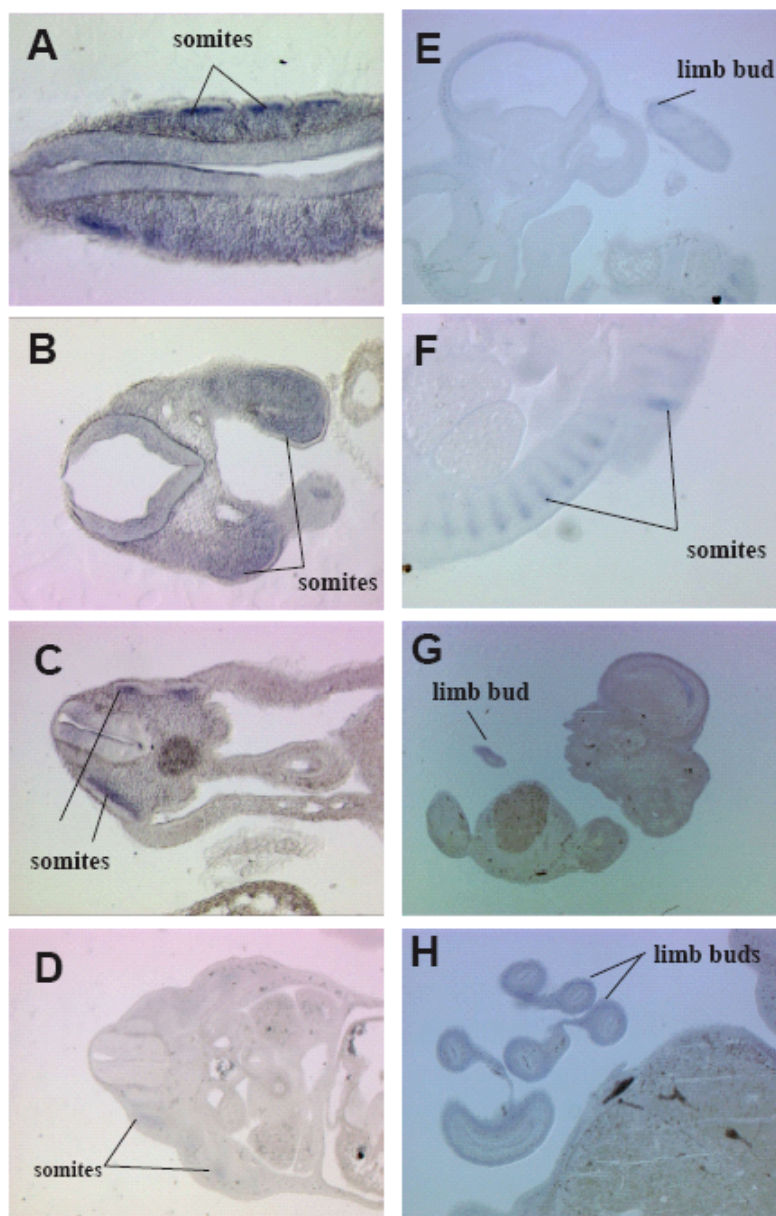
Figure 6.20: *Ostl* **expression during mouse embryonic development sections. (A and B)** horizontal and transverse sections of a whole-mount stained 9.5 d.p.c. embryo, expression is observed in the somites; **(C)** Horizontal section of a whole-mount stained 10.5 d.p.c embryos, *Ostl* expression is detected in the somites; **(D-F)** Horizontal and sagital sections of a whole-mount stained 11.5 d.p.c. embryo, expression is observed in the somites and limb bud; (G and H) sagital sections of a whole-mount stained 13.5 d.p.c. embryo, *Ostl* expression is observed in the limb buds (digits).

6.5. Preparation and purification of OSTL-GST protein

Cloning

In order to produce antibodies against OSTL for the further characterization of the protein, we tried to express sufficient quantities of OSTL as a GST fusion protein in bacteria (see 5.7). We constructed three plasmids: the first with the full length h*OSTL* (~ 275 aa) was cloned into pGEX4T-2 vector. The insert was obtained from the plasmid pEGFP-C1-*OSTL* (see 6.3) using the *BglII* and *SalI* restriction enzymes and cloned into pGEX4T-2 cut with *BamHI* and *XhoI* (figure 6.21 A). Two *Ostl* mutants were constructed: one containing the RING finger 2 and the C terminus (~ 127 aa) named *Ostl* mutant 4 and the other containing only the C terminus (~ 78 aa) called *Ostl* mutant 6. Both mutants were PCR amplified from the mouse J16 clone using the primers J16-836TEcoRI and J16-1218BXhoI (mutant 4) and J16-982TEcoRI and J16-1218BXhoI (mutant 6) (see table 5.1). The mutants were cloned into the *EcoRI* and *XhoI* sites of pGEX4T-2 (Figures 3.21 B and C).

The integrity of all constructs was veryfied by sequencing with primer pGEX 5' (table 5.1). Unfortunately, all three constructs failed to express sufficient amounts of protein.
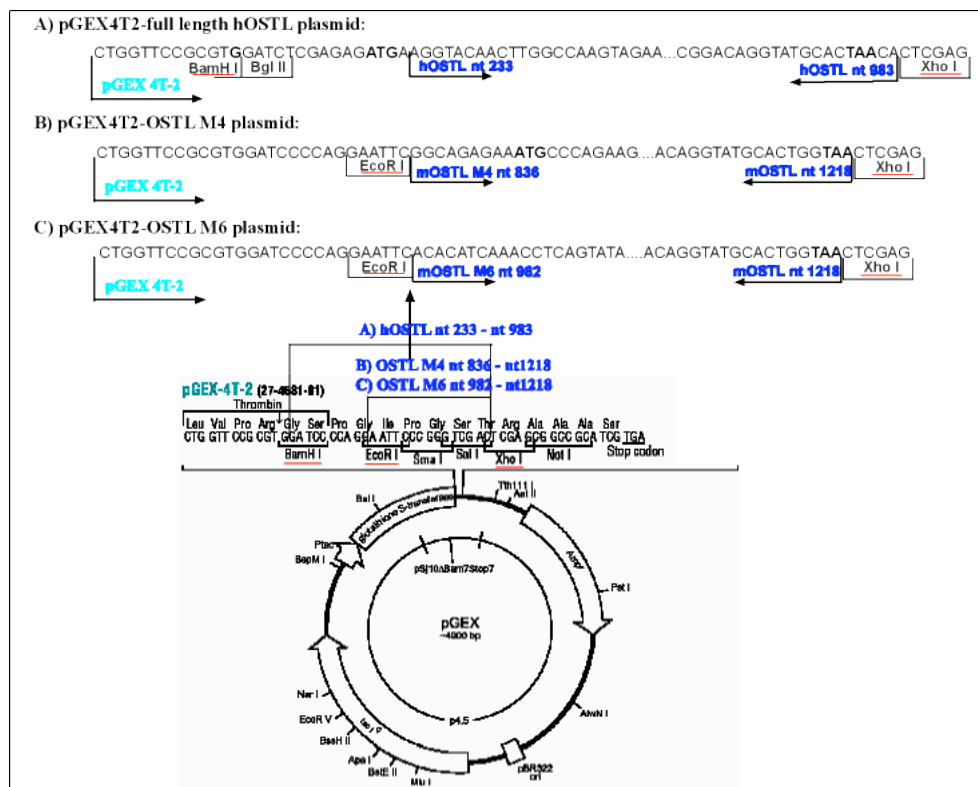
Figure 6.21: Schematic representation of pGEX4T-2-*OSTL* plasmids. (A) Human full length *OSTL* into pGEX4T-2; **(B)** Mouse *Ostl* mutant 4 into pGEXT4-2; **(C)** Mouse *Ostl* mutant 6 into pGEX4T-2. The diagram indicates the restriction enzyme sites (underlined in red), and the start and stop codons (in bold) of *OSTL* inserts (in blue) for all three constructs.

6.6. Identification of OSTL-interacting proteins using the yeast two-hybrid system

To identify OSTL-interacting proteins a yeast two-hybrid protein interaction screen was performed. The OSTL protein served as bait and a cDNA Hela S3 library encoding possible OSTL-interacting factors supplied the prey (schematically represented in Figures 6.22 A and B).
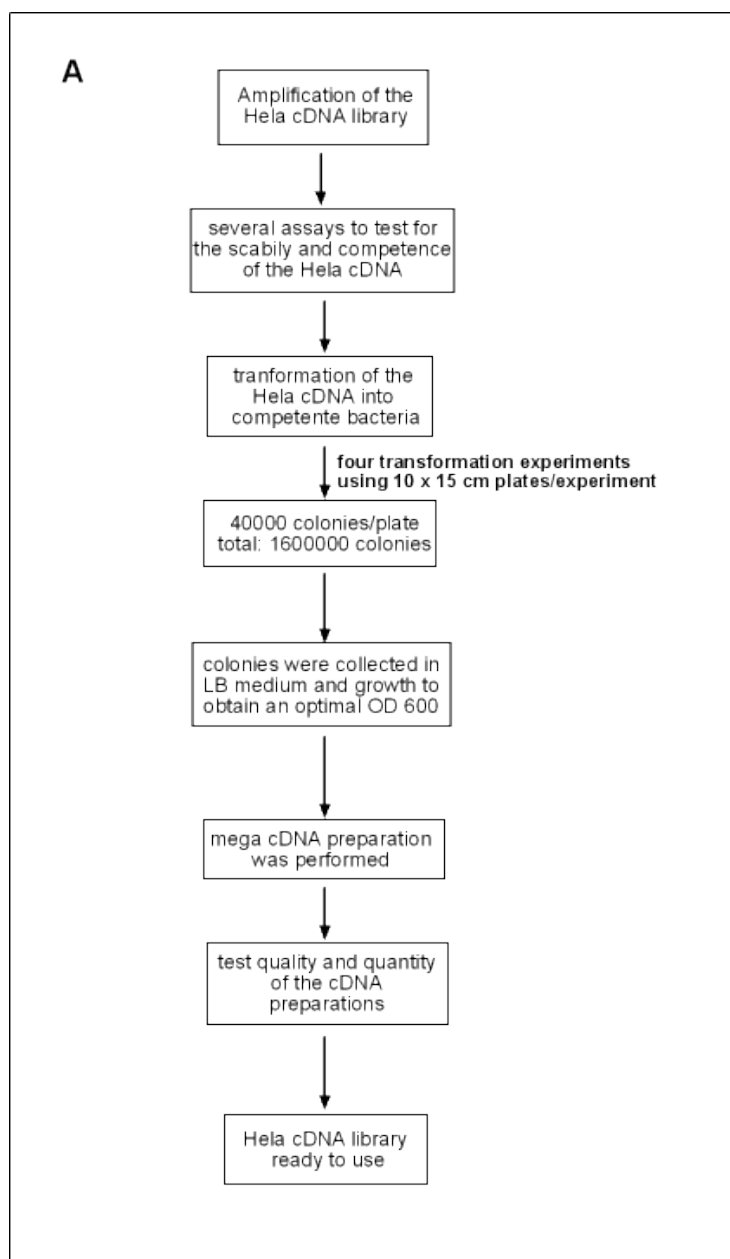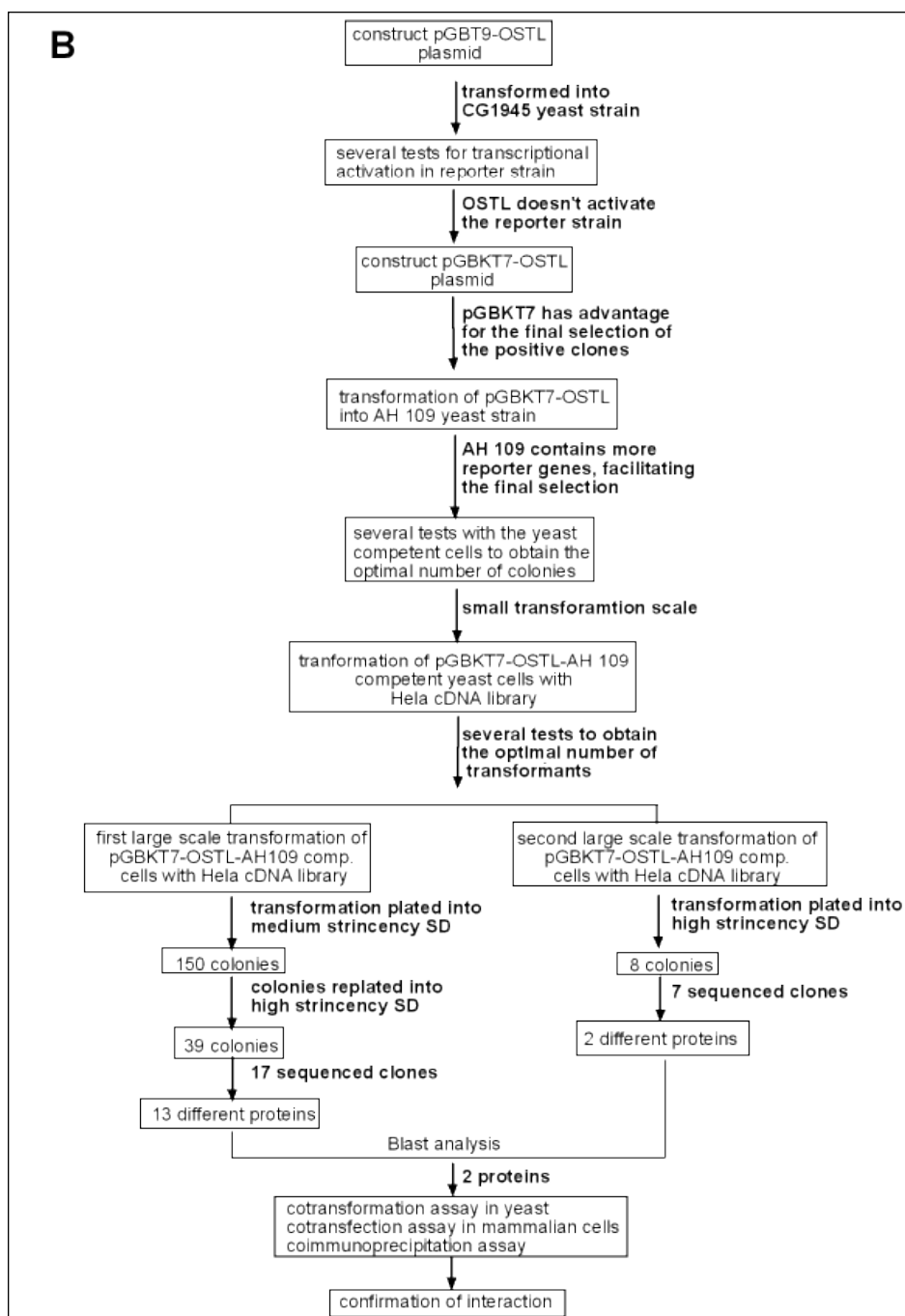
Figure 6.22: Flow diagrams for the identification of OSTL-interacting proteins. **(A)** Schematic representation of the Hela cDNA library amplification; **(B)** Schematic representation of the yeast two hybrid screening using *OSTL* as bait gene and the Hela cDNA library as prey.

6.6.1. Preparation and test of *OSTL* as a bait protein

Cloning

With standard cloning techniques (see 5.3.4), the *OSTL* cDNA was inserted into the polylinker of the pGBT9 plasmid to produce an in frame GAL4DBD-OSTL fusion protein. Briefly, the human *OSTL*-ORF (E06-ORF) was PCR amplified with the primers OSTLEx1dATGXhoI and OSTL983BPstI (table 5.1) and inserted in frame with GAL4-DNA-BD into the *SalI* and *PstI* restriction sites of the pGBT9 vector. The pGBT9-*OSTL* construct is schematically shown in the figure 6.23.

Using the lithium acetate procedure, the yeast strain CG 1945 (see 5.2.3) was transformed with the plasmid pGBT9-*OSTL*. Since the prey plasmid pGAD-GH and the bait expression plasmid pGBT9 harbor the *LEU2* and *TRP1* genes, respectively (see 5.2.3 and 5.2.8.4), transformants which were selected grew in synthetic selective dropout medium lacking leucine and tryptophan. To investigate whether *OSTL* as a bait protein activates transcription of the reporter genes in the absence of the "prey" protein, each yeast transformant was diluted 100 and 1000-fold in sterile water and plated on SD -Trp and SD -Trp, -His plates. The growth of the cells was monitored for several days. All yeast clones grew well to a similar density on the SD -Trp plates. However, in the presence of histidine the yeast clones did not grow.

These results showed that the binding of the OSTL-GAL4-BD fusion protein upstream of the reporter genes *HIS3* and *lacZ* was not enough to activate their transcription. Therefore, it was concluded that the OSTL protein is suitable as a bait protein for the yeast two-hybrid assay. For the actual yeast two hybrid screen, the *OSTL* cDNA was inserted into the polylinker of the pGBKT7 plasmid to produce an in frame GAL4-BD-OSTL fusion protein.

The pGBKT7 vector was choose for the further analysis because it carries a kanamycin resistence marker and contains a c-Myc epitope, facilitating the selection of OSTL-interactors from the library transformants and also the confirmation of positively selected clones through *in vitro* CoIP. The pGBKT7-*OSTL* construct is schematically shown in figure 6.24.

To confirm expression of the OSTL protein, the yeast strain harboring the bait plasmid was analyzed with a Western blot.

The yeast clone (pGBKT7-*OSTL*) showed a clear band around 50 kDa on Western analysis corresponding to the pGBKT7-OSTL fusion protein.
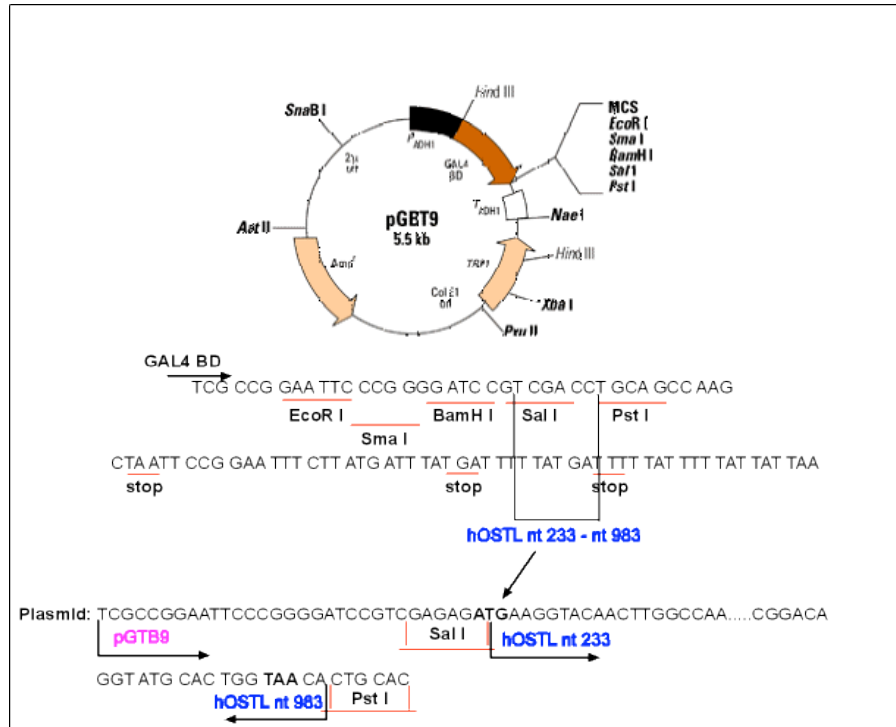
Figure 6.23: Diagram of the pGBT9-*OSTL* plasmid. The restriction enzyme sites from the vector and insert are underlined (in red). The human *OSTL* insert is shown in blue (h*OSTL* nucleotides are indicated). The vertical arrow indicates the plasmid pGBT9-*OSTL* with start and stop codons of the *OSTL* sequence insert in bold.
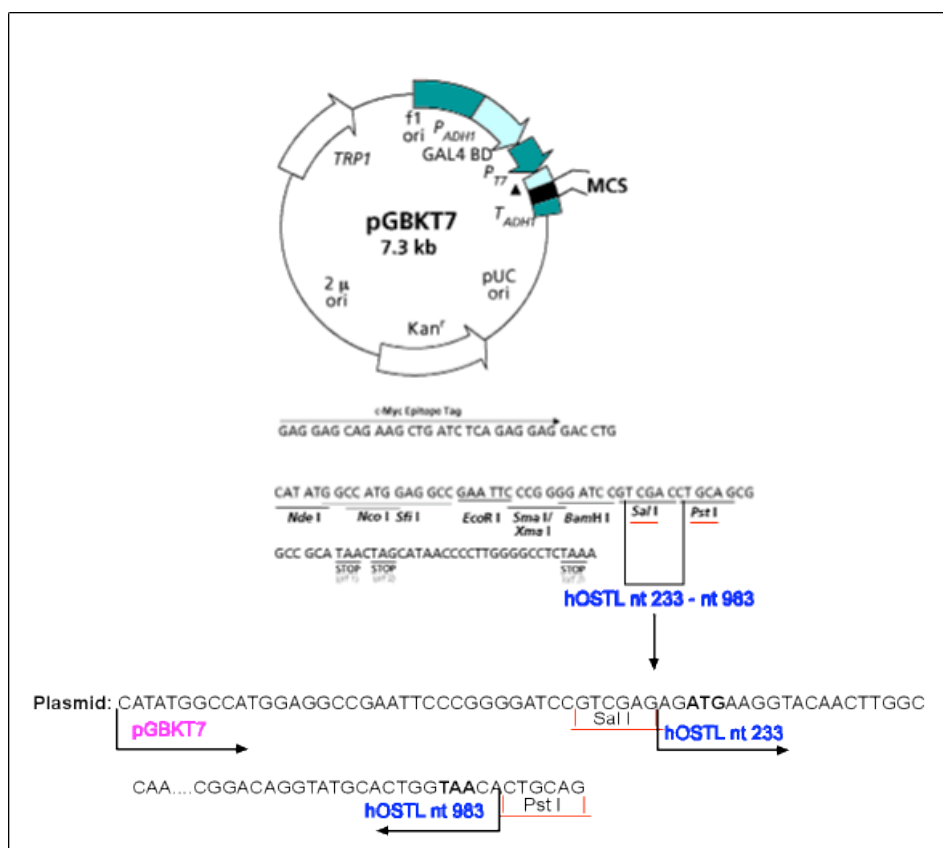
Figure 6.24: Schematic representation of pGBKT7-*OSTL* plasmid. The pGBKT7 vector and MCS are indicated. The restriction enzyme sites from the vector and insert are underlined (in red). Human *OSTL* insert is represented in blue (h*OSTL* nucleotides are indicated). The vertical arrow indicates the plasmid pGBKT7-*OSTL* with start and stop codons of *OSTL* sequence insert in bold.

6.6.2. Screening for OSTL interactors

The interactor screen was performed in two consecutive large plating steps (see 5.4.5 and Figure 6.22 B). First 22 µg and then 33 µg DNA of pGAD-GH plasmid containing the human cDNA Hela S3 library (Clontech) were transformed into AH109 cells with the bait plasmid (pGBKT7-*OSTL*) plasmid (see 5.4.5). In order to obtain a high number of primary transformants expressing an individual library plasmid, the yeast strain was transformed in large scale in 8 different sterile tubes per experiment (2 large scale experiments = 16 tubes). For each experiment the transformation efficiency[*] expressed as colony forming units (cfu) per µg of input DNA was around 3×10^4 (table 6.5). The content of the 8 tubes was pooled, and 250 µl of the transformation reaction were plated on thirty 15 cm SD-TRP, -LEU, -HIS, -ADE plates in the first transformation and on thirty 15 cm SD-TRP, -LEU, -HIS plates in the second transformation.

The plates were incubated at 30°C for 3-7 days until colony growth could be detected.

*Transformation efficiency = cfu/ μg transformed DNA

cfu = colony forming units (into SD/ -TRP-LEU selective yeast medium)

Number of tested clones = total number of clones per experiment

Table 6.5: Transformation efficiency and number of tested clones

Experiments	Amount of transformed DNA in μg	Transformation-efficiency in cfu/μg	Number of tested clones
First transformation	22	29920	660.000
Second transformation	33	26666	880.000

After seven days, 8 clones from the first experiment and 150 clones from the second experiment were detected. The clones from the first experiment were selected on SD –TRP-LEU-HIS-ADE + X-α-gal master plates (15 cm). The clones from the second experiment were selected on SD –TRP-LEU-HIS-ADE and finally on X-α-gal master plate (see 5.4.5.1). At this point 8 out of 8 and 39 out of 150 clones grew in the absence of tryptophan, leucine, histidine, adenine, and showed X-gal positivity (= blue colonies).

6.6.3. Isolation and classification of library plasmids

From each of the 8 (first screen) and 39 (second screen) positive yeast clones prey plasmids were isolated by performing a rapid yeast plasmid preparation and the isolated DNA was transformed into competent XL1 bacteria by electroporation (see 5.4.7 and 5.4.8).

Seven of 8 and 17 of 39 yeast DNAs were successfully transformed, while the prey clones from 23 colonies could not be transformed into XL1 bacteria. From these bacteria, DNA was isolated and analyzed by restriction enzyme digestion. Each bacterial miniprep DNA was digested with *EcoRI* and *XhoI* restriction enzymes to release the insert of the library plasmids.

6.6.4. Sequencing of the interaction clones and BLAST analysis

The 24 clones harboring an *EcoRI/XhoI* insert in the library plasmid were sequenced with the primers Y2H2 and 3'AD (table 5.1). NCBI's BLAST search (see 5.12) of available sequence databases identified the proteins shown in tables 6.6 and 6.7. A brief description of each interaction-protein is given in table 6.8.

As observed in tables 6.6 and 6.7, HAX1 was the most frequent protein found in the two screens. Interestingly, not only full length HAX1 protein (represented by clone 5) but also eight different fragments of the protein (represented by clones 1 (= 4), 2 (= 104), 3, 6, 15 (= 41), 79 (= 87), 118, and 127 were found as OSTL interacting proteins (see figure 6.25).

Only one clone coding for the following proteins was found: SIVA was found in both screens as OSTL-interacting protein (represented by clone 7 and as diagram in figure 6.25), Dpy-30 (clone 19), Luman (clone 21), RPLP1 (clone 27), Metallothionein 2A (clone 43), FLJ31231 (clone 52), LMS3 (clone 67), a hypothetical protein containing a RING-finger motif (clone 115).

PKM2 was found two times in the medium stringency Hela screening as OSTL-interacting protein (clones 85 = 107).

Figure 6.25 schematically shows the full length cDNA and protein sequences of the OSTL interacting proteins and their clones found in the HeLa library.

**Table 6.6: First screening of the Hela-library (SD −T, L, H, A) –
7 positive clones**

Hela Clones	Protein Interaction partners of OSTL
1, 3	HAX-1 NM_006118.3[*]
2	HAX-1
4, 6	HAX-1
5	HAX-1
7	SIVA NM_006427.2[*]

Table 6.7: Second screening of the Hela-library (SD –T, L, H) –
17 positive clones

Hela Clones	Protein Interaction partners of OSTL
15, 41	HAX-1
19	DPY-30 BC_015970.1[*]
21	Luman AF_009368[*]
27	RPLP1 NM_001003[*]
43	Metallothionein 2A BC_007034[*]
52	FLJ31231 NM_030919.1[*]
67	LSM3 NM_014463.1[*]
79, 87	HAX-1
85, 107	PKM2 NM_002654.1[*]
104, 2	HAX-1
115	MGC 33993 (Hypothetical Protein RING-Finger motif) NM_152737.1[*]
118	HAX-1
127	HAX-1

[*]: Genbank accession numbers

Table 6.8: Yeast two hybrid OSTL-interacting proteins

Protein name	Cell localization	Protein description[*]
HAX1	cytoplasm	HS1-associated protein X-1, is an anti-apoptotic protein, involved in signal transduction in B cells
SIVA	nucleus	Intracellular ligand of CD27, is highly expressed in lymphoid cells and exhibits pro-apoptotic activity
DPY-30	nucleus	A ubiquitous factor that promote the hermaphrodite-specific association of DPY-27 with X by affecting the activity of a sex-specific dosage compensation gene
Luman	cytoplasm	Human basic leucine zipper transcription factor, requires the host cell factor (HCF) for activity, implicated in cell growth
RPLP1	cytoplasm	Homo sapiens ribosomal protein, large, P1 (RPLP1), transcript variant 1
Metallothionein 2A (MT2A)	nucleus	Metallothionein (MT) belong to a family of cysteine-rich, metal-binding intracellular proteins, which are encoded by 10 functional MT isoforms, and involved in cell proliferation, differentiation and apoptosis
FLJ31231 or chromosome 20 ORF 129 (C20orf129)	nucleus	Homo sapiens chromosome 20 open reading frame 129 (C20orf129)
LSM3 or MDSO17	cytoplasm	Homo sapiens LSM3 homolog, U6 small nuclear RNA associated *S. cerevisiae* (LSM3). LSM (1-7) proteins form heptameric complexes that are involved in various steps of RNA metabolism
PKM2	cytoplasm	Homo sapiens pyruvate kinase, muscle (PKM2)
MGC33993 (Hypothetical Protein RING-Finger motif)	cytoplasm	Homo sapiens ring finger protein 182 (RNF182)

[*]Literature information
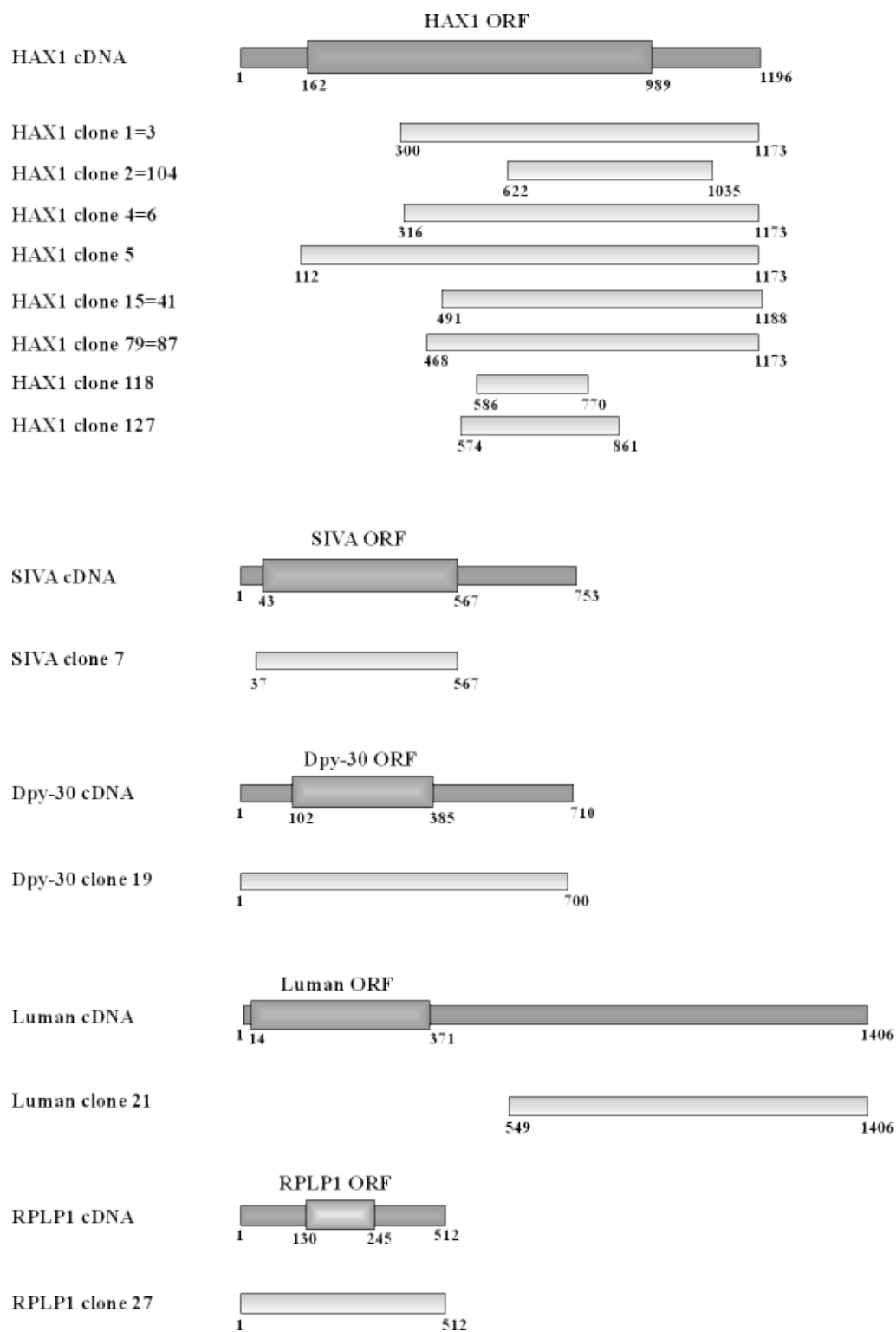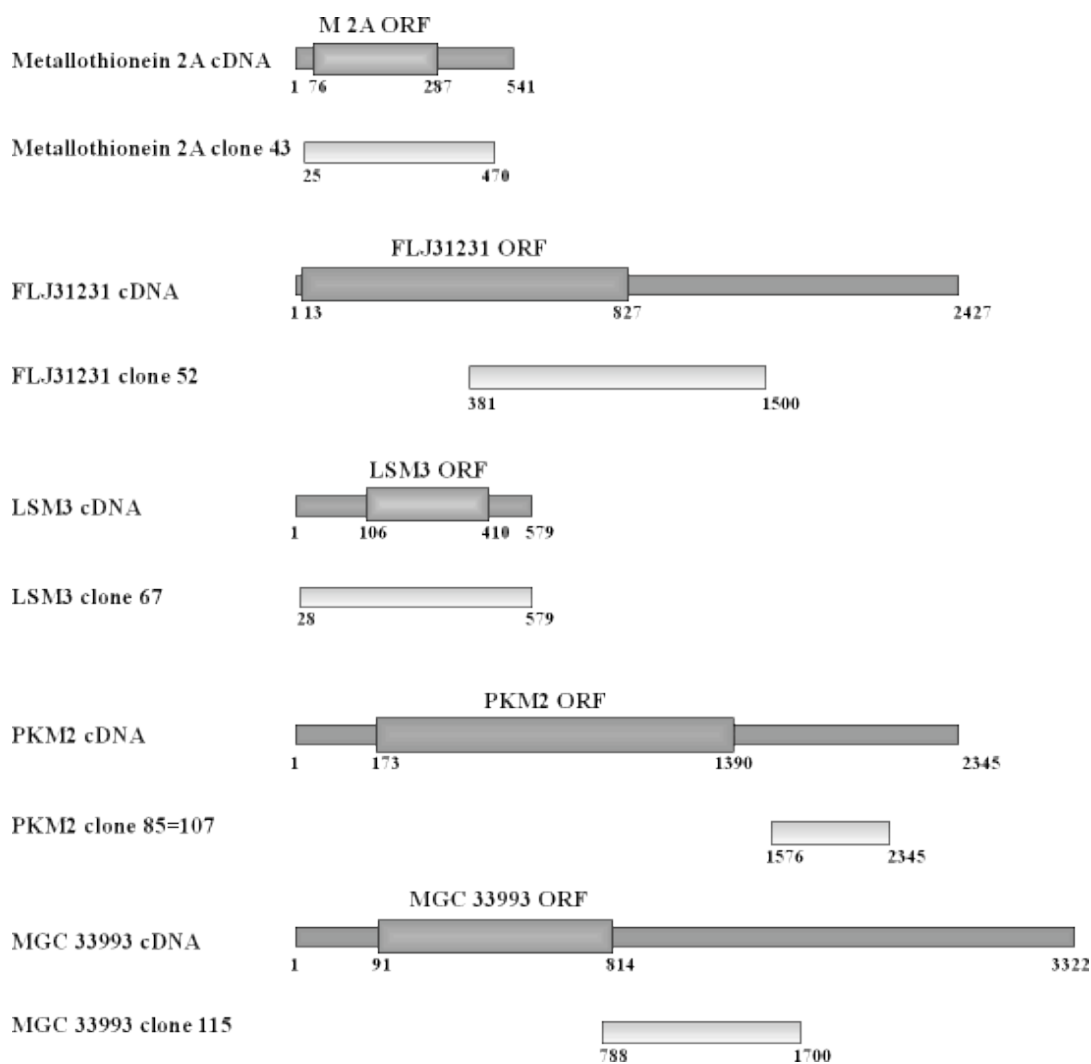
Figure 6.25: cDNAs and Open Reading Frames (ORFs) of full length proteins and clones 1-6, 7, 15, 19, 21, 27, 41, 43, 52, 67, 79 85, 87, 104, 107, 115, 118, and 127 isolated in yeast two hybrid screen as OSTL interaction partner.

6.6.5. Confirmation of the interaction between OSTL and HAX1 and OSTL and SIVA

Cotransformation assay in yeast

For further analysis, we focused on the interaction of OSTL with HAX1 and SIVA. In order to perform the first confirmation assay, HAX1 (2, 3, and 5) and SIVA (7) clones obtained from a Hela cDNA library were cotransformed with pGBKT7-*OSTL* into competent yeast cells (strain AH109) (see 5.4.3). The cotransformants were plated on highly selective SD plates lacking tryptophan, leucine, histidine, and adenine, supplemented with X-α-gal (figure 6.26).

All the tested clones, HAX1 clones 2, 3, and 5 and SIVA clone 7 showed activation of the reporter genes indicated by growth on the selective plate and the development of blue colonies when cotransformed with pGBKT7-*OSTL* as shown in figure 6.26.
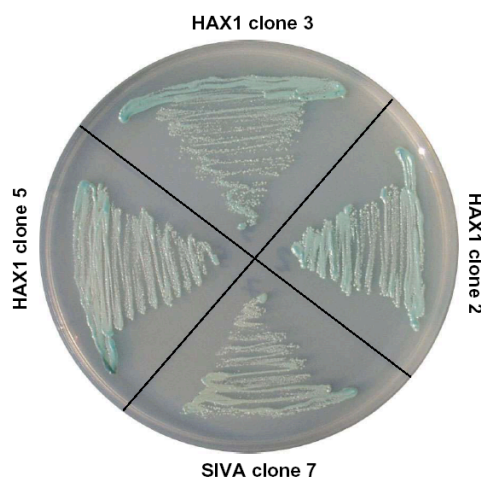
Figure 6.26: Highly selective SD plate lacking TRY, LEU, HIS, and ADE supplemented with X-α-gal. Blue colonies are observed in all library clones (HAX1 2, 3, and 5) and (SIVA 7) cotransformed with pGBKT7-*OSTL* bait plasmid.

Mapping of the HAX1 and SIVA interaction domain with OSTL

Cloning

In order to analyze which OSTL protein domains are responsible for the interaction with HAX1 and SIVA, we constructed several deletion mutants of *Ostl*.

For these experiments and further *in vitro* assays, *HAX1* and *SIVA* cDNAs were cloned into pGADT7 (figures 6.27 and 6.28). The full length human *HAX1* insert was cut with the restriction enzymes *EcoRI* and *BamHI* from the plasmid pEYFP-*HAX1* (Figure 6.31 A) and cloned into a modified pGADT7 vector (cutt with *Nde*I, blunt ended and religated) (Figure 6.27). *SIVA* variant 1 (V1) from Hela library clone 7 was digested with *EcoRI* and *Xho* and cloned into pGADT7. Unfortunately, plasmid pGADT7-*SIVA* was out of frame. To correct this, the plasmid was cut with *NdeI*, blunt ended and religated (Figure 6.28).

Full length mouse *Ostl* and six m*Ostl* mutants (M1-M6) were cloned into pGBKT7 (Figures 6.28 and 6.29 B). Mouse *Ostl* was choose because it has the complete N terminal variant RING1, while the human *OSTL* clone lacks 15 aa of the first RING domain (Figures 6.29 and 6.30 B lane 8).

To construct mouse *Ostl* deletion mutant expression vectors, the desired sequences were amplified from the m*Ostl* coding region by PCR and cloned into *NcoI/PstI* sites of the pGBKT7 vector.

The forward and reverse primers used to amplify the full-length *OSTL* were J16-295TNcoI and OSTL983BPstI; for *Ostl* (58 to 307) mutant 1 J16ATG1dNcoI and J16-996BPstI; for *Ostl* (1 to 111) mutant 2 J16-295TNcoI and J16-605BPstI; for *Ostl* (58 to 187) mutant 3 J16ATG1dNcoI and J16-855BPstI; for *Ostl* (166 to 307) mutant 4 J16-838TNcoI and OSTL983BPstI; for *Ostl* (166 to 223) mutant 5 J16-838TNcoI and J16-996BPstI; for *Ostl* (207 to 307) mutant 6 J16-949NcoI and OSTL983BPstI (Figures 6.29 and 6.30 B). All constructs were verified by sequencing using primers 5' Y2H1 for the pGBKT7 vector and Y2H3'AD for the pGADT7 vector (see table 5.1 for primer details).
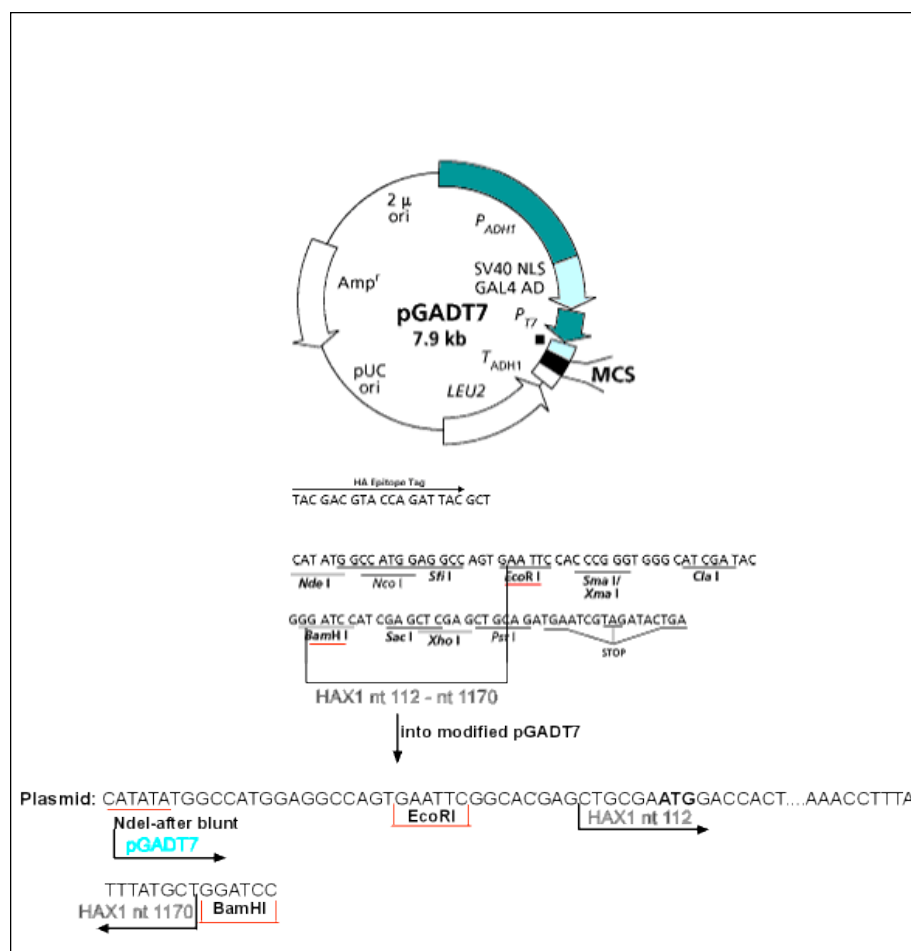
Figure 6.27: Schematic representation of pGADT7-*HAX1* plasmid. The restriction enzyme sites from the vector and insert are underlined (in red). Human *HAX1* insert is shown in blue (*HAX1* Nt 112 – Nt 1170 are indicated). The vertical arrow indicates the plasmid pGADT7-*HAX1* with start and stop codons of *HAX1* sequence insert in bold.
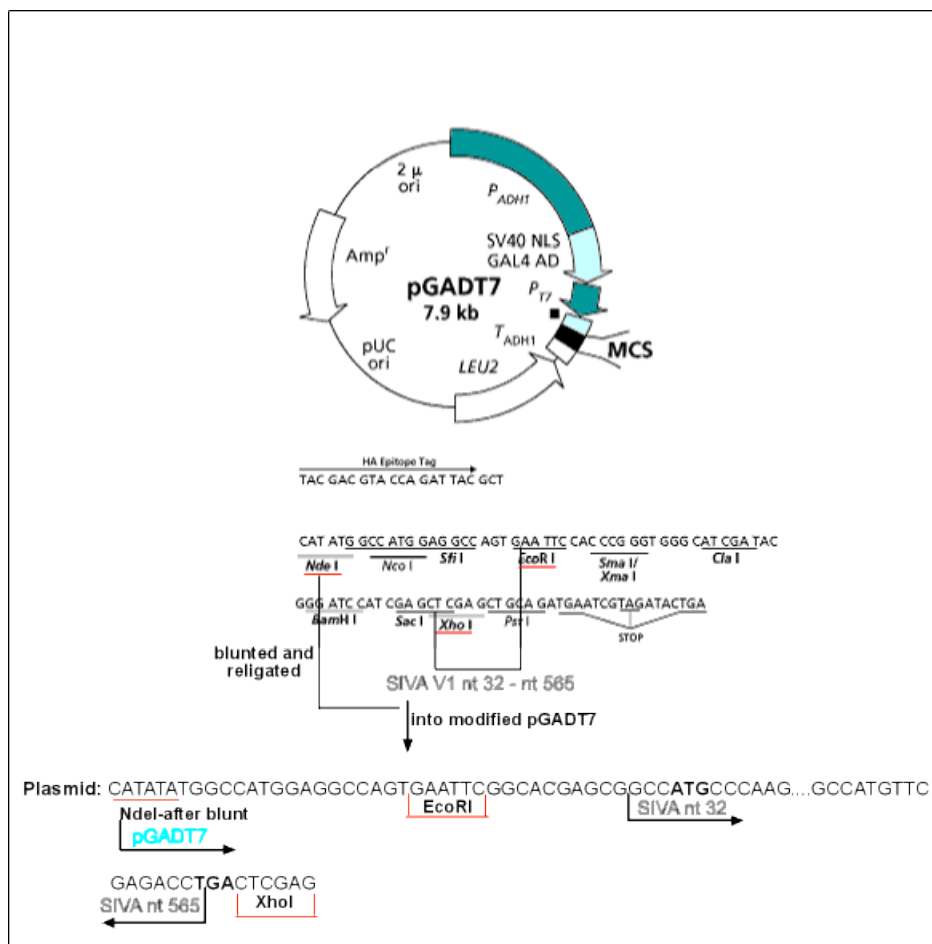
Figure 6.28: Schematic representation of pGADT7-*SIVA* plasmid. The restriction enzyme sites from the vector and insert are underlined (in red). *SIVA* V1 insert is shown in blue (*SIVA* Nt 32 – Nt 565 are indicated). The vertical arrow indicates the plasmid pGADT7-*HAX1* with start and stop codons of *HAX1* sequence insert in bold.

Cotransformation assay in yeast to map the HAX and SIVA interaction domains of OSTL

Cotransformation of pGBKT7-m*Ostl*, h*OSTL*, and mouse deletion mutant plasmids and pGADT7-*HAX1* or pGADT7-*SIVA* were performed using the yeast strain AH109 (as described in 5.4.3). Cotransformants were plated into SD lacking TRY and LEU and SD lacking TRP, LEU and HIS as shown in figure 6.29 A for HAX1-OSTL cotransformation and in figure 6.30 A for SIVA-OSTL cotransformation.

For each cotransformation reaction, three serial dilutions were performed (1:1000, 1:10000, and 1:100000), from 100 µl of total reaction 5 µl were plated on each selection plate (shown in A). In B, the lanes 1-9 indicate the *Ostl* fragments used for the cotransformation. Lane 1 shows full length mouse *Ostl* (with all three domains); lane 2: - mutant 1, lacking 15 aa of the first RING domain and the C terminus; lane 3: - mutant 2, containing the complete first RING; lane 4: - mutant 3, lacking RING 2 and C terminus; lane 5: - mutant 4, RING 2 and C terminus; lane 6: - mutant 5, containing only RING 2; lane 7: - mutant 6, C terminus only;

lane: - 8 human *OSTL* (used for the library screening), lacking the first 15 aa of the first RING; lane 9: mOstl full length co-transformed with the empty prey plasmid as negative control for the growth on SD lacking TRY, LEU and HIS.

Interaction efficiency are shown in B as +++ or -. As can be seen in fig. 6.29, HAX1 interacts with OSTL through its variant RING finger 1.

For the SIVA-OSTL interaction, shown in figure 6.30, the interaction seems to occur through RING finger 1 of OSTL, but here, the C terminus is also involved.
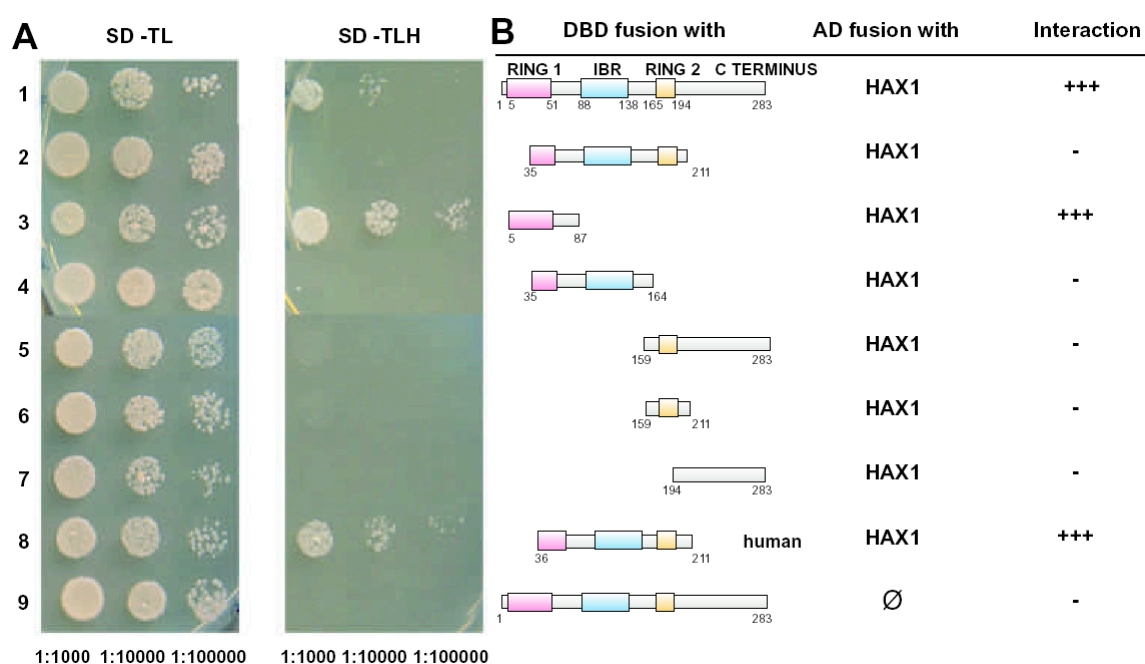
Figure 6.29: Mapping of the HAX1 interaction domain of OSTL. (A) Growth of serially diluted yeast colonies (1:100, 1:1000, 1:10000) on SD lacking tryptophan and leucine (SD -TL) or on SD lacking tryptophan, leucine and histidine (SD –TLH). The yeast cells AH109 were cotransformed with a plasmid expressing a DBD-OSTL or DBD-OSTL deletion mutant proteins (pGBKT7-*OSTL*) and a plasmid expressing an AD-HAX1 fusion (pGADT7-*HAX1*) shown in lanes 1-8. Lane 9 indicates the cotransformation control where the DBD-OSTL protein was co-transformed with the empty prey plasmid. **(B)** First column shows the structure of the DBD-OSTL deletion mutants; the second column represent AD fusion, and the third column shows the interaction levels.
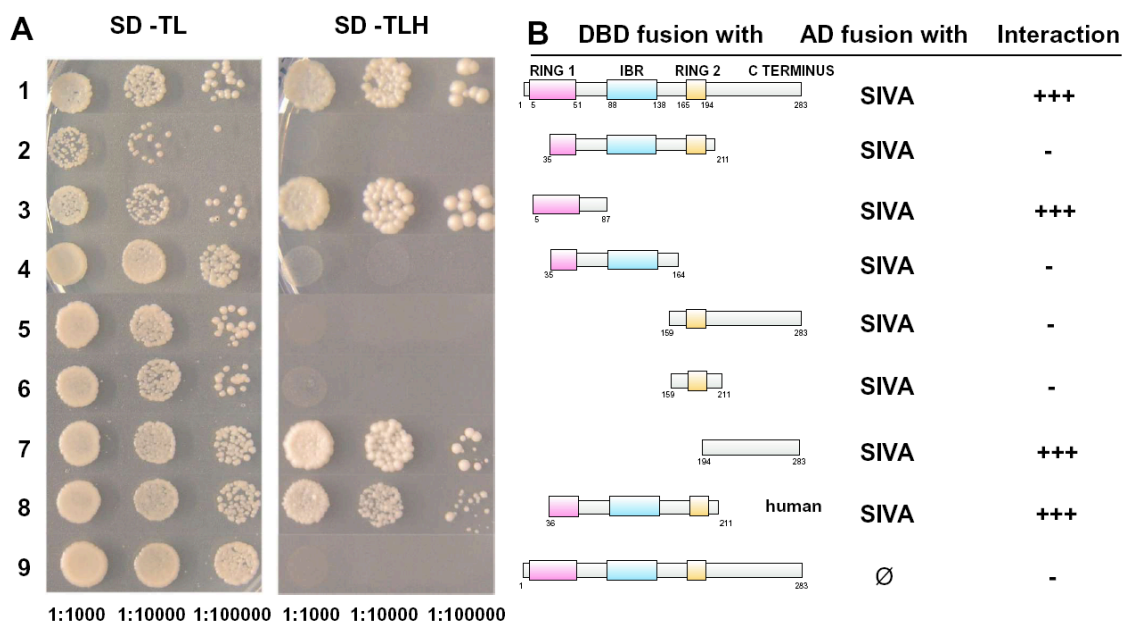
Figure 6.30: Mapping of the SIVA interaction domain of OSTL. (A) Growth of serially diluted yeast colonies (1:100, 1:1000, 1:10000) on SD lacking tryptophan and leucine (SD -TL) or on SD lacking tryptophan, leucine and histidine (SD –TLH). The yeast cells AH109 were cotransformed with a plasmid expressing a DBD-OSTL or DBD-OSTL deletion mutant proteins (pGBKT7-*OSTL*) and a plasmid expressing an AD-SIVA fusion (pGADT7-*SIVA*) in lanes 1-8. Lane 9 has the control where the DBD-OSTL protein was co-transformed with empty AD in yeast. **(B)** First column shows DBD-OSTL deletion mutants; the second column shows the AD fusions, and the third column indicates the level of interaction.

Cotransfection assays in mammalian cells

In order to confirm the OSTL interaction with HAX1 and SIVA through co-localization in mammalian cells, we performed cotransfection assays in NIH3T3 cells (see 5.5.1.1).

Cloning

In order to analyse the sub-cellular localization of OSTL, HAX1 and SIVA, the open-reading frame (ORF) of *OSTL* was cloned in frame with the gene coding for the enhanced cyan fluorescent protein (pECFP vector). The ORFs of *HAX1* and *SIVA* were cloned in frame with the gene coding for the enhanced yellow fluorescent protein (pEYFP vector).

Full length human *HAX1* was digested from the Hela library clone 5 (Table 6.6 and Figure 6.25) with the restriction enzymes *EcoRI* and *KpnI* and cloned into pEYFP using the same enzymes (Figure 6.31 A). The *SIVA* insert was released from the plasmid pGADT7-*SIVA* (Figure 6.28) using the restriction enzymes *EcoRI* and *XhoI* and cloned into pEYFP digested with *EcoRI* and *SalI* (Figure 6.31 B). Expressing a CFP-*OSTL* and an YFP-*HAX1* or YFP-*SIVA* fusion protein in mammalian cells allowed us to colocalize these proteins.

A

EYFP
TCAAAGTCCGGACTCAGATCTCGAGCTCAAGCTTCGAATTCTGCAGTCGACGGTACCGCGGGCCCG

GGATCCACCGGATCTAGATAACTG

EcoR I   Sal I   Kpn I

HAX1 nt 112 - nt 1170

Plasmid: GCTCAAGCTTCGAATTCGGCACGAGCTGCGAATGGACCACTGGAGGGGTTCAAAGGTTCGCGT
pEYFP   EcoR I   hHAX1 nt 112

CCCAGTACGGGA**ATG**AGC.....AAAACCTTTATTTATGCTGGTACC
hHAX1 nt 1170   Kpn I

B

EYFP
TCAAAGTCCGGACTCAGATCTCGAGCTCAAGCTTCGAATTCTGCAGTCGACGGTACCGCGGGCCCG

GGATCCACCGGATCTAGATAACTG

EcoR I   Sal I   Kpn I

SIVA V1 nt 32 - nt 565

Plasmid: GCTCAAGCTTCGAATTCGGCACGAGCGGCC**ATG**CCC......GCCATGTTCGAGACC**TGA**CTCGAG
pEYFP   EcoR I   SIVA V1 nt 32   SIVA V1 nt 565   Xho I

Figure 6.31: (A) Schematic representation of pEYFP-C1-h*HAX1* and **(B)** pEYFP-C1-*SIVA* V1.

Cotransfection and sub-cellular colocalization experiments

Cells transfected with CFP-*OSTL* and YFP-*HAX1* or CFP-*OSTL* and YFP-*SIVA* were observed 24 hours after transfection with an inverted epi-fluorescence microscope (see 5.5.3). After formaldehyde fixation, the cotransfected cells were photographed using an inverted epi-fluorescence microscope (see 5.5.2 and 5.5.3). Both OSTL and HAX1 co-localize in the

cytoplasm of the cells as shown in figure 6.32 A-D. Figure 6.32 A represented CFP-*OSTL* in the cyan channel, in 6.32 B YFP-*HAX1* in the YFP channel, in C the merged image of YFP and CFP is shown and in D is phase contrast image of the same cell.

OSTL and SIVA co-localization was observed in the cytoplasm. As shown in figure 6.33, OSTL localization is restricted to the cytoplasm and SIVA, which normally localizes to the nucleus, goes also to cytoplasm when OSTL is cotransfected (Figure 6.33 B). In most of the examined cells, the pattern observed is the same as shown in figure 6.33. In a few cells (about 10%) OSTL, when cotransfected with SIVA can also be seen in the nucleus.
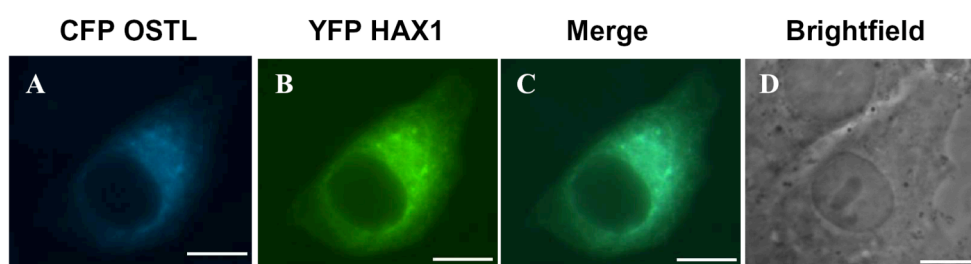
Figure 6.32: **Subcellular localization and colocalization of OSTL and HAX1 in mouse fibroblast cells (NIH3T3). (A)** CFP-OSTL fusion protein. **(B)** YFP-HAX1 fusion protein. **(C)** Merge of CFP-OSTL and YFP-HAX1. **(D)** Phase contrast. Scale bar: 10μm
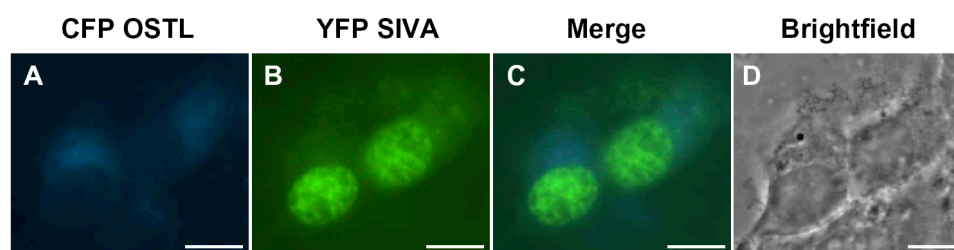
Figure 6.33: Subcellular localization and colocalization of OSTL and SIVA in mouse fibroblast cells (NIH3T3). **(A)** CFP-OSTL fusion protein. **(B)** YFP-SIVA fusion protein. **(C)** Merge of CFP-OSTL and YFP-SIVA. **(D)** Phase contrast. Scale bar: 10μm

Protein expression

In order to confirm expression of the OSTL, HAX1, and SIVA proteins in our fluorescent constructs, we expressed the proteins in the embryonal kidney cell line HEK293T and performed Western analysis (see 5.6). All constructs could be detected in a 10% SDS-PAGE gel as shown in figure 6.34. The protein sizes are indicated on the left in kDa. Bands of 27, 62, 57, and 44 kDa molecular weight correspond to YFP, YFP-HAX1, CFP-OSTL, YFP-SIVA proteins, respectively.
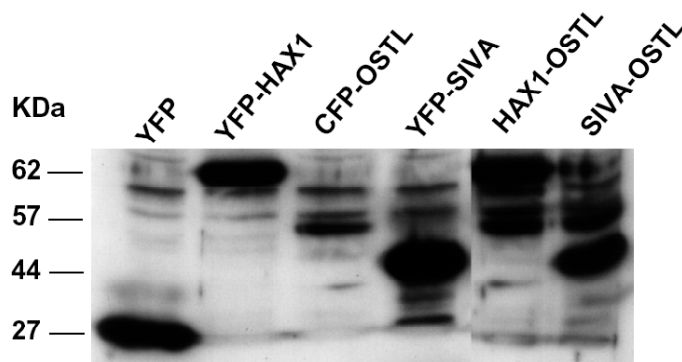
Figure 6.34: Protein expression of the different constructs used in the cotransfection assays. Western blot of protein extract (10 μg/lane) from HEK 293T cells transiently transfected with pEYFP (first lane) or pEYFP-*HAX1* (second lane), pECFP-*OSTL* (third lane), pEYFP-*SIVA* (fourth lane), co-OSTL-HAX1 (fifth lane) and co-OSTL-SIVA (sixth lane). Protein extracts were incubated with a rabbit anti-GFP antibody (1:3000) for 1 hour at RT and a secondary donkey anti-rabbit HRP-conjugated antibody. Exposure time was 3 sec.

In vitro coimmunoprecipitation assay

We were able to confirm the association between OSTL and HAX1 by using the CoiP in vitro system from Clontech (see 5.4.8.3). Both proteins were immunoprecipitated using the TNT-reticulocyte lysate system (Promega) (see 5.4.8.3). The CoiP was performed with mAb c-myc Ab against GAL4DBD-OSTL and pAb anti-HA against AD-HAX1. As observed in figure 6.35 lane 1, both proteins OSTL (30 kDa) and HAX1 (35 kDa) were coimmunoprecipitated with the anti-myc Ab. The expression of OSTL and HAX1 can be observed in lanes 2 and 3. The negative controls are shown in lanes 4 and 5, where OSTL was immunoprecipitated with anti-HA and HAX1 with anti-myc antibodies.
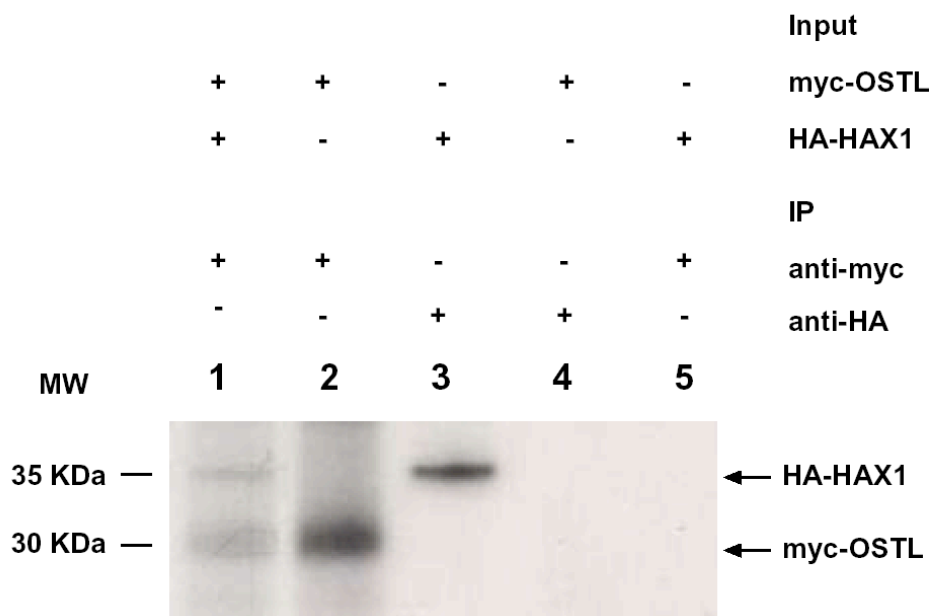
Figure 6.35: *In vitro* **coimmunoprecipitation of OSTL and HAX1.** OSTL and HAX1 were immunoprecipitated with a in vitro transcription/translation coupled reticulocyte lysate system. CoIP was performed using a mAb c-myc against GAL4DBD-OSTL. Lane 1 shows the CoIP of OSTL and HAX1, lane 2 IP of OSTL identified as a 30 kDa molecular weight band, lane 3 IP of HAX1 identified as a 35 kDa molecular weight band, lane 4 IP of OSTL with pAb anti-HA as negative control and lane 5 IP of HAX1 with mAb anti-myc as negative control.

In vivo coimmunoprecipitation assay

We were able to confirm the association between OSTL and HAX1 by overexpressing both proteins in HEK293T cells and coimmunoprecipitation (see 5.4.8.4). Immunoprecipitation was performed using the anti-HAX1 Ab (Clontech) (see 5.2.7.) (Figure 6.36 lower panel). As controls, untransfected 293T cells or control goat polyclonal Ab were used (lanes 1 and 3). The coprecipitation was performed with anti-GFP Ab (Molecular Probes) (Figure 6.36 upper panel). Both proteins CFP-OSTL (57 kDa) and YFP-HAX1 (62 kDa) were coimmunoprecipitated with the anti-GFP Ab (lane 2 upper panel). In lanes 4 and 5, approximately 10 μg of total cell lysates of untransfected 293T or CFP-*OSTL* and YFP-*HAX1* cotransfected cells is shown.
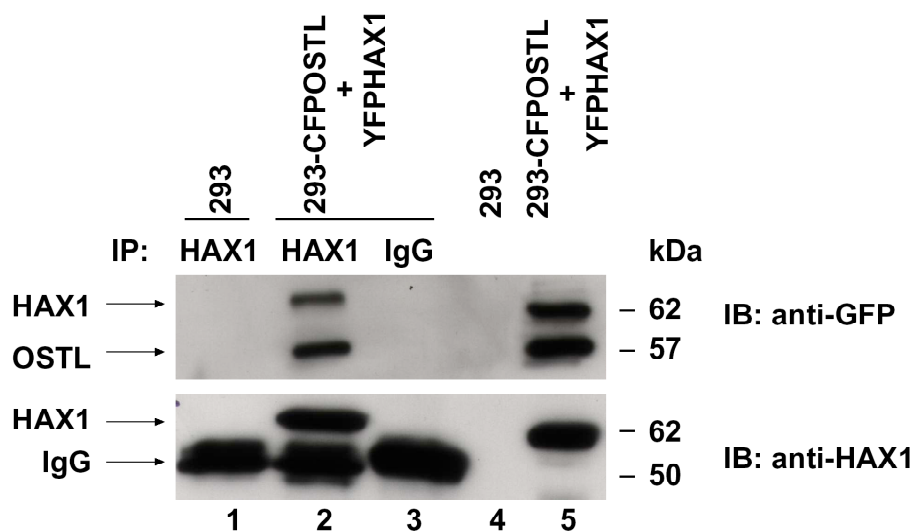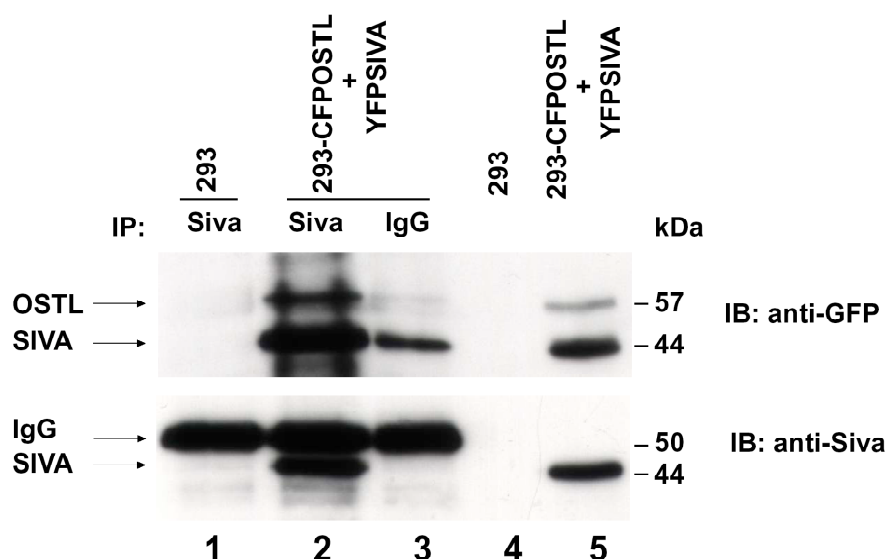
Figure 6.36: Interaction of OSTL and HAX1 in mammalian cells. Immunoblot detection of HEK293T cells cotransfected with CFP-OSTL and YFP-HAX1 proteins was performed. After 24 h, cells were lysed (2×10^6/lane) and analyzed by 10% SDS-PAGE followed by immunoblotting with mouse anti-HAX1 Ab (lower panel). Untransfected 293T cells were used as control (lane 1) or control mouse polyclonal Ab (lane 3). The same filter was immunoblotted with anti-GFP Ab (upper panel). Lane 2, the coprecipitated OSTL and HAX1 fused proteins (upper panel). Lanes 4 and 5, 10 μg of total cell lysates of untransfected 293T and cotransfected cells.

The association between OSTL and SIVA could also be confirmed by overexpressing both proteins in HEK293T cells (see 5.4.8.4). Immunoprecipitation was performed using a polyclonal anti-Siva Ab (Santa Cruz) (see 5.2.7.) (Figure 6.37 lower panel). As controls, untransfected 293T cells or control goat polyclonal Ab were used (lanes 1 and 3). The coimmunoprecipitation was performed with anti-GFP Ab (Molecular Probes) (Figure 6.37 upper panel).

Both proteins CFP-OSTL (57 kDa) and YFP-SIVA (44 kDa) were coimmunoprecipitated with the anti-GFP Ab (lane 2 upper panel). In lanes 4 and 5, approximately 10 μg of total cell lysates of untransfected 293T or CFP-*OSTL* and YFP-*SIVA* cotransfected cells is showed.

Figure 6.37: Interaction of OSTL and SIVA in mammalian cells. Immunoblot detection of HEK293T cells cotransfected with CFP-OSTL and YFP-SIVA proteins was performed. After 24 h, cells were lysed (3x10^6/lane) and analyzed by 10% SDS-PAGE followed by immunoblotting with goat anti-Siva Ab (lower panel). Untransfected 293T cells (lane 1) or control goat polyclonal Ab (lane 3) were used as controls. The same filter was immunoblotted with anti-GFP Ab (upper panel). Lane 2, the coprecipitated OSTL and SIVA fused proteins (upper panel). Lanes 4 and 5, 10 µg of total cell lysates of untransfected 293T and cotransfected cells.

6.7. Ubiquitination assay

Most RING finger proteins known are ubiquitin ligases (Lorick, *et al.*, 1999). *OSTL* encodes a protein that has a variant RING 1, a DRIL (double RING finger linked) or IBR (in between RING fingers) and a RING finger 2 motif (Capili, *et al.*, 2004) (see 6.1.1).

We have performed experiments to study the involvement of OSTL in the ubiquitin cascade. These experiments were done in collaboration with Stefan Müller and Andreas Ledl at the Max Planck Institute, Martinsried. We examined whether OSTL plays a role as an E3 ligase for HAX1 and or for SIVA, both interaction partners of OSTL (see 6.6.4). We also performed a test for ubiquitination of a putative substrate protein (modified from Treier *et al.*, 1994). In these experiments, we tested whether OSTL can enhance the ubiquitination of HAX1 and/or SIVA (see 5.9).

We repeated the assays three times and we were unable to show an increased ubiquitination of either HAX1 or SIVA in the presence of OSTL (Figures 6.39 and 6.40).

Cloning

For these experiments the presence of both RING finger domains is essential, therefore we cloned the ORF of the whole mouse *Ostl* gene (J16) in frame with the gene coding for the enhanced cyan fluorescent protein (pECFP). m*Ostl* was PCR amplified with the primers OSTLj16T302XhoI and OSTLj16B1272XhoI (see table 5.1) and subcloned into pECFP vector using the restriction enzyme *Xho*I.

The plasmid was sequenced with the primer pEGFP-C11240 (Table 5.1) to confirm that the insert was in frame with the cyan fluorescent protein open reading frame. The plasmid is schematically shown in figure 6.38.
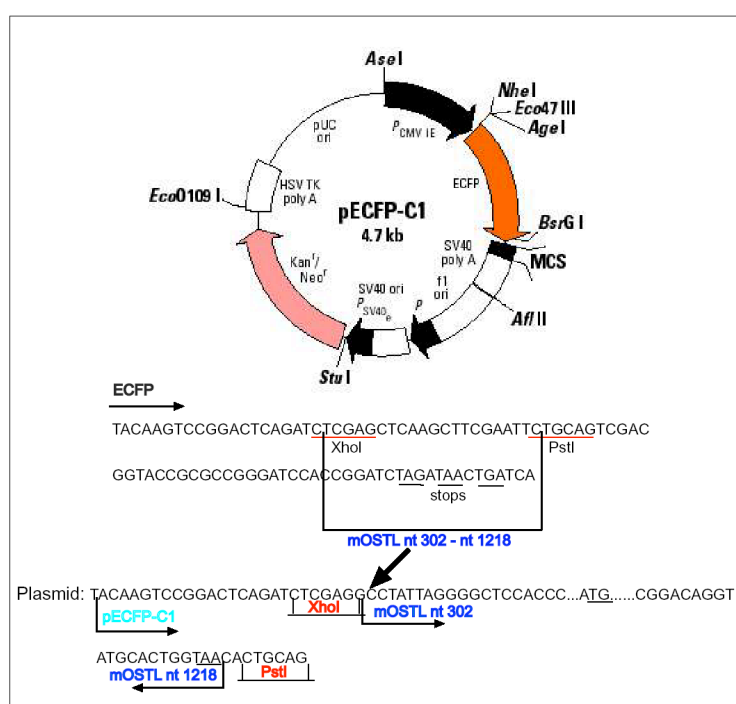
Figure 6.38: Schematic representation of the pECFP-m*Ostl* construct. The mouse *Ostl* insert (J16) is represented in blue (Nt 302 – Nt 1218). The open reading frame (ATG) and stop codon (TAA) of *Ostl* insert are underlined. The restriction enzymes used to clone *Ostl* into pECPF vector are shown in red (*XhoI* and *PstI*).

Western blot analysis of in vitro ubiquitination test using HAX1 and SIVA as candidates substrates for Ostl

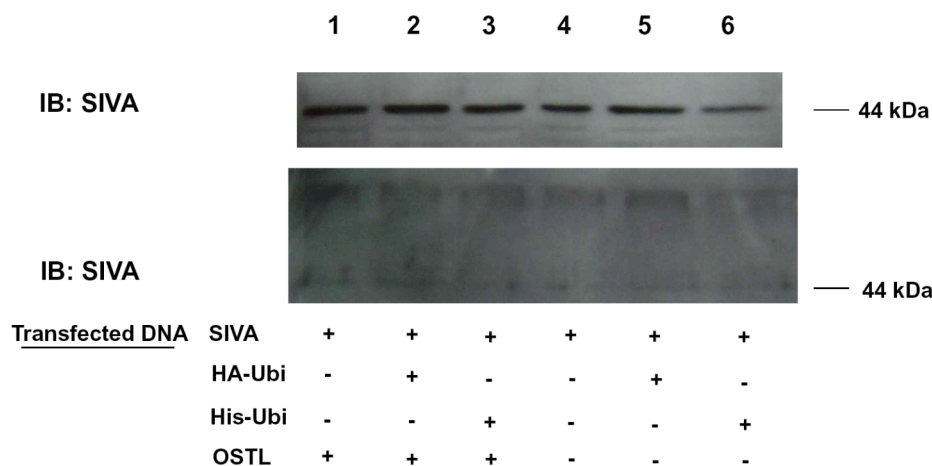| Transfected DNA		1	2	3	4	5	6
	HAX1	+	+	+	+	+	+
	HA-Ubi	-	+	-	-	+	-
	His-Ubi	-	-	+	-	-	+
	OSTL	-	-	-	+	+	+
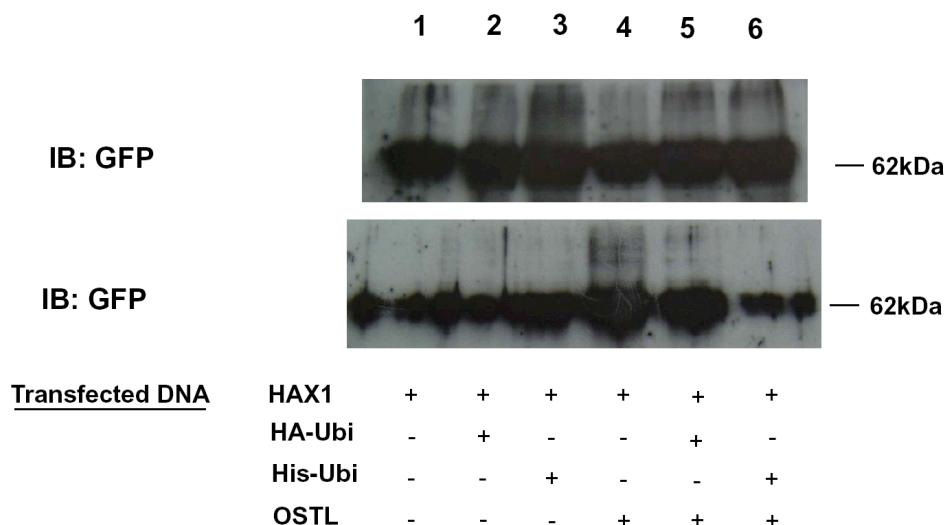
Figure 6.39: Test of *in vitro* ubiquitination with cotransfected HEK293 cells in the presence of Ostl and HAX1. HEK293 cells were transfected with the indicated combinations of expression plasmids. DNA amounts were YFP-*HAX1* and/or CFP-*Ostl*, 3 μg; HA-Ubi and/or His-Ubi, 1μg, per 35 mm dish. Cells were harvested 48 hr after transfection, and extracts were immunoprecipitated with anti-GFP antibody. In the upper panel the protein lysates are shown. Immunoprecipitated material, shown in the upper panel, was taken for *in vitro* ubiquitination reactions in the presence of His-Ubi (lanes 3 and 6) or HA-Ubi as negative control (lanes 2 and 5). Reaction products were resolved by SDS-PAGE, followed by Western blot analysis with an anti-GFP antibody. Positions of molecular size markers are indicated on the right and represented HAX1 + YFP vector (35 kDa+27 kDa).

Transfected DNA		1	2	3	4	5	6
	SIVA	+	+	+	+	+	+
	HA-Ubi	-	+	-	-	+	-
	His-Ubi	-	-	+	-	-	+
	OSTL	+	+	+	-	-	-

Figure 6.40: Test of *in vitro* ubiquitination with cotransfected HEK293 cells in the presence of OSTL and SIVA. HEK293 cells were transfected with the indicated combinations of expression plasmids. Amounts of DNA were SIVA-YFP and/or OSTL-CFP, 3 μg; HA-Ubi and/or His-Ubi, 1μg, per 35 mm dish. Cells were harvested 48 hr after transfection, and extracts were immunoprecipitated with a SIVA-specific polyclonal antibody. In the upper panel the protein lysates are shown. Immunoprecipitated material, shown in the upper panel, was used for *in vitro* ubiquitination reactions in the presence of His-Ubi (lanes 3 and 6) or HA-Ubi as negative control (lanes 2 and 5). Reaction products were resolved by SDS-PAGE, followed by Western blot analysis with an anti-GFP antibody. Positions of molecular size markers are indicated on the right and represented SIVA+YFP (17 kDa+27 kDa).

6.8. Overexpression of Ostl in primary hematopoietic cells

To analyze whether the ectopic expression of the *Ostl* gene is able to transform early murine hematopoietic progenitors we expressed *Ostl* in murine bone marrow cells using a MSCV-based retroviral construct.

Cloning

The mouse *Ostl* cDNA insert was subcloned into the modified MSCV retroviral vector with a green fluorescent protein (GFP) selection marker (called MIG). m*Ostl* was PCR amplified with the primers OSTLj16T302XhoI and OSTLj16B1272XhoI (see table 5.1 for primer informations) and cloned into the *Xho*I restriction site of MIG. The construct was sequenced for us using the primers pMSCV-F and pMSCV-R (see table 5.1) to confirm the correct orientation of the insert. Figure 6.41 chematically represent the MIG-*Ostl* construct.

Figure 6.41 Schematic diagram of MSCV-m*Ostl* construct. MSCV based retroviral vector were used to express whole mouse *Ostl* **in murine Bone marrow. LTR = long terminal repeats; IRES = internal ribosomal entry site; GFP = green fluorescente protein.**

Results of *in vitro* assays

6.8.1. Ectopic expression of *Ostl in vitro* is not enough to induce cell proliferation or blast colony formation

We checked the proliferative potential of bone marrow (BM) cells transduced with *Ostl in vitro* by analyzing sorted GFP positive cells (see 5.10.4.1). Expression of *Ostl* after 2 weeks in liquid expansion cultures (supplemented with IL-3, IL-6 and SCF) compared to BM cells transduced with GFP as a control did not show any significant (8.8±12.4) proliferation advantage (p>0.05) of *Ostl*-transduced cells (Figure 6.42).

Cells expressing *Ostl* were not able to grow in liquid culture supplemented only with IL-3 for longer than one week and did not show blast cell morphology.

Cytomorphological analysis of the cultured cells showed that BM cells expressing the *Ostl* gene and GFP were able to differentiate to normal terminally differentiated macrophages and granulocytes (data not showed).
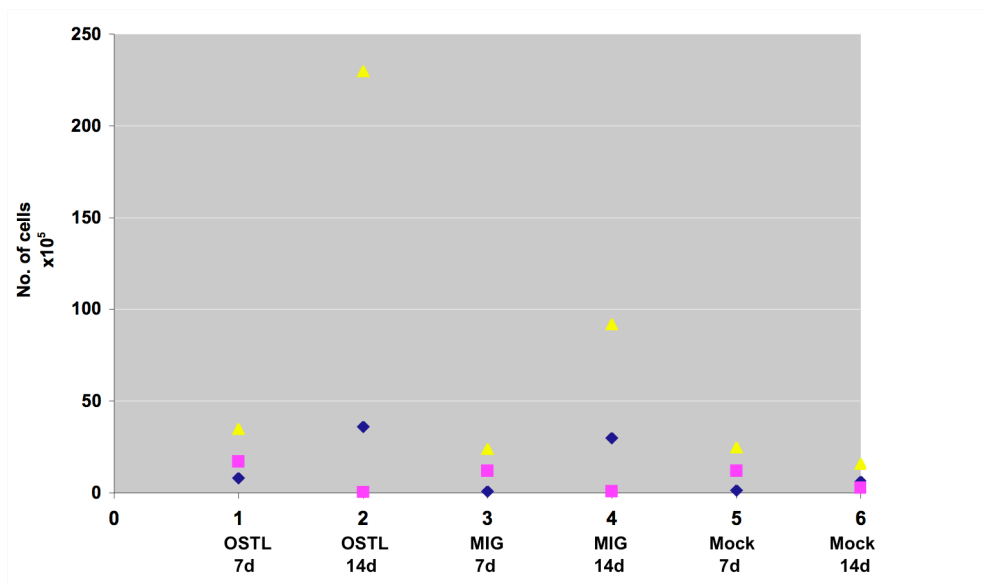

Figure 6.42 Ectopic expression of *Ostl* is not enough to increase the proliferation rate or to block cell differentiation. BM cells expressing *Ostl* did not show a significant proliferative advantage compared to GFP transduced cells (N=3) in liquid expansion medium supplemented with cytokines (IL-3, IL-6, and SCF). The symbols represent three independent experiments.

Results *in vivo*

6.8.2. Ectopic expression of *Ostl in vivo* leads to leukemia in transplanted mice

To analyze whether the ectopic expression of *Ostl* is able to transform early murine hematopoietic progenitors *in vivo,* total retrovirally transduced murine hematopoietic progenitors were injected into lethally irradiated recipient mice without sorting (6 x 10^5 – 1.2 x 10^6 cells/mouse; containing around 4% GFP$^+$ cells).

Mice transplanted with BM cells expressing *Ostl* became moribund after a median of 300 days post transplantation (n=3) (Figure 6.43). Diseased mice were characterized by cachexia, shortness of breath and lethargy, at which time they were sacrificed for further analysis. All *Ostl* mice analyzed (n=4) suffered from splenomegaly with an average spleen weight of 400 mg (4 fold increase compared to control animals).

Immunophenotypic characterization of cells from BM and spleen from the Ostl leukemic mice showed predominance of lymphoid $CD4^+CD8^+$ cells (~96% in the BM; 82% in the spleen; n=2) compared to the MIG control mice (~0.1% in the BM; ~1% in the spleen; n=1) (Figure 6.44).

Unfortunately, the cells obtained from diseased $Ostl$ mice were not GFP positive. To confirm the expression of the $Ostl$ gene in these cells, we extracted RNA and we were able to show by RT-PCR the Ostl expression, using appropriate controls and primers from $OSTL$ gene (E06 OSTL 374T and E06 OSTL 734B) (see table 5.1). RT-PCR was performed using normal and leukemic mouse cell subpopulations. In figure 6.45 the lower panel shows the mouse GAPDH (mGAPDH) control and the upper panel, lanes 1-6 are show subpopulations from normal mice. $Ostl$ expression could be observed in $Gr\text{-}1^+Mac\text{-}1^+$ cells, a very weak expression was detected by $B220^+CD19^+$ and $CD4^+CD8^+$ subpopulations. On the other hand, strong expression of $Ostl$ was observed in the T-ALL $CD4^+CD8^+$ cell subpopulation (Figure 6.45 lane 7).
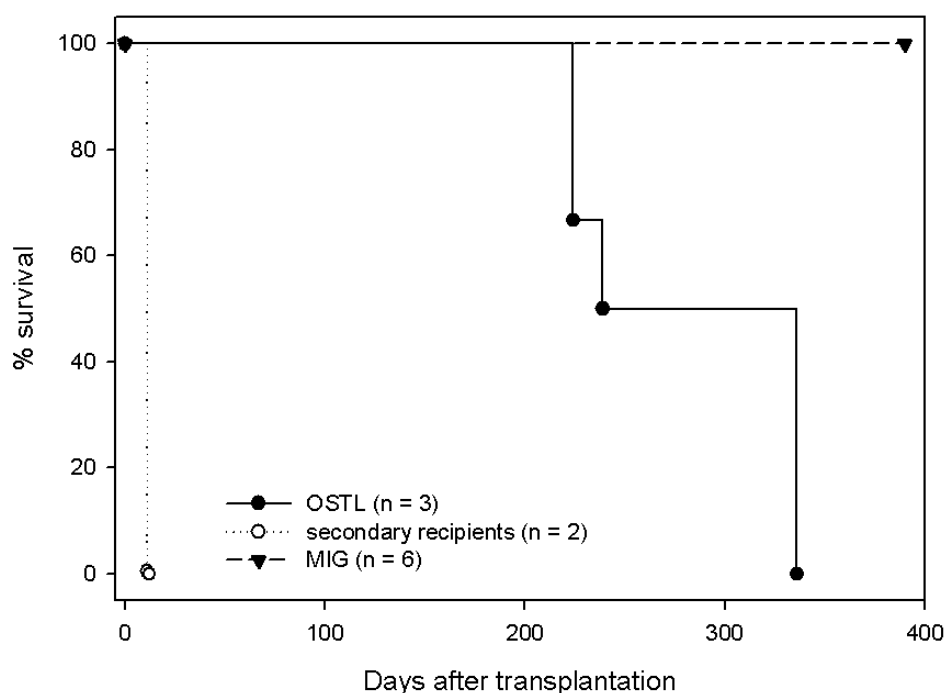
Figure 6.43 Survival of transplanted mice. Survival curve of mice transplanted with BM cells expressing $Ostl$ (n=3), MIG (n=6), and of secondarily transplanted mice (n=2).
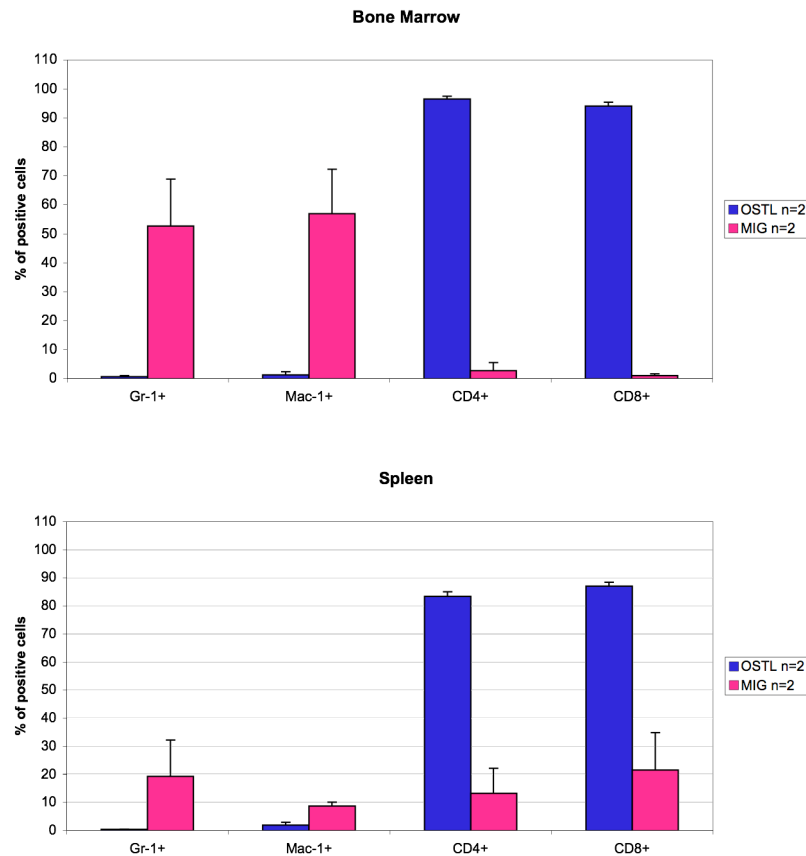
Figure 6.44 *Ostl* expression increases the proportion of early T cells and reduces that of myeloid cells. Immnophenotyping of the BM and spleen of *Ostl* diseased mice showed a predominance of lymphoid CD4^{+}, CD8^{+} cells (n=2). The Gr-1^{+}, Mac-1^{+} myeloid subpopulations in the BM and spleen were greatly reduced compared to MIG control mice.
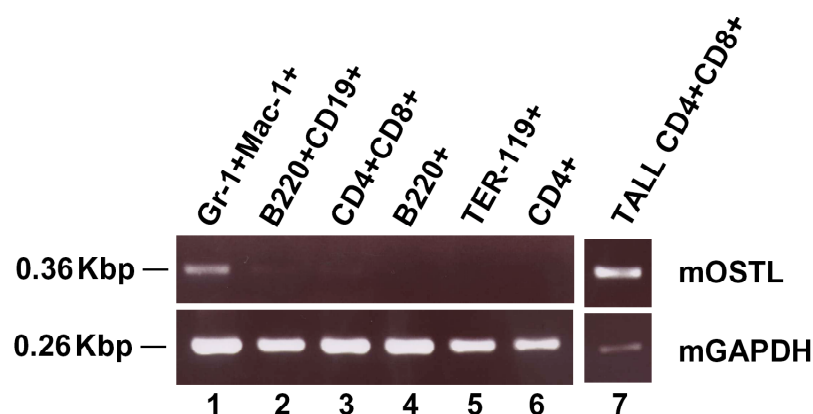

Figure 6.45 *Ostl* expression in normal and leukemic mice cell subpopulations. mGAPDH primers were used as control in the lower panel, lanes 1-6 represent cell subpopulations from BM and spleen of normal C57bl mice and lane 7, CD4^{+} CD8^{+} cells from spleen of the T-ALL C57bl mouse.

143

6.8.3. Immunohistochemistry showed blast infiltration in multiple organs

Histopathology report of one of these diseased *Ostl* mice (performed at the GSF Institute of Pathology by Dr. Leticia Quintanilla-Fend) showed that liver and kidney were diffusely infiltrated with neoplastic cells characterized by small to medium-sized cells with open blastic chromatin, one small nucleolus and inconspicuous chromatin (Figure 6.46). The cells showed a high mitotic index with abundant tingible body macrophages.

Immunohistochemistry performed with anti-CD3 and Tdt showed positivity for both markers (Figure 6.46 E, G, and H). Cells were negative for PAX5 and B220 (Figure 6.46 F and I). These findings suggested a diagnosis of a T-cell acute lymphoblastic leukemia (T-ALL). Wright-Giemsa-stained cytospins of BM and spleen demonstrated the lymphoblastic nature of disease (Figure 6.47).
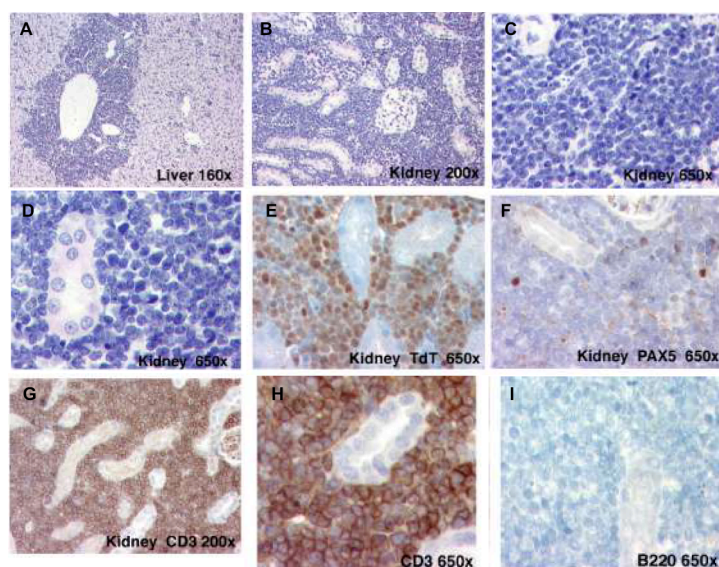
Figure 6.46 Histological analysis of diseased *Ostl* (T-ALL mouse) showed multiple organ infiltration of blast cell population. Histological analysis of diseased *Ostl* mouse. A) Liver (H&E stainning) immuno-histochemistry showed that the liver is hypercellular (160X); B, C and D) Kidney (H&E staining) showed that the kidney is hypercellular (200X and 650X); E) Histology of the kidney showed positivity for Tdt (650X); F) negativity for PAX5 (650X) and G and H) positiviy for CD3 (200X and 650X) and I) negativity for B220 (650x).
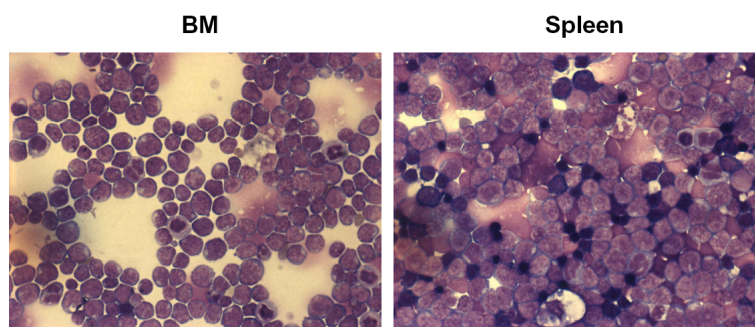
BM　　　　　　　　Spleen

Figure 6.47: Cytospin of BM and spleen of a diseased mouse (T-ALL) confirmed the lymphoblastic phenotype. Cytospin preparations of BM and spleen were analyzed after Giemsa staining and photographs were taken with an inverted microscope (Axiovert-135, Zeiss) at 250X.

7. Discussion

7.1. Identification and characterization of OSTL gene

Since the identification of *ETV6* about a decade ago it has become increasingly clear that *ETV6* plays an important role in various forms of leukemia (Golub, 1994a, b; Kobayashi, 1994; Buijs, 1995; Golub, 1995; Sato, 1995; Papadopoulos, 1995; Romana, 1995a; Shurtleff, 1995). Recently several studies and reviews have examined the role of *ETV6* in hematologic malignancies (Belloni, 2004; Tirado, 2005; Vieira, 2005; Bohlander, 2005).

The mechanism that is used by *ETV6* to effect malignant transformation appears to be variable. Not only have numerous fusion partners of *ETV6* been reported but *ETV6* was also found to be deleted frequently while the other *ETV6* allele was affected by a translocation (Raynaud, 1996; Romana, 1996; Bohlander, 2005). The occurrence of this two-hit pattern (one allele is rearranged and the other is deleted) is unusual among genes known from translocation breakpoints.

The t(6;12)(q23;p13) translocation involving *ETV6* at 12p13 was found in a cell line derived from the malignant blasts of a child with B-cell precursor ALL (Suto, 1997). Up to now, this is the only ALL or leukemia case with this translocation. However, two cases of a similar t(6;12)(q21;p13) were observed in a large series of childhood ALLs; in both cases a pre-B immunophenotype was observed (Hayashi, 1990). Although the breakpoints were reported as 6q21 in this series, it is not clear whether they were really different from the 6q23 case. The t(6;12) in the SUB-B2 cell line was only correctly identified after fluorescence in situ hybridization (FISH) analysis with probes from 12p. The original karyotype was reported to have a t(2;4;12)(q13;q25;p13) and a del(6)(q23q27). It could be that the 6;12 translocation is more common than conventional cytogenetic analysis suggests. This was also the case with the t(12;21)(p13;q22), which had only been reported in very few cases of childhood ALL by traditional cytogenetics (Romana, 1994), but which was found to be the most common translocation in childhood ALLs ten years ago (Golub et al., 1995; Romana, 1995b).

The molecular analysis of the (6;12) translocation in SUB-B2 identified a partner gene of *ETV6* on chromosome 6 that was named *STL* (Six twelve Leukemia gene) (Suto, 1997). Like with all the previous translocations partners of *ETV6* (*PDG-FRB*, *ABL*, *CBFA2*, and *MN1*), was expected to find a gene with a long open-reading frame. Instead, a fusion mRNAs was identified that showed no long open-reading frame (ORF) which would continue the ORF of

146

ETV6 either in the *ETV6/STL* fusion transcript or in the reciprocal *STL/ETV*6 fusion transcript (Figure 4.11 A).

Suto et al., 1997 tried two different strategies to characterize the *STL* gene: the first was to clone the mouse homologue of *STL*, to be able to identify human and murine conserved sequences. The second strategy was the use of a 3' probe of *STL* from the t(6;12) breakpoint, but this was also not successfully. A 5' *STL* probe was able to identify human and mouse homologuous sequences of the *STL* gene in Genbank. Intriguingly, an EST (Expressed Sequence Tag) was identified that belonged to a gene transcribed in the opposite direction to the *STL* gene. This gene was named for us *OSTL* (opposite *STL*).

OSTL shares the first exon with *STL* but is transcribed in the opposite direction, as shown in figure 6.6. The t(6;12) translocation in SUB-B2 interrupts not only *STL* but might also affect the regulation of *OSTL* (Figure 6.1).

OSTL was characterized by sequencing using a human and a mouse EST clones (see 6.1). The open-reading frame of mouse *Ostl* encodes a 307 aa protein and of human *OSTL* a 275 aa protein (Table 6.3) with a calculated molecular mass of 30 kDa (Figure 6.17). The OSTL protein contains three domains, a N-terminal variant RING finger (variant RING1), a DRIL or IBR domain and a C-terminal RING (RING2). These domains are evolutionarily highly conserved and have homologies in other genes from human, *C.elegans*, *D. melanogaster*, and *S. cerevisae* (Figures 6.4 and 6.5). The variant RING1 in OSTL has the same pattern as the C terminal RING (RING2) described in the human homologue of the *Drosophila Ariadne* gene (HHARI) (Capili, 2004). In the OSTL variant RING1 one of the apparently conserved metal binding ligand H4 is replaced by a Lys (Figure 7.1). The same situation is found in RNF14, a novel RING finger protein (RING finger 14) (Capili, 2004).

However, in RNF14 and other proteins that belong to the RING-IBR-RING family, such as Ariadne-1, Parkin, PARC, UIP28 (Capili, 2004) the amino acid residues show a consensus, which is not observed in OSTL (Figure 6.4 and 7.1).

In OSTL C7 and C8 of variant RING1 are separated by 4 aa residues but only by two aa in the other proteins (Figure 7.1).
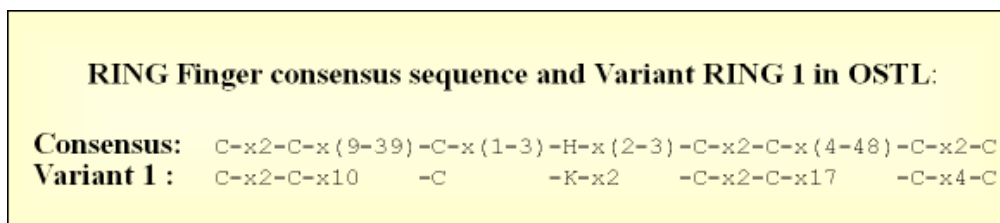
Figure 7.1: Schematic representation of RING finger domain consensus sequence and Variant RING 1 sequence in OSTL.

Comparison between human and mouse OSTL protein showed a 98% identity and between OSTL and puffer fish (*Fugu rubripes*) protein the identity is about 68% (Figure 6.5), suggesting an important, evolutionary conserved cellular function of this protein.

Sequence analysis of *OSTL* revealed the presence of six exons and five introns (Tables 6.1 and 6.2) and several alternatively spliced exons. However, only a minority of the alternatively spliced *OSTL* transcripts would code for longer proteins with functional domains (Table 6.3). At least seven "productive" alternatively spliced transcripts of *OSTL* were identified through sequencing and database searches (Table 6.4 and Figure 6.7).

Our mouse multiple tissues Northern analysis with the mouse 5' Ostl probe (Figure 6.8) revealed that *Ostl* is not very abundant in any of the tissues and the same was observed when human multiple tissue Northern blots were analyzed with a similar probe (Figure 6.9). The *Ostl* transcripts are not restricting to hematopoietic tissues as there is also strong expression in muscle tissue. Interestingly, the expression pattern of *OSTL* was similar to that observed for the *STL* gene, suggesting that these two genes are coregulated (Suto, 1997). Since we were not able to obtain the SUP-B2 cell line which was originally characterized by Zhang and coworkers in 1993 (it was lost in the freezer thaw of the 1999/2000 transition) we chose other B and B-related cell lines to perform the Northern analysis with the human 5' *OSTL* probe (Figure 6.10). Like in the human multiple tissue Northerns, the OSTL mRNA was not very abundant in these cell lines. *OSTL* transcripts were detected in one B-NHL and three EBV transformed B cell lines (Figure 6.10).

RT-PCR analysis detected expression of *OSTL* in two patient lymphoblastoid cell lines, a pre-B cell line, and showed expression in another different B-NHL cell (Figure 6.11). This discrepancy could be explained by the presence of different alternatively spliced transcripts in these cell lines or variations in the RNA quality.

Our RT-PCR using B-cells of different developmental stages (Figure 6.12) suggested the possible involvement of the gene in the course of B cell development.

We were able to show the *OSTL* expression in several B and also T-ALL samples from patients (Figures 6.13 and 6.14), demonstrating the presence of the gene in these types of leukemias.

The OSTL protein is found predominantly in the cytoplasm (Figure 6.16). During mouse developmental, *Ostl* expression was detected in all embryos examined from E9.5 until E14.5 dpc (Figure 6.18).

In accordance with the Northern data where *OSTL* transcripts were observed in skeletal muscle and liver, in the mouse embryos, *Ostl* expression was mainly observed in the somites, during limb development and in the branchial arches (Figures 6.18, 6.19 and 6.20). The primitive gut and its derivatives (liver, thymus, etc) originate from the branchial arches (from the first until the sixth branchial arches).

We attempted to express an OSTL-GST fusion protein in bacteria (Figure 6.21), which we planned to use for immunization to obtain OSTL antibodies, but we failed to obtain expression. This was probably due to the high number of cysteines in the OSTL protein. For such proteins, it has been reported that the proteins do not fold correctly and may be toxic for the bacteria. To circumvent this problem one could express an insoluble OSTL fusion protein (e.g. with tiorredoxin or the maltose binding protein).

7.2. The protein interaction partners of OSTL

In a yeast two hybrid screen we were able to identify several OSTL-interacting proteins from a Hela-cDNA bank (Figure 6.22). Interestingly, two OSTL-interacting proteins are involved in B-cell survival and B-cell receptor signaling.

HAX-1 (HS1-associated protein X-1) was first described to interact with HS1 in B-cells (Suzuki, 1997). HS1 (hematopoietic lyn substrate 1) is a component of the B-cell receptor (BCR) signaling pathway, its expression restricted to hematopoietic cells and it is rapidly tyrosine phosphorylated by a variety of non-receptor tyrosine kinases after lymphocytes stimulation (Kitamura, 1989; Yamanashi, 1993; Brunati, 1995). The activity of HS1 and possibly HAX1 may be important for survival of lymphocytes (Taniuchi, 1995; Suzuki, 1997). Suzuki and coworkers found that the *HAX1* open reading frame encoded a protein consisting of 279 amino acids (Figure 7.2 A) with a calculated molecular mass of 35 kDa. The HAX1 protein is hydrophilic, but contains a presumptive membrane-spanning hydrophobic domain at its carboxy terminus.

HAX1 as a whole has no significant homologies to other proteins, but shows some similarity to Nip3, which has been reported to interact with the adenovirus E1B and Bcl-2 protein (Boyd, 1994). HAX-1 possesses two Bcl-2 homologous domains BH1 and BH2 that are conserved among the Bcl-2 family proteins and are known to be critical for the regulation of apoptosis (Figure 7.2 A) (Yin, 1994; Suzuki, 1997). HAX1 contains a PEST sequence, suggesting that this protein may be degraded rapidly (Rogers, 1986) (Figure 7.2 A). Its mRNA is found in all tissues suggesting an essential function of this gene in intracellular signaling (Suzuki, 1997). The HAX1 protein has been reported to localize to the mitochondria, cytoplasm or plasma membrane (Suzuki, 1997; Gallagher, 2000; Dufva, 2001; Sharp, 2002).

HAX1 interacts with the polycystic kidney disease protein (PKD2) and this interaction probably mediates its association with the actin cytoskeleton (Gallagher, 2000).

Interaction between HAX1 and Epstein-Barr virus nuclear antigen leader protein (EBNA-LP or EBNA5) was demonstrated by Kawaguchi, 2000 and by Dufva, 2001 and again suggesting a role of HAX1 in apoptosis.

Recently a model of complex formation was proposed for the EBNA-LP, HAX1 and Bcl-2 proteins. EBNA-LP interacts with HAX1 via its nuclear localization signal (NLS) and HAX1 associates with Bcl-2 through its BH2 domain, further supporting the hypothesis that HAX1 is a regulator of apoptosis (Matsuda, 2003). Yin and coworkers in 2001 reported interaction between HAX1 and IL-1α and suggested that HAX1 may modulate multiple facets of the N-terminal peptide of interleukin-1α (IL-1 NTP) biochemistry.

Through interaction between HAX1 and Kaposi's Sarcoma-associated herpesvirus protein (K15), Sharp and coworkers in 2002 were able to show that HAX1 is able to block BAX induced apoptosis (BAX is a Bcl-2 family member with a strong proapoptotic function). HAX1 was found to be upregulated in psoriatic lesions (Mirmohammadsadegh, 2003). Mirmohammadsadegh and coworkers analyzed UBV-induced apoptosis in HaCaT keratinocytes overexpressing *HAX1* mRNA or its antisense and found further evidence for the role of HAX1 in antiapoptotic processes.

HAX1-specific antisense led to a marked increase in caspase-3 mediated apoptosis, strongly suggesting an antiapoptotic role for HAX1 (Mirmohammadsadegh, 2003). HAX1 interacts with bile salt export protein (BSEP) and regulates its abundance in the apical membrane of Madin-Darby canine kidney cells (Ortiz, 2004). A mechanism was proposed suggesting HAX1 involvement in clathrin-mediated endocytosis: BSEP and HAX1 are present in clathrin-coated vesicles; expression of dominant negative EPS15, which selectively blocks

clathrin mediated endocytosis (Benmerah, 1999), doubled the apical membrane concentration of BSEP; and expression of dominant negative cortactin also doubled the amount of BSEP in the apical membrane. Cortactin, an actin and HAX1-binding protein, participates in clathrin endocytosis (Lynch, 2003; Cao, 2003).

HAX1 interacts with $G\alpha_{13}$, the α-subunit of the heterotrimeric G protein G13, this protein has been shown to stimulate cell migration in addition to inducing oncogenic transformation (Radhika, 2004).

HAX1 potentiate activation of Rac through $G\alpha_{13}$; Rac stimulates the translocation of cortactin (Patel, 1998; Weed, 1998); cortactin stimulates actin polymerization leading to lamellipodia formation (Weed, 1998; Uruno, 2001; Uruno, 2003); and HAX1 promotes $G\alpha_{13}$-mediated cell motility, suggesting that $G\alpha_{13}$ and HAX1 are part of a signaling complex involved in cell motility (Radhika, 2004).

Finally, HAX1 interacts with Omi/HtrA2, a nuclear-encoded mitochondrial serine protease that has a pro-apoptotic function in mammalian cells (Cilenti, 2004). Cilenti and coworkers could show that through this interaction, Omi cleaves HAX1 and can initiate apoptosis from mitochondria.

In our work we could show interaction between OSTL and HAX1 and this interaction was confirmed by using *in vivo* and *in vitro* assays. Interestingly, by using OSTL as bait in a yeast two hybrid assay we were able to identify eight different HAX1 clones (Figure 6.25). We selected three clones (2, 3, and 5) and confirmed the interaction by cotransformation assay in yeast (Figure 6.26). Further assays to confirm the interaction between OSTL and HAX1 were performed using HAX1 clone 5, which contains almost the whole *HAX1* cDNA (Figure 6.25). The interaction was mapped by cotransformation between different Ostl mutants with HAX1 clone 5 (Figure 6.29). The OSTL variant RING1 (the N terminal RING finger of OSTL) seems to be involved in the interaction with HAX1 (Figure 6.29).

Surprisingly, *Ostl* mutants 1 and 3 (lanes 2 and 4 in figure 6.29) did not show any interaction with HAX1 (any growth in the yeast cotransformation), although they have only one amino acid that is different from the *Ostl* mutant 2 and human *OSTL* (lanes 3 and 8 in figure 6.29) which are capable of interaction with HAX1 (they showed a very nice growth in the yeast cotransformation assay). In *Ostl* mutants 2 and 4 a serine (S) at position 2 is substituted by a adenine (A), this substitution might be responsible for the difference observed in the interaction assay (Figure 6.29).

The interaction between OSTL and HAX1 was also confirmed in mammalian cells (NIH3T3) by cotransfection assays (Figure 6.32), where we could show colocalization of both proteins

in the cytoplasm of the mouse fibroblast cells. Colocalization was also observed in the mitochondria (data not showed).

The *in vitro* confirmation of interaction was by coimmunoprecipitation using S^{35} labeled myc-GAL4DBD-OSTL and HA-GAL4AD-HAX1 proteins. Both proteins could be coprecipitated using an anti myc antibody (Figure 6.35).

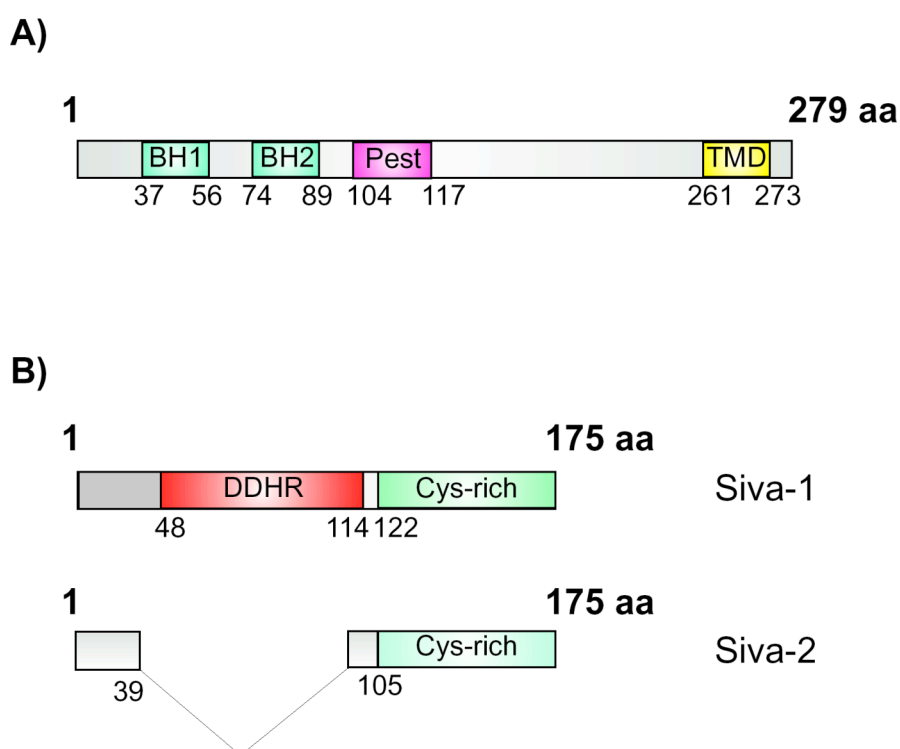CFP-*OSTL* and YFP-*HAX1* overexpressed in 293 cells could be coprecipitated (Figure 6.36). This assay confirmed *in vivo* the association of the two proteins.

Figure 7.2: A) Schematic representation of HAX1 amino acid (aa) sequence and domains. BCL-2 homology domains 1 and 2 (BH1 and -2), a PEST domain, and a transmembrane domain (TMD) are indicated (Figure adapted from Sharp, 2002). **B)** Schematic representation of Siva-1 and Siva-2 aa sequences. A death domain homology region (DDHR), and a cysteine-rich domain are represented in Siva-1 diagram. Siva-2 lacks the exon 2, corresponding to the 65 aa of the DDHR (Figure adapted from Py, 2004).

SIVA (from Shiva, the Hindu god of destruction) was first described to bind to the CD27 cytoplasmic tail in a yeast two hybrid assay and function as a proapoptotic protein (Prasad, 1997). The human SIVA protein contains 189 aa (Prasad, 1997), the rat Siva 177 aa. Human and rat SIVA are 92% homologous (Padanilam, 1998). Analysis of the primary amino acid sequence revealed an amino-terminal region that has a 40% homology to the death domains (DDs) of FADD and RIP. The homologies between SIVA and TRADD/Ankyrin DDs is 16% and between SIVA and FADD DDs 14% (Yoon, 1999). SIVA has a carboxy-terminal region

rich in cystein residues that could form a B-box-like ring finger (Yang, 1997) (Figure 7.2 B). The B-box region of SIVA, however, lacks any histidine residues. The amino-terminal RING finger and the carboxy-terminal coiled-coil domain, which are characteristic of other B-box-containing proteins (Yang, 1997), are absent in SIVA. Instead, SIVA has additional cystein residues at the carboxy terminus that can potentially form a zinc finger (residues 164-184 in the human SIVA).

Alternatively, the Cys-rich region of SIVA could represent a novel metal binding motif involved in either protein-protein or protein-DNA interactions. The architecture of SIVA is unlike that of any other protein known to bind to the cytoplasmic tails of TNFR family members. The human *SIVA* mRNA is expressed mainly in thymus and testis, but also in spleen, prostate, ovary, small intestine, PB and to a lesser amount in colon. The SIVA expression was also observed in some cell lines including HL60, HeLa, Raji, K562, MOLT4, SW480, and G361 (Prasad, 1997). In 1997 Prasad and coworkers could demonstrate the proapoptotic properties of SIVA in various cell lines (293, Jurkat, Raji, a murine pre-B cell (SKW), and Ramos) by transiently expressing SIVA as a GFP fusion protein.

In 1999, Yoon and coworkers showed that mouse SIVA is 80% homologous to human SIVA. The murine *Siva* mRNA is mainly expressed in testis, muscle, and heart with brain expressing the least. Two forms of mouse *Siva* cDNA were identified by Yoon and coworkers. The longer form was named *Siva-1* and the shorter form *Siva-2* (Yoon et al., 1999) (Figure 7.2 B). Part of the amino terminal region and most of the death domain homology region (DDHR) including the conserved 13 amino acids stretch is missing in *Siva-2*. Although *Siva-2* lacks the major portion of the DDHR, it showed association with the cytoplasmic tail of the CD27 receptor, as did *Siva-1* (Figure 7.2 B). However, murine and human SIVA-2 are much less proapoptotic than SIVA-1 (Yoon, 1999). SIVA was also reported to be up-regulated in colorectal cancer (Okuno, 2001) and research groups have recently reported the apoptotic activity of SIVA (Lin, 1999; Xiao, 2000; Henke, 2000; Cao, 2001; Qin, 2002; Xue, 2002; Spinicelli; 2002; Daoud, 2003; Chu, 2004; Seseke, 2004; Py, 2004; Fortin, 2004; Novikowa, 2005).

We found interaction between OSTL and the proapoptotic human SIVA-1 in our yeast two hybrid assay (Tables 6.6 and 6.8; Figure 6.25; and attachment 4). We were able to confirm the interaction through *in vivo* (Figure 6.33, 6.37) and *in vitro* assays (Figure 6.26, 6.30). The RING finger at the N terminal region of OSTL (variant RING1) and the C terminal region of OSTL seems to be involved in the interaction between OSTL and SIVA (Figure 6.30).

The mapping of OSTL-SIVA interaction showed the same pattern of yeast growth that was observed for the OSTL-HAX1 interaction mapping. The amino acid substitutions (V→Q), is probably responsible for the negative interaction results between *Ostl* mutants 1 and 3 and SIVA (Figures 6.29 and 6.30).

CFP-*OSTL* and YFP-*SIVA* overexpressed in 293 cells could be coprecipitated (Figure 6.37). This assay confirmed *in vivo* the association of the two proteins.

Summarizing our yeast two hybrid data, we propose a functional pathway for OSTL through its interaction with HAX1 and SIVA (Figure 7.3). SIVA and HAX1 are involved in pro- and antiapoptotic decisions in the cell, respectively.
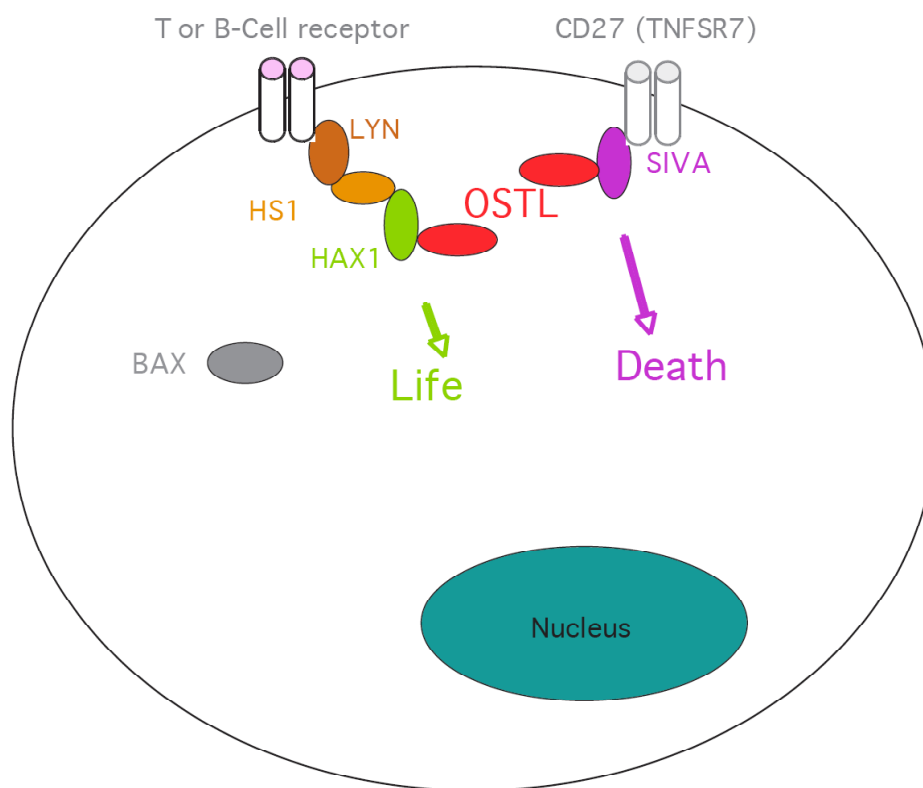

Figure 7.3: Hypothetical role of OSTL mediated through its interactions with HAX1 and SIVA.

7.3. *Functional characterization of Ostl*

Most of RING finger proteins function as E3 ubiquitin protein ligases in the ubiquitin conjugation pathway where they catalyze the transfer of an activated ubiquitin from an E2 ubiquitin conjugating enzyme to a substrate protein (Joazeiro, 2000; Fang, 2003). In our work, we performed an ubiquitination assay using HAX1 and SIVA as possible substrates for Ostl function as an E3 ubiquitin ligase (Figures 6.39 and 6.40). But neither HAX1 nor SIVA showed increased ubiquitination in this assay. However, these results do not completely rule out that Ostl functions as an E3 ubiquitin protein ligase. More potential Ostl substrates have to be tested.

In order to investigate the potential of *Ostl* to transform primary hematopoietic cells, we overexpressed *Ostl* in primary bone marrow cells and assayed the transforming activity in various assays.

In vitro assays, such as liquid culture assays in the presence of myeloid cytokines (IL-3, IL-6, and SCF) did not show a significant transformation potential of *O*stl, in comparison to GFP positive cells (MIG) or to negative cells (Mock) (Figure 6.42). However, when we overexpressed *Ostl in vivo*, injecting lethally irradiated mice with *Ostl*-positive cells, leukemias developed after a median of 300 days (Figure 6.43). The immunophenotypic and histopathologic analysis of the leukemic mice revealed a T-ALL (Figures 6.44 and 6.46). The BM and spleen cells from such an *Ostl*-induced T-ALL showed 96% positivity for CD4 and CD8 as shown in figure 6.44. The histopathology of one of the mice showed multiple organ infiltration with blasts cells, which were positive for CD3 and Tdt (Figure 6.46). Figure 6.47 shows the microscopic analysis of BM and spleen from an *Ostl*-induced T-ALL, with a high percentage (more than 60% of the cells) of lymphoid cells. The expression of the *Ostl* gene in the leukemic mice was assayed by RT-PCR (Figure 6.45).

Although the expression of *Ostl* was observed only in the cell subpopulation of the leukemic mice and not in controls cells, the leukemic cells did not show expression of GFP. In order to confirm the presence of the OSTL carrying retrovirus in the leukemic cells of these mice we are in the process of analyzing the retroviral integration sites in these leukemias. It has been reported that retroviral integration by itself will only rarely lead to hematologic malignancies (Duesberg, 1987). This information strongly suggests that the expression of OSTL is the cause of the leukemias in our model. These OSTL-induced leukemias could be transplanted into secondary recipient mice, which also developed leukemia and died four weeks after injection of primary leukemic cells (Figure 6.43).

In 2005, Schessl and coworkers reported leukemia in mice expressing the *AML1-ETO* fusion gene and a *FLT3* length mutation showing a latency period for the leukemia phenotype ranging from 100 until more than 600 days after transplantation. The 300 days latency of leukemia development observed in our model could be due to the need of secondary *in vivo* genetic events in the animals.

OSTL was first identified in an B-cell acute lymphoblastic leukemia cell line, which a t(6;12)(q23;p13), and in our work its expression was also observed in leukemic cells with different immunophenotypes and genetic backgrounds. In our mouse model, *Ostl* caused a T-ALL, but the high expression of this gene observed in AML and B-ALL patients might reflect the importance of this gene in a wider range of leukemias (Figures 6.13 and 6.14).

Our data suggest that *OSTL* is one of the genes on the long arm of chromosome 6 that might be important in the development of childhood acute lymphoblastic leukemia (ALL) and lymphomas of B and T-cell types (Hayashi, 1990), and adult ALL (Merup, 1998).

8. References

Aaronson S. A, Todaro G. J. (1968). Development of 3T3-like lines from Balb-c mouse embryo cultures: transformation susceptibility. *J Cell Physiol.* **72** (2), 141-8.

Adolfsson J., Borge O. J., Bryder D., Theilgaard-Monch K., Astrand-Grundstrom I., Sitnicka E., Sasaki Y., Jacobsen S. E. (2001). Upregulation of Flt3 expression within the bone marrow Lin(-)Sca1(+)c-kit(+) stem cell compartment is accompanied by loss of self-renewal capacity. *Immunity.* **15** (4), 659-69.

Akashi K., Traver D., Kondo M., Weissman I. L. (1999). Lymphoid development from hematopoietic stem cells. *Int J Hematol.* **69** (4), 217-26.

Akashi K., Traver D., Miyamoto T., Weissman I. L. (2000). A clonogenic common myeloid progenitor that gives rise to all myeloid lineages. *Nature.* **404** (6774), 193-7.

Allman D., Sambandam A., Kim S., Miller J. P., Pagan A., Well D., Meraz A., Bhandoola A. (2003). Thymopoiesis independent of common lymphoid progenitors. *Nat Immunol.* **4** (2), 168-74.

Antonchuk J., Sauvageau G., Humphries R, K. (2001). HOXB4 overexpression mediates very rapid stem cell regeneration and competitive hematopoietic repopulation. *Exp Hematol.* **29** (9), 1125-34.

Baer R. (1993). TAL1, TAL2 and LYL1: a family of basic helix-loop-helix proteins implicated in T cell acute leukaemia. *Semin Cancer Biol.* **34** (6), 341-7.

Bartram C. R., de Klein A., Hagemeijer A., van Agthoven T., Geurts van Kessel A. (1983). Translocation of c-ab1 oncogene correlates with the presence of a Philadelphia chromosome in chronic myeloid leukaemia. *Nature.* **306** (5940), 277-80.

Belloni E., Trubia M., Mancini M., Derme V., Nanni M., Lahortiga I., Riccioni R., Confalonieri S., Lo-Coco F., Di Fiore P. P. (2004). ETV6: A new complex rearrangment involving the ETV6, LOC114448, and MN1 genes in a case of acute myeloid leukemia. *Genes Chromosomes Cancer.* **41** (3), 272-7.

Benmerah A., Bayrou M., Cerf-Bensussan N., Dautry-Varsat A. (1999). Inhibition of clathrin-coated pit assembly by an Eps15 mutant. *J Cell Sci.* 11**2** (9), 1303-11.

Beverloo H. B., Panagopoulos I., Isaksson M., et al. (2001). Fusion of the homeobox gene HLXB9 and the ETV6 gene in infant acute myeloid leukemias with the t(7;12)(q36;p13). *Cancer Res.* **61**, 5374-77.

Boehm T., Foroni L., Kennedy M., Rabbitts T. H. (1990). The rhombotin gene belongs to a class of transcriptional regulators with a potential novel protein dimerisation motif. *Oncogene.* **5** (7), 1103-5.

Bohlander S. K. (2005). ETV6: A versatile player in leukemogenesis. *Semin Cancer* Biol. **15** (3), 162-74.

Bonnet D. (2003). Hematopoietic stem cells. *Birth Defects Res C Embryo Today*. 69 (3), 219-29.

Borrow J., Goddard A. D., Sheer D., Solomon E. (1990). Molecular analysis of acute promyelocytic leukemia breakpoint cluster region on chromosome 17. *Science.* 249, 1577-80.

Boyd J. M., Malstrom S., Subramanian T., Venkatesh L. K., Schaeper U., Elangovan B., D'Sa-Eipper C., Chinnadurai G. (1994). Adenovirus E1B 19 kDa and Bcl-2 proteins interact with a common set of cellular proteins. *Cell.* **79** (2), 341-51.

Brunati A. M., Ruzzene M., James P., Guerra B., Pinna L. A. (1995). Hierarchical phosphorylation of a 50-kDa protein by protein tyrosine kinases TPK-IIB and C-Fgr, and its identification as HS1 hematopoietic-lineage cell-specific protein. *Eur J Biochem.* **229** (1), 164-70.

Buijs A., Sherr S., van Baal S., van Bezouw S., van der Plas D., Geurts van Kessel A., Riegman P., Lekanne Deprez R., Zwarthoff E., Hagemeijer A., et al. (1995). Translocation (12;22) (p13;q11) in myeloproliferative disorders results in fusion of the ETS-like TEL gene on 12p13 to the MN1 gene on 22q11. *Oncogene.* **11** (4), 809.

Burmeister T., Thiel E. (2001). Molecular genetics in acute and chronic leukemias. *J Cancer Res Clin Oncol.* **127** (2), 80-90.

Buske C., Feuring-Buske M., Abramovich C., Spiekermann K., Eaves C. J., Coulombel L., Sauvageau G., Hogge D. E., Humphries R. K. (2002). Deregulated expression of HOXB4 enhances the primitive growth activity of human hematopoietic cells. *Blood.* **100** (3), 862-8.

Busslinger M. (2004). Transcriptional control of early B cell development. *Annu Rev Immunol.* **22**, 55-79.

Cao C., Ren X., Kharbanda S., Koleske A., Prasad K. V., Kufe D. (2001). The ARG tyrosine kinase interacts with Siva-1 in the apoptotic response to oxidative stress. *J Biol Chem.* **276** (15), 11465-8.

Cao H., Orth J. D., Chen J., Weller S. G., Heuser J. E., McNiven M. A. (2003). Cortactin is a component of clathrin-coated pits and participates in receptor-mediated endocytosis. *Mol Cell Biol.* **23** (6), 2162-70.

Capili A. D., Schultz D. C., Rauscher F. J., Borden K. L. (2001). Solution structure of the PHD domain from the KAP-1 corepressor: structural determinants for PHD, RING and LIM zinc-binding domains. EMBO *J.* **20**, 165-77.

Capili A. D., Edghill E. L., Wu K., Borden K. L. (2004). Structure of the C-terminal RING finger from a RING-IBR-RING/TRIAD motif reveals a novel zinc-binding domain distinct from a RING. *J Mol Biol.* **340** (5), 1117-29.

Cazzaniga G., Tosi S., Aloisi A., et al. (1999). The tyrosine kinase abl-related gene ARG is fused to EYV6 in an AML-M4Eo patient with a t(1;12)(q25;p13): molecular cloning of both reciprocal transcripts. *Blood.* **94**, 4370-73.

Chase A., Reiter A., Burci L., et al. (1999). Fusion of ETV6 to the caudal-related homeobox gene CDX2 in acute myeloid leukemia with the t(12;13)(p12;q12). *Blood.* **93**, 1025-31.

Chien C. T., Bartel P. L., Sternglanz R., Fields S. (1991). The two-hybrid system: a method to identify and clone genes for proteins that interact with a protein of interest. *Proc Natl Acad Sci U S A.* **88** (21), 9578-82.

Christensen J. L., Weissman I. L. (2001). Flk-2 is a marker in hematopoietic stem cell differentiation: a simple method to isolate long-term cells. *Proc Natl Acad Sci U S A.* **98** (25), 14541-6.

Chu F., Borthakur A., Sun X., Barkinge J., Gudi R., Hawkins S., Prasad K. V. (2004). The Siva-1 putative amphipathic helical region (SAH) is sufficient to bind to BCL-XL and sensitize cells to UV radiation induced apoptosis. *Apoptosis.* **9** (1), 83-95.

Cilenti L., Soundarapandian M. M., Kyriazis G. A., Stratico V., Singh S., Gupta S., Bonventre J. V., Alnemri E. S., Zervos A. S. (2004). Regulation of HAX-1 anti-apoptotic protein by Omi/HtrA2 protease during cell death. *J Biol Chem.* **279** (48), 50295-301.

Cools J., Mentens N., Odero M. D., et al. (2002). Evidence for position effects as a variant ETV6-mediated leukemogenic mechanism in myeloid leukemias with a t(4;12)(q11-q12;p13) or t(5;12)(q31;p13). *Blood.* **99**, 1776-84.

Cohen N., Sharma M., Kentsis A., Perez J. M., Strudwick S., Borden K. L. (2001). PML RING suppresses oncogenic transformation by reducing the affinity of eiF4E for mRNA. *EMBO J.* **20**, 4547-59.

Copeland N. G., Zelenetz A. D., Cooper G. M. (1979). Transformation of NIH/3T3 mouse cells by DNA of Rous sarcoma virus. *Cell.* **17** (14), 993-1002.

Daoud S. S., Munson P.J., Reinhold W., Young L., Prabhu V. V., Yu Q., LaRose J., Kohn K. W., Weinstein J. N., Pommier Y. (2003). Impact of p53 knockout and topotecan treatment on gene expression profiles in human colon carcinoma cells: a pharmacogenomic study. *Cancer Res.* **63** (11), 2782-93.

Dash A., Gilliland D. G. (2001). Molecular genetics pf acute myeloid leukaemia. *Best Pract Res Clin Haematol.* **14**, 49-64.

Dawid I. B., Breen J. J., Toyama R. (1998). LIM domains: multiple roles as adapters and functional modifiers in protein interactions. *Trends Genet.* **14**, 156-62.

Dear T. N., Sanchez-Garcia I., Rabbitts T. H. (1993). The HOX11 gene encodes a DNA-binding nuclear transcription factor belonging to a distinct family of homeobox genes. *Proc Natl Acad Sci USA.* **90** (10), 4431-5.

De Klein A., Hagemeijer A., Bartram C. R., Houwen R., Hoefsloot L., Carbonell F., Chan L., Barnett M., Greaves M., Kleinhauer E, et al. (1986). bcr rearrangement and translocation of the c-abl oncogene in Philadelphia positive acute lymphoblastic leukemia. *Blood.* **68** (6), 1369-75.

Dernburg A. F., Sedat J. W. (1998). Mapping three-dimensional chromosome architecture in situ. *Methods Cell Biol.* **53**, 187-233.

De The H., Chomienne C., lanotte M., Degos L., Dejean A. (1990). The t(15;17) translocation of acute promyelocytic leukaemia fuses the retinoic acid receptor alpha gene to a novel transcribed locus. *Nature.* **347**, 558-61.

Detrich H. W. 3rd', Kieran M. W., Chan F. Y., Barone l. M., Yee K., Rundstadler J. A., Pratt S, Ransom D., Zon L. I. (1995). Intraembyonic hematopoietic cell migration during vertebrate development. *Proc Natl Acad Sci USA.* **92** (23), 10713-7.

Domen J., Gandy K. L., Weissman I. L. (1998). Systemic overexpression of BCL-2 in the hematopoietic system protects transgenic mice from the consequences of lethal irradiation. *Blood.* **91** (7), 2272-82.

Domen J., Weissman I. L. (2000). Hematopoietic stem cells need two signals to prevent apoptosis; BCL-2 can provide one of these, Kitl/c-Kit signaling the other. *J Exp Med.* **192** (12), 1707-18.

Dube I. D., Kamel-Reid S., Yuan C. C., Lu M., Wu X., Corpus G., Raimondi S. C., Crist W. M., Carroll A. J., Minowasa J. et al. (1991). A novel human homeobox gene lies at the chromosome 10 breakpoint in lymphoid neoplasias with chromosomal translocation t(10;14). *Blood.* **78** (11), 2996-3003.

Duesberg P. H. (1987). Retroviruses as carcinogens and pathogens: expectations and reality. *Cancer Research.* **47** (5), 1199-220.

Dufva M., Olsson M., Rymo L. (2001). Epstein-Barr virus nuclear antigen 5 interacts with HAX-1, a possible component of the B-cell receptor signalling pathway. *J Gen Virol.* **87** (7), 1581-7.

Dyer M. J., Fischer P., Nacheva E., Labastide W., Karpas A. (1990). A new human B-cell non-Hodgkin's lymphoma cell line (Karpas 422) exhibiting both t(14;18) and t(4;11) chromosomal translocations. *Blood.* **75** (3), 709-14.

Eaves C., Miller C., Cashman J., Conneally E., Petzer A., Zandstra P., Eaves A. (1997). Hematopoietic stem cells: inferences from in vivo assays. *Stem Cells.* **15** (1), 1-5.

Fang S., Iorick K. L., Jensen J. P., Weissman A. M. (2003). RING finger ubiquitin protein ligases: implications for tumorigenesis, metastasis and for molecular targets in cancer. *Semin Cancer Biol.* **13** (1), 5-14.

Feilotter H. E., Hannon G. J., Ruddell C. J., Beach D. (1994). Constructions of an improved host strain for two hybrid screening. *Nucleic Acids Res.* **22** (8), 1502-3.

Fenrick R., Amann J. M., Lutterbach B., et al. (1999). Both TEL and AML-1 contribute repression domains to the t(12;21) fusion protein. *Mol Cell biol.* **19**, 6566-74.

Feuring-Buske M., Frankel A. E., Alexander R. L., Gerhard B., Hogge D. E. (2002). A diphtheria toxin-interleukin 3 fusion protein is cytotoxic to primitive acute myeloid leukemia progenitors but spares normal progenitors. *Cancer Res.* **62** (6), 1730-6.

Fields S., Song O. (1989). A novel genetic system to detect protein-protein interactions. *Nature.* **340** (6230), 245-6.

Fontanari Krause L., Przemeck G., Hrabe de Angelis M., Bohlander S. K. (2003). The OSTL gene encodes for a conserved RING finger protein which interacts with HAX1 and SIVA: possible role in B cell signaling and survival. *Blood.* **102**, 848a.

Fortin A., MacLaurin J. G., Arbour N., Cregan S. P., Kushwaha N., Callaghan S. M., Park D. S., Albert P. R., Slack R. S. (2004). The proapoptotic gene SIVA is a direct transcriptional target for the tumor suppressors p53 and E2F1. *J Biol Chem.* **79** (27), 28706-14.

Freemont P. S., Hanson I. M., Trowsdale J. (1991). A novel Cysteine-rich sequence motif. *Cell.* **64** (3), 483-84.

Freemont P. S. (1993). The RING finger. A novel protein sequence motif related to the zinc finger. *Ann N Y Acad Sci.* **684**, 174-92.

Gallagher A. R., Cedzich A., Gretz N., Somlo S., Witzgall R. (2000). The polycystic kidney disease protein PKD2 interacts with the actin cytoskeleton. *Proc Natl Acad Sci USA.* **97** (8), 4017-22.

Golub, T. R., Barker G.F., Lovett M., Gilliland D. G. (1994a). Fusion of PDGF receptor beta to a novel ets-like gene, tel, in chronic myelomonocytic leukemia with t(5;12) chromosomal translocation. *Cell.* **77** (2), 307-16.

Golub, T. R., Barker B.F., Bohlander S. K., Stegmaier K., Bray-Ward P., Ward D. C., Sato Y., Suto Y., Rowley J. D., Gilliland D. G. (1994b). Evidence implicating the TEL gene at 12p13 in multiple mechanisms of leukemogenesis. *Blood.* **84**, 229a.

Golub, T. R., Barker G.F., Bohlander S. K., Hiebert S. W., Ward D. C., Bray-Ward P., Morgan E., Raimondi S. C., Rowley J. D., Gilliland D. G. (1995). Fusion of the TEL gene on 12p13 to the AML1 gene on 21q22 in acute lymphoblastic leukemia. *Proc Natl Acad Sci U S A.* **92** (11), 4917-21.

Gounari F., Aifantis I., Martin C., Fehling H. J., Hoeflinger S., Leder P., von Boehmer H., Reizis B. (2002). Tracing lymphopoiesis with the aid of a pTalpha-controlled reporter gene. *Nat Immunol.* **3** (5), 489-96.

Graham F. L., Smiley J., Russell W. C., Nairn R. (1977). Characteristics of a human cell line transformed by DNA from human adenovirus type 5. *J Gen Virol.* **36** (1), 59-74.

Greil J., Gramatzki M., Burger R., Marschalek R., Peltner M., Trautmann U., Hansen-Hagge T. E., Bartram C. R., Fey G. H., Stehr K., Beck J. (1994). The acute lymphoblastic leukaemia cell line SEM with t(4;11) chromosomal rearrangement is biphenotypic and responsive to interleukin-7 . *Br J Haematol.* **86** (2), 275-83.

Grimshaw S. J., Mott H. r., Stott K. M., Nielson P. R., Evetts K. A., Hopkins L. J., et al. (2004). Structure of the sterile alpha motif (SAM) domain of the *Saccharomyces cerevisiae* mitogen-activated protein kinase pathway-modulating protein STE50 and analysis of its interaction with the STE11 SAM. *J Biol Chem.* **279**, 2192-201.

Hardy R. R., Carmack C. E., Shinton S. A., Kemp J. D., Hayakawa K. (1991). Resolution and characterization of pro-B and pre-B cell stages in normal mouse bone marrow. *J Exp Med.* **173** (5), 1213-25.

Hardy R. R., Li Y. S., Allman D., Asano M., Gui M., Hayakawa K. (2000). B-cell commitment, development and selection. *Immunol Rev.* **175**, 23-32.

Hatano M., Roberts C. W., Minden M., Crist W. M., Korsmeyer S. J. (1991). Deregulation of a homeobox gene, HOX11, by the t(10;14) in T cell leukemia. *Science.* **253**, 79-82.

Hayashi Y., Raimondi S. C., Look A. T., Behm F. G., Kitchingman G. R., Pui C. H., Rivera G. K., Williams D. L. (1990). Abnormalities of the long arm of chromosome 6 in childhood acute lymphoblastic leukemia. *Blood.* **76** (8), 1626-30.

Henke A., Launhardt H., Klement K., Stelzner A., Zell R., Munder T. (2000). Apoptosis in coxsackievirus B3-caused diseases: interaction between the capsid protein VP2 and the proapoptotic protein siva. *J Virol.* **74** (9), 4284-90.

Hershko A., and Ciechanover A. (1998). The ubiquitin system. *Ann Rev Biochem.* **67**, 425-79.

Hicke L. & Dunn R. (2003). Regulation of membrane protein transport by ubiquitin and ubiquitin-binding proteins. *Annu Rev Cell Dev Biol.* **19**, 141-72.

Hilden J. M., Smith F. O., Frestedt J. L., McGlennen R., Howells W. B., Sorensen P. H., Arthur D. C., Woods W. G., Buckley J., Bernstein I. D., Kersey J. H. (1997). MLL gene rearrangement, cytogenetic 11q23 abnormalities, and expression of the NG2 molecule in infant acute myeloid leukemia. *Blood.* **89**, 3801-05.

Hock H., Meade E., Medeiros S., Schindler J. W., Valk P. J., Fujiwara Y., Orkin S. H. (2004). Tel/Etv6 is an essential and selective regulator of adult hematopoietic stem cell survival. *Genes Dev*. **18** (19), 2336-41.

Holyoake T. L., Nicolini F. E., Eaves C. J. (1999). Functional differences between transplantable human hematopoietic stem cells from fetal liver, cord blood, and adult marrow. *Exp Hematol*. 2**7** (9), 1418-27.

Hurwitz R., Hozier J., LeBien T., Minowada J., Gajl-Peczalska K., Kubonishi I., Kersey J. (1979). Characterization of a leukemic cell line of the pre-B phenotype. *Int J Cancer*. **23** (2), 174-80.

Igarashi H., Gregory S. C., Yokota T., Sakagucgi N., Kincade P. W. (2002). Transcription from the RAG1 locus marks the earliest lymphocyte progenitors in bone marrow. *Immunity*. 1**7** (2), 117-30.

Jadayel D. M., Lukas J., Nacheva E., Bartkova J., Stranks G., De Schouwer P. J., Lens D., Bartek J., Dver M. J., Kruger A. R., Catovsky D. (1997). Potential role for concurrent abnormalities of the cyclin D1, p16^{CDKN2} and p15^{CDKN2B} genes in cetain B cell non-hodgkin's lymphomas. Functional studies in a cell line (Granta 519). *Leukemia*. **11** (1), 64-72.

Jainchill J. L., Aaronson S. A., Todaro G. J. (1969). Murine sarcoma and leukemia viruses: assay using clonal lines of contact-inhibited mouse cells. *J Virol*. **4** (5), 549-53.

James P., Haliaday J., Craig E. A. (1996). Genomic libraries and a host strain designed for highly efficient two-hybrid selection in yeast. *genetics*. **144**, 1425-36.

Joazeiro C. A., Weissman A. M. (2000). RING finger proteins: mediators of ubiquitin ligase activity. *Cell*. **102** (5), 2061-2.

Jones R. J., Collector M. I., Barber J. P., Vala M. S., Fackler M. J., May W. S., Griffin C. A., Hawkrins A. L., Zehnbauer B. A., Hilton J., Colvin O. M., Sharkis S. J. (1996). Caracterization of mouse lymphohematopoietic stem cells lacking spleen colony-forming activity. *Blood*. **88** (2), 487-91.

Jordan C. T., Lemischka I. R. (1990). Clonal and systemic analysis of long-term hematopoiesis I the mouse. *Genes Dev*. **4** (2), 220-32.

Jumaa H., Hendriks R. W., Reth M. (2005). B cell signaling and tumorigenesis. *Annu Rev Immunol*. **23**, 415-45.

Kaufman M. H. (1994). The atlas of mouse development. **2nd ed**.

Kawaguchi Y., Nakajima K., Igarashi M., Morita T., Tanaka M., Suzuki M., Yokoyama A., Matsuda G., Kato K., Kanamori M., Hirai K. (2000). Interaction of Epstein-Barr virus nuclear leader protein (EBNA-LP) with HS1-associated protein X-1: implication of cytoplasmic function of EBNA-LP. *J Virol*. **74** (21), 10104-11.

Kennedy M. A., Gonzales-sarmiento R., Kees U. R., Lampert F., Dear N., Boehm T., Rabbits T. H. (2001). HOX11, a homeobox-containing T-cell oncogene on human chromosome 10q24. *Proc Natl Acad Sci USA.* **88** (20), 8900-4.

Kentsis A., Dwyer E. C., Perez J. M., Sharma M., Chen A., Pan Z. Q., Borden K. L. (2001). The RING domains of the promyelocytic leukemia protein PML and the arenaviral protein Z repress translation by directly inhibiting translation initiation factor eIF4E. *J Mol Biol.* **312**, 609-23.

Kispert A., Vainio S., Shen L., Rowitch D. H., McMahon A. P. (1996). Proteoglycans are required for maintenance of Wnt-11 expression in the ureter tips. *Development.* **122** (11), 3627-37.

Kitamura D., Kaneko H., Taniuchi I., Akagi I., Yamamura K., Watanabe T. (1989). Molecular cloning and characterization of mouse HS1. *Biochem Biophys Res Commun.* **208** (3), 1137-43.

Kluin-Nelemans H. C., Limpens J., Meerabux J., Beverstock G. C., Jansen J. H., de Jong D., Kluin P. M. (1991). A new non-Hodgkin's B-cell line (DoHH2) with a chromosomal translocation t(14;18)(q32;q21). *Leukemia.* **5** (3), 221-4.

Kobayashi H., Montgomery K. T., Bohlander S. K., Adra C. N., Lim B. L., Kucherlapati R. S., Donis-Keller H., Holt M. S., Le Beau M. M. (1994). Fluorescence in situ hybridization mapping of translocations and deletions involving the short arm of human chromosome 12 in malignant hematologic diseases. *Blood.* **84** (10), 3473-82.

Koegl M. T., Hoppe S., Schenkler H. D., Ulrich T. U., Mayer, et al. (1999). A novel ubiquitination factor, E4, is involved in multiubiquitin chain assembly. *Cell.* **96**, 635-44.

Kondo M., Weissman I. L., Akashi K. (1997). Identification of clonogenic common lymphoid progenitors in mouse bone marrow. *Cell.* **91** (5), 661-72.

Kuno Y., Abe a., Emi N., Iida M., Yokozawa t., towatari M., et al. (2001). Constitutive kinase activation of the TEL-Syk fusion gene in myelodysplastic syndrome with t(9;12)(q22;p12). *Blood.* **97**, 1050-5.

Lemischka I. (2001). Stem cell dogmas in the genomics era. *Rev Clin Exp Hematol.* **5** (1), 15-25.

Lemons R. S., Eilender D., Waldmann R. A., Rebentisch M., Frej A. K., Ledbetter D. H., Willman C., McConnell T., O'Connell P. (1990). Cloning and characterization of the t(15;17) translocation breakpoint region in acute promyelocytic leukemia. *Genes Chromosomes Cancer.* **2**, 79-87.

Lescher B., Haenig B., Kispert A. (1998). sFRP-2 is a target of the Wnt-4 signaling pathway in the developing metanephric kidney. *Dev Dyn.* **213** (4), 440-51.

Li Y. S., Wasserman R., Hayakawa K., Hardy R. R. (1996). Identification of the earliest B lineage stage in mouse bone marrow. *Immunity.* **5** (6), 527-35.

Li Y. S., Hayakawa K., Hardy R. R. (1993). The regulated expression of B lineage associated genes during B cell differentiation in bone marrow. *J Exp Med.* **178** (3), 951-60.

Lin S., Ying S. Y. (1999). Differentially expressed genes in activin-induced apoptotic LNCaP cells. *Biochem Biophys Res Commun.* **257** (1), 187-92.

Lorick K. L., Jensen J. P., Fang S., Ong A. M., Hatakeyama S., Weissman A. M. (1999). RING fingers mediate ubiquitin-conjugating enzyme (E2)-dependent ubiquitination. *Proc Natl Acad Sci U S A* **96** (20), 11364-9.

Lu M., Gong Z. Y., Shen W. F., Ho A. D. (1991). The tcl-3 proto-oncogene altered by chromosomal translocation in T-cell leukemia codes for a homeobox protein. *EMBO J.* **10** (10), 2905-10.

Ludwig W. D., Rieder H., Bartram C. R., Heinze B., Schwartz S., Gassmann W., Löffler H., Hossfeld D., Heil G., Handt S., Heyll A., diedrich H., Fischer K., Weiss A., Volkers B., Aydemir U., Fonatsch C., Gökbuget N., Thiel E., Hoelzer D. (1998). Immunophenotypic and genotypic features, clinical characteristics, and treatment outcome of adult pro-B acute lymphoblastic leukemia: results of the German multicenter trials GMALL 03/87 and 04/89. *Blood.* **92**, 1898-909.

Lynch D. K., Winata S. C., Lyons R. J., Hughes W. E., Lehrbach G. M., Wasinger V., Corthals G., Cordwell S. (2003). A Cortactin-CD2-associated protein (CD2AP) complex provides a novel link between epidermal growth factor receptor endocytosis and the actin cytoskeleton. *J Biol Chem.* **278** (24), 21805-13.

McKenna H. J., Stocking K. L., Miller R. E., Brasel K., De Smedt T., Maraskovsky E., Maliszewski C. R., Lynch D. H., Smith J., Pulendran B., Roux E. R., Teepe M., Lyman S. D., Peschon J. J. (2000). Mice lacking flt3 ligand have deficient hematopoiesis affecting hematopoietic progenitor cells, dendritic cells, and natural killer cells. *Blood.* **95** (11), 3489-97.

Martin C. H., Aifantis I., Scimone M. L., von Andrian U. H., Reizis B., von Boehmer H., Gounari F. (2003). Efficient thymic immigrtion of B220+ lymphoid-restricted bone marrow cells with T precursor potential. *Nat Immunol.* **4** (9), 866-73.

Matsuda G., Nakajima K., Kawaguchi Y., Yamanashi Y., Hirai K. (2003). Epstein-Barr virus (EBV) nuclear antigen leader protein (EBNA-LP) forms complexes with a cellular anti-apoptosis protein Bcl-2 or its EBV counterpart BHRF1 through HS1-associated protein X-1. *Microbiol Immunol.* **47** (1), 91-9.

Meffre E., Casellas R., Nussenzweig M. C. (2000). Antibody regulation of B cell development. *Nat Immunol.* **1** (5), 379-85.

Merup M., Moreno T. C., Heyman M., Ronnberg K., Grander D., Detlofsson R., Rassol O., Liu Y., Soderhall S., Juliusson G., Gahrton G., Einhorn S. (1998). 6q deletions in acute lymphoblastic leukemia and non-Hodgjin's lymphomas. *Blood.* **91** (9), 3397-400.

Miller J. P., Izon D., DeMuth W., Gerstein R., Bhandoola A., Allman D. (2002). The earliest step in B lineage differentiation from common lymphoid progenitors is critically dependent upon interleukin 7. *J Exp Med.* **196** (5), 705-11.

Mirmohammadsadegh A., Tartler U., Michel G., Baer A., Walz M., Wolf R., Ruzicka T., Hengge U. R. (2003). HAX-1, identified by differencial display reverse trancription polymerase chain reaction, is overexpressed in lesional psoriasis. *J Invest Dermatol.* **120** (6), 1045-51.

Mohamed A. N., al-Katib A. (1988). Establishment and characterization of a human lymphoma cell line (WSU-NHL) with 14;18 translocation. *Leuk Res.* **12** (10), 833-43.

Morrison S. J., Weissman I. L. (1994). The long-term repopulating subset of hematopoietic stem cells is deterministic and isolatable by phenotype. *Immunity.* **1** (8), 661-73.

Morrison S. J., Wandycz A. M., Hemmati H. D., Wright D. E., Weissman I. L. (1997). Identification of a lineage of multipotent hematopoietic progenitors. *Development.* **124** (10), 1929-39.

Novell P. C., Hungerford D. A. (1960). A minute chromosome in human chronic granulocyte leukemia. *Science.* **132**, 1497.

Novikova S. I., He F., Bai J., Badan I., Lidow I. A., Lidow M. S. (2005). Cocaine-induced changes in the expression of apoptosis-related genes in the fetal mouse cerebral wall. *Neurotoxicol Teratol.* **27** (1), 3-14.

Oikawa T., Yamada T. (2003). Molecular biology of the Ets family of transcription factors. *Gene.* **303**, 11-34.

Okuno K., Yasutomi M., Nishimura N., Arakawa T., Shiomi M., hida J., Ueda K., Minami K. (2001). Gene expression analysis in colorectal canceer using practical DNA array filter. *Dis Colon Rectum.* **44** (2), 295-9.

Ortiz D. F., Moseley J., Calderon G., Swift A. L., Li S., Arias I. M. (2004). Identification of HAX-1 as a protein that binds bile salt export protein and regulates its abundance in the apical membrane of Madin-Darby canine kidney cells. *J Biol Chem.* **279** (31), 32761-70.

Osawa M., Hanada K., Hamada H., Nakauchi H. (1996). Long-term lymphohematopoietic reconstitution by a single CD34-low/negative hematopoietic stem cell. *Science.* **273** (5272), 242-5.

Padanilam B. J., Lewington A. J., Hammerman M. R. (1998). Expression of CD27 and ischemia/reperfusion-induced expression of its ligand Siva in rat kidneys. *Kidney Int.* **54** (6), 1967-75.

Palis & Yoder. (2001). Yolk-sac hematopoiesis: the first blood cells of mouse and man. *Exp Hematol.* **29** (8), 927-36.

Papadopoulos P., Rigde S. A., Boucher C. A., Stocking C., Wiedemann L. M. (1995). The novel activation of ABL by fusion to an ets-related gene, TEL. *Cancer Res.* **55** (1), 34-8.

Patel A. S., Schechter G. L., Wasilenko W. J., Somers K. D. (1998). Overexpression of EMS1/cortactin in NIH3T3 fibroblasts causes increased cell motility and invasion in vitro. *Oncogene.* **16** (25), 3227-32.

Peeters P., Raynaud S. D., Cools J., et al. (1997). Fusion of TEL. the ETS-variant gene 6 (ETV6), to the receptor-associated kinase JAK2 as a result of t(9;12) in a lymphoid and t(9;15;12) in a mueloid leukemia. *Blood.* **90**, 2535-40.

Peng H., Begg G. E., Schultz D. C., Friedman J. R., Jensen D. E., Speicher D. W., Rauscher F. J. (2000). Reconstituition of the KRAB-KAP-1 repressor complex: a model system for defining the molecular anatomy of RING-B box-coiled-coil domain-mediated protein-protein interactions. *J Mol Biol.* **295**, 1139-62.

Pineault N., Buske C., Feuring-Buske M., Abramovich C., Rosten P., Hogge D. E., Aplan P. D., Humphries R. K. (2003). Induction of acute myeloid leukemia in mice by the human leukemia-specific fusion gene NUP98-HOXD13 in concert with Meis1. *Blood.* **101** (11), 4529-38.

Prasad K. V., Ao Z., Yoon Y., Wu M. X., Rizk M., Jacquot S., Schlossman S. F. (1997). CD27, a member of the tumor necrosis factor receptor family, induces apoptosis and binds to Siva, a proapoptotic protein. *Proc Natl Acad Sci USA.* **94** (12), 6346-51.

Py B., Slomianny C., Auberger P., Petit P. X., Benichou S. (2004). Siva-1 and an alternative splice form lacking the death domain, Siva-2, similarly induce apoptosis in T lymphocytes via a caspase-dependent mitochondrial pathway. *J Immunol.* **172** (7), 4008-17.

Qin L. F., Lee T. K., Ng I. O. (2002). Gene expression profiling by cDNA array in human hepatoma cell line in response to cisplatin treatment. *Life Sci.* **70** (14), 1677-90.

Rabbttis T. H. (1994). Chromosomal translocations in human cancer. *Nature.* **372** (6502), 143-9.

Radhika V., Onesime D., Ha J. H., Dhanasekaran N. (2004). Galpha13 stimulates cell migration throuh cortactin-interacting protein Hax-1. *J Biol Chem.* **279** (47), 49406-13.

Raynaud S., Mauvieux L., Cayuela J. M., Bastard C., Bilhou-Nabera C., Debuire B., Bories D., Boucheix C., Charrin C., Fiere D., Gabert J. (1996). TEL/AML1 fusion gene is a rare event in adult lymphoblastic leukemia. *Leukemia.* **10** (9), 1529-30.

Reddy B. A., Etkin L. D., Freemont P. S. (1992). A novel zinc finger coiled-coil domain in a family of nuclear proteins. *Trends Biochem Sci.* **17**, 344-45.

Reichel M., Gillert E., Nilson I., Siegler G., Greil J., Fey G. H., Marschalek R. (1998). Fine structure of translocation breakpoints in leukemic blasts with chromosomal translocation t(4;11): the DNA damage-repair model of translocation. *Oncogene.* **17** (23), 3035-44.

Reya T., Duncan A. W., Ailles L., Domen J., Scherer D. C., Willert K., Hintz L., Nusse R., Weissman I. L. (2003). A role for Wnt signaling in self-renewal of hematopoietic stem cells. *Nature.* **423** (6938), 409-14.

Reya T., Morrison S. J., Clarke M. F., Weissman I. L. (2001). Stem cells, cancer, and cancer stem cells. *Nature.* **414** (6859), 105-11.

Rogers S., Wells R., Rechsteiner M. (1986). Amino acid sequences common to rapidly degraded proteins: the PEST hypothesis. *Science.* **234** (4774), 364-8.

Rolink A. G., ten Boekel E., Yamagami T., Ceredig R., Andersson J., Melchers F. (1999). B cell development in the mouse from early progenitors to mature B cells. *Immunol Lett.* **68** (1), 89-93.

Romana S. P., Poirel H., Le Coniat M., Berger R. (1994). t(12;21): a new recurrent translocation in acute lymphoblastic leukemia. *Genes Chromosomes Cancer.* **9** (3), 186-91.

Romana S. P., Mauchauffe M., Le Coniat M., Chumakov I., Le Paslier D., Berger R., Bernard O. A. (1995a). The t(12;21) of acute lymphoblastic leukemia results in a tel-AML1 gene fusion. *Blood.* **85** (12), 3662-70.

Romana S. P., Poirel H., Le Coniat M., Flexor M. A., Mauchauffe M., Jonveaux P., Macintyre E. A., Berger R., Bernard O. A. (1995b). High frequency of t(12;21) in childhood B-lineage acute lymphoblastic leukemia. *Blood.* **86** (11), 4263-9.

Romana S. P., Le Coniat M., Poirel H., Marynen P., Bernard O., Berger R. (1996). Deletion of the short arm of chomosome 12 is a secondary event in acute lymphoblastic leukemia with t(12;21). *Leukemia.* **10** (1), 167-70.

Rowley J. D. (1999). The role of chromosome translocations in leukemogenesis. *Semin Hematol.* **4** (7), 59-72.

Rudolph C., Steinemann d., Von Neuhoff N., Gadzicki D., Ripperger T., Drexler H. G., Mrasek K., Liehr T., Claussen U., Emura M., Schrock E., Schlegelberger B. (2004). Molecular cytogenetic characterization of the mantle cell lymphoma cell line GRANTA-519. *Cancer Genet Cytogenet.* **153** (2), 144-50.

Saltman D. L., Cachia P. G., Dewar A. E., Ross F. M., krajewsk A. S., Ludlam C., Steel C. M. (1988). Characterization of a new non-Hodgkin's lymphoma cell line (NCEB-1) with a chromosomal (11:14) translocation [t(11;14)(q13;q32)]. *Blood.* **72** (6), 2026-30.

Sambrook J., Fritsch E. F., Maniats T. (1989). Molecular cloning: a laboratory manual. **2nd ed.**

Sambrook J., Russel D. W. (2001). Molecular cloning: a laboratory manual. **3nd ed.**

Sanchez-Garcia I., Rabbitts T. H. (1993). LIM domain proteins in leukaemia and development. *Semin Cancer Biol.* **4** (6), 349-58.

Sato Y., Suto Y., Pietenpol J., Golub, T. R., Gilliland D. G., Davis E. M., Le Beau M. M., Roberts J. M., Rowley J. D. et al. (1995). TEL and KIP1 define the smallest region of deletions on 12p13 in hematopoietic malignancies. *Blood.* **86** (4), 1525-33.

Saurin A. J., Borden K. L., boddy M. N., Freemont P. S. (1996). Does this have a familiar RING?. *Trends Biochem Sci.* **21**, 208-14.

Sawyers C. L., Denny C. T., Witte O. N. (1991). Leukemia and the disruption of normal hematopoiesis. *Cell.* **64** (2), 337-50.

Schebesta M., Heavey B., Busslinger M. (2002). Transcriptional control of B-cell development. *Curr Opin Immunol.* **14** (2), 21-23.

Schessl C., Rawat V. P. S., Cusan M., Desphande A., Kohl T. M., Rosten P. M., et al. (2005). The AML1-ETO fusion gene and the FLT3 length mutation collaborate in inducing acute leukemia in mice. *J. Clin. Invest.* **115** (8), 2159-68.

Schmeichel K. L., Beckerle M. C. (1994). The LIM domain is a modular protein-binding interface. *Cell.* **79**, 211-19.

Schwabe J. W., Klug A. (1994). Zinc mining for protein domains. Nat Struct Biol. **1**, 345-49.

Schwaller J., Frantsve J., Aster J., Williams I. R., Tomasson M. H., Ross T. S., Peeters P., Van Rompaey L., Van Etten R. A., Ilaria R. Jr., Marynen P., Gilliland D. G. (1998). Transformation of hematopoietic cell lines to growth-factor independente and induction of a fatal myelo- and lymphoproliferative disease in mice by retrovirally transduced TEL/JAK2 fusion genes. EMBO *J.* **17** (18), 5321-33.

Secker-Walker L. M., Mehta A., Bain B. (1995). Abnormalities of 3q21 and 3q26 in myeloid malignancy: a United Kingdom Cancer Cytogenetic Group study. *Br J Haematol.* **91**, 490-501.

Sell S. &Pierce G. B. (1994). Maturation arrest of stem cell differentiation is a common pathway for the cellular origin of teratocarcinomas and epithelial cancers. *Lab Invest.* **70** (1), 6-22.

Seseke F., Thelen P., Ringert R. H. (2004). Characterization of an animal model of spontaneous congenital unilateral obstructive uropathy by cDNA microarray analysis. *Eur Urol.* **45** (3), 374-81.

Sharp T. V., Wang H. W., Koumi A., Hollyman D., Endo Y., Ye H., Du M. Q., Boshoff C. (2002). K15 protein of Kaposi's sarcoma-associated herpes virus is latently expressed and binds to HAX-1, a protein with antiapoptotic function. *J Virol.* **76** (2), 802-16.

Shurtleff S. A., Buijs A., Behm F. G., Rubnitz J. E., Raimondi S. C., Hancock M. L., Chan G. C., Pui C. H., Grosveld G., Downing J. R. (1995).TEL/AML1 fusion resulting from a cryptic t(12;21) is the most common genetic lesion in pediatric ALL and defines a subgroup of patients with an excellent. *Leukemia.* **9** (12), 1985-9.

Sitnicka E., Bryder D., Theilgaard-Monch K., Buza-Vidas N., Adolfsson J., Jacobsen S. E. (2002). Key role of flt3 ligand in regulation of the common lymphoid progenitor but not in maintenance of the hematopoietic stem cell pool. *Immunity.* **17** (4), 463-72.

Slupsky C. M., Gentile L. N., Donaldson L. W., Mackereth C. D., Seidel J. J., Graves B. J., Mcintosh L. P. (1998). Structure of the Ets-1 pointed domain and mitogen-activated protein kinase phosphorylation site. *Proc. Natl. Acad. Sci. USA.* **95** (21), 12129-12134.

Smith C. (2003). Hematopoietic stem cells and hematopoiesis. *Cancer Control.* 10 (1), 9-16.

Spinicelli S., Nocentini G., Ronchetti S., Krausz L. T., Bianchini R., Riccardi C. (2002). GITR interacts with the pro-apoptotic protein Siva and induces apoptosis. *Cell Death Differ.* **9** (12), 1382-4.

Suto Y., Sato Y., Smith S. D., Rowley D. R., Bohlander S. K. (1997). A t(6;12)(q23;p13) results in the fusion of ETV6 to a novel gene, STL, in a B-cell ALL cell line. *Genes Chromosomes Cancer.* **18** (4), 254-68.

Suzuki Y., Demoliere C., Kitamura D., Takeshita H., Deuschle U., Watanabe, T. (1997) HAX-1, a novel intracellular protein, localized on mitochondria, directly associates with HS1, a substrate of Src family tyrosine kinases. *J Immunol.* **158** (6), 2736-44.

Taipale J., Beachy P. A. (2001). The hedgehog and Wnt signaling pathways in cancer. *Nature.* **411** (6835), 349-54.

Taniuchi I., Kitamura D., Maekawa Y., Fukuda T., Kishi H., Watanabe T. (1995). Antigen-receptor induced clonal expansion and deletion of lymphocytes are impaired in mice lacking HS1 protein a substrate of the antigen-receptor-coupled tyrosine kinases. *EMBO J.* **14** (15), 3664-78.

Tirado C. A., Sebastian S., Moore J. O., Gong J. Z., Goodman B. K. (2005). Molecular and cytogenetic characterization of a novel rearrangement involving chromosomes 9, 12, and 17 resulting in ETV6 (TEL) and ABL fusion. *Cancer Genet Cytogenet.* **157** (1), 74-7.

Traver D., Akashi K., Manz M., Merad M., Miyamoto T., Engleman E. G., Weissman I. L. (2000). Development of CD8alpha-positive dendritic cells from a common myeloid progenitor. *Science.* **290** (5499), 2152-4.

Traver D., Herbomel P., Patton E. E., Murphey R. D., Yoder J. A., Litman G. W., Catic A., Amemiya C. T., Zon L. I., Trede N. S. (2003). The zebrafish as a model organism to study development of the immune system. *Adv Immunol.* **81**, 253-330.

Treier M., Staszewski L. M., Bohmann D. (1994). Ubiquitin-dependent c-Jun degradation in vivo is mediated by the delta domain. *Cell.* **78** (5), 787-98.

Tudor K. S., Payne k. J., Yamashita Y., Kincade P. W. (2000). Functional assessment of precursors from murine bone marrow suggests a sequence of early B lineage differentiation events. *Immnunity.* **12** (3), 335-45.

Turpen J. B., Kelley C. M., Mead P. E., Zon L. L. (1997). Bipotential primitive-definitive hematopoietic progenitors in the vertebrate embryo. *Immunity.* **7** (3), 325-34.

Tyers M., and Willems A. R. (1999). One ring to rule a superfamily of E3 ubiquitin ligases. *Science.* **284**, 601-04.

Uruno T., Liu J., Zhang P., Fan Yx., Egile C., Li R., Mueller S. C., Zhan X. (2001). Activation of Arp2/3 complex-mediated actin polymerization by cortactin. *Nat Cell Biol.* **3** (3), 259-66.

Uruno T., Zhang P., Liu J., Hao J. J., Zhan X. (2003). Haematopoietic lineage cell-specific protein 1 (HS1) promotes actin-related protein (Arp) 2/3 complex-mediated actin polymerization. *Biochem J.* **371** (2), 485-93.

Van der Reijden B. A., Erpelinck-Verschueren C. A., Lowenberg B., Jansen J. H. (1999). TRIADs: a new class of proteins with a novel Cysteine-rich signature. *Protein Sci.* **8**, 1557-61.

Vieira L., Marques B., Cavaleiro C., Ambrosio A. P., Jorge M., Neto A., Cost J. M., Junior E. C., Boavida M. G. (2005). Molecular cytogenetic characterization of rearrangements involving 12p in leukemia. *Cancer Genet Cytogenet.* **157** (2), 134-9.

Wang L. C., Kuo F., Fujiwara Y., Gilliland D. G., Golub T. R., Orkin S. H. (1997). Yolk sac angiogenic defect and intra-embryonic apoptosis in mice lacking the Ets-related factor TEL. *EMBO J.* **16**, 4374-83.

Waring P. M., Cleary M. L. (1997). Disruption of a homolog of trithorax by 11q23 translocations: leukemogenic and transcriptional implications. *Curr Top Microbiol Immunol.* **220**, 1-23.

Waskow C., Pauls S., Haller C., Gassmann M., Rodewald H. R. (2002). Viable c-Kit(W/W) mutants reveal pivotal role for c-kit in the maintenance of lymphopoiesis. *Immunity.* **17** (3), 277-88.

Wasylyk B., Hahn S. L., Giovane A. (1993). The Ets family of transcription factors. *Eur J Biochem.* **211**, 7-18.

Weed S. A., Du Y., Parsons J. T. (1998). Translocation of cortactin to the cell periphery is mediated by the samll GTPase Rac1. *J Cell Sci.* **111** (16), 2433-43.

Weissman I. L. (2000). Stem cells: units of development, units of regeneration, and units in evolution. *Cell.* **100** (1), 157-68.

Weissman A. M. (2001). Themes and variations on ubiquitination. *Nat Rev Mol Cell Biol.* **2** (3), 169-78.

Xiao H., Palhan V., Yang Y., Roeder R. G. (2000). TIP30 has an intrinsic kinase activity required for up-regulation of a subset of apoptotic genes. EMBO *J.* **19** (5), 956-63.

Xue L., Chu F., Cheng Y., Sun X., Borthakur A., Ramarao M., Pandey P., Wu M., Sclossman S. F., Prasad K. V. (2002). Siva-1 binds to and inhibits BCL-X(L)-mediated protection against UV radiation-induced apoptosis. *Proc Natl Acad Sci USA.* **99** (10), 6925-30.

Yamanashi Y., Okada M., Semba T., Yamori T., Umemori H., Tsunasawa S., Toyoshima K., Kitamura D., Watanabe T., Yamamoto T. (1993). Identification of HS1 protein as a major substrate of protein-tyrosine kinase(s) upon B-cell antigen receptor-mediated signaling. *Proc Natl Acad Sci USA.* **90** (8), 3631-5.

Yang X., Khosravi-Far R., Chang H. Y., Baltimore D. (1997). Daxx, a novel Fas-binding protein that activates JNK and apoptosis. *Cell.* **89** (7), 1067-76.

Yin X. M., Oltvai Z. N., Korsmeyer S. J. (1994). BH1 and BH2 domains of Bcl-2 are required for inhibition of apoptosis and heterodimerization with Bax. *Nature.* **369** (6478), 321-3.

Yoon Y., Ao Z., Cheng Y., Sclossman S. F., Prasad K. V. (1999). Murine Siva-1 and Siva-2, alternate splice forms of the mouse Siva gene, both bind to CD27 but differentially transduce apoptosis. *Oncogene.* **18** (50), 7174-9.

Zhang L. Q., Downie P. A., Goodell W. R., McCabe N. R., LeBeau M. M., Morgan R., Sklar J., Raimondi S. C., Miley D., Goldberg A., Lu M. M., Montag A., Smith S. D. (1993). Stablishment of cell lines from B-cell precursor acute lymphoblastic leukemia. *Leukemia.* **7** (11), 1865-74.

9. Appendix

1) BLAST search of HAX-1 (Hela clone 2)

```
gi|15680006|gb|BC014314.1|    Homo sapiens HS1 binding protein, mRNA (cDNA clone
MGC:22696
IMAGE:3931852), complete cds
Length = 1147

Score =  638 bits (322), Expect = e-180
Identities = 334/337 (99%), Gaps = 2/337 (0%)
Strand = Plus / Plus

Query: 49   cccaaccagcaccagactggggctcccagaggccatttcataggtttgatgatgtatggc 108
            ||||||||||||||||||||||||||||||||||||||||||||||||||||||||||||
Sbjct: 543  cccaaccagcaccagactggggctcccagaggccatttcataggtttgatgatgtatggc 602

Query: 109  ctatggacccccatcctagaaccagagaggacaatgatcttgattcccaggtttcccagg 168
            ||||||||||||||||||||||||||||||||||||||||||||||||||||||||||||
Sbjct: 603  ctatggacccccatcctagaaccagagaggacaatgatcttgattcccaggtttcccagg 662

Query: 169  agggtcttggcccggttctacagccccagcccaaatcctatttcaagagcatctctgtga 228
            ||||||||||||||||||||||||||||||||||||||||||||||||||||||||||||
Sbjct: 663  agggtcttggcccggttctacagccccagcccaaatcctatttcaagagcatctctgtga 722

Query: 229  ccaagatcactaaaccagatgggatagtggaggagcgccggactgtgggtgggacagtga 288
            ||||||||||||||||||||||||||||||||||||||||||||||    ||||||||||
Sbjct: 723  ccaagatcactaaaccagatgggatagtggaggagcgccggactgtgg--tggacagtga 780

Query: 289  gggccggacagagactacagtaacccgacacgaagcagatagcagtcctaggggtgatcc 348
            ||||||||||||||||||||||||||||||||||||||||||||||||||||||||||||
Sbjct: 781  gggccggacagagactacagtaacccgacacgaagcagatagcagtcctaggggtgatcc 840

Query: 349  agaatcaccaagacctccagccctggatgatgccttt 385
            |||||||||||||||||||||||||||||||||||||
Sbjct: 841  agaatcaccaagacctccagccctggatgatgccttt 877
```

Appendix 1: Genbank nucleotide sequence (156 nucleotides, primer Y2H2) of cDNA 2 (Query)

2) BLAST search of HAX-1 (Hela clone 3)

```
gi|15680006|gb|BC014314.1|    Homo sapiens HS1 binding protein, mRNA (cDNA clone
MGC:22696
             IMAGE:3931852), complete cds
           Length = 1147

 Score =  551 bits (278), Expect = e-154
 Identities = 285/286 (99%), Gaps = 1/286 (0%)
 Strand = Plus / Plus

Query: 71   gggaacccaaggttccatagtcctcagcaccccctgaggaatttggcttcggcttcagc 130
            |||||||||||||||||||||||||||||||||||||||||||||||||||||||||||
Sbjct: 221  gggaacccaaggttccatagtcctcagcaccccctgaggaatttggcttcggcttcagc 280

Query: 131  ttcagcccaggaggagggatacgtttccacgataacttcggctttgatgacctagtacga 190
            ||||||||||||||||||||||||||||||||||||||||||||||||||||||||||||
Sbjct: 281  ttcagcccaggaggagggatacgtttccacgataacttcggctttgatgacctagtacga 340

Query: 191  gatttcaatagcatcttcagcgatatgggggcctggaccttgccttcccatcctcctgaa 250
            ||||||||||||||||||||||||||||||||||||||||||||||||||||||||||||
Sbjct: 341  gatttcaatagcatcttcagcgatatgggggcctggaccttgccttcccatcctcctgaa 400
```

```
Query: 251 cttccaggtcctgagtcagagacacctggtgagagactacgggaggggacagacacttcg 310
            |||||||||||||||||||||||||||||||||||||||||||||| ||||||||||||||
Sbjct: 401 cttccaggtcctgagtcagagacacctggtgagagactacggga-gggacagacacttcg 459


Query: 311 ggactcaatgcttaagtatccagatagtcaccagcccaggatcttt 356
            ||||||||||||||||||||||||||||||||||||||||||||||
Sbjct: 460 ggactcaatgcttaagtatccagatagtcaccagcccaggatcttt 505
```

Appendix 2: Genbank nucleotide sequence (156 nucleotides, primer Y2H2) of cDNA 3 (Query)

3) BLAST search of HAX-1 (Hela clone 5)

gi|1916621|gb|U68566.1|HSU68566 Human HS1 binding protein HAX-1 mRNA, nuclear gene
encoding mitochondrial
          protein, complete cds
        Length=1196

```
 Score =  248 bits (125),  Expect = 6e-63
 Identities = 127/128 (99%), Gaps = 0/128 (0%)
 Strand=Plus/Plus

Query   125  CTGCGAATGGACCACTGGAGGGGTTCAAAGGTTCGCGTCCCAGTACGGGAATGAGCCTCT   184
             ||||||||||||||||||||||||||||||||||||||||||||||||||||||||||||
Sbjct   112  CTGCGAATGGACCACTGGAGGGGTTCAAAGGTTCGCGTCCCAGTACGGGAATGAGCCTCT   171

Query   185  TTGATCTCTTCCGGGGCTTTTTCGGCTTTCCTGGACCTNGGAGCCACAGAGATCCCTTTT   244
             |||||||||||||||||||||||||||||||||||||| |||||||||||||||||||||
Sbjct   172  TTGATCTCTTCCGGGGCTTTTTCGGCTTTCCTGGACCTCGGAGCCACAGAGATCCCTTTT   231

Query   245  TTGGAGGG   252
             ||||||||
Sbjct   232  TTGGAGGG   239
```

Appendix 3: Genbank nucleotide sequence (156 nucleotides, primer Y2H2) of cDNA 5 (Query)

4) BLAST search of SIVA (Hela clone 7)

>gi|11277467|ref|NM_006427.2| Homo sapiens CD27-binding (Siva) protein (SIVA),
transcript variant 1, mRNA
Length = 751

```
Score =  377 bits (190), Expect = e-102
Identities = 194/196 (98%)
Strand = Plus / Plus

Query: 78   gcggccatgcccaagcggagctgcccccttcgcggacgtggccccgctacagctcaangtc 137
            ||||||||||||||||||||||||||||||||||||||||||||||||||||||||| |||
Sbjct: 32   gcggccatgcccaagcggagctgcccccttcgcggacgtggccccgctacagctcaaggtc 91

Query: 138  cgcgtgagccagagggagttgagccgcggcgtgtgcgccgagcgctactcgcaggaggtc 197
            ||||||||||||||||||||||||||||||||||||||||||||||||||||||||||||
Sbjct: 92   cgcgtgagccagagggagttgagccgcggcgtgtgcgccgagcgctactcgcaggaggtc 151


Query: 198  ttcgagaagaccaagcgactcctgttcctcggggcccaggcctacctggaccacgtgtgg 257
            ||||||||||||||||||||||||||||||||||||||||||||||||||||||||||||
Sbjct: 152  ttcgagaagaccaagcgactcctgttcctcggggcccaggcctacctggaccacgtgtgg 211

Query: 258  gatgaaggctgtgccg 273
            ||||||||||||||||
Sbjct: 212  gatgaaggctgtgccg 227
```

Appendix 4: Genbank nucleotide sequence (195 nucleotides, primer Y2H2) of cDNA 7 (Query)

10. Acknowledgements

11. Curricullum Vitae

Personal data:	**Luciana M. Fontanari Krause**
Date and place of birth:	Santa Cruz das Palmeiras – SP – Brazil

School:

February 1982 – December 1985	Primary School at the Escola de Primeiro Grau Dr. Carlos Guimaraes, Santa Cruz das Palmeiras – SP
February 1986 – December 1988	High School at the Escola de Primeiro Grau Dr. Carlos Guimaraes, Santa Cruz das Palmeiras – SP
February 1989 – December 1989	High School at the Escola de Primeiro e Segundo Grau Lauro Barreira, Santa Cruz das Palmeiras – SP
February 1990 – December 1992	High School at the College John Kennedy, Pirassununga – SP
February 1993 – December 1994	College Oswaldo Cruz, Ribeirao Preto – SP

University:

February 1995 – December 1998	University, study of biomedicine at the Júlio de Mesquita Filho University (Unesp), Botucatu, Brazil
January 1998 – December 1998	Diploma thesis at the Microbiology and Imunology Department of the Júlio de Mesquita Filho University, in the group of Dr. Ramon Kaneno, "Effects of aqueous extract of *Agaricus blazei* mushroom in the adaptative response mechanisms in the Ehrlich tumor evolution in mice."
19.12.1998	Diploma of biomedicine, Júlio de Mesquita Filho University, Botucatu, Brazil

February 1999 – March 2000	Research at the Microbiology and Imunology Department of the Júlio de Mesquita Filho University, in the group of Dr. Ramon Kaneno,"Antitumoral activity of *Lentinus edodes* mushroom in mouse model."
September 2001 – October 2005	PhD-student in the group of Prof. Dr. Stefan Bohlander at the GSF-Clinical Cooperation Group at the Ludwig Maximilian-Universtity, Grosshadern, Germany, "Identification and functional characterization of the human and murine *OSTL* gene."

Publications:

Kaneno R., Fontanari L. M., Santos S. A., Di Stasi L. C., Rodriguez Filho E., Eira A. F. (2004). Effects of extracts from Brazilian sun-mushroom (*Agaricus blazei*) on the NK activity and lymphoproliferative responsiveness of Ehrlich tumor-bearing mice. *Food and Chem Toxicol.* **42** (6), 909-16.

Kaneno R., Belik A. V. F., Frantz F. G., Lorenzo J. S. F., Fontanari L. M., Castoldi L., Dias B. R., Spinardi Barbisan A. L. T., Eira A. F. (2004). Antitumor and immunomodulatory effects of culinary-medicinal Shiitake mushroom *Lentinus edodes* (Berk.) Singer: Analysis of NK activity, lymphoproliferative response, and antibody production. *Internacional Journal of Medicinal Mushrooms.* **6**, 315-25.

12. Statement

Herewith I certify to have written this thesis independently, without help of others. The results of this thesis are based on experiments I performed by myself.

Luciana Fontanari Krause